

# **Stony Brook University**



OFFICIAL COPY

**The official electronic file of this thesis or dissertation is maintained by the University Libraries on behalf of The Graduate School at Stony Brook University.**

**© All Rights Reserved by Author.**

Investigation of Menaquinone Biosynthetic Pathway in *Mycobacterium*  
*Tuberculosis*: Catalytic Mechanism and Inhibition Studies of MenB and MenE

A Dissertation Presented  
by  
Huaning Zhang  
to  
The Graduate School  
in Partial Fulfillment of the  
Requirements  
for the Degree of  
Doctor of Philosophy  
in  
Chemistry

Stony Brook University

December 2008

**Stony Brook University**

The Graduate School

**Huaning Zhang**

We, the dissertation committee for the above candidate for the

Doctor of Philosophy degree, hereby recommend

Acceptance of this dissertation

Peter J. Tonge – Dissertation Advisor

Professor of Chemistry Department

Dale G. Drueckhammer – Chairperson of Defense

Professor of Chemistry Department

Daniel P. Raleigh – Committee Member of Defense

Professor of Chemistry Department

Luis E. N. Quadri – External Committee Member of Defense

Professor of Microbiology and Immunology of Weill Cornell Medical College

This dissertation is accepted by the Graduate School

Lawrence Martin

Dean of the Graduate School

## Abstract of the Dissertation

Investigation of Menaquinone Biosynthesis Pathway in *Mycobacterium  
Tuberculosis*: Catalytic Mechanism and Inhibition Studies of MenB and MenE

by

Huaning Zhang

Doctor of Philosophy

in

Chemistry

Stony Brook University

2008

The lipid soluble redox cofactor menaquinone is an essential component of the mycobacterial respiratory chain. Selective inhibitors of menaquinone biosynthesis are thus promising lead compounds for the treatment of latent tuberculosis (TB) infections. Menaquinone is synthesized from chorismate by the action of at least 8 enzymes including MenB which catalyzes an intramolecular Dieckmann condensation to form the naphthalenoid aromatic compound 1,4-dihydroxynaphthoyl-CoA from o-succinylbenzoyl-CoA (OSB-CoA), and MenE, an acyl-CoA synthetase, which converts OSB to OSB-CoA.

Currently we are comparing and contrasting the mechanism of the *M. tuberculosis* MenB enzyme with that of MenB from *E. coli* as well as with other members of the crotonase superfamily including BadI, which catalyzes a retroDieckmann reaction. Crystallographic and kinetic data indicate that

conserved catalytic residues play similar roles in the reactions catalyzed by MenB and BadI. However, the studies also suggest differences in the mechanisms of the reactions catalyzed by the *M. tuberculosis* and *E. coli* MenB enzymes and they might utilize the different substrates for catalysis.

In our studies, several inhibitors, targeting MenB, have been selected and optimized from the initial high throughput screening. The most potent compound against MenB exhibits excellent inhibition *in vitro* with an IC<sub>50</sub> value of 262 nM. On the other hand, a series of mechanism-based inhibitors of MenE have been designed and synthesized. The most potent compound inhibits MenE with an IC<sub>50</sub> value of 5.7 μM. These studies will help us to validate that the enzymes in menaquinone biosynthetic pathway are targets for the development of novel microbial chemotherapeutics.

## Table of Contents

Abstract.....	iii
Table of Contents.....	v
List of Figures.....	xii
List of Tables.....	xviii
List of Abbreviations and Symbols.....	xx

### CHAPTER 1: TUBERCULOSIS AND THE MENAQUINONE BIOSYNTHETIC PATHWAY

Overview of tuberculosis (TB).....	1
Current diagnosis, prevention and treatment of TB.....	3
Mechanisms of action of anti-TB drug.....	6
Multi-drug resistant TB (MDR-TB) and extensively drug-resistant TB (XDR-TB).....	7
Persistence and latency of TB.....	9
Drug targets in persistent and latent <i>M. tuberculosis</i> infection.....	12
Menaquinone biosynthesis in respiratory chain.....	14
Menaquinone (Vitamin K <sub>2</sub> ) biosynthetic pathway is absent in humans and might be an attractive target for anti-TB drug discovery.....	16
Menaquinone biosynthetic pathway in <i>E. coli</i> .....	17
Menaquinone biosynthesis in <i>M. tuberculosis</i> .....	19
The alternative biosynthetic pathway is not present in <i>M. tuberculosis</i> .....	20

Overview of my research.....	22
References.....	24
CHAPTER 2: MECHANISM OF REACTION CATALYZED BY 1, 4-DIHYDROXY- 2-NAPHTHOYL-COA SYNTHASE FROM <i>M. TUBERCULOSIS</i> (MTMENB)	
Background.....	38
<i>Introduction of crotonase superfamily.....</i>	38
<i>MenB catalyzes Dieckmann condensation reaction.....</i>	48
Materials and methods.....	50
<i>Reagents and general methods.....</i>	50
<i>Expression and purification of wild-type MenB from M. tuberculosis (mtMenB).....</i>	51
<i>Cloning, expression and purification of mutant mtMenB.....</i>	52
<i>Cloning, expression and purification of wild-type MenB from E. coli (ecMenB).....</i>	52
<i>Cloning and expression of mutant ecMenB.....</i>	54
<i>Cloning, expression and purification of wild-type MenB from S. aureus (saMenB).....</i>	54
<i>Cloning, expression and purification of mutant saMenB.....</i>	55
<i>Cloning, expression and purification of Wild-type YfbB from E. coli.....</i>	56
<i>Coupled assay of MenB reaction.....</i>	57
<i>Pre-incubation of the MenB coupled assay.....</i>	58
<i>Ellman assay for detecting thioesterase activity.....</i>	58

<i>Kinetic data analysis</i> .....	58
<i>Purification of chorismate from E. coli cells</i> .....	58
<i>Enzymatic synthesis of o-succinylbenzoic acid (OSB) from chorismate</i> .....	60
<i>Synthesis of o-succinylbenzoic acid (OSB)</i> .....	60
<i>Synthesis of N-[2'-(3-carboxypropionyl) benzoyl] imidazole</i> .....	62
<i>Synthesis of methyl ester OSB</i> .....	63
<i>HMBC spectrum of methyl ester of OSB</i> .....	64
<i>Synthesis of methylamine OSB</i> .....	65
<i>Synthesis of dimethylamine OSB</i> .....	66
<i>Standard procedure for the synthesis of acyl-CoA thioester</i> .....	67
<i>Synthesis of 3-benzoylpropionic CoA (3-BP CoA)</i> .....	68
<i>Synthesis of o-(3-carboxypropyl)-benzoic CoA (OCPB-CoA)</i> .....	72
<i>Synthesis of methyl ester OSB-CoA</i> .....	74
<i>Synthesis of methylamine OSB-CoA and dimethylamine OSB-CoA</i> .....	76
<i>Synthesis of dimethoxy DHNA-CoA</i> .....	76
<i>Circular dichroism (CD) spectra of wild-type mtMenB and its mutants</i> .....	76
<i>Isothermal titration calorimetry (ITC) binding experiment of mtMenB</i> .....	77
<i>Alpha-proton exchange reactions catalyzed by mtMenB</i> .....	78
<i>Observing the degradation of DHNA in D<sub>2</sub>O</i> .....	78
<i>X-Ray crystallography of mtMenB bound with dimethoxy DHNA-CoA</i> .....	80
<i>Structural analysis</i> .....	80
Results and discussion.....	81



<i>Expression and catalytic activity of MenBs (mtMenB, ecMenB and saMenB).....</i>	81
<i>Binding and alpha-proton exchange studies of substrate analogues of mtMenB.....</i>	82
<i>Lactone OSB-CoA might be the substrate for mtMenB.....</i>	85
<i>Catalytic functional role of D185 mtMenB.....</i>	92
<i>mtMenB and ecMenB might utilize difference mechanism for catalysis.....</i>	107
<i>YfbB and MenB cannot catalyze the hydrolysis of DHNA-CoA.....</i>	108
<i>Crystal structure of mtMenB in complex with dimethoxy DHNA-CoA.....</i>	112
Conclusions.....	115
References.....	117

### CHAPTER 3: MENB AND BADI CATALYZE DIECKMANN CONDENSATION AND REVERSE DIECKMANN CONDENSATION

Background.....	125
Materials and methods.....	127
<i>Expression and purification of wild-type BadI from R. palustris.....</i>	127
<i>Expression and purification of mutant BadI.....</i>	128
<i>CD spectra of wild-type BadI and its Mutants.....</i>	129
<i>Assay of BadI reaction.....</i>	129
<i>Magnesium dependence of BadI reaction.....</i>	130
<i>Synthesis of 2-ketohexanecarboxyl-CoA.....</i>	131
<i>Synthesis of cyclohexenecarboxyl-CoA.....</i>	132

<i>X-Ray crystallography of BadI</i> .....	133
Results and discussion.....	134
<i>BadI catalyzes reverse Dieckmann condensation</i> .....	134
<i>Comparison of crystal structures of mtMenB and BadI</i> .....	137
<i>Stereochemistry of reactions catalyzed by MenB and BadI</i> .....	142
Conclusions.....	145
References.....	146

#### CHAPTER 4: INHIBITION STUDIES OF MTMENB

Introduction.....	149
Materials and methods.....	150
<i>Pilot screening to establish assay conditions for high throughput screening</i> .....	150
<i>High throughput screening of potent inhibitors of mtMenB</i> .....	150
<i>Pyrophosphate release assay</i> .....	151
<i>Fluorescence titration of mtMenB with hexachlorophene</i> .....	151
<i>Assay for inhibition of mtMenB</i> .....	152
<i>Determination of M. tuberculosis antimicrobial activity</i> .....	152
<i>Determination of B. subtilis antimicrobial activity</i> .....	153
<i>Supplement experiment with DHNA by agar overlay method</i> .....	153
<i>Supplement experiment with menadione and menaquinone-7 (MK-7)</i> .....	153
Results and discussion.....	155
<i>Pilot screening of mtMenB and hexachlorophene</i> .....	155

<i>High throughput screening of mtMenB</i> .....	158
<i>Second screens of “cherry picks”</i> .....	162
<i>In vitro enzymatic inhibition assay of “substrate-like” inhibitors</i> .....	165
<i>In vitro enzymatic inhibition assay of “product-like” inhibitors</i> .....	171
<i>MK-7 can partially rescue the growth of B. subtilis</i> .....	172
<i>In vitro antibacterial activity of inhibitors against M. tuberculosis</i> .....	174
Conclusions.....	175
References.....	176

## CHAPTER 5: EXPRESSION AND INHIBITION STUDIES OF MENE

Background.....	178
Materials and methods.....	183
<i>Expression and purification of ecMenE</i> .....	183
<i>Cloning and expression of mtMenE in M. smegmatis cells</i> .....	184
<i>Cloning and expression of mtMenE in E. coli cells</i> .....	185
<i>E. coli rare codon mutagenesis</i> .....	186
<i>Expression and purification of rare codon mutant of mtMenE in E. coli cells</i> .....	187
<i>Coupled assay of MenE reaction</i> .....	188
<i>Assay for inhibition of ecMenE</i> .....	188
Results and discussion.....	190
<i>Expression of ecMenE and enzymatic activity</i> .....	190
<i>Expression of mtMenE</i> .....	190

<i>Design of mechanism-based inhibitors of MenE</i> .....	194
<i>Inhibition of ecMenE</i> .....	196
Conclusions.....	198
References.....	199
REFERENCES.....	204

## List of Figures

Figure 1.1: Current five first-line anti-TB drugs and <i>p</i> -aminosalicylic acid (PAS).....	4
Figure 1.2: Dual role of TLR2 in immunity against <i>M. tuberculosis</i> .....	11
Figure 1.3: Structure of metronidazole and PA-824.....	13
Figure 1.4: Structure of phenothiazines: chlorpromazine and trifluoperazine.....	14
Figure 1.5: Proposed pathway of aerobic electron flow in mycobacteria.....	15
Figure 1.6: Oxidized and reduced forms of ubiquinone and menaquinone.....	15
Figure 1.7: The men operon in <i>E. coli</i> .....	17
Figure 1.8: Menaquinone biosynthetic pathway in <i>E. coli</i> .....	18
Figure 1.9: Clustering of men gene homologs in <i>M. tuberculosis</i> .....	20
Figure 1.10: Menaquinone biosynthetic pathway in <i>S. coelicolor</i> A3(2).....	21
Figure 2.1: Sequence alignment of characterized crotonase superfamily members.....	39
Figure 2.2: Reactions catalyzed by members of the crotonase superfamily.....	41
Figure 2.3: Structures of enzymes from the crotonase superfamily.....	44
Figure 2.4: Structure of acetoacetyl CoA (AcAc-CoA).....	45
Figure 2.5: Crystal structures of mtMenB bound with AcAc-CoA.....	46
Figure 2.6: Structure of saMenB showing G233V mutation may alter the C-terminus.....	47
Figure 2.7: Structures of mtMenB and saMenB.....	48

Figure 2.8: Reaction catalyzed by MenB.....	49
Figure 2.9: The formation of the naphthoic ring catalyzed by MenB and the spirodilactone in a non-enzymatic reaction.....	57
Figure 2.10: Synthesis of o-succinylbenzoic acid (OSB).....	61
Figure 2.11: <sup>1</sup> H NMR spectrum ((CD <sub>3</sub> ) <sub>2</sub> CO) of OSB, 12-0 ppm.....	61
Figure 2.12: <sup>13</sup> C NMR spectrum ((CD <sub>3</sub> ) <sub>2</sub> CO) of OSB, 220-0 ppm.....	62
Figure 2.13: Synthesis of N-[2'-(3-carboxypropionyl) benzoyl] imidazole.....	62
Figure 2.14: <sup>1</sup> H NMR spectrum ((CD <sub>3</sub> ) <sub>2</sub> SO) of N-[2'-(3-carboxypropionyl) benzoyl] imidazole, 13-0 ppm.....	63
Figure 2.15: Synthesis of methyl ester OSB.....	63
Figure 2.16: <sup>1</sup> H NMR spectrum (CD <sub>3</sub> OD) of methyl ester OSB, 10-2 ppm.....	64
Figure 2.17: <sup>13</sup> C NMR spectrum (CD <sub>3</sub> OD) of methyl ester OSB, 220-0 ppm.....	64
Figure 2.18: HMBC spectrum (500 MHz, CD <sub>3</sub> OD) of methyl ester OSB.....	65
Figure 2.19: Synthesis of methylamine OSB.....	66
Figure 2.20: <sup>1</sup> H NMR spectrum (CD <sub>3</sub> OD) of methylamine OSB, 9-0 ppm.....	66
Figure 2.21: Synthesis of dimethylamine OSB.....	66
Figure 2.22: <sup>1</sup> H NMR spectrum (CD <sub>3</sub> OD) of dimethylamine OSB, 9-0 ppm.....	67
Figure 2.23: Synthesis of CoA thioester.....	67
Figure 2.24: <sup>1</sup> H NMR spectrum (D <sub>2</sub> O) of 3-BP CoA, 10-0 ppm.....	68
Figure 2.25: COSY spectrum of 3-BP CoA (600 HMz, D <sub>2</sub> O).....	71
Figure 2.26: HMBC spectrum of 3-BP CoA (600 HMz, D <sub>2</sub> O).....	72
Figure 2.27: <sup>1</sup> H NMR spectrum (D <sub>2</sub> O) of OCPB-CoA, 10-0 ppm.....	73
Figure 2.28: Synthesis of methyl ester OSB-CoA.....	74

Figure 2.29: $^1\text{H}$ NMR spectrum ( $\text{D}_2\text{O}$ ) of methyl ester OSB-CoA, 10-0 ppm.....	75
Figure 2.30: CD spectra of wild-type and mutant mtMenB.....	77
Figure 2.31: Degradation of DHNA.....	79
Figure 2.32: SDS-PAGE gels of mtMenB, ecMenB and saMenB.....	81
Figure 2.33: Structures of MenB substrate analogues.....	83
Figure 2.34: Proposed mechanism of reaction catalyzed by MenB.....	85
Figure 2.35: The degradation of OSB-CoA to spirodilactone.....	86
Figure 2.36: The equilibrium of OSB and lactone OSB.....	86
Figure 2.37: $^{13}\text{C}$ NMR spectra of OSB and lactone OSB.....	87
Figure 2.38: Synthesis of $^{13}\text{C}$ labeled OSB-CoA from chorismate.....	88
Figure 2.39: Sequence alignment of mtMenB, ecMenB and saMenB.....	91
Figure 2.40: S-specific reaction catalyzed by enoyl-CoA hydratase.....	93
Figure 2.41: Crystal structures of mtMenB and enoyl-CoA hydratase.....	94
Figure 2.42: Part of sequence alignment of MenBs from different organisms...	105
Figure 2.43: The phylogenetic tree of MenBs from different organisms.....	106
Figure 2.44: Proposed mechanism of the reaction catalyzed by mtMenB.....	107
Figure 2.45: Proposed mechanism of the reaction catalyzed by ecMenB.....	108
Figure 2.46: Hydrolysis of DHNA-CoA to DHNA.....	108
Figure 2.47: SDS-PAGE gel of YfbB shows it has a molecular weight of 27 kD.....	109
Figure 2.48: YfbB from <i>E. coli</i> catalyzes the conversion from SEPHCHC to SHCHC.....	109

Figure 2.49: UV scan monitoring the degradation of DHNA-CoA at different pH conditions.....	110
Figure 2.50: Proposed degradation reaction of DHNA-CoA in solution.....	111
Figure 2.51: Degradation reaction of DHNA in solution.....	112
Figure 2.52: Structures of AcAc-CoA, OSB-CoA, DHNA-CoA and dimethoxy DHNA-CoA.....	112
Figure 2.53: Inhibition of mtMenB with dimethoxy DHNA-CoA.....	113
Figure 2.54: Crystal structure of mtMenB bound with dimethoxy DHNA-CoA.....	114
Figure 3.1: Reactions catalyzed by MenB and BadI.....	125
Figure 3.2: Pathway for anaerobic benzoate degradation in <i>R. palustris</i> .....	126
Figure 3.3: CD spectra of wild-type and mutant BadI.....	129
Figure 3.4: Formation of an Mg <sup>2+</sup> -enolate complex of 2-ketohexanecarboxyl-CoA.....	130
Figure 3.5: Assay of BadI reaction based on the disappearance of Mg <sup>2+</sup> -enolate complex.....	130
Figure 3.6: BadI reaction is not magnesium dependent.....	131
Figure 3.7: Synthesis of 2-ketohexanecarboxyl-CoA.....	132
Figure 3.8: SDS-PAGE gel of BadI after DE52 and Q sepharose columns.....	134
Figure 3.9: Keto enol tautomerism of BadI substrates and interconversion of the S and R diastereomers.....	135
Figure 3.10: Apparent $k_{cat}/K_m$ values of BadI mutants.....	136
Figure 3.11: Proposed mechanism of BadI reaction.....	137



Figure 3.12: Structure of cyclohexenecarboxyl-CoA.....	137
Figure 3.13: Structure of BadI.....	138
Figure 3.14: Active site of BadI.....	139
Figure 3.15: Crystal structures of mtMenB, BadI and enoyl-CoA hydratase...	141
Figure 3.16: Mechanism of the reaction catalyzed by rat mitochondrial enoyl-CoA hydratase.....	142
Figure 3.17: The divergent stereo-specificities of the reactions catalyzed by crotonase, mtMenB, ecMenB, and BadI.....	144
Figure 4.1: Stages of drug discovery process.....	149
Figure 4.2: The structures of hexachlorophene and triclosan.....	156
Figure 4.3: Inhibition and binding data of hexachlorophene of mtMenB.....	157
Figure 4.4: High throughput screening hits with strong inhibition.....	159
Figure 4.5: High throughput screening hits with medium inhibition.....	160
Figure 4.6: The structures of high throughput screening hits with weak inhibition.....	161
Figure 4.7: Structure of 2-amino-4-oxo-phenylbutanoic acids and benzoxazinones.....	165
Figure 4.8: Structures of compounds showed poor inhibition against mtMenB.....	170
Figure 4.9: Compound 8 is a competitive inhibitor.....	170
Figure 4.10: Compound 36 is a non-competitive inhibitor.....	172
Figure 4.11: Supplement experiment with MK-7.....	173
Figure 4.12: MK-7 partially overcame the inhibition of compound 8.....	173

Figure 5.1: MenE reaction.....	178
Figure 5.2: Long chain fatty acyl-CoA synthetases reaction.....	179
Figure 5.3: The schematic mechanism for the catalysis by ttLC-FACS.....	180
Figure 5.4: SDS-PAGE gel of ecMenE.....	190
Figure 5.5: Rare <i>E. coli</i> codons in <i>M. tuberculosis</i> mene DNA sequence.....	191
Figure 5.6: Expression of mtMenE after rare codon mutations.....	193
Figure 5.7: The SDS-PAGE gel showed mtMenE was not pure after purification.....	193
Figure 5.8: Structures of designed inhibitors of MenE.....	195
Figure 5.9: Mechanism of covalent inhibition.....	195
Figure 5.10: The structure of OSB methyl ester.....	197

## List of Tables

Table 1.1: Six classes of second-line drugs.....	5
Table 1.2: Mode of action of anti-TB drugs.....	7
Table 1.3: Quinones used in the electron transport.....	16
Table 1.4: Homologs of the <i>E. coli</i> menaquinone biosynthetic enzymes in <i>M. tuberculosis</i> .....	19
Table 2.1: Chemical shifts of the protons of 3-benzoylpropionic CoA (3-BP CoA).....	69
Table 2.2: Chemical shifts of the protons of OCPB-CoA.....	73
Table 2.3: Chemical shifts of the protons of methyl ester OSB-CoA.....	75
Table 2.4: Kinetic parameter for wild-type mtMenB, ecMenB and saMenB.....	82
Table 2.5: Binding affinity of mtMenB with substrate analogues (by ITC).....	84
Table 2.6: Different kinetic data of MenB reaction with/without pre-incubation.....	90
Table 2.7: Kinetic parameter mutant mtMenB, ecMenB and saMenB.....	92
Table 3.1: Apparent $k_{cat}/K_m$ values of BadI and its mutants.....	136
Table 4.1: Z' score of different reaction time.....	155
Table 4.2: Libraries of screened compounds.....	158
Table 4.3: Inhibition data of second screens for strong hits (substrate concentration is 12 $\mu$ M).....	163
Table 4.4: Inhibition data of second screens for medium hits (substrate concentration is 37.5 $\mu$ M).....	164

Table 4.5: Inhibition of “substrate-like” inhibitors.....	166
Table 4.6: Inhibition of “product-like” inhibitors.....	171
Table 5.1: Representative inhibitors of aryl acid adenylation enzymes.....	181
Table 5.2: Primer sequences for <i>E. coli</i> rare codon mutagenesis.....	186
Table 5.3: Inhibition of ecMenE by designed inhibitors 1–6.....	196

## List of Abbreviations and Symbols

2-KC-CoA	2-ketohexanecarboxyl-CoA
3-BP CoA	3-benzoylpropionic CoA
AA-CoA	acetoacetyl CoA
AIDS	acquired immunodeficiency syndrome
AMP	adenosine monophosphate
ATP	adenosine triphosphate
<i>B. subtilis</i>	<i>Bacillus subtilis</i>
BCE	before the common era
BP	before present
calcd	calculated
Carb	carboxymethylproline synthase
CBD	4-chlorobenzoyl-CoA dehalogenase
CD	circular dichroism
CDI	N, N'-carbonyldiimidazole
CoA	coenzyme A
conc.	concentrated
COSY	correlation spectroscopy
crotonase	enoyl-CoA hydratase
DCI	$\Delta^{3,5},\Delta^{2,4}$ -dienoyl-CoA isomerase
DHNA	dihydroxynaphthoic acid
DNA	deoxyribonucleic acid

<i>E. coli</i>	<i>Escherichia coli</i>
ECI	$\Delta^{3,2}$ -enoyl-CoA isomerase
ecMenB	MenB from <i>E. coli</i>
ecMenE	MenE from <i>E. coli</i>
FAD	flavin adenine dinucleotide (oxidized form)
FADH <sub>2</sub> <sup>+</sup>	flavin adenine dinucleotide (reduced form)
HICH	3-hydroxyisobutyryl-CoA hydrolase
HIV	human immunodeficiency virus
HMBC	heteronuclear multiple bond correlation
IPTG	isopropyl- $\beta$ -d-thiogalactopyranoside
ITC	isothermal titration calorimetry
LAM	lipoarabinomannans
LC-FACS	long chain acyl-CoA synthetases
LM	lipomannans
<i>M. phlei</i>	<i>Mycobacterium phlei</i>
<i>M. tuberculosis</i>	<i>Mycobacterium tuberculosis</i>
MDR-TB	multidrug-resistant TB
MenB	1, 4-Dihydroxy-2-naphthoyl-CoA synthase
MenE	OSB-CoA synthase
MGCH	3(S)-methylglutaconyl-CoA hydratase
MK	menaquinone
MMCD	methylmalonyl-CoA decarboxylase
mtMenB	MenB from <i>M. tuberculosis</i>

mtMenE	MenE from <i>M. tuberculosis</i>
NAD <sup>+</sup>	Nicotinamide adenine dinucleotide (oxidized form)
NADH	Nicotinamide adenine dinucleotide (reduced form)
NAP	nitroimidazopyran
NRP	nonreplicating persistence phase
OCH	6-oxocamphor hydrolase
OCPB-CoA	o-(3-carboxypropyl)-benzoic CoA
OSB	o-succinylbenzoic acid
PAS	<i>p</i> -aminosalicylic acid
PPi	pyrophosphate
<i>R. palustris</i>	<i>Rhodopseudomonas palustris</i>
<i>S. aureus</i>	<i>Staphylococcus aureus</i>
<i>S. coelicolor</i> A3(2)	<i>Streptomyces coelicolor</i> A3(2)
SAM	S-adenosylmethionine
saMenB	MenB from <i>S. aureus</i>
SAR	structure activity relationship
SCVs	small-colony variants
SEPHCHC	2-succinyl-5-enolpyruvyl-6-hydroxy-3-cyclohexene-1-carboxylate
SHCHC	2-succinyl-6-hydroxy-2, 4-cyclohexadiene-1-carboxylate
TB	tuberculosis
THDP	thiamin diphosphate
THF	tetrahydrofuran

TPP	thiamine pyrophosphate
WHO	World Health Organization
XDR-TB	extensively drug-resistant TB



## **CHAPTER 1: TUBERCULOSIS AND THE MENAQUINONE BIOSYNTHETIC PATHWAY**

The newest statistics from the World Health Organization (WHO) report 2008 showed that there were an estimated 9.2 million new active cases of tuberculosis (TB) in 2006, of which 709, 000 (8%) were HIV-positive. In addition the disease claims nearly 1.7 million lives annually, of which 0.2 million are among HIV-positive people (1). There were an estimated 0.5 million cases of multidrug-resistant TB (MDR-TB) in 2006 (1). The stark reality, largely overlooked, is that among infectious diseases, TB has been and still is a major global health problem and the leading cause of death (2, 3). The major problems in the treatment and control of TB include the role of this disease as a major opportunistic pathogen in patients with HIV-AIDS and the emergence of MDR-TB.

### **Overview of tuberculosis (TB)**

TB is a common and often deadly contagious disease caused by mycobacteria, mainly *Mycobacterium tuberculosis* (4). Other mycobacteria such as *Mycobacterium bovis*, *Mycobacterium africanum*, *Mycobacterium canetti*, and *Mycobacterium microti* also cause mycobacterial infection, but these species are less common.

The earliest unambiguous detection of *M. tuberculosis* is in the remains of bison dated 17, 000 years before present (BP) (5). Skeletal remains showed that prehistoric humans (4000 BCE) had TB, and tubercular decay has been found in the spines of mummies from 3000-2400 BCE (6). The answer of whether TB

originated in cattle and then transferred to humans, or diverged from a common ancestor infecting a different species, is currently unclear (7).

*M. tuberculosis*, is an aerobic rod-shaped bacillus that divides every 16 to 20 hours, an extremely slow rate compared with other bacteria such as *Escherichia coli* (8). Since *M. tuberculosis* has a cell wall but lacks a phospholipid outer membrane, it is classified as a Gram-positive bacterium. However, *M. tuberculosis* does not retain the crystal violet stain or stains very weakly by Gram staining due to its high lipid and mycolic acid content of its cell wall (9), and so is classified as an acid-fast bacterium (10). This unique waxy cell wall makes it hydrophobic and resistant to oral fluids.

Although *M. tuberculosis* can only replicate and grow within a host organism, it can survive in the dry state for weeks as an endospore in the environment and withstand weak disinfectants (11).

TB is transmitted through the air when people who have the disease cough, sneeze, or spit. A single sneeze can release up to 40,000 droplets (0.5 to 5  $\mu\text{m}$  in diameter of each droplet) (12). Each one of these droplets may transmit the disease, since the infectious dose of TB is very low and the inhalation of just a single bacterium can cause a new infection (13). Transmission can only occur from people with active not latent TB (4). People of close contact (prolonged, frequent, or intense contact) with patients are at particularly high risk of being infected, with an estimated 22% infection rate.

The distribution of TB is not uniform across the globe with about 80% of the population in many Asian and African countries testing positive in tuberculin tests, while only 5-10% of the US population testing positive (1).

About 90% of those infected with *M. tuberculosis* have asymptomatic, latent TB infection, with only a 10% lifetime chance that a latent infection will progress to TB disease (4). However, if untreated, the death rate for these active TB cases is more than 50% (14).

### **Current diagnosis, prevention and treatment of TB**

TB usually attacks the lungs (75% of active cases are pulmonary TB) but can also affect the central nervous system, the lymphatic system, the circulatory system, the genitourinary system, the gastrointestinal system, bones, joints, and even the skin. The typical symptoms of TB include a chronic cough with blood-tinged sputum, fever, night sweats, and weight loss (15). Infection of other organs causes a wide range of symptoms. The diagnosis relies on radiology (commonly chest X-rays), a tuberculin skin test, blood tests, as well as microscopic examination and microbiological culture of bodily fluids (16). Prevention relies on screening programs and vaccination, usually with Bacillus Calmette-Guérin (BCG) vaccine (17, 18).

TB treatment is difficult and requires long courses of multiple antibiotics. Five current first-line drugs for treating TB are isoniazid, rifampicin, ethambutol, pyrazinamide, and streptomycin (**Figure 1.1**).

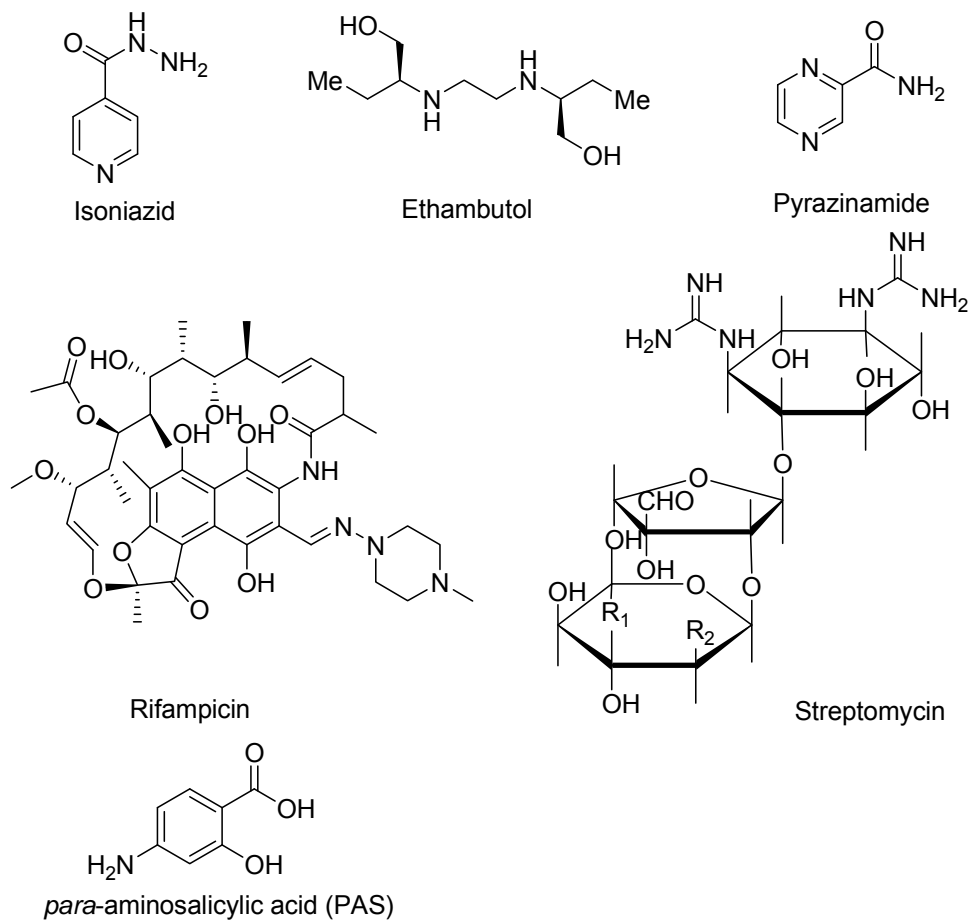


**Figure 1.1: Current five first-line anti-TB drugs and *p*-aminosalicylic acid (PAS)**

Second-line drugs (SLDs) include six classes of antibiotics (**Table 1.1**). A drug may be classed as second-line instead of first-line for one of three possible reasons: it may be less effective than the first-line drugs (e.g., *p*-aminosalicylic acid (PAS) (**Figure 1.1**)); or, it may cause a range of serious side-effects including hepatitis, depression and hallucinations (e.g., cycloserine); or it may be unavailable in many developing countries (e.g., fluoroquinolones).

---

**Table 1.1: Six classes of second-line drugs**

---

Type	Examples
Aminoglycosides	Amikacin (AK) and kanamycin
Polypeptides	Capreomycin, viomycin and enviomycin
Fluoroquinolones	Ciprofloxacin (CIP), levofloxacin and moxifloxacin (MXF)
Thioamides	Ethionamide and prothionamide
Cycloserine	
<i>p</i> -Aminosalicylic acid (PAS)	

---

Soon after the discovery of the anti-TB activity of streptomycin in 1944, it became apparent that *M. tuberculosis* was capable of rapidly developing drug resistance. It was then found that PAS could be used in combination with streptomycin to prevent, or delay, streptomycin resistance (19-21). With the discovery of isoniazid in 1951, it was found that it was much more powerful in combinations with streptomycin and PAS than when used alone and the first combination chemotherapy regimens (included daily isoniazid, streptomycin and high dose of PAS) were standardized with long duration of 18-24 months (22-24). The introduction of rifampicin in 1966 shortened the course of treatment (25-27). Eventually, the 6 months short-course chemotherapy, with combinations of rifampicin, isoniazid and pyrazinamide and ethambutol or streptomycin became standard. These drugs are administered for the first two months of treatment followed by four months of treatment with isoniazid and rifampicin alone (15). The

initial two month treatment destroys bacteria in all growth stages, whereas in the four month continuation phase rifampicin kills any residual dormant bacilli and isoniazid kills any rifampicin-resistant mutants that commence replication (28). For latent TB, the standard treatment is six to nine months of isoniazid alone.

### **Mechanisms of action of anti-TB drugs**

The main issue in anti-TB drug discovery is to develop compounds that have a new mode of action and the potential to shorten the treatment of TB to less than 2 months. Indeed, long-term therapies increase the chances of treatment failure, TB relapse, and emergence of multidrug-resistant (MDR) *M. tuberculosis* strains (29).

Hence there are two main objectives in the treatment of TB: to kill actively metabolizing bacilli in the lung cavities and to destroy less actively replicating and near-dormant bacilli in acidic and oxygen-free lesions that may otherwise cause a relapse of the disease (28). The determination of the biochemical processes targeted by anti-TB drugs is still undergoing and has been reviewed (30-33). The reality is that there are still many anti-TB drugs that have been used for decades with little or no knowledge of their mechanism of action. Therefore understanding the mechanisms of current anti-TB drugs can lead to the identification of already validated biological targets of *M. tuberculosis*. These targets can then be used for the search of better inhibitors starting with the use of modern high-throughput screening of chemical libraries. **Table 1.2** shows several known targets of anti-TB drugs including first-line, second-line and some of the new drugs.

---

**Table 1.2: Mode of action of anti-TB drugs**

---

Anti-TB drugs	Mechanisms of action
Isoniazid, pyrazinamide, ethionamide, prothionamide, thiacetazone, and PA-824 or OPC-67683	Fatty acid biosynthesis inhibitors
Ethambutol, <i>d</i> -cycloserine and amoxicillin, clofazimine	Arabinogalactam and peptidoglycan biosynthesis inhibitors
Streptomycin, kanamycin, amikacin, capreomycin, clarithromycin, and linezolid	Inhibitors of protein synthesis
Rifampin, rifapentin, and fluoroquinolones	Inhibitors of DNA-based processes
<i>p</i> -Aminosalicylic acid	Inhibitors of dihydrofolate reductase or siderophore biosynthesis
TMC 207	Inhibitors of the proton pump $F_0F_1H^+$ ATPase

---

### **Multi-drug resistant TB (MDR-TB) and extensively drug-resistant TB (XDR-TB)**

Multidrug-resistant TB (MDR-TB) is TB that is resistant to at least two of the major first-line bactericidal drugs, isoniazid and rifampicin. With widespread use of rifampicin-containing regimens, resistance to multiple drugs, notably against isoniazid and rifampicin, appeared. In the US, 0.5% of new cases and 3.0% of recurrent cases were resistant to both isoniazid and rifampicin in 1982 but this

proportion increased to 3.1% and 6.9% by 1991(34) and similar data have been reported worldwide (35). Hence, the growth of MDR-TB prevalence has become the major threat that the TB epidemic poses today.

The genes coding for multi-drug, membrane proteins that recognize different toxic compounds and pump them out of bacterial cells, have been identified in mycobacteria, and *M. tuberculosis*. However, they do not seem to play a major role in the emergence of MDR strains (36-38). To the contrary, multi-drug resistance is thought to be the consequence of stepwise accumulation of random mutations in the chromosome selected under the environmental pressure of chemotherapy (39).

In this regard, it was observed that short-course chemotherapy regimens including four or five drugs (rifampicin, isoniazid, pyrazinamide and ethambutol or streptomycin) were still effective in the presence of resistance to isoniazid alone and longer course protocols could still treat patients with rifampicin mono-resistance (40). In contrast, with the resistance to isoniazid and rifampicin combined i.e., MDR-TB, the course of treatment needs prolongation from the standard 6 months to 18–24 months and the cure rate decreases from nearly 100% to less than, or equal to, 60% (34).

Extensively drug resistant TB (XDR-TB) is a relatively rare type of MDR-TB and defined as TB which is resistant to isoniazid and rifampicin, plus resistant to any fluoroquinolone and at least one of three injectable second-line drugs (i.e., amikacin, kanamycin, or capreomycin). It has emerged from the mismanagement of MDR-TB and once created, can spread from one person to another.



Worldwide prevalence of XDR-TB is estimated to be 6.6% in all the studied countries among multidrug-resistant *M. tuberculosis* strains (41).

Because XDR-TB is resistant to first-line and second-line drugs, treatment options for patients are much more limited. XDR-TB is of special concern for persons with HIV infection or other conditions that can weaken the immune system. These persons are more likely to develop TB disease once they are infected, and also have a higher risk of death once they develop TB.

### **Persistence and latency of TB**

Progression from TB infection to TB disease occurs when *M. tuberculosis* overcomes the immune system and begins to replicate. In primary TB disease, this occurs soon after infection (4). However, in the majority of cases, a latent infection occurs that shows no obvious symptoms (4). These dormant bacilli can reproduce active TB in 2-23% per lifetime of these latent cases, often many years after infection (42). The risk of reactivation increases when the immune system is suppressed. For instance, in TB patients co-infected with HIV, the risk of reactivation increases to 10% per year (14).

While the biology and mechanism of *M. tuberculosis* latency is not fully understood, theories on how *M. tuberculosis* enters into the host system and subverts host immune responses in favor of survival, growth and persistence of mycobacteria in macrophages have been put forward.

TB infection begins when the mycobacteria reach the pulmonary alveoli, where they invade and replicate within the endosomes of alveolar macrophages

(4, 43). The primary site of infection in the lungs is called the Ghon focus, and is generally located in either the upper part of the lower lobe, or the lower part of the upper lobe (4). Bacteria are transported by dendritic cells through the bloodstream to other tissues and organs where secondary TB lesions can develop in other parts of the lung (particularly the apex of the upper lobes), peripheral lymph nodes, kidneys, brain, and bone (4, 44). All parts of the body can be affected by the disease, though it rarely affects the heart, skeletal muscles, pancreas and thyroid (45).

TB is classified as one of the granulomatous inflammatory conditions. Macrophages, T lymphocytes, B lymphocytes and fibroblasts are among the cells that aggregate to form a granuloma, with lymphocytes surrounding the infected macrophages. The granuloma functions not only to prevent dissemination of the mycobacteria, but also provides a local environment for communication of cells in the immune system. Within the granuloma, T lymphocytes (CD4<sup>+</sup>) secrete cytokines such as interferon gamma, which activates macrophages to destroy the bacteria with which they are infected (46). T lymphocytes (CD8<sup>+</sup>) can also directly kill infected cells (43). However, bacteria are not always eliminated within the granuloma, but can become dormant, resulting in a latent infection (4).

The entry and persistence of *M. tuberculosis* within the host immune system is attributed to lipoarabinomannans (LAM) and their precursors lipomannans (LM), two predominant glycolipids of *M. tuberculosis* cell wall (47).

LM are recognized by TLR2, one of pattern-recognizing receptors, and induce pro-inflammatory activation of macrophages against *M. tuberculosis* infection.

However, the TLR2-dependent activation of macrophages and dendritic cells favors the direction of adaptive immune responses toward the Th2-type responses, which results in intracellular survival of *M. tuberculosis* (47) (Figure 1.2).

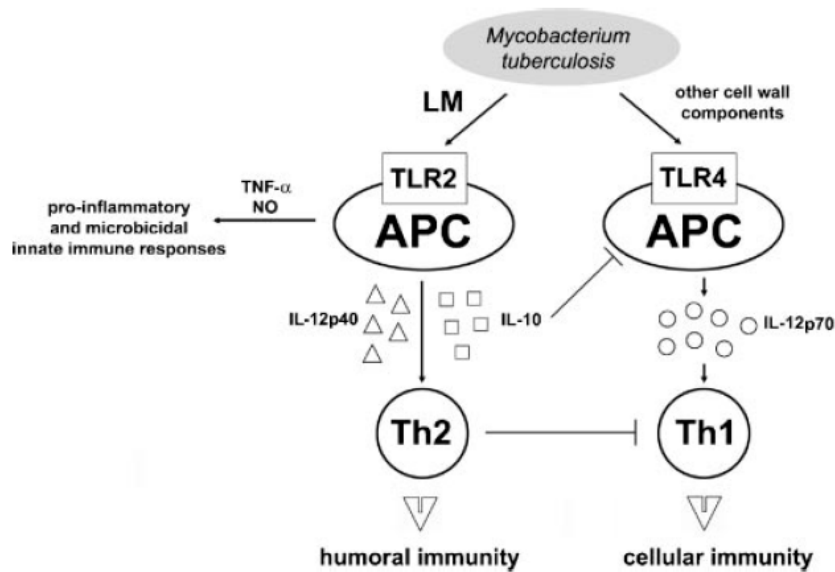


**Figure 1.2: Dual role of TLR2 in immunity against *M. tuberculosis*.** Activation of TLR2 by LM, most likely by its tri-acylated forms, leads to pro-inflammatory innate immune responses. On the other hand, TLR2-mediated activation of APC skews adaptive immune responses toward those of Th2-type, e.g., by blocking TLR4-mediated production of IL-12, and boosts humoral immunity not harmful to *M. tuberculosis*, an intracellular pathogen (47).

At the same time, LAM mimic endogenous host components through the modification of LAM with oligomannosides upon binding to macrophage and dendritic cell receptors, thus evoking immunosuppression and evading from the host defense mechanisms (47).

Wayne and Hayes (48) have conducted pioneering studies of the dormant state of *M. tuberculosis*. In their famous *in vitro* Wayne model of persistence, *M. tuberculosis* cultures are subjected to self-generated oxygen depletion in sealed containers. Growth under such conditions leads to a physiologically well defined anaerobic non-replicating synchronized state of the bacilli. When the oxygen tension in the sealed tubes is reduced to 0.06%, *M. tuberculosis* enters in a non-replicating persistence (NRP) phase where it can survive for extended period without a significant drop in viability (48). Synchronized replication can be relapsed upon reintroduction of oxygen (48, 49). Their work also suggested that *in vitro*-grown non-replicating tubercle bacilli have a reduced susceptibility to the cidal activity of TB drugs (48). This physiological state of the bacillus is being referred to as “drug tolerant” or “phenotypically drug resistant” (50-52).

However, the poor understanding of the mechanisms used by *M. tuberculosis* to persist in the total absence of visible growth is still one of the major obstacles in finding and developing drugs that are active against non-replicating bacilli.

### **Drug targets in persistent and latent *M. tuberculosis* infection**

The non-replicating persistence phenotype of *M. tuberculosis* (NRP-MTB) is assumed to be responsible for the maintenance of latent infection and the requirement of long treatment duration for active TB due to the reduced drug susceptibility (48, 53).

The latent or non-replicating persistent *M. tuberculosis* are resistant to all conventional anti-TB drugs but they become sensitive to metronidazole (**Figure**

**1.3) *in vitro*** (54). Nitroimidazopyran (NAP) drugs such as PA-824 (**Figure 1.3**) were reported to inhibit the synthesis of protein and cell wall lipid (55). In contrast to current anti-TB drugs, nitroimidazopyrans exhibited bactericidal activity against both replicating and static *M. tuberculosis*. Lead compound PA-824 inhibits a more terminal step than isoniazid, namely the oxidation of hydroxymycolates to ketomycolates, a lipid class making up the mycobacterial pseudo-outer membrane and over one-third of the dry weight of *M. tuberculosis* (56). In addition, PA-824 demonstrates potential bactericidal activity against multidrug-resistant (55).

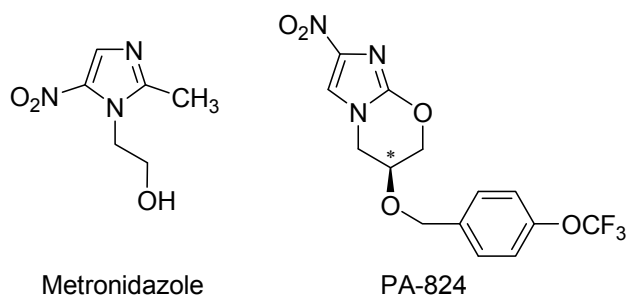


**Figure 1.3: Structure of metronidazole and PA-824**

Significant progress in this area was recently made by Boshof *et al.* who utilized groupings of DNA microarray profiles to analyze the transcriptional response of *M. tuberculosis* to drugs and growth-inhibitory conditions (57). These profiles accurately clustered mechanisms of action of several known drugs and successfully predicted novel mechanisms for previously unknown drugs. Given the critical role of oxygen in the generation of cellular energy and bacterial long-term survival, oxidative phosphorylation is a central component in the production of adenosine triphosphate (ATP) and the subsequent growth and pathogenesis

of *M. tuberculosis*. Cellular respiration, and more specifically the type II NADH menaquinone oxidoreductase, then was identified as the target of a novel class of phenothiazines (**Figure 1.4**) (58).

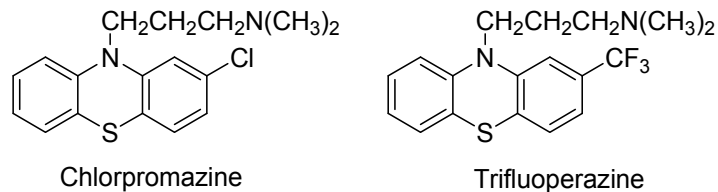


**Figure 1.4: Structure of phenothiazines: chlorpromazine and trifluoperazine**

### **Menaquinone biosynthesis in respiratory chain**

In the respiratory chain, which is also called the electron transport chain, electrons flow from electron donors such as NADH and FADH<sub>2</sub> (succinate) to downstream electron acceptors. In aerobic respiration the electron acceptor is oxygen, while in anaerobic respiration a variety of molecules such as nitrate, dimethyl sulfoxide, fumarate and sulfate, can act as electron acceptors. At the same time, protons are pumped across the membrane to generate a proton gradient that is then used to produce ATP, the main energy intermediate in living organisms. **Figure 1.5** shows the proposed pathway of aerobic electron flow in mycobacteria.

Quinones including ubiquinones and menaquinones are lipid-soluble molecules that shuttle electrons and protons between the membrane-bound protein complexes in the electron transport chain (**Figure 1.6**). The major structural difference within these classes lies on different length of the repeated isoprenoid units.

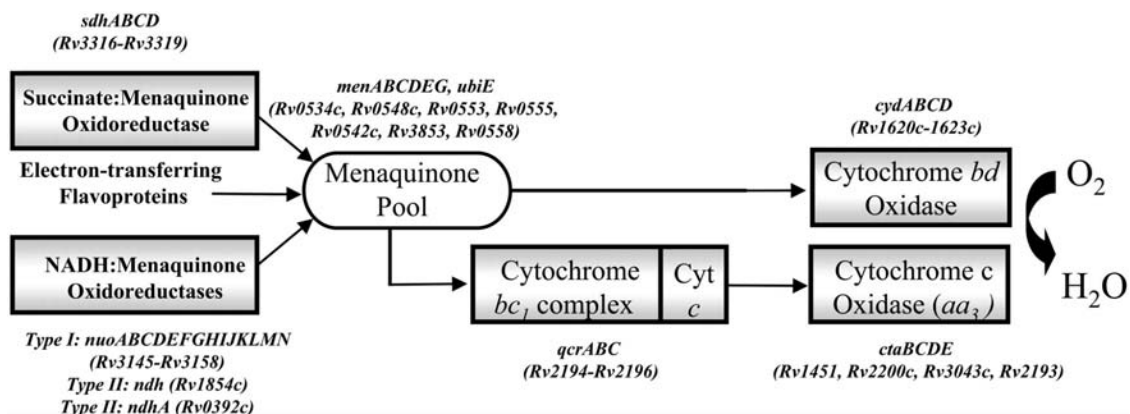


**Figure 1.5: Proposed pathway of aerobic electron flow in mycobacteria.** Complexes are shown in boxes, with corresponding gene names and GenBank accession numbers given outside of the boxes (58).

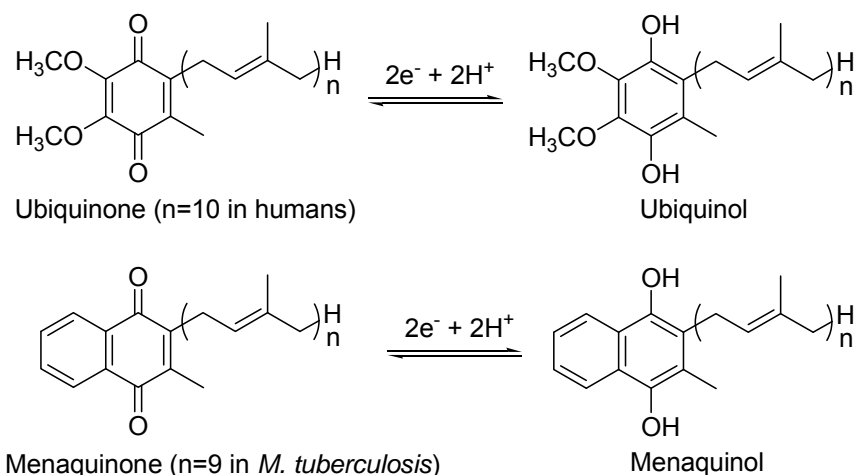


**Figure 1.6: Oxidized and reduced forms of ubiquinone and menaquinone.**

The quinones in mammals are ubiquinone (Coenzyme Q) with 10 isoprene units (**Table 1.2**) (59). They are located in the inner mitochondrial membrane and participate in electron transport. By contrast, prokaryotes employ either the ubiquinone or menaquinone (MK) in the electron transport system. The specific quinones employed also differ in the chain length of the isoprene chain (**Table**

1.3). The enzymes responsible for electron transport are located in membranes, or associated with structures related to membranes or membranes fragments.

**Table 1.3: Quinones used in the electron transport**

Mammals	Ubiquinone (Coenzyme Q)	CoQ-10 (n=10)
Prokaryotes	Menaquinone (MK) and ubiquinone	<i>E. Coli</i> : CoQ-8 (n=8) – aerobic MK-8 (n=8) – anaerobic <i>Bacillus subtilis</i> : MK-7 (n=7) <i>M. tuberculosis</i> : MK-9 (n=9)

n: units of the isoprene chain

Eukaryotes and aerobic Gram negative bacteria use only ubiquinones in the electron transport. Facultative anaerobic bacteria, such as *E. coli*, use ubiquinones in aerobic conditions and menaquinones in anaerobic conditions (59, 60). Most Gram positive bacteria and anaerobic bacteria, e.g. *M. tuberculosis* (MK-9) and *Bacillus subtilis* (MK-7) use only menaquinones (60).

**Menaquinone (Vitamin K<sub>2</sub>) biosynthetic pathway is absent in humans and might be an attractive target for anti-TB drug discovery**

Although latent *M. tuberculosis* are not replicating, they must presumably respire in order to survive. Compounds that target components of the mycobacterial respiratory chain thus have the potential to sterilize latent TB infections. Menaquinone is an essential component of the electron transport chain in *M. tuberculosis*. Hence the menaquinone biosynthetic pathway might be



an intriguing target for the development of antimycobacterial drugs against both replicating as well as non-replicating bacteria populations (61).

Menaquinone in the form of vitamin K<sub>2</sub> plays an important role in blood clotting for humans because it is involved as a cofactor in  $\gamma$ -carboxylation of glutamic acid residues in thrombin (62). However, humans lack the biosynthetic pathway for menaquinone and therefore this compound must be obtained in the diet or from intestinal bacteria. It is possible that the menaquinone biosynthesis pathway may be a novel drug target against TB for the following reasons, although humans require menaquinone (vitamin K<sub>2</sub>): first, menaquinone is the sole quinone in *M. tuberculosis*; and second, this pathway is absent in humans: humans obtain menaquinone either in their diet or from intestinal bacteria. The ideal hypothetical TB therapeutic would be one that inhibited menaquinone biosynthesis in *M. tuberculosis* but not in the intestinal bacteria that supply menaquinone for vitamin K<sub>2</sub>.

### Menaquinone biosynthetic pathway in *E. coli*

The biosynthesis of menaquinone has been most heavily studied in *E. coli* (63) and to a lesser extent in *B. subtilis* (64-66) and *Mycobacterium phlei* (67-76). The first six enzymes in the *E. coli* pathway are encoded by an operon (**Figure 1.7**), and the proposed biosynthetic pathway in *E. coli* is shown in **Figure 1.8**.

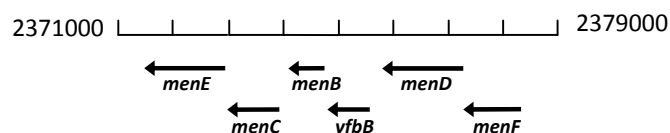


**Figure 1.7: The *men* operon in *E. coli***

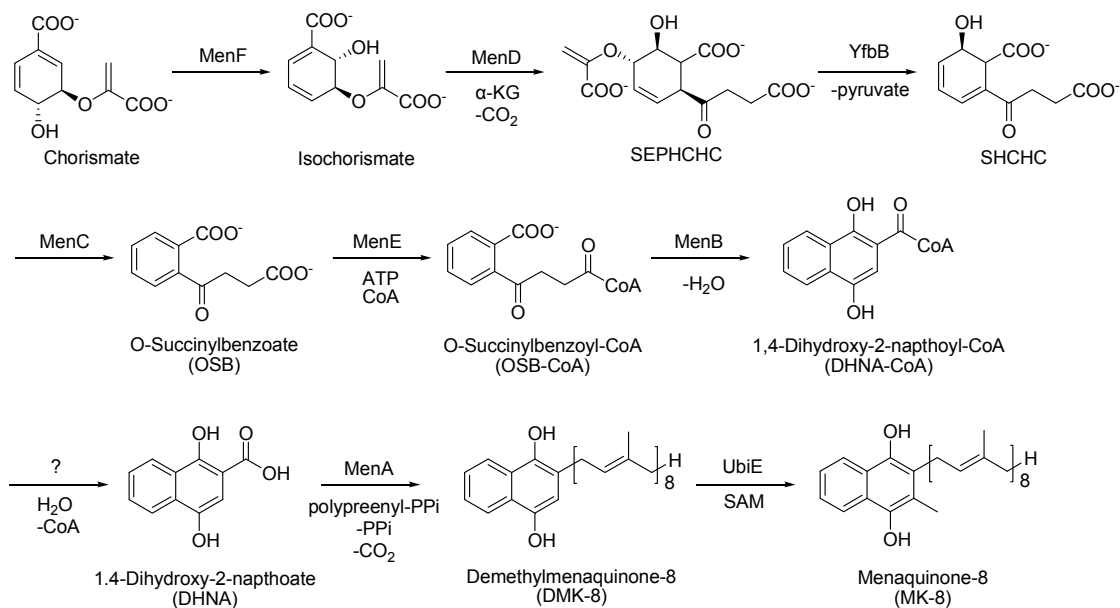


**Figure 1.8: Menaquinone biosynthetic pathway in *E. coli***

Chorismate, derived from the shikimate pathway, is converted into isochorismate catalyzed by MenF, an isochorismate synthase (77). The condensation of isochorismate with  $\alpha$ -ketoglutarate is catalyzed by MenD, and requires thiamine pyrophosphate (TPP) to form 2-succinyl-5-enolpyruvyl-6-hydroxy-3-cyclohexene-1-carboxylate (SEPHCHC) (78, 79). The transformation of SEPHCHC to 2-succinyl-6-hydroxy-2, 4-cyclohexadiene-1-carboxylate (SHCHC) requires an additional enzyme, YfbB (80, 81). SHCHC is dehydrated to the aromatic compound O-succinyl benzoic acid (OSB) by MenC (82). The activation of OSB to aliphatic mono-CoA thioester (OSB-CoA), catalyzed by MenE, requires the cofactor CoA and ATP (83). MenB catalyzes the cyclization reaction to form the naphthalenoid aromatic compound (DHNA-CoA) (84). After the DHNA-CoA is hydrolyzed to dihydroxynaphthoic acid (DHNA), MenA catalyzes the attachment of the prenyl side chain with the loss of a carboxyl

group(85). The last step of the pathway is methylation, catalyzed by UbiE, an S-adenosylmethionine (SAM)-dependent methyl transferase (86).

### **Menaquinone biosynthesis in *M. tuberculosis***

The *M. tuberculosis* genome contains homologs of all the *E. coli* men genes (**Table 1.4**) except the MenF and YfbB homologs. In *E. coli*, the key enzymes of the menaquinone pathway are organized into a distinct operon, while in *M. tuberculosis*, homologs of *menA*, *menB*, *menC*, *menD*, *menE*, and *menH* are clustered in one region of the genome (**Figure 1.9**).

**Table 1.4: Homologs of the *E. coli* menaquinone biosynthetic enzymes in *M. tuberculosis***

<i>E. coli</i> enzymes	Homologs in <i>M. tuberculosis</i>
ecMenD (P17109. 556 aa.) SEPHCHC synthase	Rv0555 (mtMenD); 556 aa. 30% identical / 43% similar over 503 aa.
ecMenC (P29208. 320 aa.) OSB synthase	Rv0553 (mtMenC); 321 aa. 29% identical / 46% similar over 181 aa.
ecMenE (P37353. 451 aa.) OSB-CoA synthase	Rv0542c (mtMenE); 451 aa. 29% identical / 47% similar over 275 aa.
ecMenB (P27290. 285 aa.) DHNA synthase	Rv0548c (mtMenB); 285 aa. 48% identical / 62% similar over 285 aa.
ecMenA (P32166. 308 aa.) DHNA prenyl transferase	Rv0534c (mtMenA); 292 aa. 36% identical / 51% similar over 271 aa.
ecUbiE (P0A887. 251 aa.) DMK methyl transferase	Rv0558 (mtMenH); 234 aa. 43% identical / 56% similar over 226 aa.

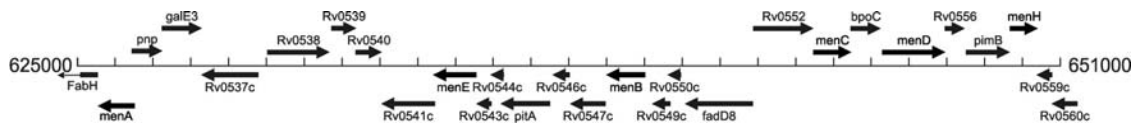


**Figure 1.9: Clustering of *men* gene homologs in *M. tuberculosis***

### **The alternative biosynthetic pathway is not present in *M. tuberculosis***

Menaquinone is an obligatory component of the electron-transfer pathway in some bacteria. However, there is no trace of *men* gene orthologs in the genome of *Streptomyces coelicolor* A3(2) (87-89), even though it produces menaquinones. Similarly, some pathogens that synthesize menaquinone, including *Helicobacter pylori* and *Campylobacter jejuni*, have also been reported to lack *men* gene homologs (90-93). Recent studies support the existence of an alternative biosynthetic pathway, the futasine pathway, in *S. coelicolor* A3(2) (**Figure 1.10**) (94, 95). However, there is no evidence for the presence of this alternate pathway in *M. tuberculosis*.

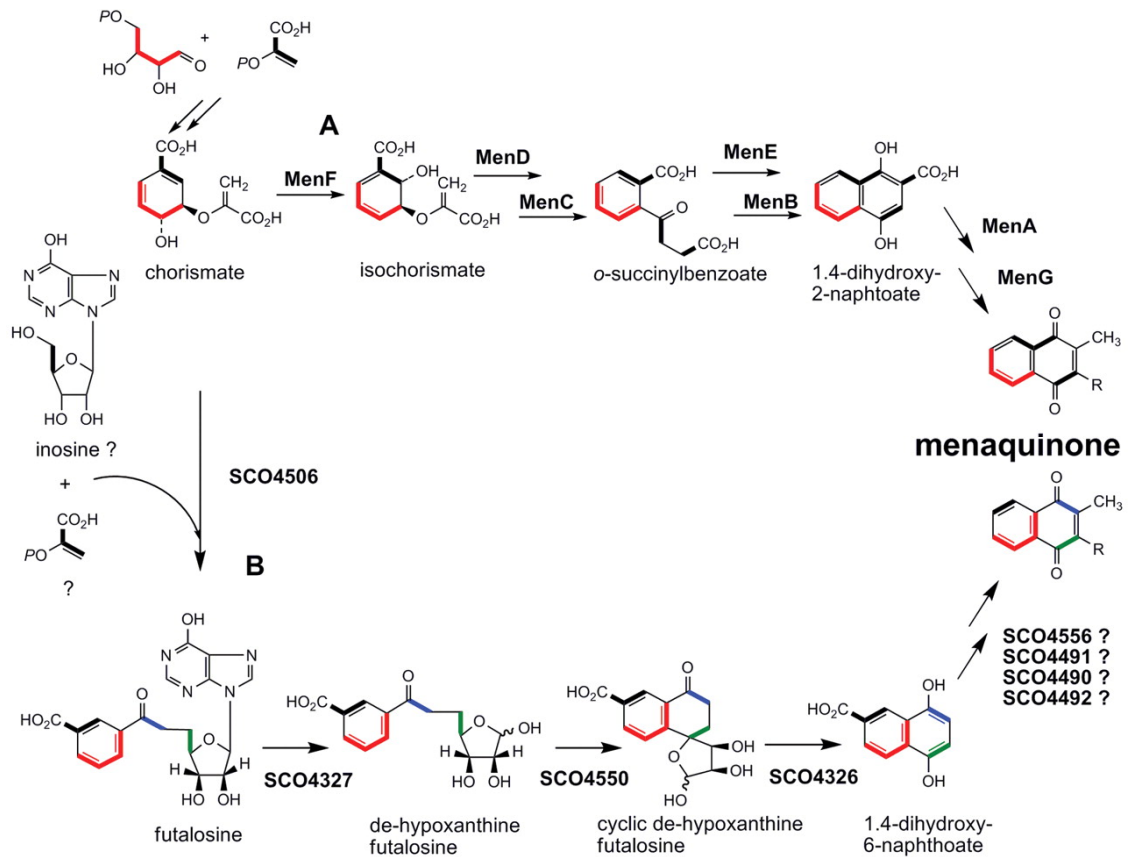


**Figure 1.10: Menaquinone biosynthetic pathway in *S. coelicolor* A3(2).** (A) Classical pathway in *E. coli*. Red and black bold lines show carbons originated from erythrose-4-phosphate and phosphoenolpyruvate, respectively. (B) Alternative pathway. Green and blue bold lines indicate two carbon units derived from C-5 and C-6 of glucose via different metabolic pathways. Based on the annotation of the open reading frames of *S. coelicolor* A3(2), SCO4491 (prenylation), SCO4556 (methylation), SCO4490 (decarboxylation), and SCO4492 (decarboxylation) (modified from (94)).

## Overview of my research

My research is mainly focused on the central portion in the menaquinone biosynthetic pathway in *M. tuberculosis*. The long term goal of our research is to completely understand the enzymes from the menaquinone biosynthetic pathway, to design and develop potent inhibitors targeting this pathway, and to validate this pathway as a target for the development of novel microbial chemotherapeutics.

MenB catalyzes the formation of a carbon-carbon bond through an intramolecular Claisen/Dieckmann condensation. In chapter 2, mechanistic studies of the reaction catalyzed by MenB will focus on comparing the mechanism of the *M. tuberculosis* MenB (mtMenB) enzyme with that of MenB from *E. coli* (ecMenB). We will address the following questions: what are the substrates for both enzymes, what is the functional role of D185 mtMenB which is not conserved in ecMenB, and can MenB catalyze the hydrolysis of DHNA-CoA?

In chapter 3, we will continue to discuss the mechanism of MenB reaction by contrasting with BadI, a member of the crotonase superfamily which catalyzes a retroDieckmann reaction. mtMenB shares 35% sequence identity with orthologs of BadI. The proposed catalytic roles for the residues in the active site of MenB are complementary to the roles proposed for the active-site residues of BadI. However, the usage of different stereochemistry by MenB and BadI provides us new understanding of MenB reaction mechanism.

The SAR studies on MenB inhibitors are based on the two types of leads (2-amino-4-oxo-phenylbutanoic acids and benzoxazinones) identified from high throughput screening, which will be discussed in chapter 4. In chapter 5, a series of 5'-O-(*N*-acylsulfamoyl) adenosines (acyl-AMS) and related compounds which inhibit MenE by mimicking tightly-bound OSB-AMP intermediates will be introduced. Information obtained from these studies will help us to evaluate the importance of MenB or MenE in menaquinone biosynthesis, and to design better inhibitors for the development of novel microbial antibiotics.

## References

1. World Health Organization (WHO) REPORT 2008: Global Tuberculosis Control.
2. Bloom, B. R., and Murray, C. J. (1992) Tuberculosis: commentary on a reemergent killer, *Science*. 257, 1055-1064.
3. Kochi, A. (1991) The global tuberculosis situation and the new control strategy of the World Health Organization, *Tubercle* 72, 1-6.
4. Kumar, V., Abbas, A. K., Fausto, N., and Mitchell, R. N., (Eds.) (2007) *Robbins Basic Pathology (8th ed.)*, Saunders Elsevier.
5. Rothschild, B. M., Martin, L. D., Lev, G., Bercovier, H., Bar-Gal, G. K., Greenblatt, C., Donoghue, H., Spigelman, M., and Brittain, D. (2001) Mycobacterium tuberculosis complex DNA from an extinct bison dated 17,000 years before the present, *Clin Infect Dis* 33, 305-311.
6. Zink, A. R., Sola, C., Reischl, U., Grabner, W., Rastogi, N., Wolf, H., and Nerlich, A. G. (2003) Characterization of Mycobacterium tuberculosis complex DNAs from Egyptian mummies by spoligotyping, *J Clin Microbiol* 41, 359-367.
7. Pearce-Duvel, J. M. (2006) The origin of human pathogens: evaluating the role of agriculture and domestic animals in the evolution of human disease, *Biol Rev Camb Philos Soc* 81, 369-382.
8. Cox, R. A. (2004) Quantitative relationships for specific growth rates and macromolecular compositions of Mycobacterium tuberculosis,



- Streptomyces coelicolor A3(2) and Escherichia coli B/r: an integrative theoretical approach, *Microbiology (Reading, England)* 150, 1413-1426.
9. Madison, B. M. (2001) Application of stains in clinical microbiology, *Biotech Histochem* 76, 119-125.
  10. Ryan, K. J., and Ray, C. G., (Eds.) (2004) *Sherris Medical Microbiology (4th ed.)*, McGraw Hill.
  11. Finlay, B. B., and Falkow, S. (1997) Common themes in microbial pathogenicity revisited, *Microbiol Mol Biol Rev* 61, 136-169.
  12. Cole, E. C., and Cook, C. E. (1998) Characterization of infectious aerosols in health care facilities: an aid to effective engineering controls and preventive strategies, *Am J Infect Control* 26, 453-464.
  13. Nicas, M., Nazaroff, W. W., and Hubbard, A. (2005) Toward understanding the risk of secondary airborne infection: emission of respirable pathogens, *J Occup Environ Hyg* 2, 143-154.
  14. (December 2004) World Health Organization Disease Watch: Focus: Tuberculosis.
  15. (March 2006) Tuberculosis Fact sheet N°104 - Global and regional incidence, World Health Organization (WHO).
  16. (2000) *Core Curriculum on Tuberculosis: What the Clinician Should Know (4th edition)*, Centers for Disease Control and Prevention (CDC), Division of Tuberculosis Elimination.

17. Bonah, C. (2005) The 'experimental stable' of the BCG vaccine: safety, efficacy, proof, and standards, 1921-1933, *Stud Hist Philos Biol Biomed Sci* 36, 696-721.
18. Comstock, G. W. (1994) The International Tuberculosis Campaign: a pioneering venture in mass vaccination and research, *Clin Infect Dis* 19, 528-540.
19. Pfuetze, K. H., Pyle, M. M., Hinshaw, H. C., and Feldman, W. H. (1955) The first clinical trial of streptomycin in human tuberculosis, *Am Rev Tuberc* 71, 752-754.
20. Medical\_Research\_Council. (1948) Streptomycin treatment of pulmonary tuberculosis, *BMJ* 2, 769-782.
21. Medical\_Research\_Council. (1952) The prevention of streptomycin resistance by combined chemotherapy, *BMJ*, 1157-1162.
22. (1952) ISONIAZID in pulmonary tuberculosis, *Lancet* 2, 19-21.
23. (1953) Second report to the Medical Research Council by their Tuberculosis Chemotherapy Trials Committee. Isoniazid in the treatment of pulmonary tuberculosis, *BMJ* 71 (4809), 521-536.
24. (1955) Seventh report to the Medical Research Council by their Tuberculosis Chemotherapy Trials Committee. Various combinations of isoniazid with streptomycin or with PAS in the treatment of pulmonary tuberculosis, *BMJ* 4911, 435-445.
25. Covacev, L., and Monzali, G. (1966) [Rifamycin SV in the therapy of tuberculosis], *Clin Ter* 39, 547-566.

26. Lucchesi, M., Pallotta, G., Rossi, P., and Sbampato, M. (1967) [The therapeutic action of Rifampicin, a derivative of 3-(4-methyl-1-piperazinyl-iminomethyl)-rifamycin SV, in pulmonary tuberculosis], *Ann Ist Carlo Forlanini* 27, 199-227.
27. Nitti, V., Catena, E., Bariffi, F., and Delli Veneri, F. (1967) [Therapeutic activity of the Rifampicin in pulmonary tuberculosis], *Arch Tisiol Mal Appar Respir* 22, 417-462.
28. Onyebujoh, P., Zumla, A., Ribeiro, I., Rustomjee, R., Mwaba, P., Gomes, M., and Grange, J. M. (2005) Treatment of tuberculosis: present status and future prospects, *Bull World Health Organ* 83, 857-865.
29. Mitchison, D. A. (2005) Shortening the treatment of tuberculosis, *Nat Biotechnol* 23, 187-188.
30. Zhang, Y., and Amzel, L. M. (2002) Tuberculosis drug targets, *Curr Drug Targets* 3, 131-154.
31. Zhang, Y. (2005) The magic bullets and tuberculosis drug targets, *Annu Rev Pharmacol Toxicol* 45, 529-564.
32. Schroeder, E. K., de Souza, N., Santos, D. S., Blanchard, J. S., and Basso, L. A. (2002) Drugs that inhibit mycolic acid biosynthesis in *Mycobacterium tuberculosis*, *Curr Pharm Biotechnol* 3, 197-225.
33. Janin, Y. L. (2007) Antituberculosis drugs: ten years of research, *Bioorg Med Chem* 15, 2479-2513.
34. (1998) Prevention and treatment of tuberculosis among patients infected with human immunodeficiency virus: principles of therapy and revised

recommendations, in *MMWR Recomm Rep.*, pp 1-58, Centres for Disease Control and Prevention.

35. Geneva\_World\_Health\_Organization. (2006) Guidelines for the programmatic management of drug-resistant tuberculosis., *HTM/TB*, 361.
36. Sander, P., De Rossi, E., Boddinhaus, B., Cantoni, R., Branzoni, M., Bottger, E. C., Takiff, H., Rodriguez, R., Lopez, G., and Riccardi, G. (2000) Contribution of the multidrug efflux pump LfrA to innate mycobacterial drug resistance, *FEMS microbiology letters* 193, 19-23.
37. De Rossi, E., Branzoni, M., Cantoni, R., Milano, A., Riccardi, G., and Ciferri, O. (1998) mmr, a Mycobacterium tuberculosis gene conferring resistance to small cationic dyes and inhibitors, *Journal of bacteriology* 180, 6068-6071.
38. Ainsa, J. A., Blokpoel, M. C., Otal, I., Young, D. B., De Smet, K. A., and Martin, C. (1998) Molecular cloning and characterization of Tap, a putative multidrug efflux pump present in Mycobacterium fortuitum and Mycobacterium tuberculosis, *Journal of bacteriology* 180, 5836-5843.
39. Saltini, C. (2006) Chemotherapy and diagnosis of tuberculosis, *Respir Med* 100, 2085-2097.
40. Mitchison, D. A., and Nunn, A. J. (1986) Influence of initial drug resistance on the response to short-course chemotherapy of pulmonary tuberculosis, *Am Rev Respir Dis* 133, 423-430.
41. Shah, N. S., Wright, A., Bai, G. H., Barrera, L., Boulahbal, F., Martin-Casabona, N., Drobniowski, F., Gilpin, C., Havelkova, M., Lepe, R., Lumb,

- R., Metchock, B., Portaels, F., Rodrigues, M. F., Rusch-Gerdes, S., Van Deun, A., Vincent, V., Laserson, K., Wells, C., and Cegielski, J. P. (2007) Worldwide emergence of extensively drug-resistant tuberculosis, *Emerg Infect Dis* 13, 380-387.
42. Parrish, N. M., Dick, J. D., and Bishai, W. R. (1998) Mechanisms of latency in Mycobacterium tuberculosis, *Trends Microbiol* 6, 107-112.
43. Houben, E. N., Nguyen, L., and Pieters, J. (2006) Interaction of pathogenic mycobacteria with the host immune system, *Curr Opin Microbiol* 9, 76-85.
44. Herrmann, J. L., and Lagrange, P. H. (2005) Dendritic cells and Mycobacterium tuberculosis: which is the Trojan horse?, *Pathol Biol (Paris)* 53, 35-40.
45. Agarwal, R., Malhotra, P., Awasthi, A., Kakkar, N., and Gupta, D. (2005) Tuberculous dilated cardiomyopathy: an under-recognized entity?, *BMC Infect Dis* 5, 29.
46. Kaufmann, S. H. (2002) Protection against tuberculosis: cytokines, T cells, and macrophages, *Ann Rheum Dis* 61 Suppl 2, ii54-58.
47. Jozefowski, S., Sobota, A., and Kwiatkowska, K. (2008) How Mycobacterium tuberculosis subverts host immune responses, *Bioessays* 30, 943-954.
48. Wayne, L. G., and Hayes, L. G. (1996) An in vitro model for sequential study of shutdown of Mycobacterium tuberculosis through two stages of nonreplicating persistence, *Infection and immunity* 64, 2062-2069.

49. Lim, A., Eleuterio, M., Hutter, B., Murugasu-Oei, B., and Dick, T. (1999) Oxygen depletion-induced dormancy in *Mycobacterium bovis* BCG, *Journal of bacteriology* 181, 2252-2256.
50. Wayne, L. G., and Sohaskey, C. D. (2001) Nonreplicating persistence of *mycobacterium tuberculosis*, *Annu Rev Microbiol* 55, 139-163.
51. Boshoff, H. I., and Barry, C. E., 3rd. (2005) Tuberculosis - metabolism and respiration in the absence of growth, *Nat Rev Microbiol* 3, 70-80.
52. Dick, T. (2001) Dormant tubercle bacilli: the key to more effective TB chemotherapy?, *J Antimicrob Chemother* 47, 117-118.
53. Wayne, L. G., and Sramek, H. A. (1994) Metronidazole is bactericidal to dormant cells of *Mycobacterium tuberculosis*, *Antimicrobial agents and chemotherapy* 38, 2054-2058.
54. Wayne, L. G. (1994) Dormancy of *Mycobacterium tuberculosis* and latency of disease, *Eur J Clin Microbiol Infect Dis* 13, 908-914.
55. Stover, C. K., Warrener, P., VanDevanter, D. R., Sherman, D. R., Arain, T. M., Langhorne, M. H., Anderson, S. W., Towell, J. A., Yuan, Y., McMurray, D. N., Kreiswirth, B. N., Barry, C. E., and Baker, W. R. (2000) A small-molecule nitroimidazopyran drug candidate for the treatment of tuberculosis, *Nature* 405, 962-966.
56. Barry, C. E., 3rd, Lee, R. E., Mdluli, K., Sampson, A. E., Schroeder, B. G., Slayden, R. A., and Yuan, Y. (1998) Mycolic acids: structure, biosynthesis and physiological functions, *Prog Lipid Res* 37, 143-179.

57. Boshoff, H. I., Myers, T. G., Copp, B. R., McNeil, M. R., Wilson, M. A., and Barry, C. E., 3rd. (2004) The transcriptional responses of *Mycobacterium tuberculosis* to inhibitors of metabolism: novel insights into drug mechanisms of action, *The Journal of biological chemistry* 279, 40174-40184.
58. Weinstein, E. A., Yano, T., Li, L. S., Avarbock, D., Avarbock, A., Helm, D., McColm, A. A., Duncan, K., Lonsdale, J. T., and Rubin, H. (2005) Inhibitors of type II NADH:menaquinone oxidoreductase represent a class of antitubercular drugs, *Proceedings of the National Academy of Sciences of the United States of America* 102, 4548-4553.
59. Lester, R. L., and Crane, F. L. (1959) The natural occurrence of coenzyme Q and related compounds, *The Journal of biological chemistry* 234, 2169-2175.
60. Bishop, D. H., Pandya, K. P., and King, H. K. (1962) Ubiquinone and vitamin K in bacteria, *Biochem J* 83, 606-614.
61. Rao, S. P. S., Alonso, S., Rand, L., Dick, T., and Pethe, K. (2008) The protonmotive force is required for maintaining ATP homeostasis and viability of hypoxic, nonreplicating *Mycobacterium tuberculosis*, *Proceedings of the National Academy of Sciences of the United States of America* 105, 11945-11950.
62. Dowd, P., Ham, S. W., Naganathan, S., and Hershline, R. (1995) The mechanism of action of vitamin K, *Annu Rev Nutr* 15, 419-440.

63. Meganathan, R. (2001) Biosynthesis of menaquinone (vitamin K2) and ubiquinone (coenzyme Q): a perspective on enzymatic mechanisms, *Vitamins and hormones* 61, 173-218.
64. Rowland, B., Hill, K., Miller, P., Driscoll, J., and Taber, H. (1995) Structural organization of a *Bacillus subtilis* operon encoding menaquinone biosynthetic enzymes, *Gene* 167, 105-109.
65. Rowland, B. M., Grossman, T. H., Osburne, M. S., and Taber, H. W. (1996) Sequence and genetic organization of a *Bacillus subtilis* operon encoding 2,3-dihydroxybenzoate biosynthetic enzymes, *Gene* 178, 119-123.
66. Rowland, B. M., and Taber, H. W. (1996) Duplicate isochorismate synthase genes of *Bacillus subtilis*: regulation and involvement in the biosyntheses of menaquinone and 2,3-dihydroxybenzoate, *Journal of bacteriology* 178, 854-861.
67. Azerad, R., Bleiler-Hill, R., Catala, F., Samuel, O., and Lederer, E. (1967) Biosynthesis of dihydromenaquinone-9 by *Mycobacterium phlei*, *Biochem Biophys Res Commun* 27, 253-257.
68. Catala, F., Azerad, R., and Lederer, E. (1970) [Properties of demethylmenaquinone C-methylase from *Mycobacterium phlei*], *Int Z Vitaminforsch* 40, 363-373.
69. Dansette, P., and Azerad, R. (1970) A new intermediate in naphthoquinone and menaquinone biosynthesis, *Biochem Biophys Res Commun* 40, 1090-1095.



70. Leduc, M. M., Dansette, P. M., and Azerad, R. G. (1970) [Incorporation of shikimic acid into the ring of bacterial and plant naphthoquinones], *Eur J Biochem* 15, 428-435.
71. McGovern, E. P., and Bentley, R. (1978) Isolation and properties of naphthoate synthetase from *Mycobacterium phlei*, *Arch Biochem Biophys* 188, 56-63.
72. Meganathan, R., and Bentley, R. (1979) Menaquinone (vitamin K2) biosynthesis: conversion of o-succinylbenzoic acid to 1,4-dihydroxy-2-naphthoic acid by *Mycobacterium phlei* enzymes, *Journal of bacteriology* 140, 92-98.
73. Meganathan, R., Folger, T., and Bentley, R. (1980) Conversion of o-succinylbenzoate to dihydroxynaphthoate by extracts of *Micrococcus luteus*, *Biochemistry* 19, 785-789.
74. Meganathan, R., Bentley, R., and Taber, H. (1981) Identification of *Bacillus subtilis* men mutants which lack O-succinylbenzoyl-coenzyme A synthetase and dihydroxynaphthoate synthase, *Journal of bacteriology* 145, 328-332.
75. Heide, L., Arendt, S., and Leistner, E. (1982) Enzymatic synthesis, characterization, and metabolism of the coenzyme A ester of o-succinylbenzoic acid, an intermediate in menaquinone (vitamin K2) biosynthesis, *The Journal of biological chemistry* 257, 7396-7400.
76. Igbavboa, U., and Leistner, E. (1990) Sequence of proton abstraction and stereochemistry of the reaction catalyzed by naphthoate synthase, an

- enzyme involved in menaquinone (vitamin K<sub>2</sub>) biosynthesis, *Eur J Biochem* 192, 441-449.
77. Daruwala, R., Kwon, O., Meganathan, R., and Hudspeth, M. E. (1996) A new isochorismate synthase specifically involved in menaquinone (vitamin K<sub>2</sub>) biosynthesis encoded by the menF gene, *FEMS microbiology letters* 140, 159-163.
78. Meganathan, R., and Bentley, R. (1983) Thiamine pyrophosphate requirement for o-succinylbenzoic acid synthesis in Escherichia coli and evidence for an intermediate, *Journal of bacteriology* 153, 739-746.
79. Palaniappan, C., Sharma, V., Hudspeth, M. E., and Meganathan, R. (1992) Menaquinone (vitamin K<sub>2</sub>) biosynthesis: evidence that the Escherichia coli menD gene encodes both 2-succinyl-6-hydroxy-2,4-cyclohexadiene-1-carboxylic acid synthase and alpha-ketoglutarate decarboxylase activities, *Journal of bacteriology* 174, 8111-8118.
80. Jiang, M., Cao, Y., Guo, Z. F., Chen, M., Chen, X., and Guo, Z. (2007) Menaquinone biosynthesis in Escherichia coli: identification of 2-succinyl-5-enolpyruvyl-6-hydroxy-3-cyclohexene-1-carboxylate as a novel intermediate and re-evaluation of MenD activity, *Biochemistry* 46, 10979-10989.
81. Jiang, M., Chen, X., Guo, Z. F., Cao, Y., Chen, M., and Guo, Z. (2008) Identification and characterization of (1R,6R)-2-succinyl-6-hydroxy-2,4-cyclohexadiene-1-carboxylate synthase in the menaquinone biosynthesis of Escherichia coli, *Biochemistry* 47, 3426-3434.

82. Sharma, V., Meganathan, R., and Hudspeth, M. E. (1993) Menaquinone (vitamin K2) biosynthesis: cloning, nucleotide sequence, and expression of the menC gene from *Escherichia coli*, *Journal of bacteriology* 175, 4917-4921.
83. Sharma, V., Hudspeth, M. E., and Meganathan, R. (1996) Menaquinone (vitamin K2) biosynthesis: localization and characterization of the menE gene from *Escherichia coli*, *Gene* 168, 43-48.
84. Truglio, J. J., Theis, K., Feng, Y., Gajda, R., Machutta, C., Tonge, P. J., and Kisker, C. (2003) Crystal structure of *Mycobacterium tuberculosis* MenB, a key enzyme in vitamin K2 biosynthesis, *The Journal of biological chemistry* 278, 42352-42360.
85. Suvarna, K., Stevenson, D., Meganathan, R., and Hudspeth, M. E. (1998) Menaquinone (vitamin K2) biosynthesis: localization and characterization of the menA gene from *Escherichia coli*, *Journal of bacteriology* 180, 2782-2787.
86. Lee, P. T., Hsu, A. Y., Ha, H. T., and Clarke, C. F. (1997) A C-methyltransferase involved in both ubiquinone and menaquinone biosynthesis: isolation and identification of the *Escherichia coli* ubiE gene, *Journal of bacteriology* 179, 1748-1754.
87. Bentley, S. D., Chater, K. F., Cerdeno-Tarraga, A. M., Challis, G. L., Thomson, N. R., James, K. D., Harris, D. E., Quail, M. A., Kieser, H., Harper, D., Bateman, A., Brown, S., Chandra, G., Chen, C. W., Collins, M., Cronin, A., Fraser, A., Goble, A., Hidalgo, J., Hornsby, T., Howarth, S.,

- Huang, C. H., Kieser, T., Larke, L., Murphy, L., Oliver, K., O'Neil, S., Rabbinowitsch, E., Rajandream, M. A., Rutherford, K., Rutter, S., Seeger, K., Saunders, D., Sharp, S., Squares, R., Squares, S., Taylor, K., Warren, T., Wietzorrek, A., Woodward, J., Barrell, B. G., Parkhill, J., and Hopwood, D. A. (2002) Complete genome sequence of the model actinomycete *Streptomyces coelicolor* A3(2), *Nature* 417, 141-147.
88. Borodina, I., Krabben, P., and Nielsen, J. (2005) Genome-scale analysis of *Streptomyces coelicolor* A3(2) metabolism, *Genome Res* 15, 820-829.
89. Collins, M. D., Pirouz, T., Goodfellow, M., and Minnikin, D. E. (1977) Distribution of menaquinones in actinomycetes and corynebacteria, *J Gen Microbiol* 100, 221-230.
90. Tomb, J. F., White, O., Kerlavage, A. R., Clayton, R. A., Sutton, G. G., Fleischmann, R. D., Ketchum, K. A., Klenk, H. P., Gill, S., Dougherty, B. A., Nelson, K., Quackenbush, J., Zhou, L., Kirkness, E. F., Peterson, S., Loftus, B., Richardson, D., Dodson, R., Khalak, H. G., Glodek, A., McKenney, K., Fitzegerald, L. M., Lee, N., Adams, M. D., Hickey, E. K., Berg, D. E., Gocayne, J. D., Utterback, T. R., Peterson, J. D., Kelley, J. M., Cotton, M. D., Weidman, J. M., Fujii, C., Bowman, C., Watthey, L., Wallin, E., Hayes, W. S., Borodovsky, M., Karp, P. D., Smith, H. O., Fraser, C. M., and Venter, J. C. (1997) The complete genome sequence of the gastric pathogen *Helicobacter pylori*, *Nature* 388, 539-547.
91. Parkhill, J., Wren, B. W., Mungall, K., Ketley, J. M., Churcher, C., Basham, D., Chillingworth, T., Davies, R. M., Feltwell, T., Holroyd, S., Jagels, K.,

- Karlyshev, A. V., Moule, S., Pallen, M. J., Penn, C. W., Quail, M. A., Rajandream, M. A., Rutherford, K. M., van Vliet, A. H., Whitehead, S., and Barrell, B. G. (2000) The genome sequence of the food-borne pathogen *Campylobacter jejuni* reveals hypervariable sequences, *Nature* *403*, 665-668.
92. Marcelli, S. W., Chang, H. T., Chapman, T., Chalk, P. A., Miles, R. J., and Poole, R. K. (1996) The respiratory chain of *Helicobacter pylori*: identification of cytochromes and the effects of oxygen on cytochrome and menaquinone levels, *FEMS microbiology letters* *138*, 59-64.
93. Moss, C. W., Lambert-Fair, M. A., Nicholson, M. A., and Guerrant, G. O. (1990) Isoprenoid quinones of *Campylobacter cryaerophila*, *C. cinaedi*, *C. fennelliae*, *C. hyointestinalis*, *C. pylori*, and "*C. upsaliensis*", *J Clin Microbiol* *28*, 395-397.
94. Hiratsuka, T., Furihata, K., Ishikawa, J., Yamashita, H., Itoh, N., Seto, H., and Dairi, T. (2008) An alternative menaquinone biosynthetic pathway operating in microorganisms, *Science (New York, N.Y)* *321*, 1670-1673.
95. Seto, H., Jinnai, Y., Hiratsuka, T., Fukawa, M., Furihata, K., Itoh, N., and Dairi, T. (2008) Studies on a new biosynthetic pathway for menaquinone, *J Am Chem Soc* *130*, 5614-5615.

## CHAPTER 2: MECHANISM OF REACTION CATALYZED BY 1, 4-DIHYDROXY-2-NAPHTHOYL-COA SYNTHASE FROM *M. TUBERCULOSIS* (MTMENB)

### Background

#### *Introduction of crotonase superfamily*

1, 4-Dihydroxy-2-naphthoyl-CoA synthase (MenB) belongs to the crotonase superfamily. Members of this family catalyze mechanistically diverse reactions and share sequence identities ranging from 15 to 45%. It has been proposed that the crotonase superfamily has evolved by divergent evolution from a common ancestor: the oxyanion hole has been retained for the stabilization of enolate anion intermediates, while the new residues have been selected to alter the substrate specificity and the catalyzed chemistry (1-4). The oxyanion hole is composed of two halves in which an amide proton forms a hydrogen bond with oxyanion intermediate. The first half is formed by sequence motif FXXGXD, with the second-to-last residue in the sequence contributing its amide proton. The second half is formed by the sequence motif GXG (normally GGG), with the second residue contributing its amide (**Figure 2.1**).

The diversity of the catalytic residues correlates with the diversity of the reactions they catalyze (**Figure 2.1 and 2.2**). Many enzymes in this superfamily catalyze the hydration of 2-enoyl-CoA thioesters and the isomerization of double bonds. Other reactions catalyzed by crotonase superfamily members include decarboxylation, thioester hydrolysis, dehalogenation, Dieckmann condensation, reverse Dieckmann condensation and reverse aldol condensation. The

1 crotonase rat-----GANFQYIITEKKGKNSVGLIQLNRPKALNA 31  
2 MGCH Human -----SSEMKTEDELVRHLEENRGIVVVLGINRAYGKNS 35  
3 BadI *R.pal* -----MQFEDLIY--EIRNGVAWIIINRPDKMNA 27  
4 MenB *M.tub* VVAPAGEQGRSSTALSNDNPFDAKAWRLVDGFDDLTIDITYHRHVDDATVRFVAFNRPEVRNA 60  
5 MMCD *E.coli* -----MSYQYVNVVTINKVAVIEFNYGRKLNA 27  
6 DCI rat -----AYESIQVTSAQKHVLHVQLNRPEKRNA 27  
7 CarB *P.car* -----MVFEENSDEVRVITLDHPNKHNP 23  
8 CBD *Ps.sp.* -----MYEAIGHRVEDGVAEITIKLPRHRNA 26  
9 FHL *P.flu* -----MSTYEGRWKTVKVEIEDGIAFVILNRPEKRNA 32  
10 HICH Human -----MTDAAEEVLLGKKGCTGVITLNRPKFLNA 29  
11 OCH *R.sp.* -----MKQLATPFQEYSQKYENIRLERDGGVLLVTVHTEGKSLV 39  
12 ECI Yeast -----MSQEIRQNEKISYRIEGPFFIIHLINPDNLNA 32

1 crotonase LCNGLIEELNQALETFEEDPAVGAIVLTG-----GEK-A**FAAGAD**IKEMQNRTFQDC-- 82  
2 MGCH Human LSKNLIKMLSKAVDALKSDKKVRTIIIRS-----EVPGI**FCAGAD**LKERAKMSSEVGP 89  
3 BadI *R.pal* FRGTTCCDELIKALYKAGYDKDVGAIVLAG-----AGDRA**FCTGGD**QSTHDGN---YDGR 78  
4 MenB *M.tub* FRPHTVDELYRVLDHARMSPDVGVVLLTGNPSPKDGGA**FCSGGD**QIRIRGRSGYQYASG 120  
5 MMCD *E.coli* LSKVFIDDLMQALSDDLNRPEIRCIILRAP-----SGSKV**FSAGHD**IHELPSGGRDPLS- 80  
6 DCI rat MNRAFWRELVECFQKISKSDSDCRAVVVSG-----AGKM**FTSGID**LMDMASDILQPPGD 80  
7 CarB *P.car* FSRTLETSVKDALARANADDSVRAVVVYG-----GAERS**FSAGGD**FNEVKQLSRSEDIE 77  
8 CBD *Ps.sp.* LSVKAMQEVTDALNRAEEDDSVGAVMITG-----AEDA**FCAGFY**LREIPLDKGVAGVR 79  
9 FHL *P.flu* MSPTLNREMIDVLETLEQDPAAGVLVLTG-----AGEA**WTAGMD**LKEYFREVDAGPEI 85  
10 HICH Human LTLNMIHQIYQQLKQWEQDPETFLIIIKG-----AGGKA**FCAGGD**IRVISEAEKAKQKI 83  
11 OCH *R.sp.* WTSTAHDDELAYCFHDIACDRENKVVILTG-----TGPS**FCNEID**FTSFNLGTPHDWDE 92  
12 ECI Yeast LEGEDYIYLGELLELADRNRDVYFTIIQS-----SGRF**FSSGAD**FKGIAKAQGDDTNK 85

1 crotonase -----YSGKFLSHWDHITRIKKPVIAAVNGYAL**GGGC****E**LAMMCDIYAG-EKAQ 130  
2 MGCH Human -----FVSKIRAVINDIANLPVPTIAAIDGLAL**GGGL****E**LALACDIRVAA-SSAK 137  
3 BadI *R.pal* GTVG-----LPMEELHTAIRDVPKPVIAVQGYAI**GGGN**VLATIICDLTICS-EKAI 128  
4 MenB *M.tub* DTADTVDVARAGRLHILEVQRLIRFMPKVVICLVNGWAA**GGG**HSLHVCDLTLASREYAR 180  
5 MMCD *E.coli* -----YDDPLRQITRMIQKFPKPIISMVEGSVW**GGAF**FEMIMSSDLIIAA-STST 128  
6 DCI rat DVARIAWYLRDLISRYQKFTFTVIEKCPKPVIAAIHGGCI**GGGV****D**LISACDIRYCT-QDAF 139  
7 CarB *P.car* E-----WIDRVIDLYQAVLNVNKPTIAAVDGYAI**GMGF**QFALMFDQRLMA-STAN 126  
8 CBD *Ps.sp.* DHFR-----IAALW**H**QMIHKIIRVKRPVLAINGVAA**GGGL**GISLASDMAICA-DSAK 132  
9 FHL *P.flu* LQEK-----IRREASQWQWKLRLMYAKPTIAMVNGWCF**GGGF**SPLVACDLAICA-DEAT 138  
10 HICH Human AP-----VFFREEYMLNNAVGSQKPYVALIHGITM**GGGV**GLSVHGQFRVAT-EKCL 134  
11 OCH *R.sp.* IIFE-----GQRLNLLSIEVPVIAAVNG-PV**TNAPEI**PVMSDIVLAAESATF 140  
12 ECI Yeast YPSETSKWVSNFVARNVYVTDFAFIKHSKVLICCLNGPAI**GLS**AALVALCDIVYSINDKVY 145

```

1 crotonase      FGQPEILLGTIPGAGGTQRLTRAVG-KSLAMEMVLTGDRISAQDAKQAGLVSKIFP---- 185
2 MGCH Human    MGLVETKLAIIPGGGGTQRLPRAIG-MSLAKELIFSARVLDGKEAKAVGLISHVLEQNQE 196
3 BadI R.pal     FGQVGPKMGSVDPGYGTAFLARVVG-EKKAREIWYMCKRYSGKEAEAMGLANLCVP---- 183
4 MenB M.tub    FKQTDADVGSFDGGYGSAYLARQVG-QKFAREIFFLGRTYTAEQMHQMGAVNAVAE---- 235
5 MMCD E.coli    FSMPVNLGVPYNLVGIHNLTRDAG-FHIVKELIFTASPITAQRALAVGILNHVVE---- 183
6 DCI rat        FQKEVDVGLAADVGTLQRLPKVIGNRSLVNELTFTARKMMADEALDSGLVSRVFP---D 196
7 CarB P.car     FVMPELKHGIG-CSVGAAILGFTHG-FSTMQEIIYQCSLDAPRCVDYRLVNQVVES--- 181
8 CBD Ps.sp.     FVCAEHTIGIGNDTATSSYSLARIVG-MRRAMELMLTNRTLYPEEAKDWGLVSRVP---- 187
9 FHL P.flu      FGLSEINWGIPPGNLVSKAMADTVG-HRFSLYYIMTGKTFGGQKAAEMGLVNSVP---- 193
10 HICH Human    FAMPETAIGLFPDVGGYFLPRLQG--KLGYFLALTGFRLKGRDVYRAGIATHFVDS-EK 191
11 OCH R.sp.     QDGPHFPSGIVPDGAHVVWPHVLG-SNRGRYFLLTGQELDARTALDGAVNEVLS---- 195
12 ECI Yeast     LLYPFANLGLITEGGTTVSLPLKFG-TNTTYECLMFNKPFKYDIMCENGFISKNFNMP-- 202

1 crotonase      VETLVEEAIQCAEKIANNSKIIVAMAKESVNAAFEMTLTEGNKLE--KKLFYSTFATDDR 243
2 MGCH Human    GDAARKALDLAREFLPOGPVAMRVAKLAINQGMEVDLVTGLAIE--EACYAQTIPTKDR 254
3 BadI R.pal     HDELDAEVQKWGEELCERSPTALAIAKRSFN-MDTAHQAGIAGMG--MYALKLYDTDES 240
4 MenB M.tub    HAELETVGLQWAAEINAKSPQAQRMLKFAFN-LLDDGLVGQQLFA--GEATRLAVMTDEA 292
5 MMCD E.coli    VEELEDFTLQMAHHISEKAPLAIAVIKEELRVLGEAHTMNSDEFERIQGMRRAVDSEDY 243
6 DCI rat        KDVMLNAAFALAADISSKSP--VAVQGSKINLIYSRDHSVDESLDYMATWNMSMLQTQDI 254
7 CarB P.car     -SALLDAAITQAHVMASYEPASAFINTKRAVNKPFIHLLEQTRDAS--KAVHKAAFQARDA 238
8 CBD Ps.sp.     KDEFREVAWKVARELAAAPTHLQVMAKERFHAGWMQPVEECTEFE--IQNVIASVTHPHF 245
9 FHL P.flu      LAQLREVTIELARNLLEKNPVVLRAAKHGFKRCRELTWEQNEDYLYAKLDQSRLLDTEGG 253
10 HICH Human    LAMLEEDLLALKSPSKENIASVLENYHTESKIDRDKSFILEEHMDKINSCFSANTVEEII 251
11 OCH R.sp.     EQELLPRAWELARGIAEKPLLARRYARKVLTRQLRRVMEADLSLGLAHEALAIDLGMES 255
12 ECI Yeast     SSNAEAFNAKVLEELREKVKGLYLPSCLGMKLLKSNHIDAFNKANSVEVNSLKYWVDG 262

```

**Figure 2.1: Sequence alignment of characterized crotonase superfamily members.**

Residues of the oxyanion hole are in blue, with the hydrogen bond donating residues marked with diamonds. Characterized catalytic residues are in red; putative and uncharacterized active-site residues are in gray. The cyan residues mark the start of the C-terminal domain in structurally characterized enzymes.



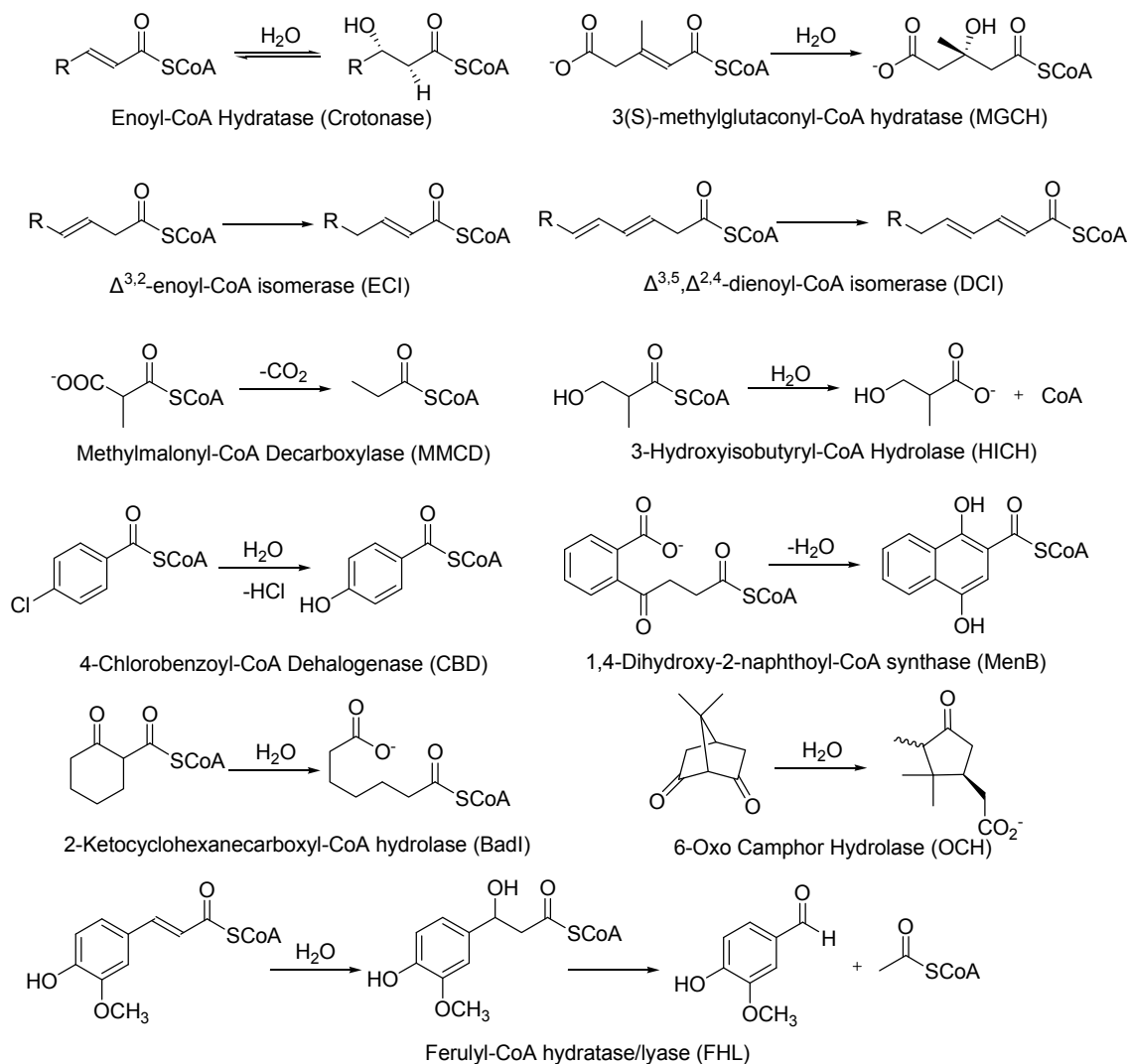
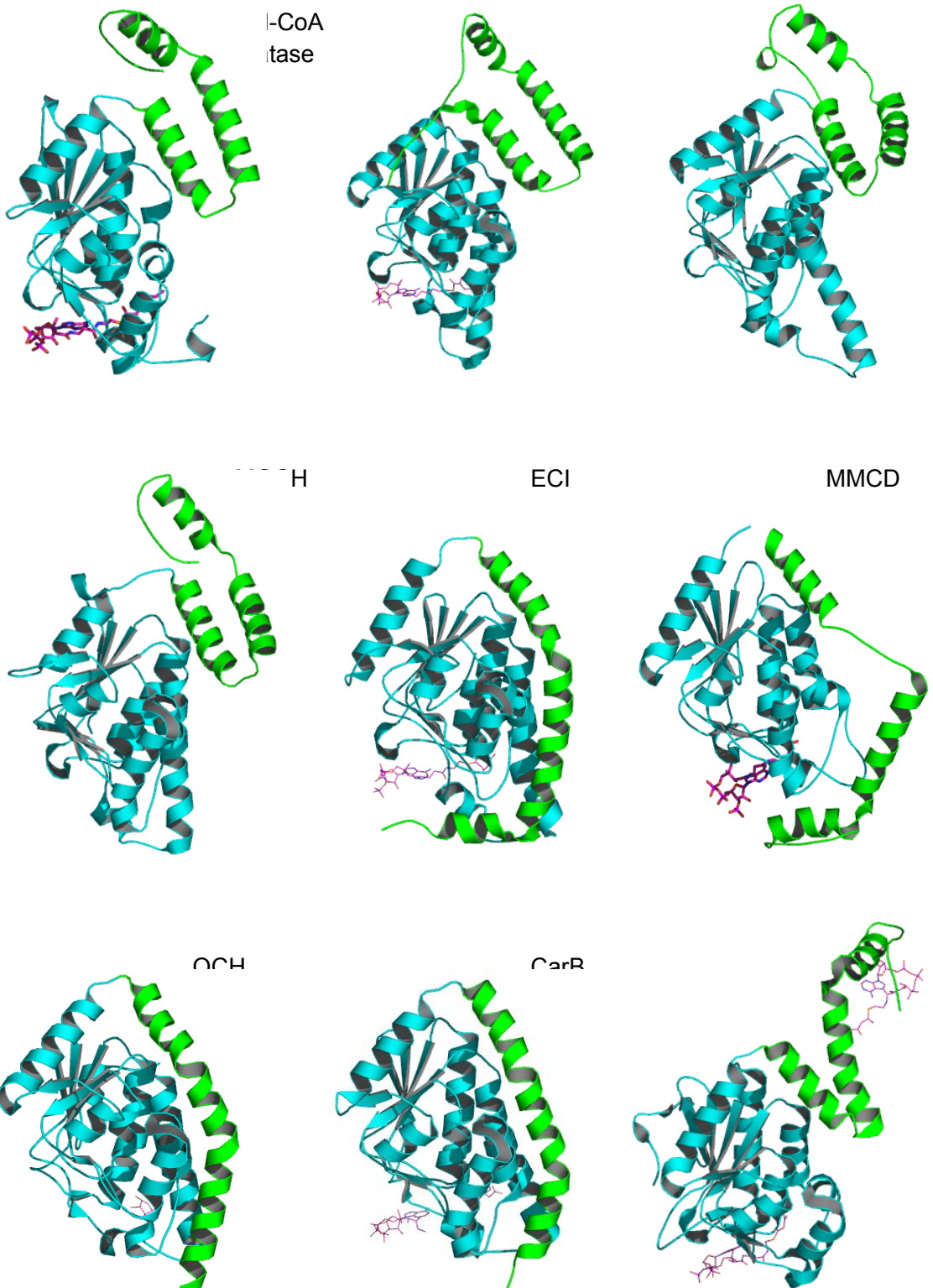


**Figure 2.2: Reactions catalyzed by members of the crotonase superfamily.** Various reactions include hydration (enoyl-CoA hydratase (5-7) and MGCH (8)), isomerization (ECI (9) and DCI (10)), decarboxylation (MMCD (11)), thioester hydrolysis (HICH (12)), dehalogenation (CBD (13)), Dieckmann condensation (MenB (14)), reverse Dieckmann condensation (OCH (15) and BadI (16)) and reverse aldol condensation (FHL (17)).

conserved oxyanion hole stabilizes oxyanion intermediate, while the divergent catalytic residues involve in substrate binding and catalysis of various reactions.

Since superfamily members may be evolved from the same ancestor, they share a common structural scaffold. The crotonase fold is a right-handed spiral composed of a core of  $\beta$ -sheets surrounded by  $\alpha$ -helices. Eleven crystal structures have been solved and published: enoyl-CoA hydratase (crotonase) from rat (18), 3(S)-methylglutaconyl-CoA hydratase (MGCH) from human (19), 4-chlorobenzoyl-CoA dehalogenase (CBD) from *Pseudomonas sp.* (13),  $\Delta^{3,5},\Delta^{2,4}$ -dienoyl-CoA isomerase (DCI) from rat (20), methylmalonyl-CoA decarboxylase (MMCD) from *E. coli* (11),  $\Delta^{3,2}$ -enoyl-CoA isomerase (ECI) from *Saccharomyces cerevisiae* (Yeast) (9), 6-oxocamphor hydrolase (OCH) from *Rhodococcus sp.* (21), MenB from *M. tuberculosis* (14) carboxymethylproline synthase (Carb) from *Pectobacterium Carotovora* (22), MenB from *S. aureus* (23), and 3-hydroxyisobutyryl-CoA hydrolase (HICH) from human (24). All these structures contain this particular arrangement of secondary structures (**Figure 2.3**). Most of crotonase members form hexamers (dimers of trimers). The active site is located at the outer edge of the trimer, near the trimer-trimer interface. The active substrate molecule is buried inside the protein, while the CoA portion threads out of the active site, occupying a cleft in the enzyme where it makes many contacts with water.

Crotonase superfamily members can be categorized into three sub-groups according to the position of their C-terminus (**Figure 2.3**). In first sub-group



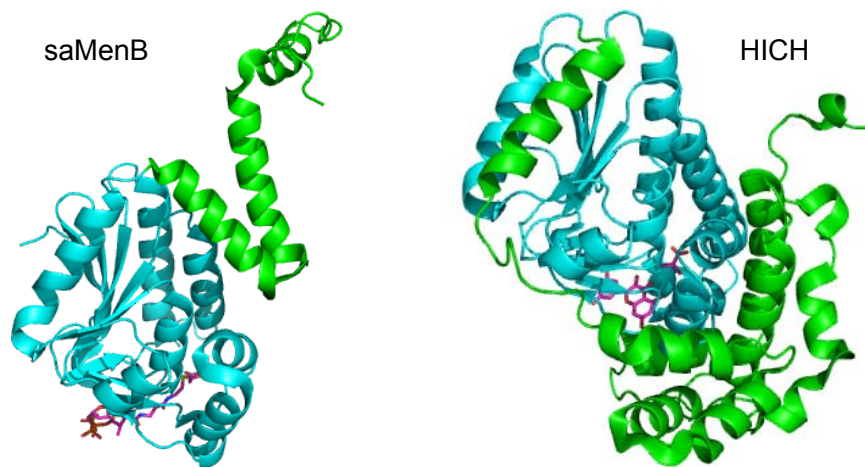


**Figure 2.3: Structures of enzymes from the crotonase superfamily.** The  $\alpha$ ,  $\beta$  core is in blue; the divergent C-terminal domain is in green; bound substrate analogs are in pink.

including enoyl-CoA hydratase, CBD, DCI and MGCH, the C-terminus protrudes away from the monomer and interacts with the active site of a neighboring monomer within the trimer. Second group includes ECI, MMCD, OCH and CarB where their C-terminus folds back to interact with active site of the same monomer. Human HICH has an extremely long C-terminus and can be categorized into second group. In third group, mtMenB and saMenB, the C-terminus crosses the trimer-trimer interface and interacts with the active site of a monomer from the opposing trimer.

#### *Crystal structures of mtMenB and saMenB Bound with Acetoacetyl CoA*

The crystal structures of mtMenB and saMenB in complex with acetoacetyl CoA (AcAc-CoA) (**Figure 2.4**) have been published by our group (14) and Ulaganathan (23) respectively.

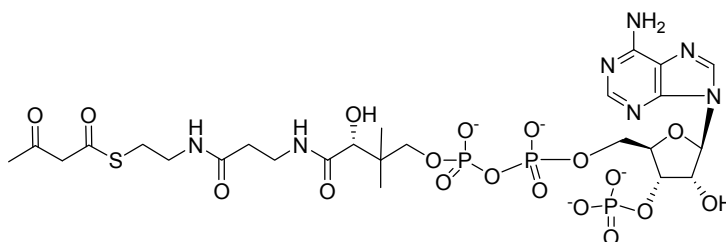


**Figure 2.4: Structure of acetoacetyl CoA (AcAc-CoA)**

Both mtMenB and saMenB proteins are hexamers (dimer of trimers). **Figure 2.5** shows the crystal structures of mtMenB. Unlike most of the members in crotonase superfamily, the C-terminus of MenB crosses the trimer-trimer interface and interacts with the active site of a monomer from the opposing trimer (**Figure 2.5A**). The active site residues are located on the outer edge of trimer, near the trimer-trimer interface. The acetoacetyl portion of the substrate analogue is buried within a cleft in the enzyme, while the CoA portion threads out of the active site making enough contacts with solvent molecules on the surface (**Figure 2.5B**). The thioester carbonyl forms hydrogen bonding with the backbone amide protons of the residues of oxyanion hole (Gly 105 and Gly 161). Catalytic residues D185, S190, D192 (mtMenB numbering) from one monomer and Y287 (mtMenB numbering) from the C-terminus of another monomer are positioned in the active site (**Figure 2.5B**).

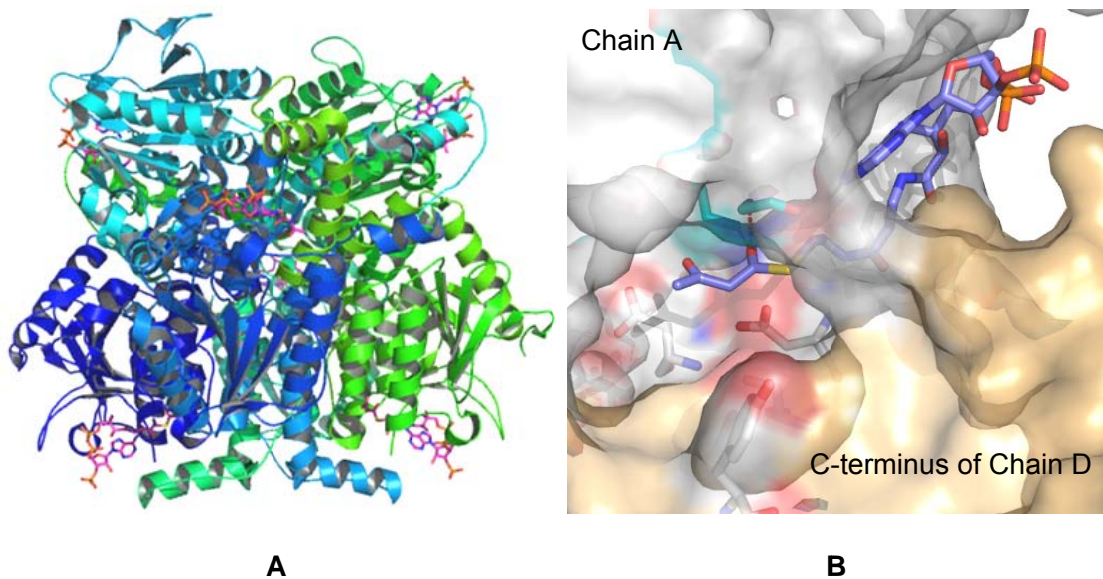


**Figure 2.5: Crystal structures of mtMenB bound with AcAc-CoA.** Figure A shows that mtMenB is a hexamer and Figure B shows the active site of mtMenB.

saMenB is associated with bacterial growth of small-colony variants (SCVs) of *S. aureus*. SCVs of *S. aureus* are associated with persistent infections and may be selectively enriched during antibiotic therapy. *S. aureus* SCV phenotype isolates were characterized by reduced susceptibility to gentamicin, reduced hemolytic activity, slow growth, and menadione auxotrophy. Sequencing of the genes involved in menadione auxotrophy revealed mutations in *menB* in all three strains with the SCV phenotype (25). The mutations included (i) a 9-bp deletion from nucleotides 55 to 63 which corresponds to the amino acid sequence of F19Y20G21, (ii) a frameshift mutation that resulted in a premature stop codon at position 230, and (iii) a point mutation that caused the amino acid substitution Gly233 to Val233 (25).

Based on the structure of saMenB (**Figure 2.6**), the bulky mutation of G233V may affect the folding at trimer-trimer interface in the C-terminus, thus impact the whole structure. The truncation of the C-terminus after residue 230 not only removes the conserved catalytic residue Y246, but also destroys the trimer-trimer interface contact.

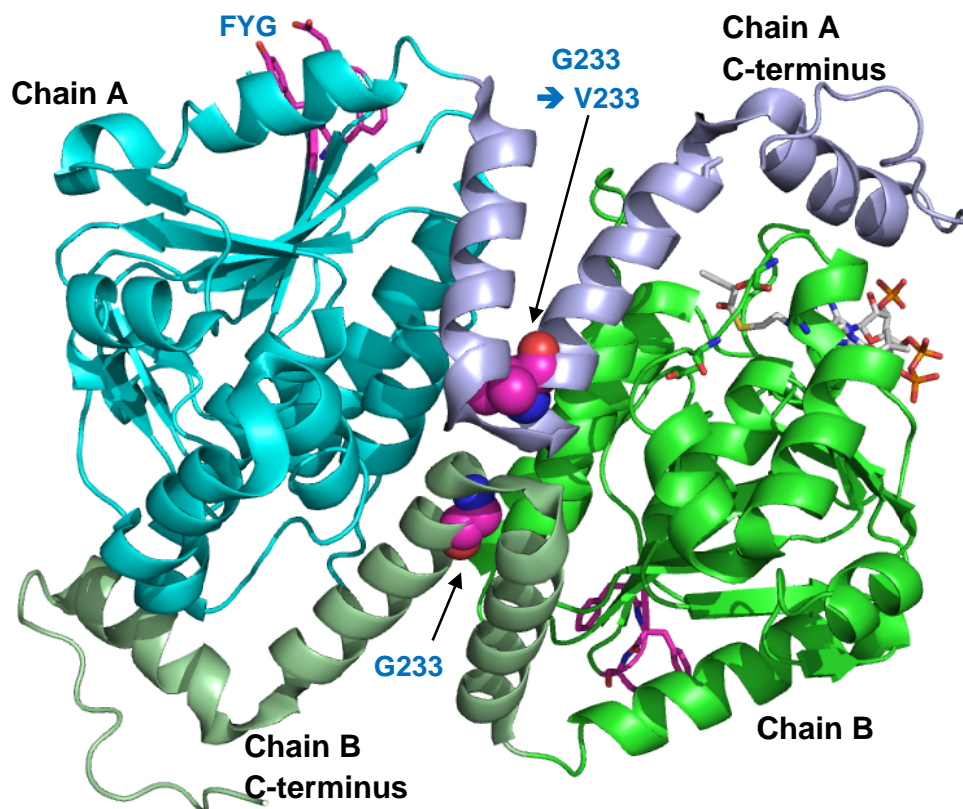


**Figure 2.6: Structure of saMenB showing G233V mutation may alter the C-terminus folding.** The G233V mutation was simulated by using PyMOL.

The active site residues of mtMenB and saMenB can be superimposable (**Figure 2.7**). The major difference lies on that the D185 mtMenB is not conserved in saMenB where there is a residue G144. The different directions the



Tyr residues point are probably because that AcAc-CoA lacks the OSB moiety for fixing the positions of the active site residues.

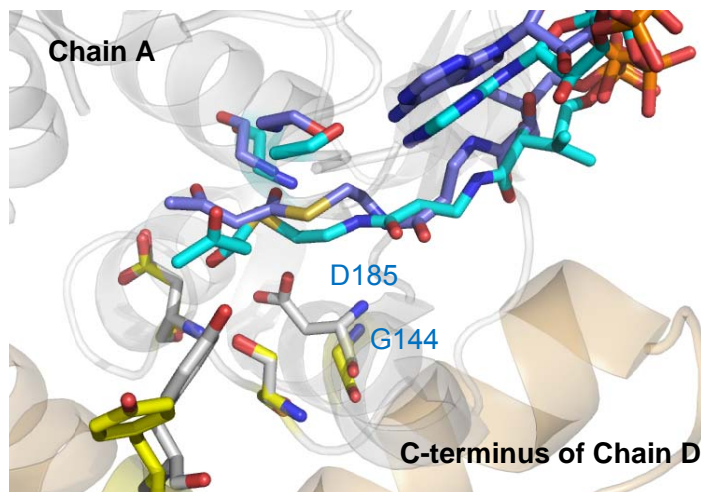


**Figure 2.7: Structures of mtMenB and saMenB.** The active site residues can be superimposable. The active site residues of mtMenB are colored in white while that of saMenB are shown in yellow.

#### *MenB catalyzes Dieckmann condensation reaction*

MenB catalyzes the formation of a carbon-carbon bond through an intramolecular Claisen/Dieckmann condensation (26, 27) (**Figure 2.8**). In the reaction, the aliphatic OSB carboxylate is activated by the formation of a CoA thioester which results in an acidification of the  $\alpha$ -protons. Subsequently, the thioester is deprotonated to form an enolate intermediate and a  $\beta$ -keto ester is generated through the nucleophilic attack of the enolate anion on the second OSB carboxylate. The enzyme catalyzes the reaction by stabilizing the enolate anion and providing a good leaving group for the carboxylate (28). The driving force of this ring closure reaction would probably also be supplied by the



aromatization process. A usual Dieckmann type reaction requires activation at two carboxyl groups whereas in this case we have shown that only one carboxyl group is activated. Ser190, Asp192 and Tyr287 are conserved in mtMenB. Asp185 is not conserved in all MenBs such as MenB from *E. coli* and from *S. aureus*.

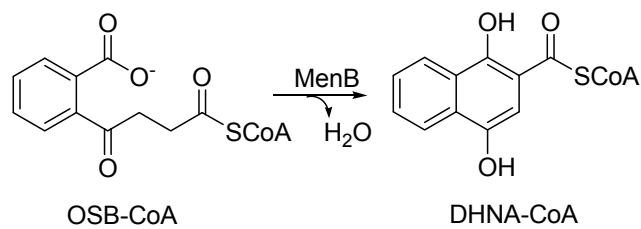


**Figure 2.8: Reaction catalyzed by MenB**

In this chapter, we will focus on the MenB reaction by comparing the mechanism of the *M. tuberculosis* MenB enzyme with that of MenB from *E. coli*. The following questions will be addressed:

1. Do mtMenB and ecMenB utilize the same mechanism and the same substrate for catalytic reaction?
2. D185 mtMenB is crucial for reaction. However, there is no homolog in ecMenB and saMenB. What is the functional role of D185 for catalysis?
3. The gene encoding for the enzyme which catalyzes the hydrolysis of DHNA-CoA to DHNA has not been found. Are the hydrolysis and instability of DHNA-CoA relevant to MenB?

## Materials and methods

### *Reagents and general methods*

The *E. coli* strains XL1-Blue, BL21 (DE3), BL21 CodonPlus, *Pfu Turbo* DNA polymerase were obtained from Stratagene. DpnI was ordered from Biolab Inc. T4 DNA ligase, and restriction enzymes (NdeI, XhoI, BamHI) were purchased from Invitrogen. High pure plasmid isolation kit (Roche) was used for minipreps of DNA plasmids. Qiaquick PCR purification kit (Qiagen) was used for purification of DNA products from agarose gels, restriction digest and PCRs. Oligonucleotides (primers) were ordered from IDT<sup>®</sup>. The thrombin, streptavidin-agarose, pET15b and pET23b vectors were purchased from Novagen. His-Bind resin and Ni-NTA His-Bind resin were obtained from Invitrogen. DE52 resin was from Whatman and Q Sepharose resin was bought from Pharmacia Biotech. Centriplus units were from Millipore. QuikChange site-directed mutagenesis kit was obtained from Stratagene<sup>®</sup> (Stratagene, La Jolla, CA).

The extinction coefficients and masses of proteins were calculated based on the amino acid sequences using ProtParam program (<http://us.expasy.org/tools/protparam.html>).

All other chemical reagents were purchased from Sigma-Aldrich or Fisher.

<sup>1</sup>H NMR and <sup>13</sup>C NMR spectra were recorded on a Varian NMR spectrometer with tetramethylsilane as an internal standard at 25 °C. Data are reported as follows: chemical shift in ppm ( $\delta$ ), multiplicity (s = singlet, d = doublet, t = triplet, q = quartet, and multiplet), and integration. Mass spectra were obtained on an Agilent Technologies MS instrument with ionization voltages of 50 eV. Column

chromatography was performed with SiO<sub>2</sub> (Silicyclo SiliaFlash 60 (230-400 mesh)).

*Expression and purification of wild-type MenB from M. tuberculosis (mtMenB)*

The *menb* gene *Rv0548c* (945 bp), used for the overexpression and purification of MenB, encoding for a putative 1,4-dihydroxynaphthoyl-CoA synthase from *M. tuberculosis*, was previously isolated by PCR from genomic DNA, cloned into the pET-15b plasmid (Novagen) and placed in frame with an N-terminal His-tag sequence, by Yuguo Feng. Protein expression was performed using *E. coli* CodonPlus cells. Transformed cells were grown in 800 mL of LB media containing 0.2 mg/mL ampicillin and induction was achieved using 1 mM isopropyl-β-d-thiogalactopyranoside (IPTG) overnight at 25 °C. Cells were harvested by centrifugation at 5,000 rpm for 20 min at 4 °C, resuspended in 30 mL of His-binding buffer (5 mM imidazole, 0.5 M NaCl, 20 mM Tris HCl, pH 7.9) and lysed by 3 passages through a French Press cell (1,000 psi). Cell debris was removed by centrifugation at 33,000 rpm for 90 min at 4 °C. MenB was purified using His affinity chromatography: the supernatant was loaded to a column containing 3 mL of His-bind resin (Novagen), charged with 9 mL of charge buffer (Ni<sup>2+</sup>). The column was washed with 20 mL of His-binding buffer and 20 mL of wash buffer (60 mM imidazole, 0.5 M NaCl, 20 mM Tris HCl, pH 7.9). MenB was eluted using a gradient of 20 mL elute buffer (0.5 M imidazole, 0.5 M NaCl, 20 mM Tris HCl, pH 7.9). Fractions containing MenB were collected and the imidazole removed by chromatography on G-25 resin using 20 mM NaH<sub>2</sub>PO<sub>4</sub>, 0.1

M NaCl at pH 7.0, as storing buffer. The concentration of MenB was determined by measuring the absorption at 280 nm using an extinction coefficient of 41,370 M<sup>-1</sup>cm<sup>-1</sup> calculated from the primary sequence. The protein was assessed by SDS-PAGE as a dominant band of 37 kDa. The enzyme was concentrated by using Centricon-30 (Amicon) and stored at -80 °C.

#### *Cloning, expression and purification of mutant mtMenB*

mtMenB D185G and D185E mutant plasmids were prepared using QuickChange site-directed mutagenesis with the following primers:

mtMenB D185G primers:

Forward: 5' CGCTTCAAGCAGACCGGGGCCGACGTCGGCAGC 3'

Reverse: 5' GCTGCCGACGTCGGCCCCGGTCTGCTTGAAGCG 3'

mtMenB D185E primers:

Forward: 5' CTTCAAGCAGACCGAGGCCGACGTCGGCAG 3'

Reverse: 5' CTGCCGACGTCGGCCTCGGTCTGCTTGAAG 3'

mtMenB mutant of D185N, S190A, D192N and Y287F were prepared by Yuguo Feng. The procedure for the expression and purification of mutant mtMenB was used as described for wild-type mtMenB.

#### *Cloning, expression and purification of wild-type MenB from E. coli (ecMenB)*

The *menb* gene *b2262* (858 bp) was amplified from crude *E. coli* cell by PCR and cloned into the pET-15b plasmid (Novagen) by using the oligonucleotides (primers) forward: (5') GGAGGAATTCCATATGATGATTTATCCTGATGA (3')

and reverse: (5') CGCGGATCCTTATTACGGATTCCGTTTGAA (3'). Use of the *NdeI* and *BamHI* restriction sites placed the *menb* gene in-frame with an N-terminal Hig-tag sequence. Protein expression was performed using BL21 (DE3) cells. Transformed cells were grown in 800 mL of LB media containing 0.2 mg/mL ampicillin and induction was achieved using 1 mM IPTG overnight at 25 °C. Cells were harvested by centrifugation at 5,000 rpm for 20 min at 4 °C, resuspended in 30 mL of Ni-NTA Bind Buffer (10 mM imidazole, 300 mM NaCl, 50 mM sodium phosphate buffer, pH 8.0) and lysed by 3 passages through a French Press cell (1,000 psi). Cell debris was removed by centrifugation at 33,000 rpm for 90 min at 4 °C. MenB was purified using His affinity chromatography: the supernatant was loaded to a column containing 3 mL of Ni-NTA His-Bind resins (Novagen). The column was washed with 20 mL of Ni-NTA Bind Buffer and 20 mL of wash buffer (20 mM imidazole, 300 mM NaCl, 20 mM sodium phosphate buffer, pH 8.0). MenB was eluted using a gradient of 20 mL elute buffer (250 mM imidazole, 300 mM NaCl, 20 mM sodium phosphate buffer, pH 8.0). Fractions containing MenB were collected and the imidazole removed by chromatography on G-25 resin using 20 mM NaH<sub>2</sub>PO<sub>4</sub>, 0.1 M NaCl at pH 7.0, as storing buffer. N-terminal His-tag was cleavage by thrombin overnight at room temperature. With the His-tag, *ecMenB* was not stable. The concentration of MenB was determined by measuring the absorption at 280 nm using an extinction coefficient of 36,040 M<sup>-1</sup>cm<sup>-1</sup> calculated from the primary sequence. The protein was assessed by SDS-PAGE as a dominant band of 31 kDa. The enzyme was concentrated by using Centricon-10 (Amicon) and stored at -80 °C.

### *Cloning and expression of mutant ecMenB*

ecMenB G156D was prepared using QuickChange site-directed mutagenesis with the following primers:

Forward: 5' GCCATCTTCGGTCAGACTGACCCGAAAGTCGGT 3'

Reverse: 5' GGAGGAACCGACTTTCGGGTCAGTCTGACCGAA 3'

The procedure for the expression and purification of mutant ecMenB was used as described for wild-type ecMenB.

### *Cloning, expression and purification of wild-type MenB from S. aureus (saMenB)*

The *menb* gene SAOUHSC\_00985 (822 bp) was amplified from *S. aureus*\_NCTC8325 genomic DNA by PCR and cloned into the pET-15b plasmid (Novagen) by using the oligonucleotides (primers) forward: (5') GGAATTCATATGATGACTAACAGACAATGGGAAAC (3') and reverse: (5') CGGGATCCTTATGGGAATTTAGGGAATTGA (3'). Use of the *NdeI* and *BamHI* restriction sites placed the *menb* gene in-frame with an N-terminal Hig-tag sequence. Protein expression was performed using BL21 (DE3) cells. Transformed cells were grown in 800 mL of LB media containing 0.2 mg/mL ampicillin and induction was achieved using 0.5 mM IPTG overnight at 25 °C. Cells were harvested by centrifugation at 5,000 rpm for 20 min at 4 °C, resuspended in 30 mL of Ni-NTA Bind Buffer (10 mM imidazole, 300 mM NaCl, 50 mM sodium phosphate buffer, pH 8.0) and lysed by 3 passages through a French Press cell (1,000 psi). Cell debris was removed by centrifugation at 33,000 rpm for 90 min at 4 °C. saMenB was purified using His affinity

chromatography: the supernatant was loaded to a column containing 3 mL of Ni-NTA His-Bind resins (Novagen). The column was washed with 20 mL of Ni-NTA Bind Buffer and 20 mL of wash buffer (20 mM imidazole, 300 mM NaCl, 20 mM sodium phosphate buffer, pH 8.0). saMenB was eluted using a gradient of 20 mL elute buffer (250 mM imidazole, 300 mM NaCl, 20 mM sodium phosphate buffer, pH 8.0). Fractions containing saMenB were collected and the imidazole removed by chromatography on G-25 resin using 20 mM NaH<sub>2</sub>PO<sub>4</sub>, 0.1 M NaCl at pH 7.5, as storing buffer. saMenB was assessed by SDS-PAGE as the dominant band at 30 kDa. N-terminal Hig-tag was cleaved by thrombin overnight at room temperature. With the Hig-tag or without Hig-tag, saMenB was not stable. The concentration of saMenB was determined by measuring the absorption at 280 nm using an extinction coefficient of 31,390 M<sup>-1</sup>cm<sup>-1</sup> calculated from the primary sequence. The enzyme was concentrated by using Centricon-10 (Amicon) and stored at -80 °C.

#### *Cloning, expression and purification of mutant saMenB*

saMenB G144D was prepared using QuickChange site-directed mutagenesis with the following primers:

Forward: 5' GCTATTTTTGGACAAACTGATCCTAAAGTAGGTTTCATTTG 3'

Reverse: 5' CAAATGAACCTACTTTAGGATCAGTTTGTCCAAAATAGC 3'

The procedure for the expression and purification of mutant saMenB was used as described for wild-type saMenB.

*Cloning, expression and purification of Wild-type YfbB from E. coli*

The *yfbB* gene *b2263* (759 bp) was amplified from crude *E. coli* cell by PCR and cloned into the pET-15b plasmid (Novagen) by using the oligonucleotides (primers) forward: (5') GGAATTCCATATGATCCTGCACGCGCAGGC (3') and reverse: (5') GCCCTAGGTCAGAAACGCAAGATCTGCGCC (3'). Use of the *NdeI* and *BamHI* restriction sites placed the *yfbB* gene in-frame with an N-terminal Hig-tag sequence. Protein expression was performed using BL21 (DE3) cells. Transformed cells were grown in 800 mL of LB media containing 0.2 mg/mL ampicillin and induction was achieved using 1 mM IPTG overnight at 25 °C. Cells were harvested by centrifugation at 5,000 rpm for 20 min at 4 °C, resuspended in 30 mL of His-binding buffer (5 mM imidazole, 0.5 M NaCl, 20 mM Tris HCl, pH 7.9) and lysed by 3 passages through a French Press cell (1,000 psi). Cell debris was removed by centrifugation at 33,000 rpm for 90 min at 4 °C. YfbB was purified using His affinity chromatography: the supernatant was loaded to a column containing 3 mL of His-bind resin (Novagen), charged with 9 mL of charge buffer (Ni<sup>2+</sup>). The column was washed with 20 mL of His-binding buffer and 20 mL of wash buffer (60 mM imidazole, 0.5 M NaCl, 20 mM Tris HCl, pH 7.9). YfbB was eluted using a gradient of 20 mL elute buffer (0.5 M imidazole, 0.5 M NaCl, 20 mM Tris HCl, pH 7.9). Fractions containing YfbB were collected and the imidazole removed by chromatography on G-25 resin using 20 mM NaH<sub>2</sub>PO<sub>4</sub>, 0.1 M NaCl at pH 7.0, as storing buffer. The concentration of YfbB was determined by measuring the absorption at 280 nm using an extinction coefficient of 37,650 M<sup>-1</sup>cm<sup>-1</sup> calculated from the primary sequence. The protein was



assessed by SDS-PAGE as a dominant band of 27 kDa. The enzyme was concentrated by using Centricon-10 (Amicon) and stored at -80 °C.

#### *Coupled assay of MenB reaction*

OSB-CoA, the substrate for MenB, is unstable and decomposes rapidly to spirodilactone. The half-life of degradation is 15 min at 30 °C and more than 2 hours at 0 °C (27). Therefore, we used a coupled assay with *E. coli* MenE, the preceding enzyme in the menaquinone biosynthesis pathway, which synthesizes OSB-CoA *in situ*, to assay the MenB reaction (**Figure 2.9**). All coupled reactions were performed in 20 mM NaH<sub>2</sub>PO<sub>4</sub> pH 7.0, 150 mM NaCl, 1 mM MgCl<sub>2</sub> and an excess of *E. coli* MenE. Formation of DHNA-CoA was monitored on a CARY-300 spectrophotometer at 25 °C by following the increase in absorption at 392 nm using an extinction coefficient of 4, 000 M<sup>-1</sup>cm<sup>-1</sup>.

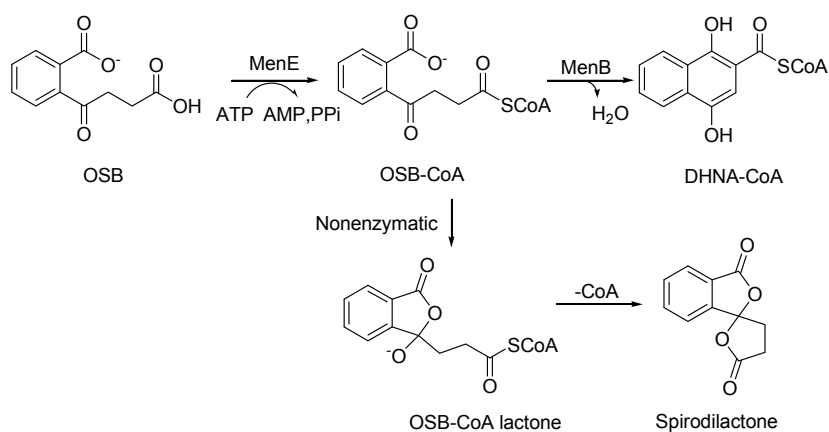


**Figure 2.9: The formation of the naphthoic ring catalyzed by MenB and the spirodilactone in a non-enzymatic reaction**

### *Pre-incubation of the MenB coupled assay*

The pre-incubation of MenE, ATP, CoA and OSB was performed in 20 mM NaH<sub>2</sub>PO<sub>4</sub> pH 7.0, 150 mM NaCl, 1 mM MgCl<sub>2</sub> and an excess of *E. coli* MenE for 3 min to allow complete conversion of OSB to OSB-CoA. MenB reaction was initiated by the addition of MenB. Formation of DHNA-CoA was monitored on a CARY-300 spectrophotometer at 25 °C by following the increase in absorption at 392 nm using an extinction coefficient of 4, 000 M<sup>-1</sup>cm<sup>-1</sup>.

### *Ellman assay for detecting thioesterase activity*

Ellman Assay was used to detect the free sulphhydryl groups using Ellman's reagent (5, 5'-Dithio-bis (2-nitrobenzoic acid) (DTNB)) (29). The thioesterase activities of MenB and YfbB were monitored at 410 nm in the presence of excess Ellman's reagent.

### *Kinetic data analysis*

Determining  $K_m$  and  $k_{cat}$ :  $V_{max}$  and  $K_m$  values were obtained by fitting all the data to the Michaelis-Menten equation using GraFit 4.0,  $v = \frac{V_{max} [S]}{K_m + [S]}$ .  $k_{cat}$  values were obtained using the relationship between  $k_{cat}$  and  $V_{max}$ :  $V_{max} = k_{cat} * [E]$ .

### *Purification of chorismate from E. coli cells*

Chorismate was purified from an *E. coli* KA12 strain that had been engineered by constructing mutant strain of *E. coli* which lacks chorismate mutase activity (30). Chorismate was subsequently purified using the procedure

described by Grisostomi C. etc. (30). 15 mL of *E. coli* KA12 cell culture was grown from a single colony at 37 °C. 800 mL of growth medium A (1.6 g casamino acids, 1.6 g yeast extract, 32.8 mg L-tryptophan, 18 mL 50 × Vogel & Bonner salts) in 4 L Erlenmeyer flask was autoclaved, added with glucose to 0.16% (w/v), and then inoculated with 15 mL preculture. The culture was grown at 30 °C for 6 hours to reach  $OD_{260} = 1.9-2.1$  and then centrifuged at 5000 g for 15 min. The cells were resuspended in nonsterile 500 mL of accumulation medium B (6.4 g  $Na_2HPO_4$ , 0.68 g  $KH_2PO_4$ , 9 g glucose, 1.35 g  $NH_4Cl$ , 10.15 mg  $MgCl_2 \cdot 6H_2O$ , 1 mg L-tryptophan). The suspension was shaken at 30 °C for 16 hours allowing for production of chorismate and its secretion into the medium. After removing the cells centrifugation, the supernatant was collected, brought to pH 9.0 and transferred to an ion-exchange column (BioRad AG1-X8, 200-400 mesh, Dowex 1-Cl; 6 × 2.4 cm). The column was washed with 80 mL water and chorismate was eluted as the ammonium salt with 1 M  $NH_4Cl$  (pH8.5). The chorismate-containing fractions were collected by monitoring the absorbance at 274 nm, acidified with concentrated HCl to pH 1.5, and extracted with dichloromethane (3 × 35 mL) to remove most of the phenylpyruvate and then extracted with ethyl acetate (4 × 25 mL). The water was dried over  $Na_2SO_4$  and ethyl acetate was removed under the vacuum. The crude chorismate was yellow oil, which was stored at -80 °C.

Crude chorismate was purified by semi-preparative HPLC (Vydac C18 column, 10 µm particle diameter, 10 mm i.d., 250 mm length). A linear gradient (0-10 min 0% acetonitrile, 10-20 to 30% acetonitrile in 5% acetic acid water) was applied. The absorbance of the eluent was monitored at 274 nm. The chorismate

fraction was eluted from 3-6 min. The peak of interest was collected over several runs, frozen, and lyophilized. Around 100 mg of chorismate was obtained. ESI-MS  $[M+Na^+]$ : calcd 249.03 ( $C_{10}H_{10}Na^+$ ); found 249.0.

#### *Enzymatic synthesis of o-succinylbenzoic acid (OSB) from chorismate*

4.4 mM Chorismate, 5 mM glutamate, 5 mM  $NAD^+$ , 50  $\mu$ M THDP, 1  $\mu$ M MenF, 1  $\mu$ M MenB, 0.5  $\mu$ M MenC, 1  $\mu$ M YfbB and 20 unit *L*-glutamic dehydrogenase were incubated in phosphate buffer (50 mM  $NaH_2PO_4$ , 2 mM  $MgSO_4$ , pH 7.8) at 37 °C for 4 hours. The product was purified by semi-preparative HPLC (Vydac C18 column, 10  $\mu$ m particle diameter, 10 mm i.d., 250 mm length). A linear gradient (0-10 min 0% acetonitrile, 10-20 to 30% acetonitrile in 5% acetic acid water) was applied. The absorbance of the eluent was monitored at 254 nm. The OSB fraction was eluted at 13 min. ESI-MS  $[M-H^-]$ : calcd 221.05 ( $C_{11}H_9O_5^-$ ); found 221.1.

#### *Synthesis of o-succinylbenzoic acid (OSB)*

40.0 g of succinic acid (0.34 mol) was heated in a three-neck round bottom flask to about 200 °C until melting. Then 30.0 g of phthalic anhydride (0.2 mol) and 16.4 g of sodium acetate (0.2 mol) were added and mixed. The reaction mixture was refluxed at the temperature of 200-220 °C for 30-40 min until  $CO_2$  and water evolution ceased. The reaction mixture was extracted with boiling water four times (4  $\times$  100 mL). 13.2 g of crude spirodilactone was precipitated from the boiling water when it was cooled down. 10.3 g (0.05 M) of pure

spirodilactone was obtained after recrystallization with MeOH (25% of yield). 10.3 g (0.05 M) of spirodilactone was then refluxed in 500 mL of 1.5 M NaOH solution for 30 min. The cooled solution was changed to pH 1-2 with HCl and extracted with 100 mL ethyl acetate for three times. Ethyl acetate was removed under the vacuum and 10.5 g (0.05 mol) of OSB was obtained as white powders (95% of yield) (**Figure 2.10**).  $^1\text{H}$  NMR (400 MHz,  $(\text{CD}_3)_2\text{CO}$ ):  $\delta$  7.85-7.62 (4H, m), 2.61(2H, t), 2.49 (2H, t) ppm (**Figure 2.11**).  $^{13}\text{C}$  NMR (400 MHz,  $(\text{CD}_3)_2\text{CO}$ ): ESI-MS  $\delta$  172.78, 166.93, 133.56, 129.83, 126.89, 125.49, 123.11, 34.42, 29.10 ppm (**Figure 2.12**). ESI-MS  $[\text{M}-\text{H}]^-$ : calcd 221.05 ( $\text{C}_{11}\text{H}_9\text{O}_5^-$ ); found 221.1.

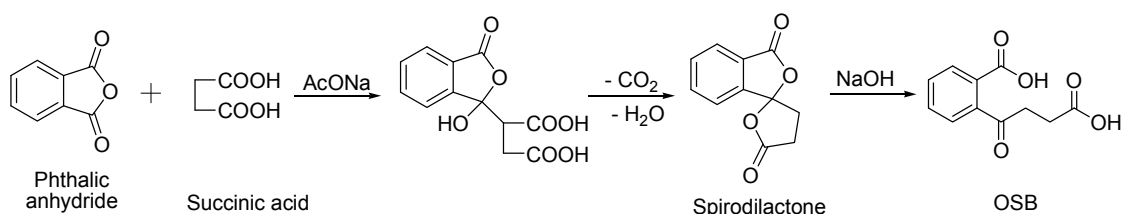


**Figure 2.10: Synthesis of o-succinylbenzoic acid (OSB)**

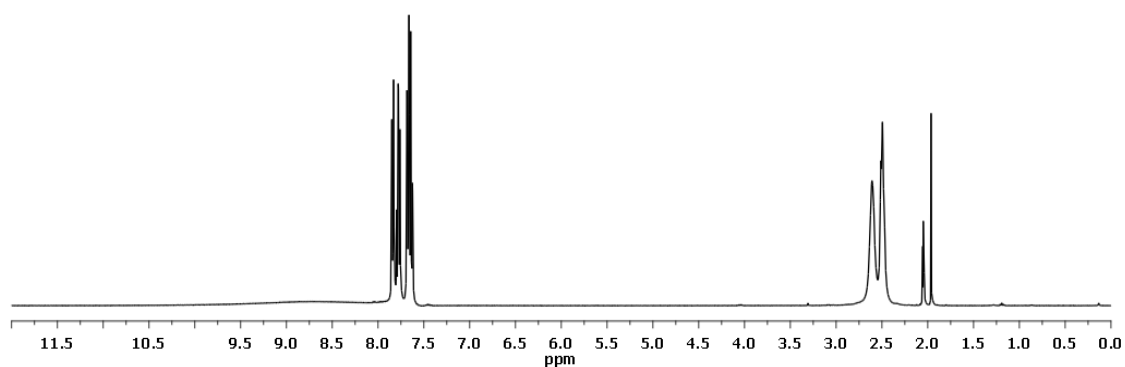


**Figure 2.11:  $^1\text{H}$  NMR spectrum ( $(\text{CD}_3)_2\text{CO}$ ) of OSB, 12-0 ppm**

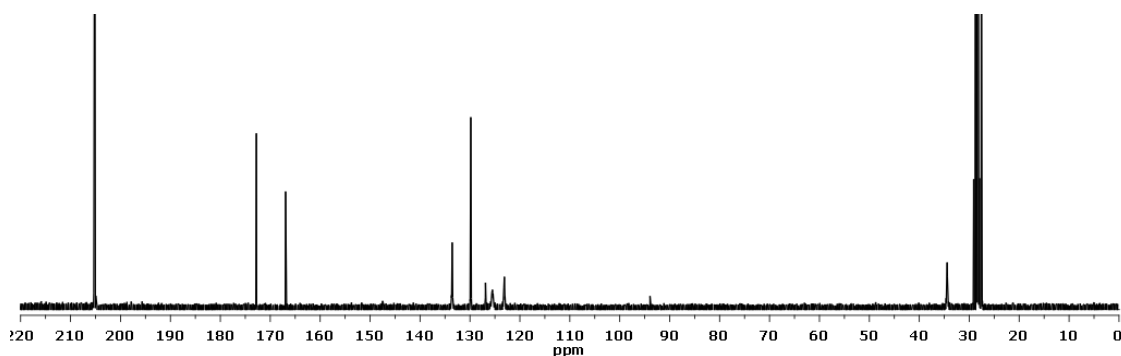


**Figure 2.12:**  $^{13}\text{C}$  NMR spectrum ( $(\text{CD}_3)_2\text{CO}$ ) of OSB, 220-0 ppm

### *Synthesis of N-[2'-(3-carboxypropionyl) benzoyl] imidazole*

N-[2'-(3-carboxypropionyl) benzoyl] imidazole synthesis was referred to Rainer Kolkmann method (31). In short, 222 mg of OSB (1 mmol) and 356 mg of N, N'-carbonyldiimidazole (CDI) (2.2 mmol) were mixed in 8 mL of anhydrous THF at 35 °C under the protection of  $\text{N}_2$ . 120  $\mu\text{L}$  of acetic acid was added after 5 hours and the reaction mixture was kept at 35 °C for another 30 min. THF and water were removed under the vacuum. The yellow oil was redissolved in 3 mL of THF and left at -20 °C for crystallization. The recovered crystals were washed with chilled water and 100 mg of product (0.36 mmol, two step yield is 36%) was obtained as white crystals after drying (**Figure 2.13**).  $^1\text{H}$  NMR (400 MHz,  $(\text{CD}_3)_2\text{SO}$ ):  $\delta$  12.32 (1H, broad s), 7.98-7.69 (5H, m), 7.27(1H, d), 6.97(1H, d), 3.07-2.87(2H, m), 2.08-1.89 (2H, m) ppm (**Figure 2.14**). ESI-MS [ $\text{M-H}^-$ ]: calcd 221.05 ( $\text{C}_{14}\text{H}_{11}\text{N}_2\text{O}_4^-$ ); found 221.1.

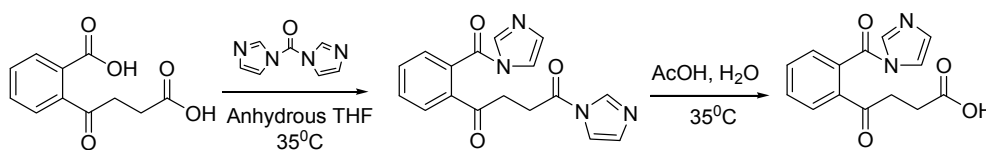


**Figure 2.13:** Synthesis of N-[2'-(3-carboxypropionyl) benzoyl] imidazole

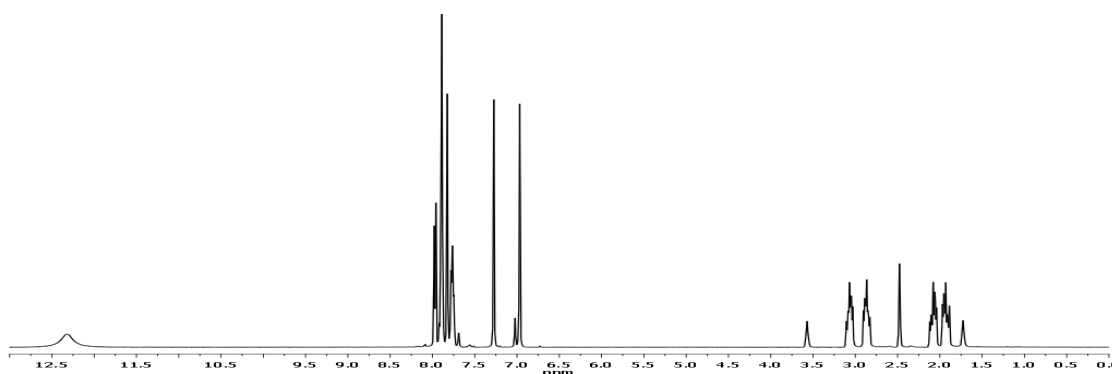


**Figure 2.14:**  $^1\text{H}$  NMR spectrum ( $(\text{CD}_3)_2\text{SO}$ ) of N-[2'-(3-carboxypropionyl) benzoyl] imidazole, 13-0 ppm

#### *Synthesis of methyl ester OSB*

100 mg N-[2'-(3-carboxypropionyl) benzoyl] imidazole (0.36 mmol) and 41 mg sodium methoxide (0.72 mmol) were incubated in 5 mL of methanol overnight at room temperature. The mixture was washed with ethyl acetate, changed pH to 2 with HCl. After extraction with ethyl acetate, removal of the organic solvent under the vacuum gave 25 mg (0.11 mmol) of the product as a white powder (the yield was 30%) (**Figure 2.15**).  $^1\text{H}$  NMR (400 MHz,  $\text{CD}_3\text{OD}$ ):  $\delta$  7.84-7.52 (4H, m), 3.85 (3H, s), 3.11 (2H, t), 2.58 (2H, t) ppm (**Figure 2.16**).  $^{13}\text{C}$  NMR (400 MHz,  $\text{CD}_3\text{OD}$ ): ESI-MS  $\delta$  206.02, 176.55, 169.18, 143.97, 133.64, 131.57, 130.98, 130.27, 128.05, 38.54, 29.37 ppm (**Figure 2.17**). ESI-MS  $[\text{M}-\text{H}]^-$ : calcd 235.07 ( $\text{C}_{12}\text{H}_{11}\text{O}_5^-$ ); found 235.1.

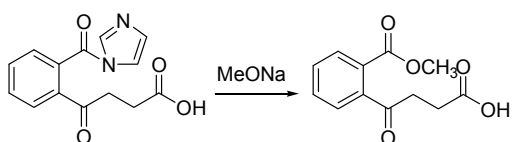


**Figure 2.15:** Synthesis of methyl ester OSB

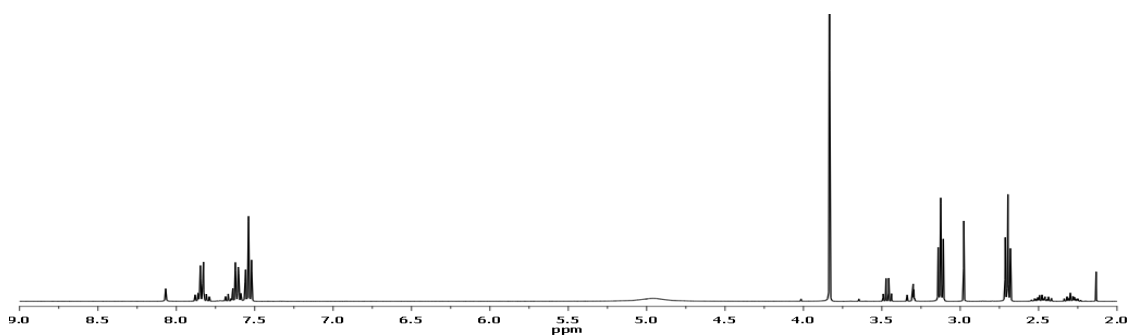


**Figure 2.16:**  $^1\text{H}$  NMR spectrum ( $\text{CD}_3\text{OD}$ ) of methyl ester OSB, 10-2 ppm.

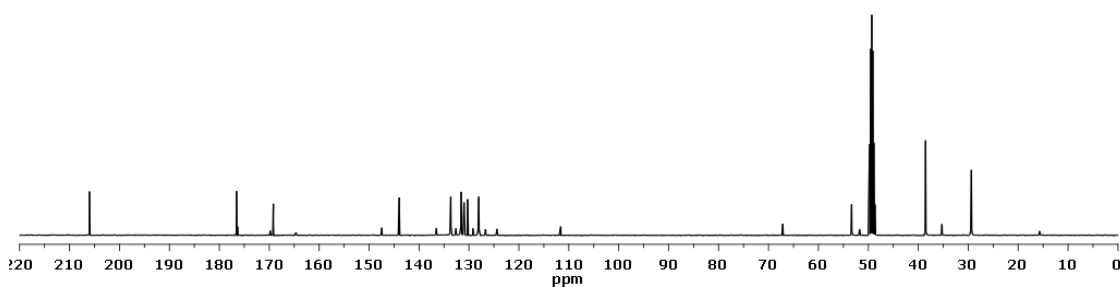


**Figure 2.17:**  $^{13}\text{C}$  NMR spectrum ( $\text{CD}_3\text{OD}$ ) of methyl ester OSB, 220-0 ppm

#### *HMBC Spectrum of methyl ester of OSB*

A two-dimensional HMBC (Heteronuclear Multiple Bond Correlation) experiment was performed to confirm regioselective incorporation of the methyl group to the aromatic carboxylic acid. In HMBC, cross peaks are between protons and carbons that are two or three bonds away ( $J = 2\text{-}15$  Hz), while direct one-bond cross-peaks are suppressed. In **Figure 2.18**, the characteristic methyl group's protons at 3.85 ppm show bond connectivity with the aromatic ketone carbon at 169.18 ppm. In addition, two adjacent methylene groups' protons ( $\delta$  3.11 and 2.58 ppm) show connectivity with the ketone and carboxylate carbonyl carbons ( $\delta$  206.02 and 176.55 ppm) forming a square.



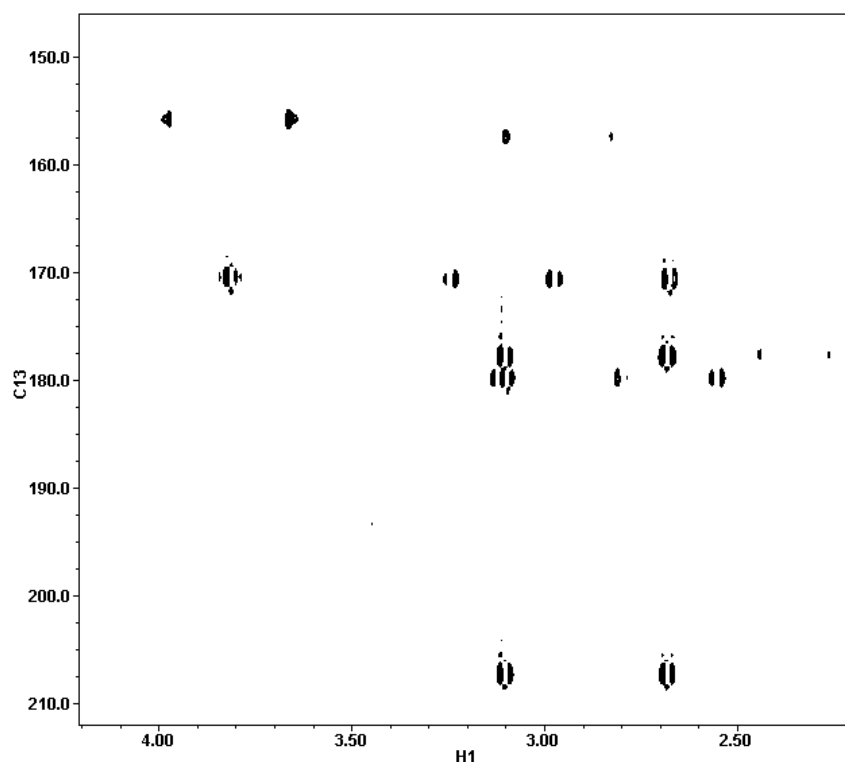


**Figure 2.18:** HMBC spectrum (500 MHz, CD<sub>3</sub>OD) of methyl ester OSB

#### *Synthesis of methylamine OSB*

52.5 mg N-[2'-(3-carbozypionyl) benzoyl] imidazole (0.19 mmol) was dissolved 1 mL of methylamine in THF (2M, 2 mmol). 1 mL each of THF and H<sub>2</sub>O were added, and the reaction mixture was stirred overnight at room temperature. The mixture was then washed with ethyl acetate. The pH of the solution was adjusted to 2 by addition of conc. HCl and the mixture was extracted with ethyl acetate. 30 mg (0.13 mmol) light yellow powder was obtained (the yield was 68%) (**Figure 2.19**). <sup>1</sup>H NMR (400 MHz, CD<sub>3</sub>OD): δ 7.74-7.52 (4H, m), 2.96 (3H, s), 2.43 (2H, m), 1.85 (1H, m), 1.72 (1H, m) ppm (**Figure 2.20**). ESI-MS [M-H]<sup>-</sup>: calcd 234.08 (C<sub>12</sub>H<sub>12</sub>NO<sub>4</sub><sup>-</sup>); found 234.0.

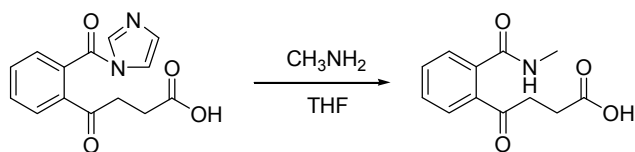


**Figure 2.19: Synthesis of methylamine OSB**

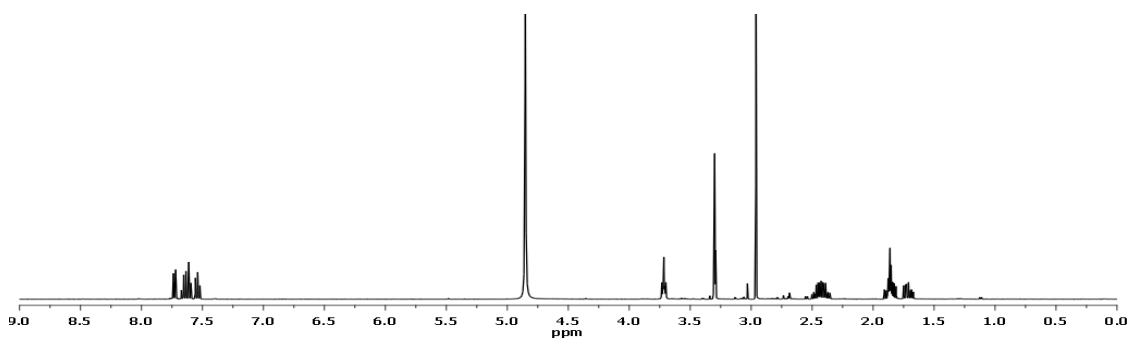


**Figure 2.20: <sup>1</sup>H NMR spectrum (CD<sub>3</sub>OD) of methylamine OSB, 9-0 ppm**

#### *Synthesis of dimethylamine OSB*

The same procedure was used for the synthesis of dimethylamine OSB as had been used for the synthesis of methylamine OSB except that dimethylamine replaced methylamine. Starting with 52.5 mg N-[2'-(3-carboxypropionyl) benzoyl]imidazole (0.19 mmol) and 250  $\mu$ L of 40% dimethylamine (2 mmol), 20 mg (0.08 mmol) of yellow powder was obtained (the yield was 50%) (**Figure 2.21**). <sup>1</sup>H NMR (400 MHz, CD<sub>3</sub>OD):  $\delta$  8.10-7.32 (4H, m), 3.32 (2H, t), 3.10 (3H, s), 2.77 (3H, s), 2.70 (2H, t) ppm (**Figure 2.22**). ESI-MS [M-H<sup>-</sup>]: calcd 248.10 (C<sub>13</sub>H<sub>14</sub>NO<sub>4</sub><sup>-</sup>); found 248.0.

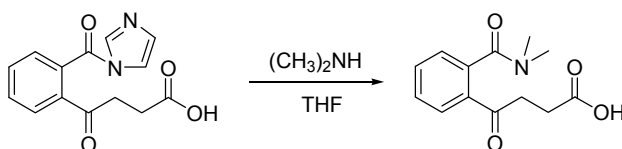


**Figure 2.21: Synthesis of dimethylamine OSB**

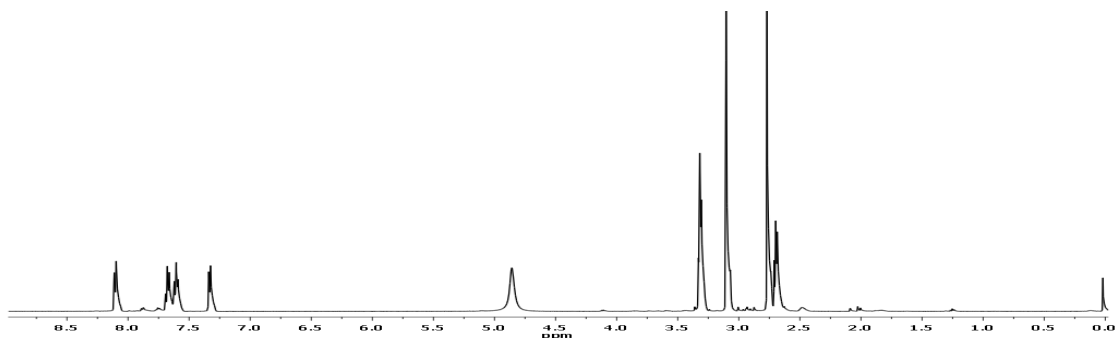


**Figure 2.22:**  $^1\text{H}$  NMR spectrum ( $\text{CD}_3\text{OD}$ ) of dimethylamine OSB, 9-0 ppm

*Standard procedure for the synthesis of acyl-CoA thioester*

Acyl-CoA thioesters were prepared *via* activation of the acid with ethylchloroformate (**Figure 2.23**) (32). The acid (1 mmol) was dissolved in 20 mL of anhydrous tetrahydrofuran (THF), with stirring and external cooling by an ice bath. Dry triethylamine (1 mmol) was added, followed by dropwise addition of ethylchloroformate (1 mmol). After an additional hour of stirring in the ice bath, the precipitated triethyl ammonium chloride was removed by gravity filtration, and the filtrate was subsequently transferred to a dry addition funnel.

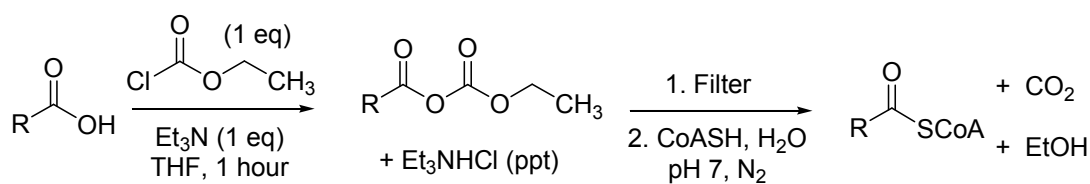


**Figure 2.23: Synthesis of CoA thioester**

CoA (40  $\mu\text{mol}$ ) was dissolved in 10 mL of water, and the pH was adjusted to 7 with 0.1 M NaOH. The solution of activated acid was added dropwise over 30 min to the CoA solution, while maintaining pH 7 by adding 0.1 M NaOH dropwise as necessary. After addition was complete, the reaction was allowed to stir

another four hours. The reaction mixture was acidified to pH 1-2 using conc. HCl and extracted with ethyl acetate. The water layer was frozen in liquid nitrogen and lyophilized.

The product was purified from the lyophilized powder by semi-preparative HPLC (Vydac C18 column, 10  $\mu\text{m}$  particle diameter, 10 mm i.d., 250 mm length). A linear gradient (0 to 40% acetonitrile, 40 min) was applied. The absorbance of the eluent was monitored at 260 nm. The peak of interest was collected over several runs, frozen, and lyophilized. The purified product was redissolved in water and quantitated by measuring the absorbance at 260 nm ( $\epsilon_{260}$  for CoA:  $1.69 \times 10^4 \text{ M}^{-1}\text{cm}^{-1}$ ).

#### *Synthesis of 3-benzoylpropionic CoA (3-BP CoA)*

Starting with 3-benzoylpropionic acid, the standard procedure for the synthesis of coenzyme A thioester was used as described on page 63.  $^1\text{H}$  NMR (600 MHz,  $\text{D}_2\text{O}$ ) spectrum (**Figure 2.24**) was assigned in **Table 2.1**. ESI-MS [ $\text{M}-\text{H}^-$ ]: calcd 926.17 ( $\text{C}_{31}\text{H}_{43}\text{N}_7\text{O}_{18}\text{P}_3\text{S}^-$ ); found 926.1.

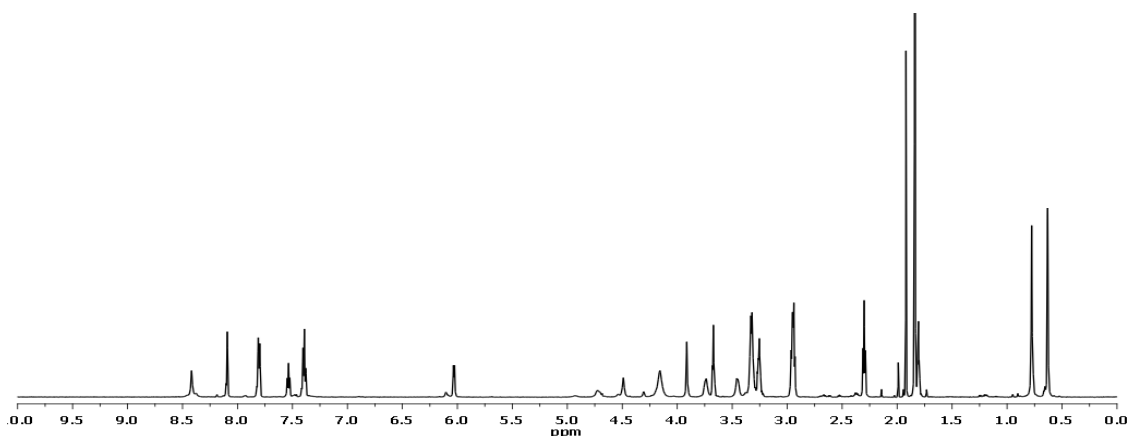


**Figure 2.24:**  $^1\text{H}$  NMR spectrum ( $\text{D}_2\text{O}$ ) of 3-BP CoA, 10-0 ppm

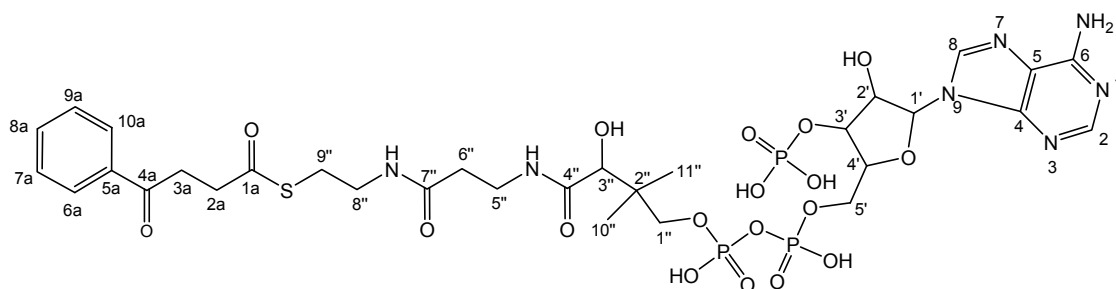


**Table 2.1: Chemical shifts of the protons of 3-benzoylpropionic CoA (3-BP CoA)**

<sup>1</sup> H	δ (ppm)	<sup>1</sup> H	δ (ppm)
2a	2.95, t, 2H	4'	4.50, d, 1H
3a	3.32, t, 2H	5'	4.17, d, 1H
6a, 10a	7.92, t, 2H	1''	3.74, 3.44, s, 2H
7a, 9a	7.50, t, 2H	3''	3.92, s, 1H
8a	7.55, m, 1H	5''	3.32, t, 2H
2	8.11, s, 1H	6''	2.30, t, 2H
8	8.42, s, 1H	8''	3.25, t, 2H
1'	6.05, d, 1H	9''	2.95, t, 2H
2'	4.72, dd, 1H	10''	0.87, s, 3H
3'	4.68, dd, 1H	11''	0.73, s, 3H

#### *COSY and HMBC of 3-BP CoA*

The assignment of <sup>1</sup>H NMR spectrum was also based on the two-dimensional COSY and HMBC analysis. In the two-dimensional COSY (CORrelation Spectroscopy) experiments, magnetization is transferred by scalar coupling. Protons that are more than three chemical bonds apart give no cross signal because the <sup>4</sup>J coupling constants are close to 0. Therefore, only signals of protons which are two or three bonds apart are visible in a COSY spectrum. The

COSY spectrum (**Figure 2.25**) of 3-BP CoA showed three pairs of cross peaks which represent the interaction between the 2a and 3a ( $\delta$  2.95 and 3.32 ppm), 5'' and 6'' ( $\delta$  3.32 and 2.30 ppm), and 8'' and 9'' ( $\delta$  3.25 and 2.95 ppm) methylene groups.

In the HMBC spectrum of 3-BP CoA (**Figure 2.26**), 4a-carbon (220 ppm) has the cross peaks with 2a-, 3a- and 5a-protons. 4''-carbon ( $\delta$  177.5 ppm) corresponds with 3''- and 5''-protons. 7''-carbon ( $\delta$  177.6 ppm) talks with 6''- and 8'' protons.

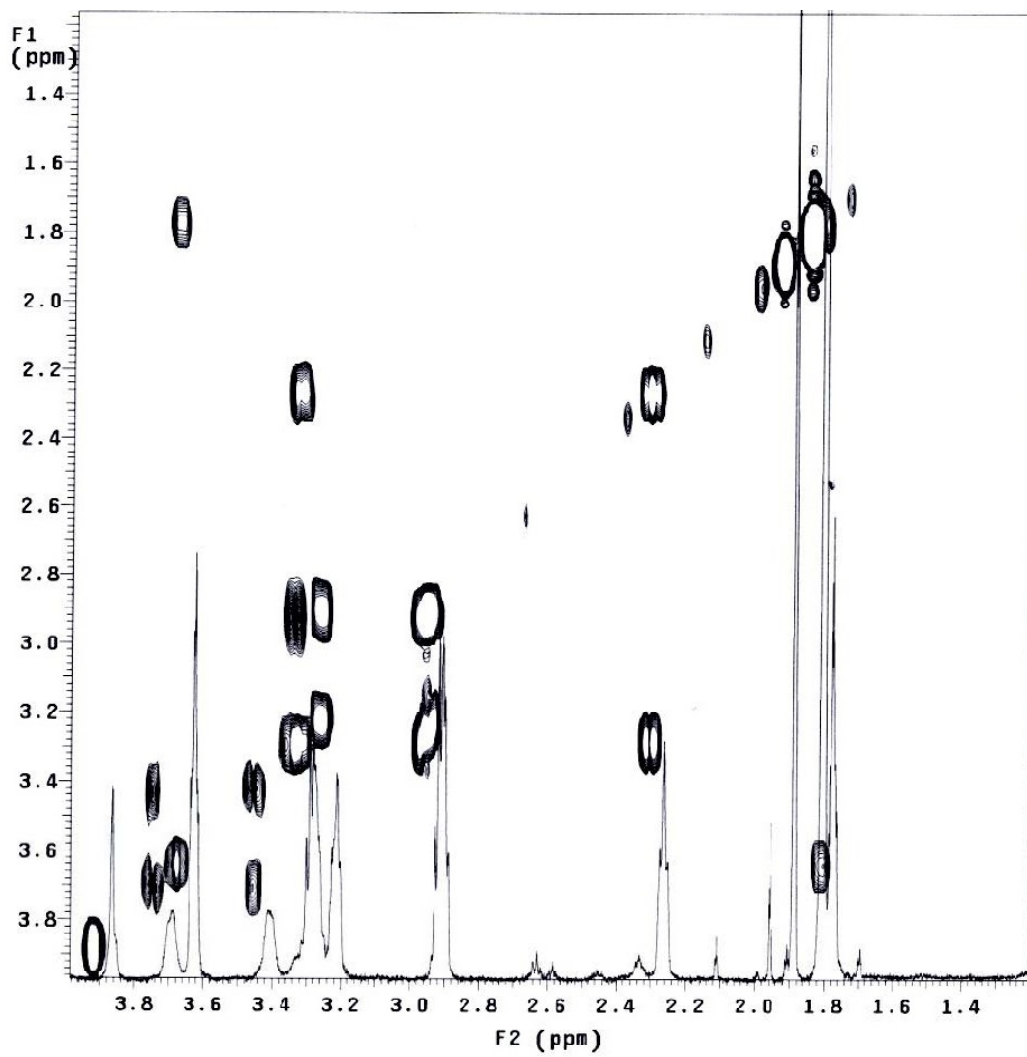
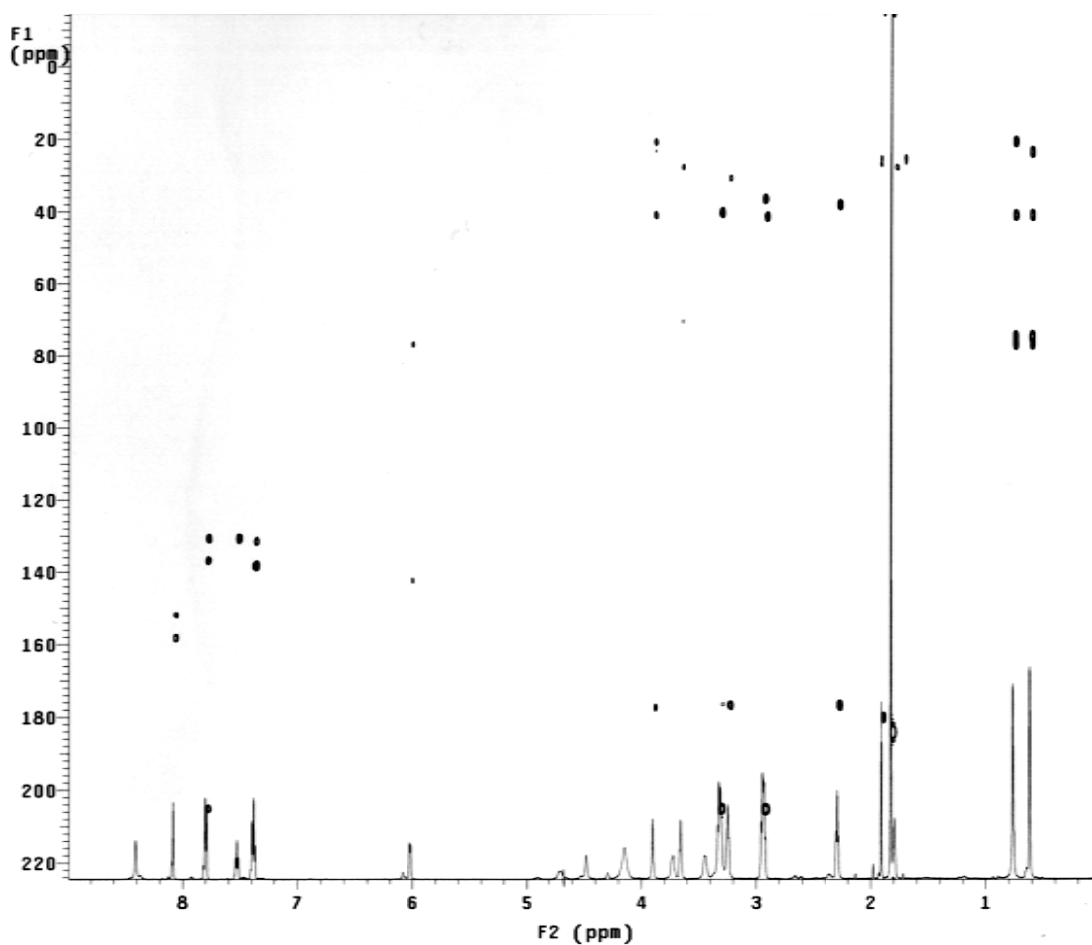


Figure 2.25: COSY spectrum of 3-BP CoA (600 MHz, D<sub>2</sub>O)



**Figure 2.26: HMBC spectrum of 3-BP CoA (600 MHz, D<sub>2</sub>O)**

*Synthesis of o-(3-carboxypropyl)-benzoic CoA (OCPB-CoA)*

OCPB-CoA was synthesized using MenE from *E. coli*. ATP, CoA, OCPB and MenE were incubated for 3 hours at room temperature in phosphate buffer (20 mM NaH<sub>2</sub>PO<sub>4</sub>, 0.1 M NaCl, 1 mM MgCl<sub>2</sub> at pH 7.0). The reaction mixture was purified by semi-preparative HPLC (Vydac C18 column, 10 μm particle, 10 mm i.d., 250 mm length). A linear gradient (0-40% acetonitrile in 20 mM ammonia acetate, 40 min) was applied. OCPB-CoA was collected, frozen and lyophilized. <sup>1</sup>H NMR (600 MHz, D<sub>2</sub>O) spectrum of OCPB-CoA was showed in **Figure 2.27**.



The assignment for OCPB-CoA was given in **Table 2.2**. ESI-MS  $[M-H]^-$ : calcd 956.18 ( $C_{32}H_{45}N_7O_{19}P_3S^-$ ); found 956.2.

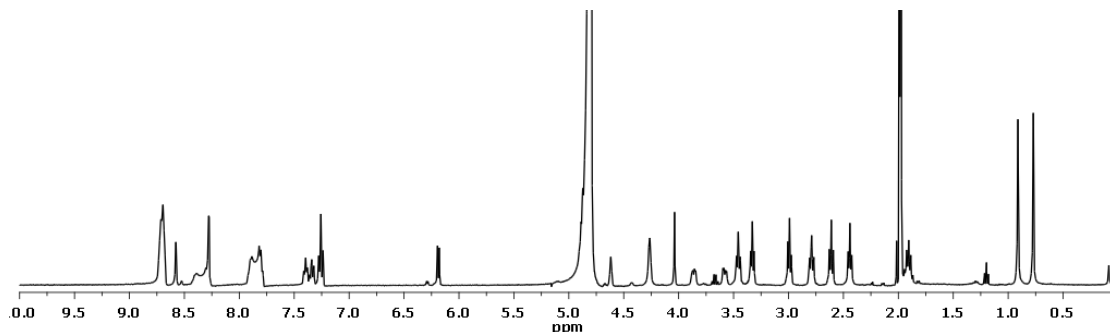


**Figure 2.27:**  $^1H$  NMR spectrum ( $D_2O$ ) of OCPB-CoA, 10-0 ppm

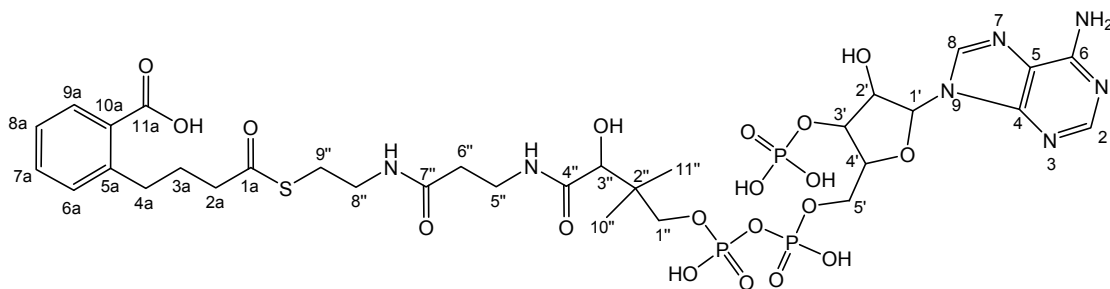


**Table 2.2: Chemical shifts of the protons of OCPB-CoA**

$^1H$	$\delta$ (ppm)	$^1H$	$\delta$ (ppm)
2a	2.44, t, 2H	4'	4.03, d, 1H
3a	1.92, m, 2H	5'	4.26, d, 2H
4a	2.79, t, 2H	3''	4.62, s, 1H
6a-8a	7.20-7.40, m, 3H	5''	3.33, t, 2H
2	8.28, s, 1H	6''	2.61, t, 2H
8	8.69, s, 1H	8''	3.46, t, 2H
1'	6.20, d, 1H	9''	2.99, t, 2H
2'	3.86, dd, 1H	10''	0.91, s, 3H
3'	3.57, dd, 1H	11''	0.77, s, 3H

### Synthesis of methyl ester OSB-CoA

24 mg (0.1 mmol) of OSB methyl ester was reacted with 19 mg CDI (0.12 mmol) in 10 mL of anhydrous THF for 2 hours at 35 °C under nitrogen. CoA (40  $\mu$ mol) was dissolved in 10 mL of water, and the pH was adjusted to 7 with 0.1 M NaOH. THF solution was added dropwise over 30 min to the CoA solution, while maintaining pH 7 by adding 0.1 M NaOH dropwise as necessary. After addition was complete, the reaction was allowed to stir another three hours (**Figure 2.28**). The reaction was acidified to pH 1-2 using 1M HCl and extracted with ethyl acetate. The water layer was frozen in liquid nitrogen and lyophilized. The product was purified from the lyophilized powder by semi-preparative HPLC (Vydac C18 column, 10  $\mu$ m particle diameter, 10 mm i.d., 250 mm length). A linear gradient (1 to 40% acetonitrile, 40 min) was applied. The absorbance of the eluent was monitored at 260 nm. Methyl ester OSB-CoA was eluted at 18 min and collected over several runs, frozen and lyophilized.  $^1\text{H}$  NMR (600 MHz,  $\text{D}_2\text{O}$ ) spectrum of methyl ester OSB-CoA was shown in **Figure 2.29**. The assignment for methyl ester OSB-CoA was given in **Table 2.3**. ESI-MS [ $\text{M-H}^-$ ]: calcd 984.17 ( $\text{C}_{33}\text{H}_{45}\text{N}_7\text{O}_{20}\text{P}_3\text{S}^-$ ); found 984.1.

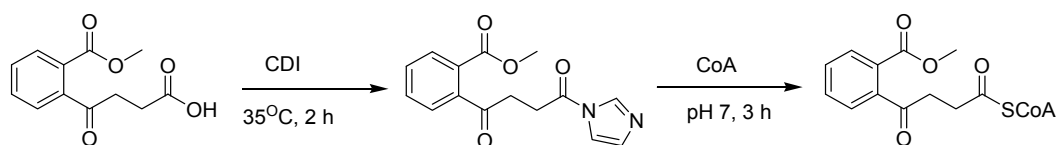


**Figure 2.28: Synthesis of methyl ester OSB-CoA**

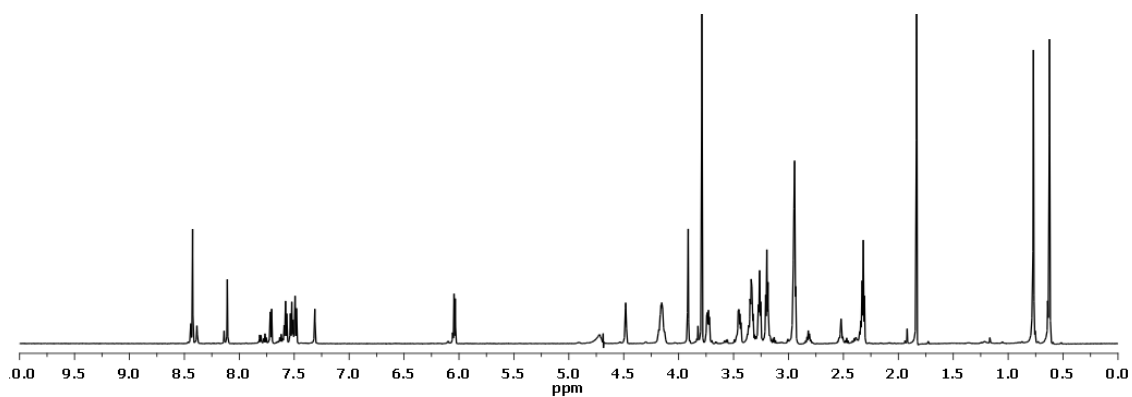


Figure 2.29:  $^1\text{H}$  NMR spectrum ( $\text{D}_2\text{O}$ ) of methyl ester OSB-CoA, 10-0 ppm

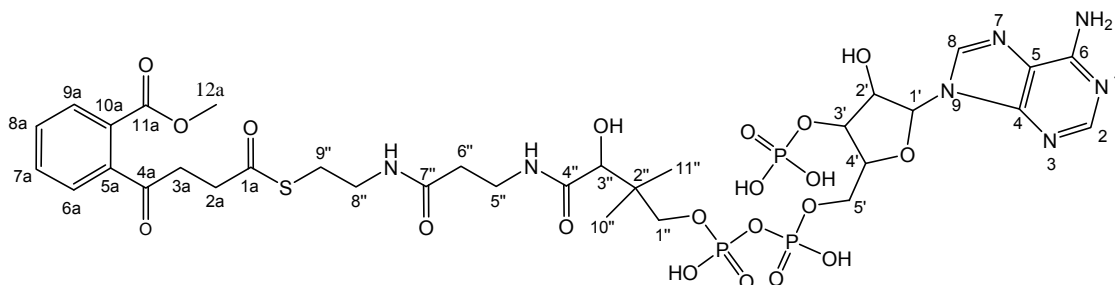


Table 2.3: Chemical shifts of the protons of methyl ester OSB-CoA

$^1\text{H}$	$\delta$ (ppm)	$^1\text{H}$	$\delta$ (ppm)
2a	2.95, t, 2H	4'	(4.50) 4.15, d, 1H
3a	3.26, t, 2H	5'	(4.17) 3.91, d, 1H
6a-10a	7.58-7.31, m, 4H	1''	3.72, 3.45, s, 2H
12a	3.79, s, 3H	3''	3.92, s, 1H
2	8.11, s, 1H	5''	3.34, t, 2H
8	8.44, s, 1H	6''	2.32, t, 2H
1'	6.04, d, 1H	8''	3.21, t, 2H
2'	(4.72) 4.48, dd, 1H	9''	2.95, t, 2H
3'	(4.68) 4.15, dd, 1H	10'', 11''	0.77, 0.64, s, 6H

### *Synthesis of methylamine OSB-CoA and dimethylamine OSB-CoA*

Starting with methylamine OSB and dimethylamine OSB, the standard procedure on page 67 was used to synthesize the methylamine and dimethylamine derivatives of OSB-CoA. Methylamine OSB-CoA was not stable due to the dilactone degradation. Dimethylamine OSB-CoA was stable with ESI-MS [M-H<sup>-</sup>]: calcd 998.20 (C<sub>34</sub>H<sub>48</sub>N<sub>8</sub>O<sub>19</sub>P<sub>3</sub>S<sup>-</sup>); found 997.1.

### *Synthesis of dimethoxy DHNA-CoA*

Starting with dimethoxy DHNA, the standard procedure on page 67 was used to synthesize dimethoxy DHNA-CoA. ESI-MS [M-H<sup>-</sup>]: calcd 980.17 (C<sub>35</sub>H<sub>47</sub>N<sub>7</sub>O<sub>19</sub>P<sub>3</sub>S<sup>-</sup>); found 980.1.

### *Circular dichroism (CD) spectra of wild-type mtMenB and its mutants*

The far-UV circular dichroism (CD) spectra of the wild-type mtMenB protein and its mutant variants were measured at a protein concentration of 20 μM in 20 mM NaH<sub>2</sub>PO<sub>4</sub>, 150 mM NaCl, pH 7.0 buffer at 25 °C by using an AVIV 62 DS spectrometer equipped with a Peltier temperature control unit. The far-UV CD spectra of the wild-type BadI protein and its mutant variants were similarly recorded at a protein concentration of 20 μM in 20 mM Tris-HCl, 150 mM NaCl, pH 7.9 buffer at 25 °C.

CD spectroscopy of different mutants indicated mtMenB mutants retained very similar overall folding as wild-type protein, suggesting that mutagenesis had not altered the overall structure of the protein and that the reduced activity of the

mutant enzymes was not a consequence of a major change in protein structure (Figure 2.30).

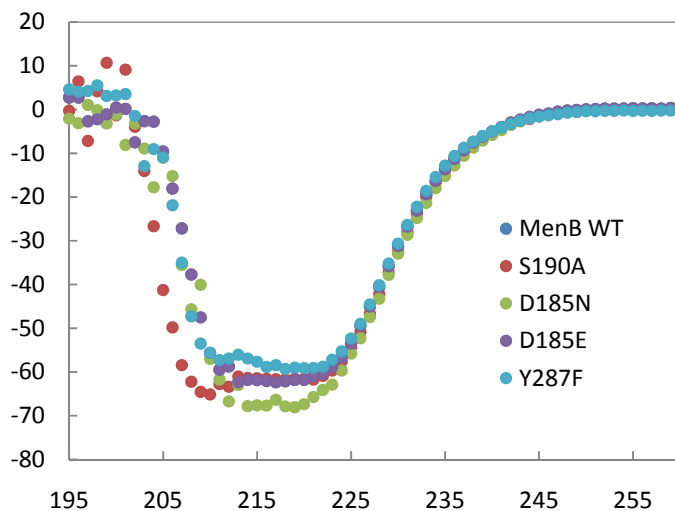


**Figure 2.30: CD spectra of wild-type and mutant mtMenB**

#### *Isothermal titration calorimetry (ITC) binding experiment of mtMenB*

Isothermal titration calorimetry (ITC) was used to analyze the interactions of mtMenB and ligands, by measuring the stepwise change of  $\Delta H^\circ$  during the titration of the ligand into the protein solution. The interaction of mtMenB with 3 BP-CoA, OCPB-CoA, acetoacetyl CoA, methyl ester OSB-CoA, dimethylamine OSB-CoA and dimethoxy DHNA-CoA was monitored. Data was analyzed by applying the one site model to the mtMenB-ligand interaction and using nonlinear least squares curve fitting. ITC experiments were performed on a MicroCal VP-ITC unit with a cell volume of 1.445 mL. All the experiments were conducted in 20 mM  $\text{NaH}_2\text{PO}_4$ , 0.1 M NaCl buffer (pH 7.0) at 25 °C. The concentration of mtMenB was 100  $\mu\text{M}$  and the ligand concentration varied from 1  $\mu\text{M}$  to 2  $\mu\text{M}$  depending on its binding affinity for the enzyme. All solutions were degassed

under the vacuum prior to use. The first data point was routinely deleted before curve fitting to eliminate the effect of diffusion at the protein/ligand interface at the titration syringe tip during the pre-titration equilibration period. Nonlinear least-squares curve fitting was performed using Origin v 5.0 using a standard one-site model supplied by MicroCal.

#### *Alpha-proton exchange reactions catalyzed by mtMenB*

Wild-type mtMenB (100  $\mu$ M) and its mutants were incubated with 2 mM of methyl ester OSB-CoA, 3-BP CoA and OCPB-CoA in a NMR tube, respectively. Proton-deuterium exchange of  $\alpha$ -proton of the ligand was monitored by NMR (600 MHz) spectroscopy at 1h, 3 h, 1 day, 3 days, and 1 week. Prior to the incubation, mtMenB was transferred into D<sub>2</sub>O phosphate buffer (150 mM NaCl, 20 mM NaH<sub>2</sub>PO<sub>4</sub> in D<sub>2</sub>O at pD of 7.0). The ligands separated from HPLC were lyophilized with D<sub>2</sub>O 3 times.

#### *Observing the degradation of DHNA in D<sub>2</sub>O*

DHNA was incubated in D<sub>2</sub>O pD 10.0 in order to observe its degradation product. Without incubation, <sup>1</sup>H NMR (400 MHz, D<sub>2</sub>O) of DHNA:  $\delta$  7.87-7.30 (4H, m), 6.89 (1H, s) ppm; <sup>13</sup>C NMR (400 MHz, D<sub>2</sub>O) of DHNA:  $\delta$  176.18, 151.76, 143.25, 127.84, 125.83, 122.58, 122.49, 110.50, 107.54 ppm. After 2 hour incubation, <sup>1</sup>H NMR (400 MHz, D<sub>2</sub>O) of DHNA degradation product:  $\delta$  7.67-7.11 (4H, m) ppm; <sup>13</sup>C NMR (400 MHz, D<sub>2</sub>O) of DHNA degradation product:  $\delta$  176.11, 151.97, 142.67, 127.59, 125.80, 124.74, 122.55, 121.17, 110.34 ppm (**Figure**

2.31). ESI-MS [M-H<sup>-</sup>]: calcd 218.02 (C<sub>11</sub>H<sub>5</sub>O<sub>5</sub><sup>-</sup>); found 217.0.

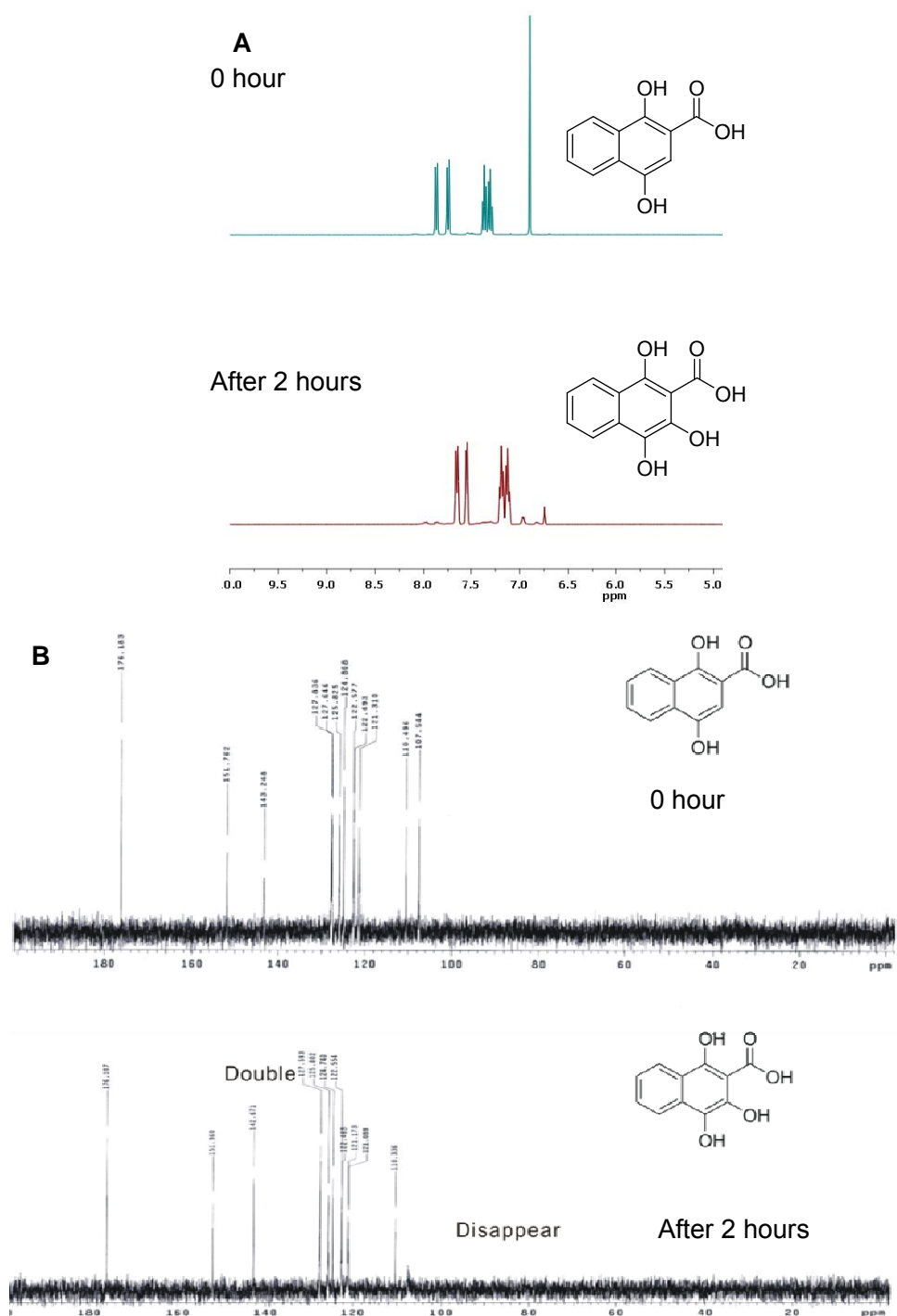


**Figure 2.31: Degradation of DHNA.** Figure A: <sup>1</sup>H NMR spectra (D<sub>2</sub>O, pD 14.0) of DHNA.

Figure B: <sup>13</sup>C NMR spectra (D<sub>2</sub>O, pD 14.0) of DHNA.

### *X-Ray crystallography of mtMenB bound with dimethoxy DHNA-CoA*

mtMenB along with dimethoxy DHNA-CoA were submitted to Dr. James J. Truglio and Prof. Caroline Kisker at the Rudolf Virchow Center, DFG Research Center for Experimental Biomedicine (Germany). The structures were solved with dimethoxy DHNA-CoA bound in the active site.

### *Structural analysis*

The structural data was analyzed using PyMOL (DeLano Scientific LLC.). Superpositions of enzymes structure were generated by aligning the residues of the oxyanion hole. Protein secondary structure analysis was obtained from website (<http://www.rcsb.org/pdb/home/home.do>) based on method mentioned in reference (33).



## Results and discussion

### *Expression and catalytic activity of MenBs (mtMenB, ecMenB and saMenB)*

The MenB enzymes from *M. tuberculosis*, *E. coli* and *S. aureus* (mtMenB, ecMenB and saMenB) were expressed with an N-terminal His-tag and purified by affinity chromatography as previously described (**Figure 2.32**).

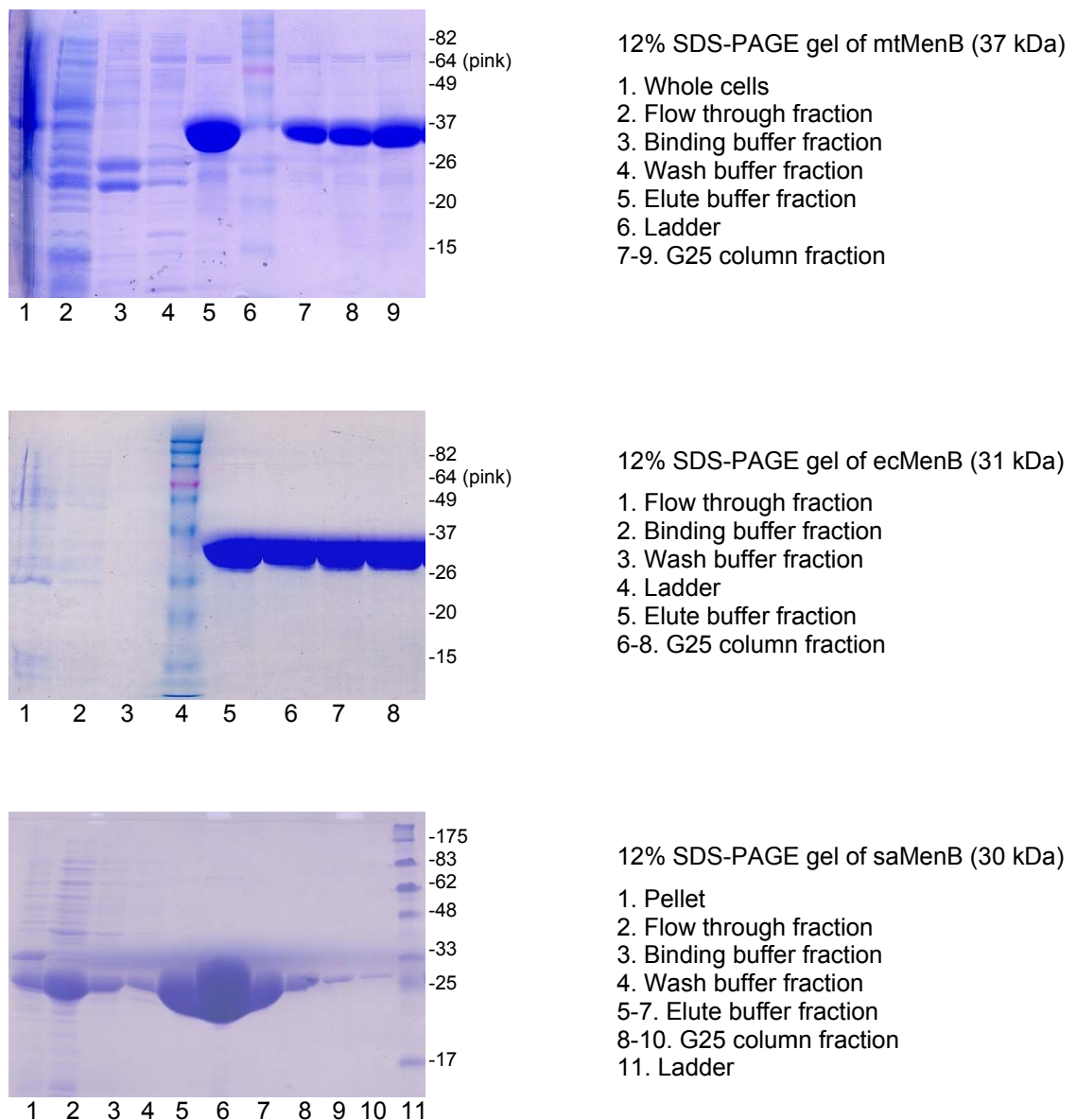


**Figure 2.32: SDS-PAGE gels of mtMenB, ecMenB and saMenB**

Because His-tagged ecMenB and saMenB precipitated readily, N-terminal His-tags were cleavage by thrombin after purification. Non-His-tagged ecMenB was then stable and its catalytic activity wasn't affected after the cleavage of the N-terminal His-tag. However, the stability of non-His-tagged saMenB wasn't improved, and both saMenBs showed extremely low catalytic activity which was only observed at 10  $\mu\text{M}$  enzyme concentration. The kinetic parameters for the MenB enzymes are shown in **Table 2.4**. Surprisingly, given the slow growth rate of *M. tuberculosis*,  $k_{cat}$  for mtMenB was significantly larger than for ecMenB and saMenB.

**Table 2.4: Kinetic parameter for wild-type mtMenB, ecMenB and saMenB**

Enzyme	$k_{cat}$ ( $\text{min}^{-1}$ )	$K_m$ ( $\mu\text{M}$ )	$k_{cat}/K_m$ ( $\text{min}^{-1}\cdot\mu\text{M}^{-1}$ )
mtMenB	$27.7 \pm 0.9$	$22.4 \pm 2.1$	$1.2 \pm 0.2$
ecMenB	$3.7 \pm 0.1$	$25.9 \pm 3.3$	$0.14 \pm 0.03$
saMenB	Showed very low activity at 10 $\mu\text{M}$ saMenB		

#### *Binding and alpha-proton exchange studies of substrate analogues of mtMenB*

A series of MenB substrate analogues have been synthesized to investigate the mechanism of the reaction catalyzed by MenB (**Figure 2.33**). The ITC data suggests that changes to the structure of the OSB acyl group only have a modest effect on the affinity of the ligands for the enzyme with the exception of the dimethylamide OSB-CoA analogue (**Table 2.5**). Based on the ITC data, it is suggested that the aromatic carboxyl group in the OSB portion and entire CoA

molecule are essential for binding. The interaction between the CoA thioester and oxyanion-hole residues contributes the major binding capacity for substrate. It has been shown that both CoA and AcAc-CoA (**Figure 2.4**) have good binding affinity with the protein although they lack the OSB framework. The aromatic carboxyl group is also important for binding since methyl ester OSB-CoA ( $K_d = 11.5 \mu\text{M}$ ) has a better binding affinity than 3-BP CoA ( $K_d = 33.0 \mu\text{M}$ ). The fact of the poor binding affinity of 3-BP CoA which is even worse than CoA and AcAc-CoA indicates that the aromatic ketone in the OSB portion might not be the key factor for binding. Dimethylamide OSB-CoA cannot bind into the active site, suggesting that the space for fitting the aromatic carboxyl group into the active site is crucial.

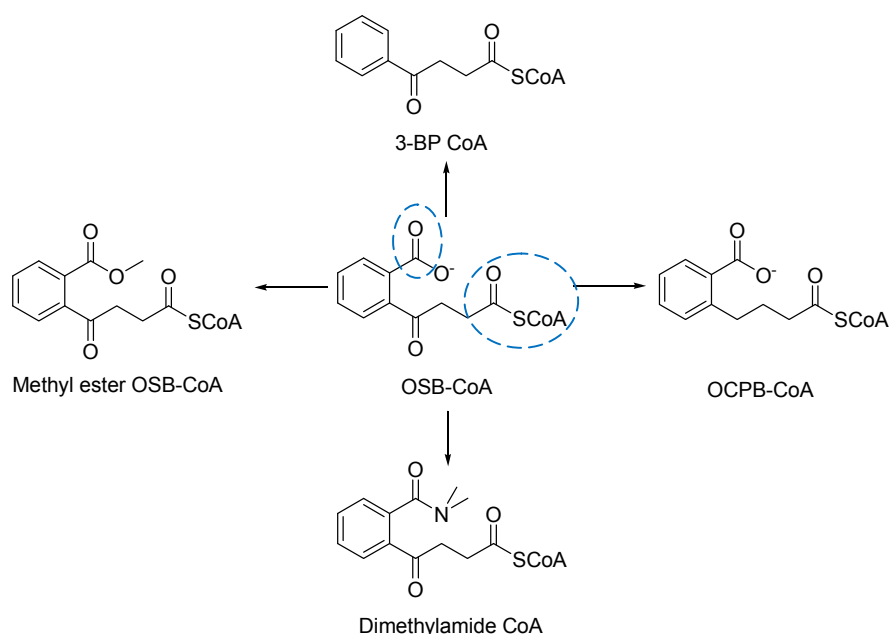


**Figure 2.33: Structures of MenB substrate analogues.** Both aromatic carboxyl group and CoA thioester are crucial for binding.

**Table 2.5: Binding affinity of mtMenB with substrate analogues (by ITC)**

Substrate analogue	$K_d$ ( $\mu\text{M}$ )
CoA	$24.2 \pm 1.4$
AcAc-CoA	$21.0 \pm 1.2$
Methyl ester OSB-CoA	$11.5 \pm 1.2$
OCPB-CoA	$16.6 \pm 1.5$
3-BP CoA	$33.0 \pm 1.6$
Dimethylamide OSB-CoA	No binding at 4 mM of ligand

Based on the mechanism of Dieckmann condensation which is proposed in reference (14), the proton at the  $\alpha$ -carbon of CoA thioester will be abstracted to form an oxyanion before the nucleophilic attack occurs (**Figure 2.34**). Therefore, a proton-deuterium exchange at this position could happen if the substrate analogues are perfectly fitted into the active site. 2 mM of methyl ester OSB-CoA, 3-BP CoA and OCPB-CoA were incubated with wild-type mtMenB (100  $\mu\text{M}$ ) and its mutants in  $\text{D}_2\text{O}$ , respectively, at different length of period. Unfortunately, no  $\alpha$ -proton exchange was observed in the experiment. One reasonable explanation is that the conformation of the active site of MenB doesn't adapt to the deprotonation upon binding with the above substrate analogues. It was suggested neither of these substrate analogues correctly position into the active site and prepare to abstract the proton of  $\alpha$ -carbon of thioester.

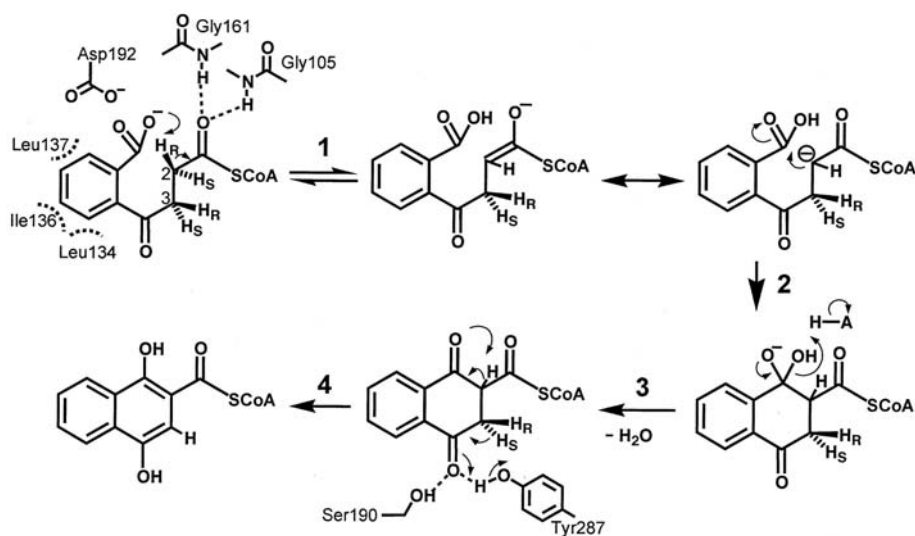


**Figure 2.34: Proposed mechanism of reaction catalyzed by MenB**

If the leaving group in the proposed mechanism is water, then methanol should work as a better leaving group. In this regard, we designed substrate analogue, methyl ester OSB-CoA, assuming it might be a good substrate for MenB since it contains a better leaving group. However, it was shown that methyl ester OSB-CoA is not a substrate for MenB. Therefore, it can be deduced that the free carboxyl group is essential for the reaction. The lack of activity of OSB methyl ester led us to reconsider the decomposition of OSB-CoA and its relationship to the enzyme catalyzed reaction.

We also tried to use the OCPB-CoA and 3-BP CoA for co-crystallization with mtMenB. Unfortunately, the experiments were not successful.

#### *Lactone OSB-CoA might be the substrate for mtMenB*

The substrate for MenB, OSB-CoA, is unstable and decomposes to spirodilactone in solution as shown in **Figure 2.35**. The decomposition might

undergo a lactone intermediate and therefore the equilibrium of OSB-CoA and lactone OSB-CoA might exist in solution before the release of the CoA molecule (**Figure 2.35**).

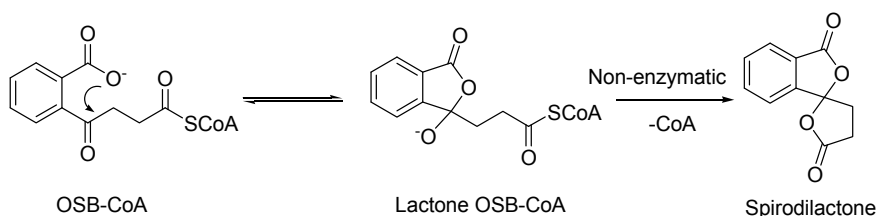


**Figure 2.35: The degradation of OSB-CoA to spirodilactone**

The study of the equilibrium between OSB and lactone OSB (**Figure 2.36**) was instead used to examine the equilibrium between OSB-CoA and lactone OSB-CoA since the existence of the molecule CoA won't affect the equilibrium. To examine the formation of a lactone from OSB, NMR spectra of OSB were acquired under a variety of conditions. It was found that in D<sub>2</sub>O at pD 14.0 the major species was OSB. However under acidic conditions or in CD<sub>3</sub>CN (0.025% DCI) the lactone of OSB was formed which was characterized by a new resonance in the NMR spectrum at 112 ppm (**Figure 2.37**). Therefore it can be concluded that basic conditions favor OSB and OSB-CoA while acidic conditions stabilize the lactone formation.

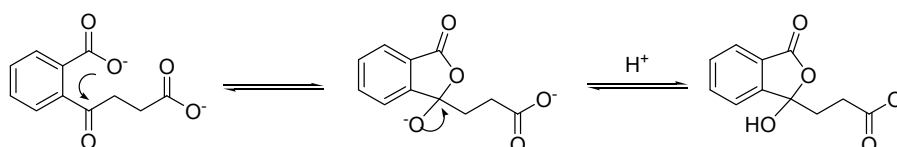


**Figure 2.36: The equilibrium of OSB and lactone OSB**

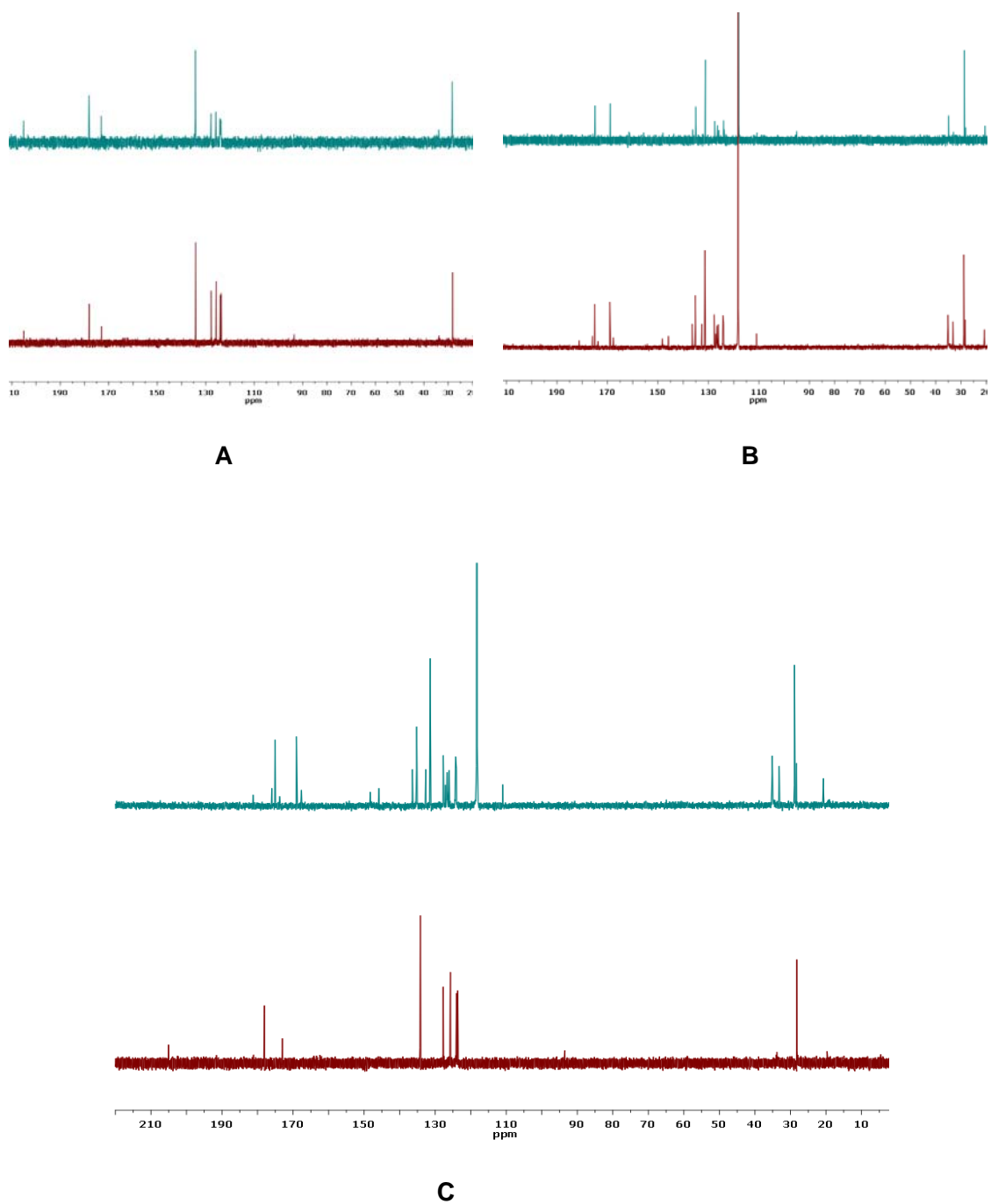


**Figure 2.37:**  $^{13}\text{C}$  NMR spectra of OSB and lactone OSB. Figure A: OSB in  $\text{D}_2\text{O}$  at pD 14.0; Figure B: OSB in  $\text{CD}_3\text{CN}$  (0.025% DCI); C: OSB in  $\text{D}_2\text{O}$  at pD 14.0 and  $\text{CD}_3\text{CN}$  (0.025% DCI) with 2 hour incubation.

In order to directly observe lactone formation we speculated that NMR spectroscopy could be used to monitor lactone formation in situ. This required synthesis of OSB labeled with  $^{13}\text{C}$  at the keto carbonyl. A synthetic route for the labeled OSB using  $^{13}\text{C}$  glutamate is shown in **Figure 2.38**. However the overall yield of OSB was only about 5-10%. Consequently, the biosynthesis of OSB needs further optimization before labeled starting material can be committed.

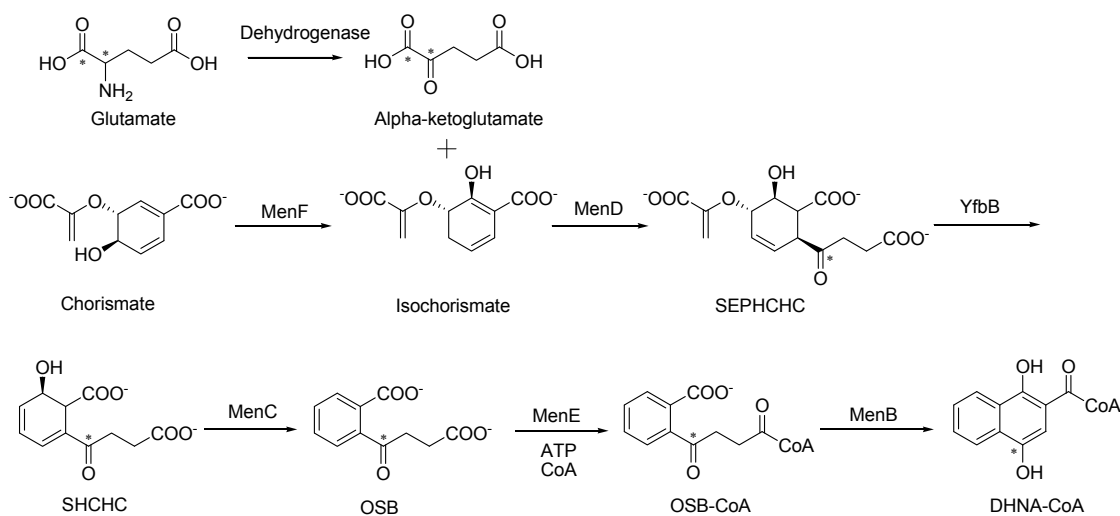


**Figure 2.38: Synthesis of  $^{13}\text{C}$  labeled OSB-CoA from chorismate**

Direct binding experiments and NMR alpha-proton exchange studies together with enzyme kinetics indicate that the aromatic carboxylate in OSB-CoA is essential for reactivity. In addition, methyl ester OSB-CoA and OCPB-CoA are not the substrates for mtMenB, indicating the requirement for the aromatic carboxyl group. Since OSB and OSB-CoA react in solution to form a lactone, we hypothesized that this could be the actual substrate for mtMenB. This possibility is attractive since the lactone carbonyl is more reactive than a free carboxylate.



In order to explore the possibility that the OSB-CoA lactone is the substrate for mtMenB, pre-incubation experiments were performed with 4  $\mu\text{M}$  of ecMenE. Since OSB-CoA will yield spirodilactone with a half-life of 15 min at 30 °C and more than 2 hours at 0 °C (27), more than 90% of substrates don't convert to spirodilactone and are in the equilibrium between OSB-CoA and lactone OSB-CoA based within 3 min's pre-incubation at 25 °C (**Figure 2.35**).

Pre-incubation for wild-type mtMenB reaction showed different kinetic results supporting the lactone intermediate (**Table 2.6**). Without pre-incubation, the values of  $k_{cat}$  and  $K_m$  values were  $27.7 \pm 0.9 \text{ min}^{-1}$  and  $22.4 \pm 2.1 \mu\text{M}$  respectively. With pre-incubation, the  $k_{cat}$  value didn't change too much since the ring closure step is the rate-limiting step. The  $K_m$  value, however, decreased about 20 fold indicating mtMenB has a better binding affinity with lactone OSB-CoA than with OSB-CoA.

In contrast, pre-incubation for wild-type ecMenB reaction relatively increased the  $K_m$  value for OSB-CoA, suggesting that ecMenB has a better binding affinity with OSB-CoA than with lactone OSB-CoA (**Table 2.6**).

**Table 2.6: Different kinetic data of MenB reaction with/without pre-incubation**

	$k_{cat}$ (min <sup>-1</sup> )	$K_m$ (μM)	$k_{cat}/K_m$ (min <sup>-1</sup> μM <sup>-1</sup> )
Wild-type mtMenB			
Pre-incubation	24.6 ± 0.4	1.3 ± 0.1	18.9 ± 1.9
No incubation	27.7 ± 0.9	22.4 ± 2.1	1.2 ± 0.2
Wild-type ecMenB			
Pre-incubation	3.9 ± 0.2	40.4 ± 4.1	0.09 ± 0.01
No incubation	3.7 ± 0.1	25.9 ± 3.3	0.14 ± 0.03
D185E mtMenB			
Pre-incubation	0.1 ± 0.01	3.7 ± 0.3	0.035 ± 0.005
No incubation	0.14 ± 0.01	4.8 ± 0.3	0.029 ± 0.004

The different pre-incubation results of wild-type mtMenB and wild-type ecMenB reactions suggest that they may utilize lactone OSB-CoA and OSB-CoA as a substrate, respectively. Since the lactone formation activates the carboxylate of OSB-CoA, why would ecMenB favor the substrate of lactone OSB-CoA? Based on the sequence assignment of mtMenB and ecMenB (**Figure 2.39**), the major difference of proposed catalytic residues in the active site of mtMenB and ecMenB is that D185 mtMenB is not conserved in ecMenB. Consequently it was anticipated that D185 would play a key role in the catalytic mechanism of mtMenB.

```

mtMenB      VVAPAGEQGRSSTALSDNPFDAKAWRLVDGFDDLTDITYHRHVDDATVRVAFNRPEVRNA 60
ecMenB      MIYPDEAMLYAPVEWHD-----CSEGFEDIR----YEKSTDGIAKITINRPQVRNA 47
saMenB      -----MTNRQWET-----LRE-YDEIK----YEFY-EGIAKVTINRPEVRNA 36
           :                               :  :::  :.  .  .:::***:***

mtMenB      FRPHTVDELYRVLDHARMSPDVGVLLTGNGPSPKDGGAFCSSGGDQRIRG-RSGYQYAS 119
ecMenB      FRPLTVKEMIQALADARYDDNIGVILTG-----AGDKAFCSSGGDQKVRGDYGGYKDDS 101
saMenB      FTPKTVAEMIDAFSRARDDQNVSVIVLTG-----EGDLAFCSSGGDQKKRG-HGGYVGED 89
           * * * * : . : * * . : : . * : : * * * * * * * * * * * * * * * *

mtMenB      GDTADTVDVARAGRLHILEVQRLIRFMPKVVICLVNGWAAFGGHSLSLHVCDLTLASREYA 179
ecMenB      -----GVHHLNVLDFQRQIRTCPKPVVAMVAGYSIFGGHVLHMMCDLTIAA-DNA 150
saMenB      -----QIPRLNVLDLQRLIRIIPKVIAMVKGYAVFGGNVLNVCDLTIAA-DNA 138
           : * : : * . * * * * * * * * * * * * * * * * * * * * * *

mtMenB      RFKQT DADVGS F D GGYGSAYLARQVGQKFAREIFFLGRTYTAEQMHQMGAVNAVAEHAEL 239
ecMenB      IFGQT GPKVGS F D GGGWASYMARIVGQKKAREIWFLCRQYDAKQALDMGLVNTVVPLADL 210
saMenB      IFGQT GPKVGS F D AGYGSGYLARIVGHKKAREIWYLCRQYNAQEALDMGLVNTVVPLEKV 198
           * * * . . * * * * . * : : * * * * * * * * * * * * * * * * * *

mtMenB      ETVGLQWAAEINAKS PQAQRMLKFAFNLLDDGLVGQQLFAGEATRLAYMTDEAVEGRDAF 299
ecMenB      EKETVRWCREMLQNSPMLRCLKAALNADCDGQAGLQELAGNATMLFYMTEEGQEGRNAF 270
saMenB      EDETVQWCKEIMKHS PTALRFLKAAMNADTDGLAGLQQMAGDATLLYTTDEAKEGRDAF 258
           * : : * . * : : * * * * * * * * * * * * * * * * * * * * * *

mtMenB      LQKRPPDWSPFPRYF 314
ecMenB      NQKRQPDFSKFKRNP 285
saMenB      KEKRDPDFDQFPKFP 273
           : * * * * . * :

```

**Figure 2.39: Sequence alignment of mtMenB, ecMenB and saMenB.** mtMenB and ecMenB share 46% identity; mtMenB and saMenB share 50% identity; and ecMenB and saMenB share 62% identity. Residues of the oxyanion hole are in blue; conserved catalytic residues are in red; and unconserved active-site residues are in gray. The cyan residues mark the start of the C-terminal domain in mtMenB and saMenB whose structures have been characterized.

### Catalytic functional role of D185 mtMenB

Although the oxyanion hole residues together with S190, D192 and Y287 (mtMenB numbering) are conserved in all MenB enzymes, D185 in mtMenB is replaced with a glycine in ecMenB and saMenB (**Figure 2.39**). Site-directed mutagenesis was used to replace each of these residues and to examine their role in the overall reaction (**Table 2.7**). D185N, D185G, D192N and Y287F mtMenB enzymes showed no activity at the concentration of 3  $\mu\text{M}$  of enzyme, while D185E and S190A mutants have  $k_{cat}/K_m$  value reduced 40 and 600-fold respectively compared to the wild-type of mtMenB.

**Table 2.7: Kinetic parameter mutant mtMenB, ecMenB and saMenB**

Enzyme	$k_{cat}$ ( $\text{min}^{-1}$ )	$K_m$ ( $\mu\text{M}$ )	$k_{cat}/K_m$ ( $\text{min}^{-1}\cdot\mu\text{M}^{-1}$ )
wt mtMenB	$27.7 \pm 0.9$	$22.4 \pm 2.1$	$1.2 \pm 0.2$
D185E	$0.14 \pm 0.01$	$4.8 \pm 0.3$	$0.029 \pm 0.004$
S190A	$0.10 \pm 0.01$	$40.2 \pm 4.5$	$0.002 \pm 0.001$
D185N, D185G, D192N, and Y287F	No activity at 3 $\mu\text{M}$ mtMenB		
wt ecMenB	$3.7 \pm 0.1$	$25.9 \pm 3.3$	$0.14 \pm 0.03$
G156D	No activity at 3 $\mu\text{M}$ ecMenB		
wt saMenB	Showed very low activity at 10 $\mu\text{M}$ saMenB		
G144D	No activity at 10 $\mu\text{M}$ saMenB		

Although D185 mtMenB is not conserved in all MenBs such as ecMenB and saMenB in which they all use a glycine, it is conserved as the E164 in enoyl-CoA hydratase from rat which involves in the addition/abstraction of  $\alpha$ -proton (34-39) and shares the same stereochemistry of pro-2*R* proton as mtMenB (40). Enoyl-CoA hydratase, the prototypical member of the crotonase superfamily, specifically catalyzes the *syn*-hydration of *trans*-2-enoyl-CoA thioesters to the corresponding 3-(*S*)-hydroxyacyl-CoA thioesters (**Figure 2.40**) (41, 42). The equilibrium of the enoyl-CoA hydratase-catalyzed reaction favors the hydration by a factor of 3.5 at 25 °C (43).

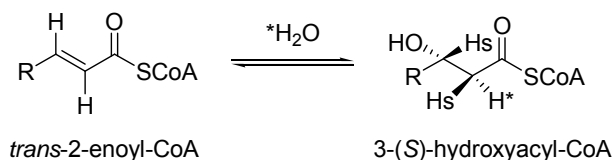


**Figure 2.40: S-specific reaction catalyzed by enoyl-CoA hydratase**

D185 mtMenB and E164 enoyl-CoA hydratase are located in similar positions in the active site (**Figure 2.41A**). Therefore, D185 may facilitate the reaction by abstracting the pro-2*R* proton. From the crystal structure of mtMenB bound with AcAc-CoA, the distance between the D185 and pro-2*R* proton is 3.87 Å (**Figure 2.41B**), which could be even shorter if the lactone OSB-CoA is bound. This is comparable with the distance between E164 enoyl-CoA hydratase and pro-2*R* proton of its ligand, which is 3.03 Å (**Figure 2.41C**).

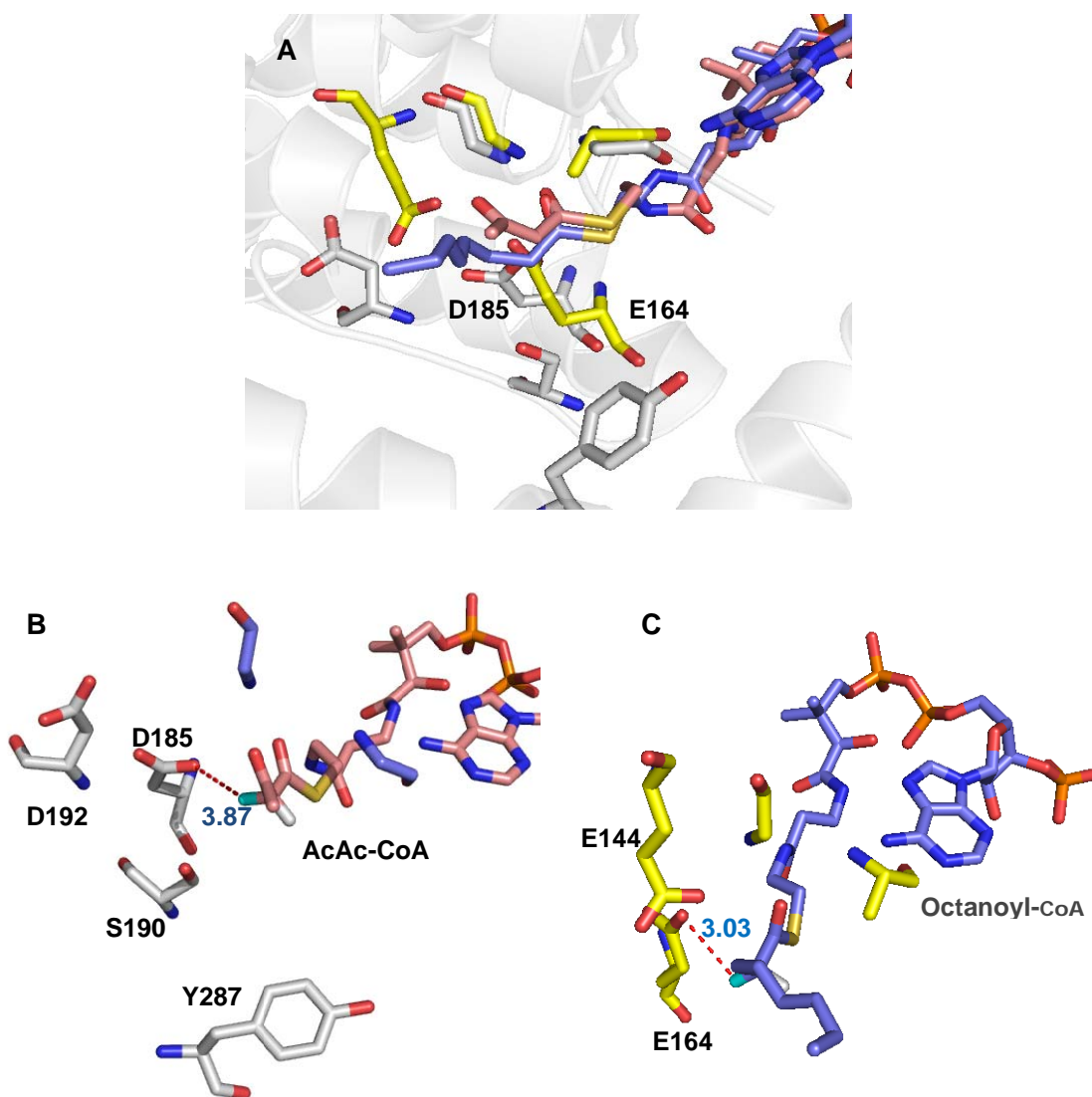


**Figure 2.41: Crystal structures of mtMenB and enoyl-CoA hydratase.** Figure A shows that D185 mtMenB is in the similar position as E164 enoyl-CoA hydratase. Figure B shows that D185 is close to the pro-2R proton of AcAc-CoA. Figure C shows that E164 is close to the pro-2R proton of octanoyl-CoA.

D185 clearly plays a critical role in the mechanism of the mtMenB reaction. Replacement of this residue with a glycine causes a complete loss of activity, while even subtle changes such as the replacement of D185 with a glutamate cause a dramatic decrease in activity (**Table 2.7**). The sensitivity of the reaction rate to changes in D185 mirrors that observed for replacements of the two glutamates in the active site of enoyl-CoA hydratase. For example, both the E164D and E164Q enoyl-CoA hydratase mutants have dramatically reduced activity (1000-330,000 folds) (44). This sensitivity to mutagenesis reflects the critical positioning of the carboxylate side chain in the active site.

However, homologue of D185 mtMenB is a G156 in ecMenB, which indicates that mtMenB and ecMenB might utilize different mechanism for catalysis. In one hand, D185 mtMenB might be involved in abstracting the pro-2*R* proton while ecMenB must use other base for the abstraction. On the other hand, this aspartic acid residue might contribute to the selectivity of the substrate between OSB-CoA and lactone OSB-CoA. Two mutations of D185N and D185G resulted in the total loss of mtMenB activity and  $K_m$  values of two mutants couldn't be estimated accordingly. Although the replacement of D185 with an aspartate caused a 150-fold decrease in activity, D185E reduced the  $K_m$  value for OSB-CoA, indicating the loss of D185 mtMenB increased the binding affinity for OSB-CoA compared to the value observed for the wild-type enzyme (**Table 2.7**).

The sequence alignment (**Figure 2.42**) of around 300 MenBs from different organisms indicate that whether D or G is conserved is a result of evolution.

**Figure 2.43** shows that G is conserved in all MenBs from organisms close to *E. coli* while D is conserved in all MenBs from organisms close to *M. tuberculosis*.

eco_b2262_menB__ECK2256__JW225	AADN-AIFGQT <b>G</b> PKVGSFDGGWGASYMARIVGQKKAREIWFLCRQYDAKQ
ecj_JW2257_menB__dihydroxynaph	AADN-AIFGQT <b>G</b> PKVGSFDGGWGASYMARIVGQKKAREIWFLCRQYDAKQ
ecc_c2805_menB__naphthoate_syn	AADN-AIFGQT <b>G</b> PKVGSFDGGWGASYMARIVGQKKAREIWFLCRQYDAKQ
eci_UTI89_C2545_menB__naphthoa	AADN-AIFGQT <b>G</b> PKVGSFDGGWGASYMARIVGQKKAREIWFLCRQYDAKQ
ecp_ECP_2306_naphthoate_syntha	AADN-AIFGQT <b>G</b> PKVGSFDGGWGASYMARIVGQKKAREIWFLCRQYDAKQ
ecv_APEC01_4299_menB__naphthoa	AADN-AIFGQT <b>G</b> PKVGSFDGGWGASYMARIVGQKKAREIWFLCRQYDAKQ
ecl_EcolC_1386_naphthoate_synt	AADN-AIFGQT <b>G</b> PKVGSFDGGWGASYMARIVGQKKAREIWFLCRQYDAKQ
ecd_ECDH10B_2423_menB__dihydro	AADN-AIFGQT <b>G</b> PKVGSFDGGWGASYMARIVGQKKAREIWFLCRQYDAKQ
ecx_EcHS_A2408_menB__naphthoat	AADN-AIFGQT <b>G</b> PKVGSFDGGWGASYMARIVGQKKAREIWFLCRQYDAKQ
ecw_EcE24377A_2558_menB__napht	AADN-AIFGQT <b>G</b> PKVGSFDGGWGASYMARIVGQKKAREIWFLCRQYDAKQ
ecy_ECSE_2522_dihydroxynaphtho	AADN-AIFGQT <b>G</b> PKVGSFDGGWGASYMARIVGQKKAREIWFLCRQYDAKQ
ecm_EcSMS35_2417_menB__naphtho	AADN-AIFGQT <b>G</b> PKVGSFDGGWGASYMARIVGQKKAREIWFLCRQYDAKQ
sfv_SFV_2333_menB__naphthoate_	AADN-AIFGQT <b>G</b> PKVGSFDGGWGASYMARIVGQKKAREIWFLCRQYDAKQ
sfx_S2475_menB__naphthoate_syn	AADN-AIFGQT <b>G</b> PKVGSFDGGWGASYMARIVGQKKAREIWFLCRQYDAKQ
sfl_SF2341_menB__naphthoate_sy	AADN-AIFGQT <b>G</b> PKVGSFDGGWGASYMARIVGQKKAREIWFLCRQYDAKQ
ecf_ECH74115_3404_menB__naphth	AADN-AIFGQT <b>G</b> PKVGSFDGGWGASYMARIVGQKKAREIWFLCRQYDAKQ
sbc_SbBS512_E2641_menB__naphth	AADN-AIFGQT <b>G</b> PKVGSFDGGWGASYMARIVGQKKAREIWFLCRQYDAKQ
sbo_SBO_2299_menB__naphthoate_	AADN-AIFGQT <b>G</b> PKVGSFDGGWGASYMARIVGQKKAREIWFLCRQYDAKQ
ssn_SSON_2323_menB__naphthoate	AADN-AIFGQT <b>G</b> PKVGSFDGGWGASYMARIVGQKKAREIWFLCRQYDAKQ
ecs_EC3150_naphthoate_synthas	AADN-AIFGQT <b>G</b> PKVGSFDGGWGASYMARIVGQKKAREIWFLCRQYDAKQ
ece_Z3522_menB__naphthoate_syn	AADN-AIFGQT <b>G</b> PKVGSFDGGWGASYMARIVGQKKAREIWFLCRQYDAKQ
sdY_SDY_2458_menB__naphthoate_	AADN-AIFGQT <b>G</b> PKVGSFDGGWGASYMARIVGQKKAREIWFLCRQYDAKQ
seg_SG2336_menB__naphthoate_sy	AAEN-AIFGQT <b>G</b> PKVGSFDGGWGASYMARIVGQKKAREIWFLCRQYDAQQ
set_SEN2289_menB__naphthoate_s	AAEN-AIFGQT <b>G</b> PKVGSFDGGWGASYMARIVGQKKAREIWFLCRQYDAQQ
sed_SeD_A2651_menB__naphthoate	AAEN-AIFGQT <b>G</b> PKVGSFDGGWGASYMARIVGQKKAREIWFLCRQYDAQQ
see_SNSL254_A2492_menB__naphth	AAEN-AIFGQT <b>G</b> PKVGSFDGGWGASYMARIVGQKKAREIWFLCRQYDAQQ
sek_SSPA0520_naphthoate_syntha	AAEN-AIFGQT <b>G</b> PKVGSFDGGWGASYMARIVGQKKAREIWFLCRQYDAQQ
seh_SeHA_C2547_menB__naphthoat	AAEN-AIFGQT <b>G</b> PKVGSFDGGWGASYMARIVGQKKAREIWFLCRQYDAQQ



sea_SeAg_B2443_menB__naphthoat	AAEN-AIFGQTGPKVGSFDGGWGASYMARIVGQKKAREIWFLCRQYDAQQ
sew_SeSA_A2535_menB__naphthoat	AAEN-AIFGQTGPKVGSFDGGWGASYMARIVGQKKAREIWFLCRQYDAQQ
spq_SPAB_00674_naphthoate_synt	AAEN-AIFGQTGPKVGSFDGGWGASYMARIVGQKKAREIWFLCRQYDAQQ
spt_SPA0556_menB__naphthoate_s	AAEN-AIFGQTGPKVGSFDGGWGASYMARIVGQKKAREIWFLCRQYDAQQ
stt_t0556_menB__naphthoate_syn	AAEN-AIFGQTGPKVGSFDGGWGASYMARIVGQKKAREIWFLCRQYDAQQ
sty_STY2537_menB__naphthoate_s	AAEN-AIFGQTGPKVGSFDGGWGASYMARIVGQKKAREIWFLCRQYDAQQ
stm_STM2307_menB__naphthoate_s	AAEN-AIFGQTGPKVGSFDGGWGASYMARIVGQKKAREIWFLCRQYDAQQ
sec_SC2307_menB__naphthoate_sy	AAEN-AIFGQTGPKVGSFDGGWGASYMARIVGQKKAREIWFLCRQYDAQQ
ses_SARI_00592_naphthoate_synt	AAEN-AIFGQTGPKVGSFDGGWGASYMARIVGQKKAREIWFLCRQYDAKQ
cko_CKO_00528_naphthoate_synth	AAEN-AIFGQTGPKVGSFDGGWGASYMARIVGQKKAREIWFLCRQYDAKQ
esa_ESA_00951_naphthoate_synth	AAEN-AVFGQTGPKVGSFDGGWGASYMARIVGQKKAREIWFLCRQYDAQQ
ent_Ent638_2812_naphthoate_syn	AAEN-AVFGQTGPKVGSFDGGWGASYMARIVGQKKAREIWFLCRQYNAQE
kpe_KPK_1489_menB__naphthoate_	AADN-AIFGQTGPKVGSFDGGWGASYMARIVGQKKAREIWFLCRQYDAQQ
kpn_KPN_02660_menB__naphthoate	AAEN-AIFGQTGPKVGSFDGGWGASYMARIVGQKKAREIWFLCRQYDAQQ
eca_ECA1213_menB__naphthoate_s	AAEN-AIFGQTGPRVGSFDGGWGASYMARIVGQKKAREIWFLCRQYDAAQ
spe_Spro_3281_naphthoate_synth	AADN-AIFGQTGPKVGSFDGGWGASYMARIVGQKKAREIWFLCRQYDAAA
ypb_YPTS_2652_naphthoate_synth	AADN-AIFGQTGPKVGSFDGGWGAAYMARIVGQKKAREIWFLCRQYDAKQ
ypy_YPK_1591_naphthoate_syntha	AADN-AIFGQTGPKVGSFDGGWGAAYMARIVGQKKAREIWFLCRQYDAKQ
ypg_YpAngola_A1783_menB__napht	AADN-AIFGQTGPKVGSFDGGWGAAYMARIVGQKKAREIWFLCRQYDAKQ
ypi_YpsIP31758_1484_menB__naph	AADN-AIFGQTGPKVGSFDGGWGAAYMARIVGQKKAREIWFLCRQYDAKQ
ypp_YPDSF_1935_naphthoate_synt	AADN-AIFGQTGPKVGSFDGGWGAAYMARIVGQKKAREIWFLCRQYDAKQ
ypn_YPN_2120_naphthoate_syntha	AADN-AIFGQTGPKVGSFDGGWGAAYMARIVGQKKAREIWFLCRQYDAKQ
ypa_YPA_2017_naphthoate_syntha	AADN-AIFGQTGPKVGSFDGGWGAAYMARIVGQKKAREIWFLCRQYDAKQ
yps_YPTB2558_menB__naphthoate_	AADN-AIFGQTGPKVGSFDGGWGAAYMARIVGQKKAREIWFLCRQYDAKQ
ypm_YP_2336_menB__naphthoate_s	AADN-AIFGQTGPKVGSFDGGWGAAYMARIVGQKKAREIWFLCRQYDAKQ
ypk_y1662_menB__naphthoate_syn	AADN-AIFGQTGPKVGSFDGGWGAAYMARIVGQKKAREIWFLCRQYDAKQ
ype_YPO2525_menB__naphthoate_s	AADN-AIFGQTGPKVGSFDGGWGAAYMARIVGQKKAREIWFLCRQYDAKQ
yen_YE1377_menB__naphthoate_sy	AADN-AIFGQTGPKVGSFDGGWGAAYMARIVGQKKAREIWFLCRQYDAKQ
plu_plu3071_menB__naphthoate_s	AADN-AIFGQTGPKVGSFDGGWGASYMARIVGQKKAREIWFLCRQYDAKQ
pmr_PMI1743_menB__naphthoate_s	AADN-AIFGQTGPKVGSFDGGWGASYMARIVGQKKAREIWFLCRQYNAQE
hsm_HSM_1612_naphthoate_syntha	AAEN-AIFGQTGPKVGSFDGGWGASYMARIVGQKKAREIWFLCRQYNAQE
hso_HS_0562_menB__naphthoate_s	AAEN-AIFGQTGPKVGSFDGGWGASYMARIVGQKKAREIWFLCRQYNAQE

hiq_CGSHiGG_08420_naphthoate_s	AAEN-AIFGQTGPKVGSFDGGWGASYMARLVGQKKAREIWFLCRQYNAQE
hin_HI0968_menB__naphthoate_sy	AAEN-AIFGQTGPKVGSFDGGWGASYMARLVGQKKAREIWFLCRQYNAQE
hip_CGSHiEE_07120_naphthoate_s	AAEN-AIFGQTGPKVGSFDGGWGASYMARLVGQKKAREIWFLCRQYNAQE
hit_NTHI1141_menB__naphthoate_	AAEN-AIFGQTGPKVGSFDGGWGASYMARLVGQKKAREIWFLCRQYNAQE
pmu_PM1096_menB__naphthoate_sy	AADN-AIFGQTGPKVGSFDGGWGASYMARIVGQKKAREIWFLCRQYDAKE
apa_APP7_1910_naphthoate_synth	AADN-AKFGQTGPKVGSFDGGWGASYMARIVGQKKAREIWFLCRMYDAQE
apj_APJL_1860_menB__naphthoate	AADN-AKFGQTGPKVGSFDGGWGASYMARIVGQKKAREIWFLCRMYDAQE
apl_APL_1824_menB__naphthoate_	AADN-AKFGQTGPKVGSFDGGWGASYMARIVGQKKAREIWFLCRMYDAQE
hdu_HD1925_menB__naphthoate_sy	AAEN-AKFGQTGPKVGSFDGGWGASYMARIVGQKKAREIWFLCRMYDAQE
msu_MS1792_menB__naphthoate_sy	AADN-AKFGQTGPKVGSFDGGWGASYMARIVGQKKAREIWFLCRMYDAKE
asu_Asuc_0650_naphthoate_synth	AADN-AKFGQTGPKVGSFDGGWGASYMARIVGQKKAREIWFLCRMYDAKE
aha_AHA_0529_menB__naphthoate_	AADN-AQFGQTGPKVGSFDGGWGASYMARIVGQKKAREIWFLCRMYDAKQ
asa_ASA_3735_menB__naphthoate_	AADN-AQFGQTGPKVGSFDGGWGASYMARIVGQKKAREIWFLCRMYDAQQ
vco_VC0395_A1559_menB__naphtho	AAEN-AQFGQTGPKVGSFDGGWGASYMARIVGQKKAREIWFLCRFYNAQE
vch_VC1973_naphthoate_synthase	AAEN-AQFGQTGPKVGSFDGGWGASYMARIVGQKKAREIWFLCRFYNAQE
vfm_VFMJ11_1794_menB__naphthoa	AAEN-AQFGQTGPKVGSFDGGWGASYMARIVGQKKAREIWFLCRFYDAQE
vfi_VF_1669_menB__dihydroxynap	AAEN-AQFGQTGPKVGSFDGGWGASYMARIVGQKKAREIWFLCRFYDAQE
vvu_VV1_3170_naphthoate_syntha	AAEN-AQFGQTGPKVGSFDGGWGASYMARIVGQKKAREIWFLCRFYDAQE
vvv_VV1118_naphthoate_synthase	AAEN-AQFGQTGPKVGSFDGGWGASYMARIVGQKKAREIWFLCRFYDAQE
vha_VIBHAR_01431_naphthoate_sy	AADN-AQFGQTGPKVGSFDGGWGASYMARIVGQKKAREIWFLCRFYNAQE
vpa_VP0931_naphthoate_synthase	AADN-AQFGQTGPKVGSFDGGWGASYMARIVGQKKAREIWFLCRFYNAQE
pin_Ping_0350_naphthoate_synth	AADN-AQFGQTGPKVGSFDGGWGASYMARIVGQKKAREIWFLCRMYDAQE
hha_Hhal_1129_naphthoate_synth	AAEN-ARFGQTGPRVGSFDGGFGASYMASVVGQKKAREIWFLCRQYDAQE
cph_Cpha266_2091_naphthoate_sy	AADN-AIFGQTGPKVGSFDGGWGASYMARLVGQKKAREIWYLCRQYNAAD
cli_Clim_2050_naphthoate_synth	AAEN-AVFGQTGPKVGSFDGGWGASYMARLVGQKKAREIWYLCRQYNAAE
cch_Cag_1719_naphthoate_syntha	AAEN-AVFGQTGPRVGSFDGGWGASYMARLVGQKKAREIWFLCRQYNAAE
cte_CT1846_menB__naphthoate_sy	AAEN-ARFGQTGPRVGSFDGGWGASYMARLVGQKKAREIWYLCRQYNAQE
cpc_Cpar_0357_naphthoate_synth	AAEN-ARFGQTGPRVGSFDGGWGASYMARLVGQKKAREIWYLCRQYNAQE
plt_Plut_0328_naphthoate_synth	AAEN-ARFGQTGPRVGSFDGGWGASYMARLVGQKKAREIWYLCRQYTAQE
pvi_Cvib_0394_naphthoate_synth	AAEN-AIFGQTGPKVGSFDGGWGASYMARLVGQKKAREIWYLCRQYNAQE
pph_Ppha_2433_naphthoate_synth	AADN-AIFGQTGPKVGSFDGGWGASYMARLVGQKKAREIWFLCRQYNAQE
cpb_Cphamn1_2077_naphthoate_sy	AAEN-AVFGQTGPKVGSFDGGWGASYMARLVGQKKAREIWYLCRQYNAQE

paa_Paes_1880_naphthoate_synth	AAEN-AIFGQTGPKVGSFDGGWGSYMARIVGQKKAREIWYLCRQYNAQE
cts_Ctha_1987_naphthoate_synth	AAEN-AIFGQTGPKVGSFDGGYGASYMARLVGQKKAREIWYLCRQYNAQQ
amu_Amuc_0351_naphthoate_synth	AADN-AKFGQTGPKVGSFDGGLGSSYLARIVGQKKAREIWYLCRQYDARQ
pcu_pc1064_menB__naphthoate_sy	AANN-ARFGQVGPKVGSFDGGLGSSYLARIVGQKKAREIWYLCRQYDAKE
ppp_PHYPADRAFT_141103_hypothes	AADN-AVFGQTGPKVGSFDAGYGCSMMARLVGQKKAREMWFLLAKFYSAEE
osa_4327859_Os01g0662700__hypo	AADN-AIFGQTGPKVGSFDAGYGTSIMSRLVGPKKAREMWFLLSRFYTADE
ath_AT1G60550_naphthoate_synth	AADN-AIFGQTGPKVGSFDAGYGSSIMSRLVGPKKAREMWFMTFRFYTASE
cre_CHLREDRAFT_112040_MEN2__na	AADN-AIFGQTGPKVGSFDAGYGSTHMARLVGQKKAREMWFLLARLYDARE
olu_OSTLU_40076_predicted_prot	AADN-AVFGQTGPKVGSFDAGYGSTHMARLIGQKKAREMWFLLARLYNASD
rxy_Rxyl_2893_naphthoate_synth	AAEN-AIFGQVGPVGSFDGGYGASVLTQLVGPKRRAKEIWFLCRQYTARE
dar_Daro_1616_naphthoate_synth	AADN-ARFGQTGPRVGSFDAGLGAGLMARTIGLKRRAKEVWLLCRQYDATT
ava_Ava_0166_naphthoate_syntha	AADN-AIFGQTGPKVGSFDGGFGASYLARIVGQKKAREIWFLCRQYDAQQ
ana_all2347_naphthoate_synthas	AADN-AIFGQTGPKVGSFDGGFGASYLARIVGQKKAREIWFLCRQYDAQQ
npu_Npun_R3968_naphthoate_synt	AADN-AIFGQTGPKVGSFDGGFGASYLARIVGQKKAREIWFLCRQYDAQQ
cyt_cce_0831_menB__naphthoate_	AADN-AVFGQTGPKVGSFDGGFGASYLARIIGQKKAREIWFLCRQYNAEQ
ter_Tery_4088_naphthoate_synth	AADN-AIFGQTGPKVGSFDGGFGASYLARIVGQKKAREIWFLCRQYTAEQ
syn_sl11127_menB__1_4-dihydrox	AADN-AIFGQTGPKVGSFDGGFGSSYLARIVGQKKAREIWYLCRQYSAQE
mar_MAE_45860_menB__naphthoate	AADN-AIFGQTGPKVGSFDGGFGSSYLARVVGQKKAREIWFLCRQYNAQQ
amr_AM1_5258_menB__naphthoate_	AADN-AIFGQTGPKVGSFDGGFGASYLARVVGQKKAREIWFLCRQYDAQA
cyb_CYB_0565_menB__naphthoate_	AADN-AIFGQTGPRVGSFDGGFGAAYLARVVGQKKAREIWFLCRQYTAQA
cya_CYA_0530_menB__naphthoate_	AADN-AIFGQTGPRVGSFDGGFGASYLARVVGQKKAREIWFLCRQYTAQA
tel_t112458_menB__naphthoate_s	AAEN-AIFGQTGPKVGSFDAGFGASYLARIVGQKKAREIWFLCRQYTAQE
ote_Oter_3116_naphthoate_synth	AADN-AIFGQVGPKMGSFDGGFGSSYLARLVGQKKAREIWFLCRQYNAQQ
syf_Synpcc7942_0597_naphthoate	AADN-AVFGQTGPKVGSFDGGFGASYLARLVGQKKAREIWFLCRQYGAKE
syc_syc0926_d_menB__naphthoate	AADN-AVFGQTGPKVGSFDGGFGASYLARLVGQKKAREIWFLCRQYGAKE
syp_SYNPC7002_A0268_menB__nap	AADN-AIFGQTGPKVGSFDGGFGASYMARIVGQKKAREIWFLCRQYDAQQ
pmb_A9601_06641_menB__naphthoa	ASEN-AIFGQTGPRVGSFDAGFGSSYLARLVGQRKAKEIWFLCRKYNSSE
pmg_P9301_06341_menB__naphthoa	AAEN-AIFGQTGPRVGSFDAGFGSSYLARLVGQRKAKEIWFLCRKYNSKE
pmh_P9215_06901_naphthoate_syn	ASEN-AIFGQTGPRVGSFDAGFGSSYLARLVGQRKAKEIWFLCRKYNSKE
pmi_PMT9312_0608_naphthoate_sy	ASEN-AIFGQTGPRVGSFDAGFGSSYLARLVGQRKAKEIWFLCRKYNSKE
pmc_P9515_06731_menB__naphthoa	ASEN-AIFGQTGPRVGSFDAGFGSSYLARLVGQRKAKEIWFLCRKYNSKE
pmm_PMM0608_menB__naphthoate_s	ASEN-AIFGQTGPRVGSFDAGFGSSYLARLVGQRKAREIWFLCRKYNSKE

pme_NATL1_06641_menB__naphthoa	AADN-AMFGQTGPKVGSFDAGFGSSYLARVVGQKKAREIWFLCRKYGAKE
pmn_PMN2A_0044_naphthoate_synt	AADN-AIFGQTGPKVGSFDAGFGSSYLARVVGQKKAREIWFLCRKYGAKE
syw_SYNW0998_menB__naphthoate_	AADN-AVFGQTGPKVGSFDGGFGAGYLARVVGQRKAREIWFLCRRYGADE
syd_Syncc9605_1123_naphthoate_	AADN-AVFGQTGPKVGSFDGGFGAGYLARVVGQRKAREIWFLCRRYGAKE
sye_Syncc9902_1333_naphthoate_	AADN-AMFGQTGPKVGSFDGGFGAGYLARVVGQRKAREIWFLCRRYGAKD
syx_SynWH7803_1022_menB__napht	AAEN-AVFGQTGPRVGSFDGGFGAGYLARVVGQRKAREIWFLCRRYGAE
syg_sync_1527_menB__naphthoate	AADN-AVFGQTGPRVGSFDGGFGAGYLARVVGQRKAKEIWFLCRQYGAEQ
pmf_P9303_18811_menB__naphthoa	AAEN-AVFGQTGPKVGSFDGGFGAGYLARVVGQRKAREIWFLCRQYGAEE
pmt_PMT0405_menB__naphthoate_s	AAEN-AVFGQTGPKVGSFDGGFGAGYLARVVGQRKAREIWFLCRQYGAEE
pma_Pro1053_menB__naphthoate_s	AADN-AVFGQTGPRVGSFDAGFGAGYLARVVGQRKAREIWFLCRKYGAQE
pmj_P9211_10421_naphthoate_syn	ASDN-AIFGQTGPKVGSFDGGFGAGYLTRVVGQRKAREIWFLCRRYSSEE
syr_SynRCC307_1141_menB__napht	AADN-AQFGQTGPRVGSFDGGYGCAHLARLVGQRKAREIWFLCRRYNAEQ
bat_BAS4748_naphthoate_synthas	AADN-AVFGQTGPKVGSFDGGYGAGYLARMVGHKKAREIWYLCRQYNAQE
btk_BT9727_4586_menB__naphthoa	AADN-AVFGQTGPKVGSFDGGYGAGYLARMVGHKKAREIWYLCRQYNAQE
bar_GBAA5109_menB__naphthoate_	AADN-AVFGQTGPKVGSFDGGYGAGYLARMVGHKKAREIWYLCRQYNAQE
baa_BA_5527_enoyl-CoA_hydratas	AADN-AVFGQTGPKVGSFDGGYGAGYLARMVGHKKAREIWYLCRQYNAQE
ban_BA5109_menB__naphthoate_sy	AADN-AVFGQTGPKVGSFDGGYGAGYLARMVGHKKAREIWYLCRQYNAQE
bt1_BALH_4419_menB__naphthoate	AADN-AVFGQTGPKVGSFDGGYGAGYLARMVGHKKAREIWYLCRQYNAQE
bcz_BCZK4608_menB__naphthoate_	AADN-AVFGQTGPKVGSFDGGYGAGYLARMVGHKKAREIWYLCRQYNAQE
bce_BC4853_naphthoate_synthase	AADN-AVFGQTGPKVGSFDGGYGAGYLARMVGHKKAREIWYLCRQYSAQE
bca_BCE_5013_menB__naphthoate_	AADN-AVFGQTGPKVGSFDGGYGAGYLARMVGHKKAREIWYLCRQYNAQE
bwe_BcerKBAB4_4695_naphthoate_	AADN-AVFGQTGPKVGSFDGGYGAGYLARMVGHKKAREIWYLCRQYSAQE
bcy_Bcer98_3491_naphthoate_syn	AADN-AVFGQTGPKVGSFDGGYGAGYLARMVGHKKAREIWYLCRQYNAQE
gka_GK2873_naphthoate_synthase	AADN-AIFGQTGPKVGSFDGGYGAGYLARIVGHKKAREIWYLCRQYTAQE
gtn_GTNG_2771_naphthoate_synt	AADN-AIFGQTGPKVGSFDGGYGAGYLARIVGHKKAREIWYLCRQYNAQE
afl_Aflv_0383_menB__dihydroxyn	AADN-AIFGQTGPKVGSFDGGYGAGYLARIVGHKKAREIWYLCRQYNAQE
bld_BLi03220_menB__naphthoate_	AADN-AIFGQTGPKVGSFDAGYGSYLARIVGHKKAREIWYLCRQYNAQE
bli_BL02406_menB__naphthoate_s	AADN-AIFGQTGPKVGSFDAGYGSYLARIVGHKKAREIWYLCRQYNAQE
bay_RBAM_027780_naphthoate_syn	AADN-AIFGQTGPKVGSFDAGYGSYLARIVGHKKAREIWYLCRQYNAQE
bsu_BSU30800_menB__naphthoate_	AADN-AIFGQTGPKVGSFDAGYGSYLARIVGHKKAREIWYLCRQYNAQE
bpu_BPUM_2716_menB__naphthoate	AADN-AVFGQTGPKVGSFDAGYGSYLARIVGHKKAREIWYLCRQYNAQE
oih_OB2323_naphthoate_synthase	AADN-AIFGQTGPKVGSFDAGYGSYLARLVGHKKAREIWYLCRQYNADE

sas_SAS0981_naphthoate_synthas	AADN-AIFGQTGPKVGSFDAGYGSGLARIVGHKKAREIWYLCRQYNAQE
sam_MW0929_menB__naphthoate_sy	AADN-AIFGQTGPKVGSFDAGYGSGLARIVGHKKAREIWYLCRQYNAQE
sax_USA300HOU_0993_menB__napht	AADN-AIFGQTGPKVGSFDAGYGSGLARIVGHKKAREIWYLCRQYNAQE
sae_NWMN_0915_memB__naphthoate	AADN-AIFGQTGPKVGSFDAGYGSGLARIVGHKKAREIWYLCRQYNAQE
sao_SAOUHSC_00985_naphthoate_s	AADN-AIFGQTGPKVGSFDAGYGSGLARIVGHKKAREIWYLCRQYNAQE
saa_SAUSA300_0948_menB__naphth	AADN-AIFGQTGPKVGSFDAGYGSGLARIVGHKKAREIWYLCRQYNAQE
sac_SACOL1054_menB__naphthoate	AADN-AIFGQTGPKVGSFDAGYGSGLARIVGHKKAREIWYLCRQYNAQE
sar_SAR1019_menB__naphthoate_s	AADN-AIFGQTGPKVGSFDAGYGSGLARIVGHKKAREIWYLCRQYNAQE
sah_SaurJH1_1127_naphthoate_sy	AADN-AIFGQTGPKVGSFDAGYGSGLARIVGHKKAREIWYLCRQYNAQE
saw_SAHV_1038_menB__naphthoate	AADN-AIFGQTGPKVGSFDAGYGSGLARIVGHKKAREIWYLCRQYNAQE
saj_SaurJH9_1104_naphthoate_sy	AADN-AIFGQTGPKVGSFDAGYGSGLARIVGHKKAREIWYLCRQYNAQE
sav_SAV1045_menB__naphthoate_s	AADN-AIFGQTGPKVGSFDAGYGSGLARIVGHKKAREIWYLCRQYNAQE
sau_SA0898_menB__naphthoate_sy	AADN-AIFGQTGPKVGSFDAGYGSGLARIVGHKKAREIWYLCRQYNAQE
sab_SAB0912_menB__naphthoate_s	AADN-AIFGQTGPKVGSFDAGYGSGLARIVGHKKAREIWYLCRQYNAQE
sha_SH1917_menB__naphthoate_sy	AADN-AIFGQTGPKVGSFDAGYGSGLARIVGHKKAREIWYLCRQYNAQE
sep_SE0746_naphthoate_synthase	AADN-AIFGQTGPKVGSFDAGYGSGLARIVGHKKAREIWYLCRQYNAQE
ser_SERP0632_menB__naphthoate_	AADN-AIFGQTGPKVGSFDAGYGSGLARIVGHKKAREIWYLCRQYNAQE
ssp_SSP1746_naphthoate_synthas	AADN-AIFGQTGPKVGSFDAGYGSGLARIVGHKKAREIWYLCRQYNAQE
lsp_Bsph_4275_naphthoate_synth	AADN-ARFGQTGPKVGSFDAGYGSGLARIVGHKKAREIWYLCRQYDAQQ
esi_Exig_0625_naphthoate_synth	AADN-AKFGQTGPKVGSFDAGYGSGLARIVGHKKAREIWYLCRQYDAQQ
llm_llmg_1831_menB__naphthoate	ASEN-AKFGQTGPRVGSFDAGYGAGLLAAMVQKKAREIWFLCRQYTAKE
llc_LACR_0771_naphthoate_synth	ASEN-AKFGQTGPRVGSFDAGYGAGLLAAMVQKKAREIWFLCRQYTAKE
lla_L0171_menB__naphthoate_syn	ASEN-AKFGQTGPRVGSFDAGYGAGLLAAMVQKKAREIWFLCRQYTAKE
dSY_DSY0520_menB__naphthoate_s	ASEN-ARFGQTGPRVGSFDAGYGAGYLARIVGHKKAREIWYLCRQYTAQE
lmf_LMof2365_1697_menB__naphth	AADN-AKFGQTGPNVGSFDAGYGSGLARIVGHKKAKEVWFMCRQYTADE
lmo_lmo1673_menB__naphthoate_s	AADN-AKFGQTGPNVGSFDAGYGSGLARIVGHKKAKEVWFMCRQYTADE
lin_lin1781_naphthoate_synthas	AADN-AKFGQTGPNVGSFDAGYGSGLARIVGHKKAKEVWFMCRQYTADE
lwe_lwe1691_menB__naphthoate_s	AADN-AKFGQTGPNVGSFDAGYGSGLARIVGHKKAKEVWFMCRQYTADE
lfe_LAF_0969_naphthoate_syntha	AADN-AMFGQTGPKVGSFDAGYGSGLARIVGHKRAKEVWFLNHFYTADE
lsl_LSL_0174_menB__naphthoate_	AADN-AMFGQTGPKVGSFDAGYGSGLARIVGHKRAKEVWFLNHFYTAQE
lrf_LAR_0833_dihydroxynaphthoic	AADN-AKFGQTGPKVGSFDAGYGSGLARIVGHKRAKEVWFLNHFYSAEE
lre_Lreu_0887_naphthoate_synth	AADN-AKFGQTGPKVGSFDAGYGSGLARIVGHKRAKEVWFLNHFYSAEE

lbr_LVIS_0066_naphthoate_synth	AADN-AQFGQTGPKVGSFDAGYGSYLARVIGHKRAKEVWFLNHFYSAEE
ooe_OEOE_0279_naphthoate_synth	AADN-AKFGQTGPKVGSFDAGYGSYLARVIGHKRAKEVWFLNHWTADE
lci_LCK_01696_menB__dihydroxyn	AADN-AKFGQTGPKVGSFDAGYGSYLARVVGHKRAKEVWFLNHVYSADE
lme_LEUM_0016_naphthoate_synth	AADN-AKFGQTGPMVGSFDAGYGSYLARVIGHKRAKEVWFLNHFYTAEE
efa_EF0445_menB__naphthoate_sy	AAEN-AKFGQTGPNVGSFDGGYGSYLARVIGHKKAKEVWFMCKQYSAQE
cau_Caur_0094_naphthoate_synth	AADN-AIFGQTGPKVGSFDGGYGSNLLARMVGDKKAREIWYLCRQYNAQQ
tfu_Tfu_1409_naphthoate_syntha	AADN-ARFGQTGPKVGSFDGGYGSWLLAQTVGLKKAREIWYLCRQYTAQE
pgi_PG1523_menB__naphthoate_sy	AAEH-ARFGQTGPKVGSFDGGFGSSYLARVCGQKKTREIWFLCRQYTAEE
dps_DP0252_naphthoate_synthase	ASEN-AKFGQTGPKVGSFDAGFGSSYLARVQVQKKAREIWFLCDQYSAQE
bfr_BF1318_naphthoate_synthase	ASEN-AIFGQTGPRVGSFDAGFGSSYLARVVQKKAREIWFLCRKYNAQE
bfs_BF1303_menB__naphthoate_sy	ASEN-AIFGQTGPRVGSFDAGFGSSYLARVVQKKAREIWFLCRKYNAQE
bth_BT_4702_naphthoate_synthas	ASEN-AIFGQTGPRVGSFDAGFGASYLARVVQKKAREIWFLCRKYNAQE
pdi_BDI_1137_naphthoate_syntha	ASEN-AIFGQTGPRVGSFDAGFGSSYLARVVQKKAREIWFLCRKYNAQE
bvu_BVU_2417_naphthoate_syntha	ASEN-AIFGQTGPKVGSFDAGFGSSYLARIVGQKKAREIWFLCRQYSAQE
lip_LI0807_menB__naphthoate_sy	ASEN-AIFGQTGPRVGSFDAGLGSSYLARIVGQKVVREIWFLCRQYTAQE
pna_Pnap_2124_naphthoate_synth	CSDK-AQFGQVGPKMGSVDPGYGTAFLARVVGEKKAREIWYLNRRYSGAE
lch_Lcho_1186_2-ketocyclohexan	ASEK-AIFGQVGPKMGSVDPGYGTAFLARVVGEKKAREIWYLNRRYSGAE
vei_Veis_4105_enoyl-CoA_hydrat	CSDK-AQFGQVGPKMGSVDPGYGTAFLARVVGEKKAREIWYLNRRYGGAE
rpa_RPA0653_badI__2-ketocycloh	CSEK-AIFGQVGPKMGSVDPGYGTAFLARVVGEKKAREIWMCKRYSGKE
rpt_Rpal_0720_2-ketocyclohexan	CSEK-AIFGQVGPKMGSVDPGYGTAFLARVVGEKKAREIWMCRYSGKE
rpe_RPE_0612_naphthoate_syntha	CSEK-AIFGQVGPKMGSVDPGYGTAFLARVVGEKKAREIWMCRYSGKE
rpc_RPC_1033_naphthoate_syntha	CSEK-AIFGQVGPKMGSVDPGYGTAFLARVVGEKKAREIWMCRYSGKQ
rpd_RPD_1542_naphthoate_syntha	CSEK-AVFGQVGPKMGSVDPGYGTAFLARVVGEKKAREIWMCRYSGKE
reh_H16_B1695_menB__naphthoate	ASDK-AVFGQVGPKVGSDVDPGYGTAFLARVVGEKKAREIWYLCRRYPAAE
xau_Xaut_0912_naphthoate_synth	ASDK-AQFGQVGPKVGSDVDPGFGTAYLARVVGEKKAREIWYLNKRYSAAE
pla_Plav_1770_naphthoate_synth	AGES-AIFGQVGPKMGSVDPGFGTAYLARVVGEKKAREIWMCRYPARE
reu_Reut_C6107_1_4-dihydroxy-2	ASDT-AIFGQVGPKVGSDVDPGFGTAFLSRVVGEKKAREIWFLCRYPKQ
bch_Bcen2424_6400_naphthoate_s	ASEA-AQLGQVGPVGSVDVDPGFGTALLARVLGEKRAREVWFLCRRYTARE
bcn_Bcen_1429_naphthoate_synth	ASEA-AQLGQVGPVGSVDVDPGFGTALLARVLGEKRAREVWFLCRRYTARE
bcm_Bcenmc03_6839_enoyl-CoA_hy	ASET-AIFGQVGPKVGSDVDPGFGTAYLARIIGEKRAREIWYLCRYSKAKE
eba_ebA1954_badI__2-ketocycloh	ASEK-AQLGQVGPVGSVDVDPGFGTALLARVVGEKKAREIWYLCRRYTAQE
afu_AF1191_menB__dihydroxynaph	ASEK-AKFGQVGPVGSFDPGFGTGELWRNVGMKRAKEIWFLCRLYTAEE

bxe_Bxe_C1035_1_4-dihydroxy-2-	AKES-AIFRQVGPMVGSFDAGYGTWYLEDLVGKKRAKEIWYCNQKITARE
rca_Rcas_4218_naphthoate_synth	AADN-AIFGQTGPIVGSFDAGFGSSYLAIVGQKKAREIWYLCRQYNAQQ
rrs_RoseRS_0024_naphthoate_syn	AADN-AIFGQTGPIVGSFDAGFGSAYLAIVGQKKAREIWYLCRQYNAQQ
mtf_TBFG_10559_naphthoate_synt	ASREYARFKQTADVGSFDGGYGSAYLARQVGQKFAREIFFLGRITYTAEQ
mra_MRA_0555_menB_naphthoate_	ASREYARFKQTADVGSFDGGYGSAYLARQVGQKFAREIFFLGRITYTAEQ
mbb_BCG_0592c_menB_naphthoate	ASREYARFKQTADVGSFDGGYGSAYLARQVGQKFAREIFFLGRITYTAEQ
mbo_Mb0562c_menB_naphthoate_s	ASREYARFKQTADVGSFDGGYGSAYLARQVGQKFAREIFFLGRITYTAEQ
mtc_MT0573_menB_naphthoate_sy	ASREYARFKQTADVGSFDGGYGSAYLARQVGQKFAREIFFLGRITYTAEQ
mtu_Rv0548c_menB_naphthoate_s	ASREYARFKQTADVGSFDGGYGSAYLARQVGQKFAREIFFLGRITYTAEQ
mle_ML2263_menB_naphthoate_sy	ASREHARFKQTADVGSFDGGYGSAYLARQIGQKFAREIFFLGRAYTAEQ
mmi_MMAR_0895_menB_naphthoate	ASRQHARFKQTADVGSFDGGYGSAYLARQVGQKFAREIFFLGRPYTAEQ
mul_MUL_0648_menB_naphthoate_	ASRQHARFKQTADVGSFDGGYGSAYLARQVGQKFAREIFFLGRPYTAEQ
mpa_MAP4044c_menB_naphthoate_	ASREHARFKQTADVGSFDGGYGSAYLARQVGQKFAREIFFLGREYTAEQ
mav_MAV_4596_menB_naphthoate_	ASREHARFKQTADVGSFDGGYGSAYLARQVGQKFAREIFFLGREYTAEQ
mgf_Mflv_0025_naphthoate_synth	ASREHARFKQTADVGSFDGGYGSAYLARQAGQKFAREIFFLGRPYTAEQ
mva_Mvan_0947_naphthoate_synth	ASREHARFKQTADVGSFDGGYGSAYLASQVGQKFAREIFFLGRAYTAEQ
mjl_Mjls_0729_naphthoate_synth	ASRQHARFKQTADVGSFDGGFGSAYLARQTGQKFAREIFFLGRAYDAET
mkm_Mkms_0749_naphthoate_synth	ASRQHARFKQTADVGSFDGGFGSAYLARQTGQKFAREIFFLGRAYDAET
mmc_Mmcs_0735_naphthoate_synth	ASRQHARFKQTADVGSFDGGFGSAYLARQTGQKFAREIFFLGRAYDAET
msm_MSMEG_1075_menB_naphthoat	ASREHARFKQTADVGSFDGGFGSAYLARQTGQKFAREIFFLGRAYDAQT
nfa_nfa51380_menB_naphthoate_	ASREHARFKQTADVGSFDGGYGSAYLAKMVGQKFAREIFFLGRPYTAEQ
rha_RHA1_ro02003_naphthoate_sy	ASREHARFKQTADVGSFDGGYGSAYLAKMVGQKFAREIFFLGETYTAEQ
mab_MAB_3945_naphthoate_syntha	ASREHARFKQTADVGSFDGGYGSAYLAKMVGQKFAREIFFLGRPYTAEQ
sen_SACE_6914_menB_naphthoate	ASAEHARFKQTADVGSFDGGFGSAYLARQVGQKFAREIFFLGRPYTAEQ
nca_Noca_0258_1_4-dihydroxy-2-	ASAEEARFKQTADVGSFDGGFGSAYLARQVGQKFAREIFFLGQEYSAED
kra_Krad_0641_naphthoate_synth	ASAEHARFKQTADVGSFDGGYGSAYLARQVGQKFAREIFFLGRPYTAQQ
cur_cu0255_naphthoate_synthase	ASREHAKFKQTADVGSFDAGYGSAYLAKQVGQKFAREIFFLGEAIDAET
cjk_jk1870_menB_naphthoate_sy	ASREHAKFKQTADVGSFDAGYGSAYLAKQVGQKFAREIFFLGEAIDAET
cgb_cg0548_menB_naphthoate_sy	ASRQEARFKQTADVGSFDAGYGSAYLAKMVGQKNAREIFFLGRITYDAER
cgl_NCg10446_cg10463__naphthoa	ASRQEARFKQTADVGSFDAGYGSAYLAKMVGQKNAREIFFLGRITYDAER
cgt_cgR_0566_naphthoate_syntha	ASRQEARFKQTADVGSFDAGYGSAYLAKMVGQKNAREIFFLGRITYDAER
cef_CE0475_naphthoate_synthase	ASRQEARFKQTADVGSFDAGYGSAYLAKMVGQKFAREIFFLGRITYSAED

cdi_DIP0421_menB__naphthoate_s	ASREHAKFKQTADVGSFDAGYGSAYLAKMVGQKFAREIFFLGRTYDAET
art_Arth_3283_1_4-dihydroxy-2-	ASRQHGFKQTVATVGSFDAGYGSALLARQIGQKAAREIFFLAREYSAED
aau_AAur_3275_menB__naphthoate	ASREHGKFKQTVATVGSFDAGYGSALLARQIGQKAAREIFFLAREYSADD
rsa_RSa133209_2700_naphthoate_	ASKEHGKFKQTVATVGSFDAGYGSALLARQIGQKRAREIFFLAREYSADD
krh_KRH_04970_menB__naphthoate	ASAEHGKFKQTVATVGSFDAGYGSALLARQVQKFAREIFFLADEYSAED
cms_CMS_2584_menB__naphthoate_	ASAEHGRFKQTVADVGSFDGGYGSAYFARQVQKKAAREVFFLAEHSAQR
cmi_CMM_0576_menB__naphthoate_	ASAEHGRFKQTVADVGSFDGGYGSAYFARQVQKKAAREVFFLAEHSAQR
lxx_Lxx01440_menB__naphthoate_	ASEEHGRFKQTVADVGSFDAGYGSAYFARQVQKFGREVFFLAREYSARR
pac_PPA0907_naphthoate_synthas	ASREYARFKQTVANVGSFDAGYGSALLARQIGDKRAREIFFLAETYDAEQ
scl_sce5310_menB__naphthoate_s	ASREHAMFKQTPDVASFDSGYGSALLARQVQKKAREIFFLGLDYTAEQ
mxa_MXAN_3154_menB__naphthoate	ASKEHAVFKQTVADVASFAGYGSALLARQIGQKRAREIFFVGANYSAEE
bba_Bd3492_menB__naphthoate_sy	ASQEHAIFKQTPDVASFDSGYGSAYLARMVGQKRAREIFFLGRNYSAQE
sat_SYN_02400_naphthoate_synth	ASKEHAVFKQTPDVASFDSGYGSAYLAKHIGQKRAREIFFLGLDYSAQD
swd_Swoo_4886_naphthoate_synth	ASKEHAIFKQTPDVASFDSGYGSAYLAKMIGQKRAREIFFLGFNYSADE
sse_Ssed_4478_naphthoate_synth	ASKEHAIFKQTPDVGSFDSGYGSAYLAKMVGQKRAREIFFLGFNYSADE
spl_Spea_4225_naphthoate_synth	ASKEHAVFKQTPDVGSFDSGYGSAYLAKMIGQKRAREIFFLGFNYTAAE
shl_Shal_4273_naphthoate_synth	ASKEHAVFKQTPDVGSFDSGYGSAYLAKMIGQKRAREIFFLGFNYSAAE
slo_Shew_3814_naphthoate_synth	ASKEHAVFKQTPDVGSFDSGYGSAYLAKMIGQKRAREIFFLGFNYSADE
sfr_Sfri_4030_naphthoate_synth	ASKEHAVFKQTPDVGSFDSGYGSAYLAKMIGQKRAREIFFLGFNYSAAE
saz_Sama_3635_naphthoate_synth	ASKEHAVFKQTPDVASFDSGYGSAYLAKMVGQKRAREIFFLGFNYSADE
sbn_Sbal195_4500_naphthoate_sy	ASKEHAIFKQTPDVASFDSGYGSAYLAKMIGQKRAREIFFCGFNYSADE
sbm_Shew185_4358_naphthoate_sy	ASKEHAIFKQTPDVASFDSGYGSAYLAKMIGQKRAREIFFCGFNYSADE
sbl_Sbal_4340_naphthoate_synth	ASKEHAIFKQTPDVASFDSGYGSAYLAKMIGQKRAREIFFCGFNYSADE
shn_Shewana3_4123_naphthoate_s	ASKEHAVFKQTPDVASFDSGYGSAYLAKMIGQKRAREIFFCGFNYSADE
she_Shewmr4_3918_naphthoate_sy	ASKEHAVFKQTPDVASFDSGYGSAYLAKMIGQKRAREIFFCGFNYSADE
shm_Shewmr7_4010_naphthoate_sy	ASKEHAVFKQTPDVASFDSGYGSAYLAKMIGQKRAREIFFCGFNYSADE
son_SO_4739_menB__naphthoate_s	ASKEHAIFKQTPDVASFDSGYGSAYLAKMIGQKRAREIFFCGFNYSADE
spc_Sputcn32_3920_naphthoate_s	ASKEHAIFKQTPDVASFDSGYGSAYLAKMIGQKRAREIFFCGFNYSADE
shw_Sputw3181_4046_naphthoate_	ASKEHAIFKQTPDVASFDSGYGSAYLAKMIGQKRAREIFFCGFNYSADE
ppr_PBPRB1048_putative_naphtho	ASKDMLFSNRQILMSHHLIQATVRLTLPR-----
hsl_OE2561R_menB__naphthoate_s	ASREHAKFKQTPDVASFDDGGFSAYLAKQVQKTAREIFFLGKTYDAEA
hal_VNG1079G_menB__naphthoate_	ASREHAKFKQTPDVASFDDGGFSAYLAKQVQKTAREIFFLGKTYDAEA



hwa_HQ1874A_menB__naphthoate_s	ASKEHAKFLQT <span style="background-color: red;">█</span> PDVASFDGGFGSAYLAKQIGQKKAREVFFRGGKTYSAAE
sru_SRU_2766_menB__naphthoate_	ASAEHATFKQT <span style="background-color: red;">█</span> PDVASFDGGFGSALLAQVGGQKKAREIFFLGGKDYSADE
hma_rrnAC0841_ech1__naphthoate	ASEEHAKFLQT <span style="background-color: red;">█</span> PDVGSFDGGFGSAYLARQVGGQKKAREVFFLGGKTYDAAE
nph_NP2730A_menB__naphthoate_s	ASEAHAKFLQT <span style="background-color: red;">█</span> PDVASFDAGFGSAYLARQIGHKKAREVFFLGGKTYSADE
tws_TW120_menB__naphthoate_syn	ASLEHAKFKQT <span style="background-color: red;">█</span> ATVASFDGGFGSAYFARQVGGQKFAREVCFLAAEYDAKT
twh_TWT110_menB__naphthoate_sy	ASLEHAKFKQT <span style="background-color: red;">█</span> ATVASFDGGFGSAYFARQVGGQKFAREVCFLAAEYDAKT
gfo_GFO_2070_menB__naphthoate_	ASKEHAIFKQT <span style="background-color: red;">█</span> ADVTSFDAGYGSAYLAKMVGQKKAREIFFLGRNYSAQE
fps_FP0478_menB__naphthoate_sy	ASKEHAIFKQT <span style="background-color: red;">█</span> ADVTSFDGGYGSAYLAKMVGQKKAREIFFLGRNYSAQE
fjo_Fjoh_2784_naphthoate_synth	ASKEHAIFKQT <span style="background-color: red;">█</span> ADVTSFDGGYGSAYLAKMVGQKKAREIFFLGRNYSAQE
chu_CHU_1897_menB__1_4-dihydro	ASKEHAIFKQT <span style="background-color: red;">█</span> ADVTSFDGGYGSAYLAKMVGQKKAREIFFLGRNYSAQE

**Figure 2.42: Part of sequence alignment of MenBs from different organisms**

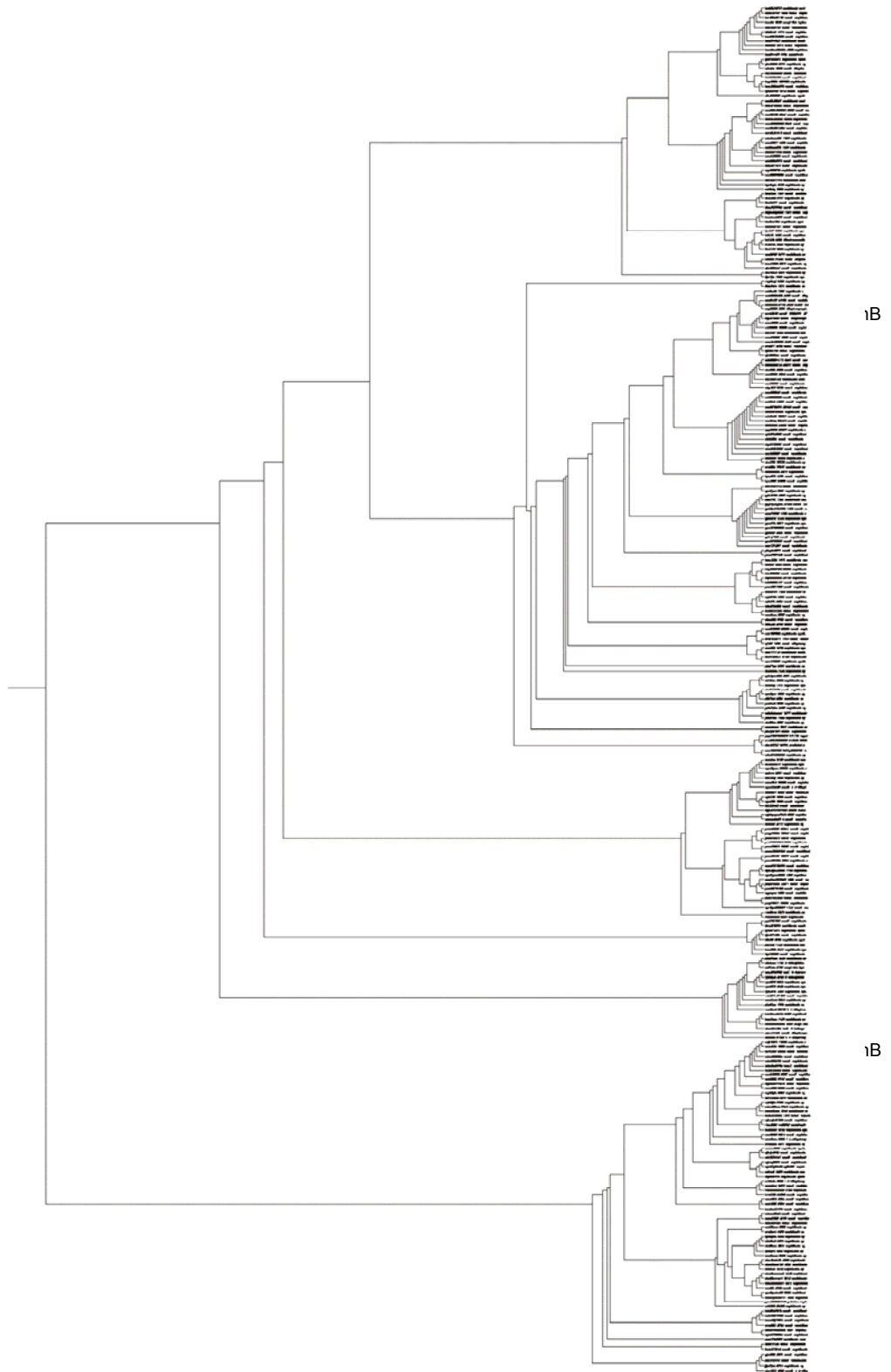


**Figure 2.43: The phylogenetic tree of MenBs from different organisms**

*mtMenB* and *ecMenB* might utilize difference mechanism for catalysis

Based on the special function role of D185 residue, a new mechanism of reaction catalyzed by *mtMenB* is proposed in **Figure 2.44** in which D185 abstracts alpha proton and is related to lactone substrate. *mtMenB* utilizes the lactone OSB-CoA as a substrate in which the carboxylate is activated. Catalytic residue D185 may function as a base and facilitate the water to abstract the pro-2*R* proton. Carbon-carbon bond is formed through the nucleophilic attack. Then residues of S190, D192 and Y287 are involved in removing water molecule and another pro-3*S* proton after the ring closure.

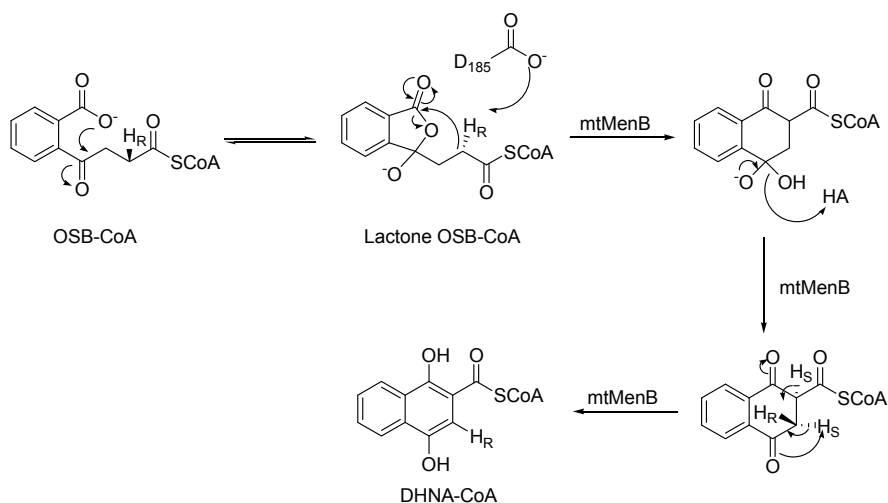


**Figure 2.44: Proposed mechanism of the reaction catalyzed by *mtMenB***

In contrast, the homolog in *ecMenB* is G156 which cannot abstract the pro-2*R* proton. Pre-incubation experiment indicated that the substrate for *ecMenB* is the OSB-CoA not lactone OSB-CoA. On the other hand, methyl ester OSB-CoA is also not the substrate of *ecMenB* suggests the carboxyl group may be involved in deprotonating the pro-2*R* proton in a way as what has been proposed in our

group's previous publication (**Figure 2.45**). The conserved catalytic residues of S119, D121 and Y216 ecMenB play similar functional role for enzymatic catalysis.

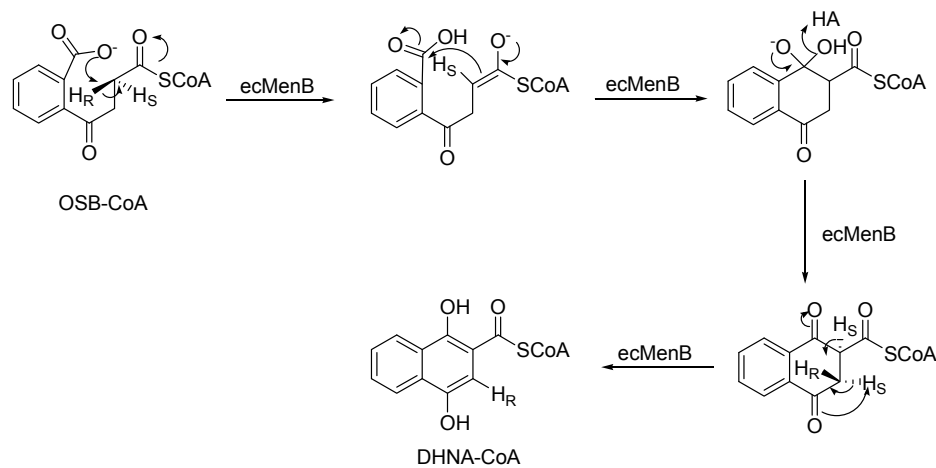


**Figure 2.45: Proposed mechanism of the reaction catalyzed by ecMenB**

*YfbB* and *MenB* cannot catalyze the hydrolysis of DHNA-CoA

The enzyme which catalyzes the hydrolysis of DHNA-CoA to DHNA is still unknown (**Figure 2.46**). It was initially suggested that product of the *MenB* reaction was DHNA. Later, the ORF *yfbB* in *E. coli* was thought to encode a hydrolase (45). There is no homolog of *yfbB* in *M. tuberculosis*.

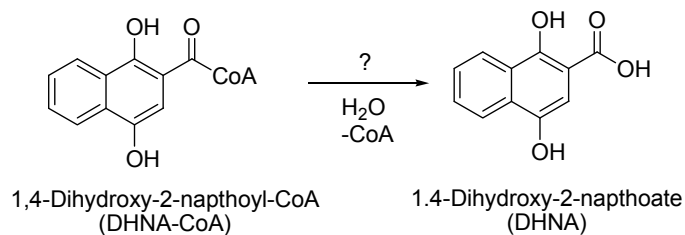


**Figure 2.46: Hydrolysis of DHNA-CoA to DHNA**

We cloned and expressed *YfbB* with an N-terminal His-tag from *E. coli*. The *YfbB* enzyme from *E. coli* was purified by affinity chromatography as a pure band

at 27 kDa (**Figure 2.47**). However, the purified YfbB was unable to catalyze the hydrolysis of DHNA-CoA. Recently, YfbB was characterized as a SHCHC synthase that catalyzes the conversion of SEPHCHC into SHCHC, an earlier step in the menaquinone biosynthetic pathway in *E. coli* (46) (**Figure 2.48**). Clearly, YfbB is not the right enzyme to catalyze the hydrolysis of DHNA-CoA.

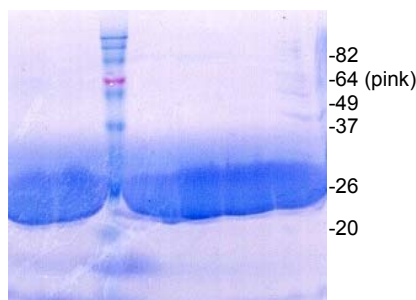


**Figure 2.47: SDS-PAGE gel of YfbB shows it has a molecular weight of 27 kDa**

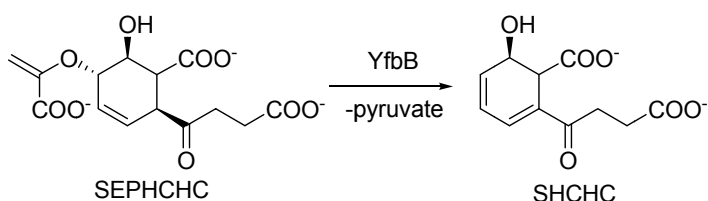


**Figure 2.48: YfbB from *E. coli* catalyzes the conversion from SEPHCHC to SHCHC**

In our attempts to characterize the product of the MenB reaction, we observed that DHNA-CoA was unstable in solution with the formation of a new peak at 340 nm, and that the decomposition of DHNA-CoA accelerated at basic pH values (**Figure 2.49**). At pH 7.0 which is the pH we use for MenB coupled assay, the DHNA-CoA is relatively stable. Since there is no gene coding for hydrolysis near the *men* cluster in *E. coli*, we therefore questioned that whether

the degradation of MenB product was due to the hydrolysis of DHNA-CoA and whether MenB can also catalyze this hydrolysis at higher pH.

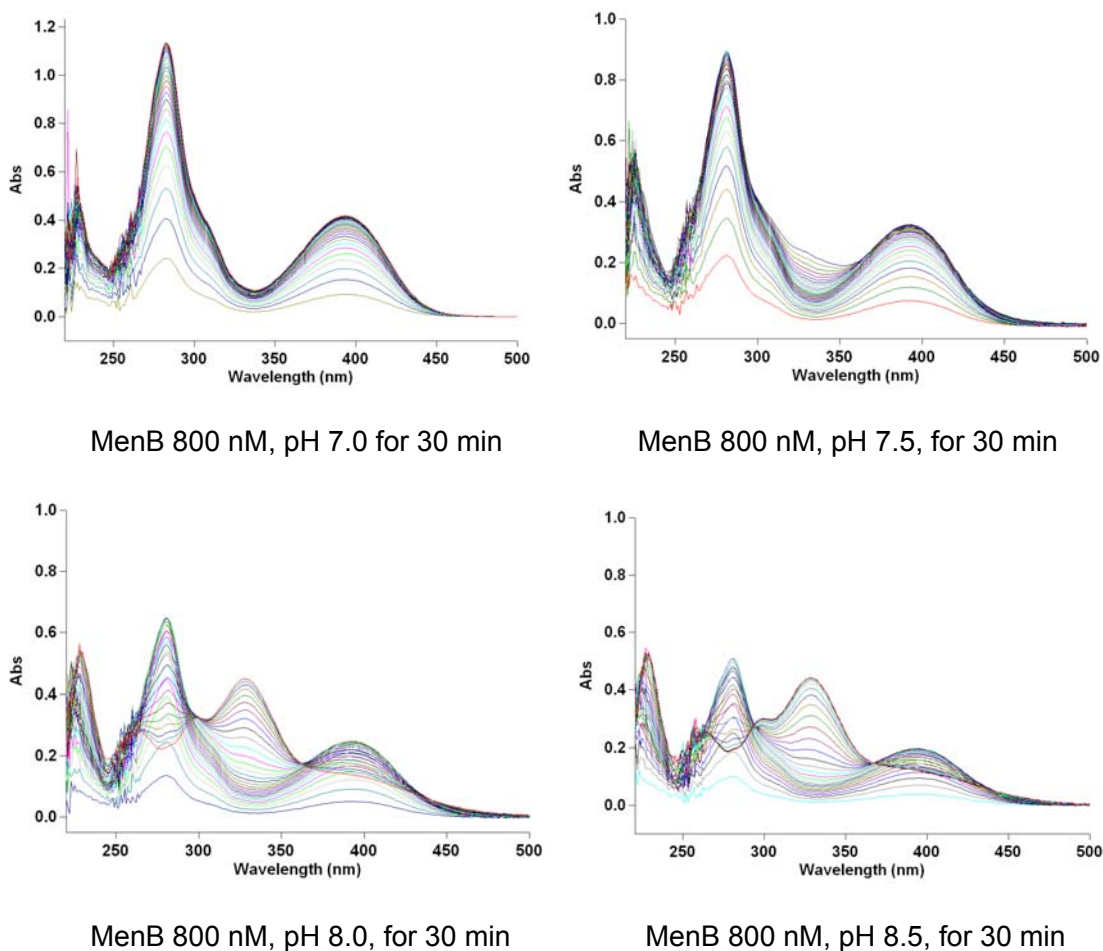


**Figure 2.49: UV scan monitoring the degradation of DHNA-CoA at different pH conditions**

Therefore, OSB, ATP, CoA, MenE and MenB were incubated at pH 7.0, pH 7.5, pH 8.0 and pH 8.5 for 30 min respectively. LC-MS analysis of the different reaction mixtures was performed to determine whether MenB can catalyze the hydrolysis of DHNA-CoA. However, DHNA was not detected in the reaction mixtures at different pH conditions, and the degradation product has the

molecular weight of 967.1 (DHNA-CoA has the molecular weight of 953.1). Based on the molecular weight of 967.1, the degradation reaction is proposed in **Figure 2.50**. Removing the MenB by HPLC didn't block the degradation of DHNA-CoA, which indicates that MenB cannot catalyze the hydrolysis of DHNA-CoA, and DHNA-CoA is intrinsically unstable in basic condition and its degradation is not related to MenB.

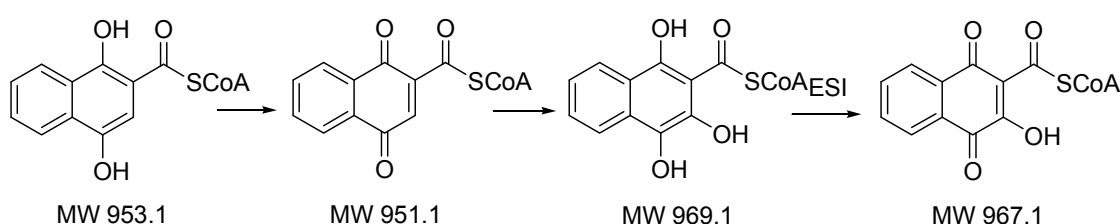


**Figure 2.50: Proposed degradation reaction of DHNA-CoA in solution**

In order to confirm the structure of the degradation product of DHNA-CoA, the NMR spectroscopy of DHNA was analyzed assuming the CoA portion won't affect the degradation reaction. DHNA was incubated in  $D_2O$  at pD 10.0 for 2 hours to accelerate the degradation.  $^1H$  NMR spectrum and  $^{13}C$  NMR spectrum confirmed that DHNA converted to structure **2** by oxidation and water addition in solution. However, ESI-MS spectra indicated that DHNA degradation product has the molecular weight of 218.1 which corresponds to the structure **3**, suggesting a further oxidation occurred during the process of ionization (**Figure 2.51**).

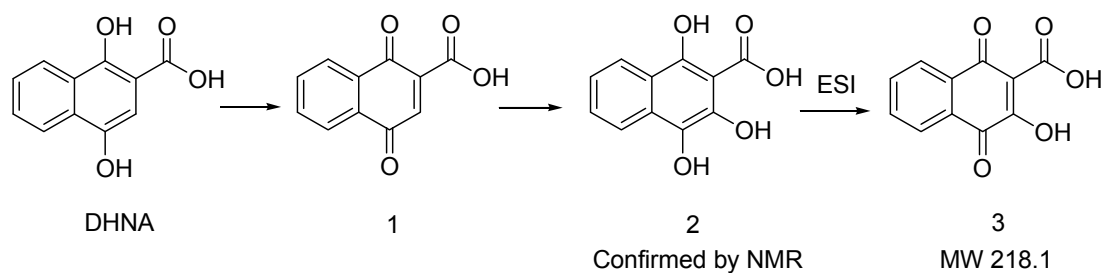


**Figure 2.51: Degradation reaction of DHNA in solution**

*Crystal structure of mtMenB in complex with dimethoxy DHNA-CoA*

The crystal structures of mtMenB and saMenB in complex with AcAc-CoA have been published by our group (14) and Ulaganathan (23) respectively. However AcAc-CoA lacks many of the structural features either of the substrate or product (**Figure 2.52**).

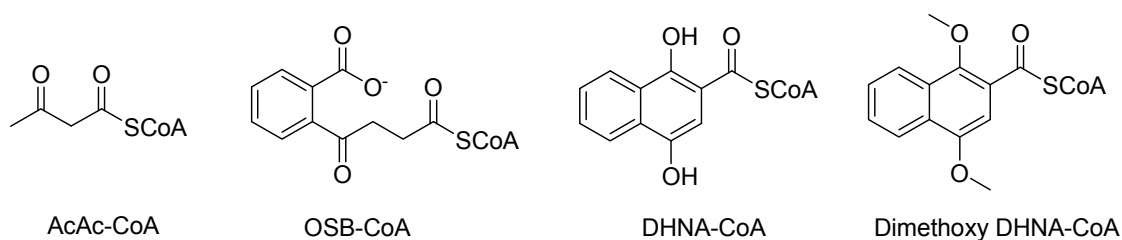


**Figure 2.52: Structures of AcAc-CoA, OSB-CoA, DHNA-CoA and dimethoxy DHNA-CoA**

We know that the product of MenB is not stable due to its oxidative degradation. We designed a stable compound by replacing the hydroxyl groups in the naphthalene moiety with methoxy groups. Dimethoxy DHNA-CoA is a stable product analogue and can be synthesized and purified by HPLC. It binds with mtMenB with a  $K_d$  value of 13.7  $\mu\text{M}$  (by ITC). In addition, this product



analogue is a competitive inhibitor of mtMenB with a  $K_i$  value of  $157.2 \pm 16.1 \mu\text{M}$  (**Figure 2.53**).

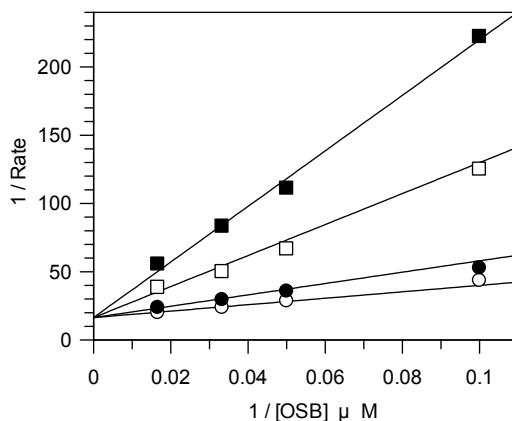


**Figure 2.53: Inhibition of mtMenB with dimethoxy DHNA-CoA.** A lineweaver-Burk plot of the inhibition of mtMenB by dimethoxy DHNA-CoA in the absence of inhibitor (○), in the presence of 120  $\mu\text{M}$  of dimethoxy DHNA-CoA (●), 600  $\mu\text{M}$  of dimethoxy DHNA-CoA (□) or 1200  $\mu\text{M}$  of dimethoxy DHNA-CoA (■).

We successfully obtained the 2.5 Å structure of dimethoxy DHNA-CoA bound to mtMenB. Interestingly, although the CoA molecule is bound in the same position as that in the AcAc-CoA structure, the dimethoxy DHNA moiety occupies a hydrophobic pocket adjacent to the active site (**Figure 2.54**). In this structure the catalytic tyrosine Y287 has rotated toward the active site in order to accommodate the dimethoxy acyl group, while the side chain of R296 has also moved. Although this structure does not provide any additional information on the location of active site residues when the substrate or product are bound in the active site, the discovery of a hydrophobic binding pocket adjacent to the active site may be useful for future inhibitor discovery efforts.

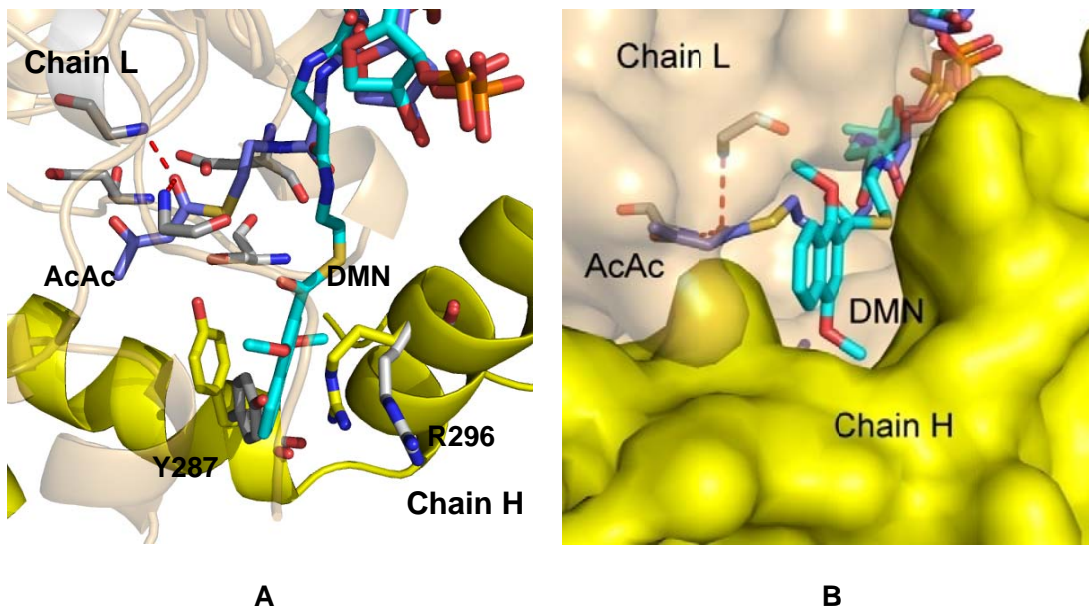


**Figure 2.54: Crystal structure of mtMenB bound with dimethoxy DHNA-CoA.** The active site residues of mtMenB bound with AcAc-CoA are colored in white and the position-changed residues of mtMenB bound with dimethoxy DHNA-CoA (DMN) are shown in yellow.

## Conclusions

MenB, a crotonase superfamily member, catalyzes the formation of a carbon-carbon bond through an intramolecular Claisen/Dieckmann condensation. Catalytic residues of Ser190, Asp192 and Tyr287 (mtMenB numbering) are conserved in all MenBs, while the residue of Asp185 (mtMenB numbering) is not conserved in all MenBs such as MenB from *E. coli* and from *S. aureus*.

mtMenB, ecMenB and saMenB were cloned and expressed. Except saMenB, both mtMenB and ecMenB showed good catalytic activities with the  $k_{cat}/K_m$  value of  $1.2 \pm 0.2 \text{ min}^{-1} \cdot \mu\text{M}^{-1}$  and  $0.14 \pm 0.03 \text{ min}^{-1} \cdot \mu\text{M}^{-1}$  respectively. Hence, the mechanism of MenB reaction catalyzed by enzyme from *M. tuberculosis* was mainly compared with the reaction catalyzed by MenB from *E. coli*.

A series of substrate analogues were synthesized to examine the mechanism of MenB reaction. Direct binding experiments and NMR alpha-proton exchange studies together with enzyme kinetics indicate that the aromatic carboxylate in OSB-CoA is essential for reactivity. Methyl ester OSB-CoA is not substrate for both mtMenB and ecMenB, indicating the free carboxyl group is essential for the reaction. The lack of activity of OSB methyl ester led us to reconsider the decomposition of OSB-CoA and its relationship to the enzyme catalyzed reaction.

The different pre-incubation results of mtMenB and ecMenB reactions suggest that they may utilize lactone OSB-CoA and OSB-CoA as a substrate, respectively. This means mtMenB and ecMenB might utilize difference mechanism for catalysis. mtMenB utilizes the lactone OSB-CoA as a substrate in which the carboxylate is activated. The catalytic residue D185 may function as a

base and facilitate the water to abstract the pro-2*R* proton. In contrast, ecMenB accepts the OSB-CoA as a substrate, and the carboxyl group of OSB-CoA may be involved in deprotonating the pro-2*R* proton in a way as what has been proposed in our group's previous publication.

It was initially suggested that MenB can also catalyze the hydrolysis of DHNA-CoA. Later, the ORF *yfbB* in *E. coli* was thought to encode a hydrolase. Our experiments confirmed that both MenB and YfbB cannot catalyze the hydrolysis reaction. The instability of DHNA-CoA in solution is not relevant to MenB.

Dimethoxy DHNA-CoA is a stable product analogue of MenB. In the crystal structure of mtMenB in complex with dimethoxy DHNA-CoA, the dimethoxy DHNA moiety occupies a hydrophobic pocket adjacent to the active site. Although this structure does not provide any additional information about the active site, the discovery of a hydrophobic binding pocket adjacent to the active site may be useful for future inhibitor discovery efforts.

## References

1. Gerlt, J. A., and Babbitt, P. C. (2001) Divergent evolution of enzymatic function: mechanistically diverse superfamilies and functionally distinct suprafamilies, *Annual review of biochemistry* 70, 209-246.
2. Glasner, M. E., Gerlt, J. A., and Babbitt, P. C. (2006) Evolution of enzyme superfamilies, *Curr Opin Chem Biol* 10, 492-497.
3. Gerlt, J. A., and Babbitt, P. C. (1998) Mechanistically diverse enzyme superfamilies: the importance of chemistry in the evolution of catalysis, *Curr Opin Chem Biol* 2, 607-612.
4. Babbitt, P. C., and Gerlt, J. A. (1997) Understanding enzyme superfamilies. Chemistry As the fundamental determinant in the evolution of new catalytic activities, *The Journal of biological chemistry* 272, 30591-30594.
5. Bahnson, B. J., Anderson, V. E., and Petsko, G. A. (2002) Structural mechanism of enoyl-CoA hydratase: three atoms from a single water are added in either an E1cb stepwise or concerted fashion, *Biochemistry* 41, 2621-2629.
6. Mohrig, J. R., Moerke, K. A., Cloutier, D. L., Lane, B. D., Person, E. C., and Onasch, T. B. (1995) Importance of historical contingency in the stereochemistry of hydratase-dehydratase enzymes, *Science (New York, N.Y)* 269, 527-529.

7. Bell, A. F., Wu, J., Feng, Y., and Tonge, P. J. (2001) Involvement of glycine 141 in substrate activation by enoyl-CoA hydratase, *Biochemistry* 40, 1725-1733.
8. Wong, B. J., and Gerlt, J. A. (2004) Evolution of function in the crotonase superfamily: (3S)-methylglutaconyl-CoA hydratase from *Pseudomonas putida*, *Biochemistry* 43, 4646-4654.
9. Mursula, A. M., van Aalten, D. M., Hiltunen, J. K., and Wierenga, R. K. (2001) The crystal structure of delta(3)-delta(2)-enoyl-CoA isomerase, *J Mol Biol* 309, 845-853.
10. Zhang, D., Liang, X., He, X. Y., Alipui, O. D., Yang, S. Y., and Schulz, H. (2001) Delta 3,5,delta 2,4-dienoyl-CoA isomerase is a multifunctional isomerase. A structural and mechanistic study, *The Journal of biological chemistry* 276, 13622-13627.
11. Benning, M. M., Haller, T., Gerlt, J. A., and Holden, H. M. (2000) New reactions in the crotonase superfamily: structure of methylmalonyl CoA decarboxylase from *Escherichia coli*, *Biochemistry* 39, 4630-4639.
12. Wong, B. J., and Gerlt, J. A. (2003) Divergent function in the crotonase superfamily: an anhydride intermediate in the reaction catalyzed by 3-hydroxyisobutyryl-CoA hydrolase, *J Am Chem Soc* 125, 12076-12077.
13. Benning, M. M., Taylor, K. L., Liu, R. Q., Yang, G., Xiang, H., Wesenberg, G., Dunaway-Mariano, D., and Holden, H. M. (1996) Structure of 4-chlorobenzoyl coenzyme A dehalogenase determined to 1.8 Å resolution:

- an enzyme catalyst generated via adaptive mutation, *Biochemistry* 35, 8103-8109.
14. Truglio, J. J., Theis, K., Feng, Y., Gajda, R., Machutta, C., Tonge, P. J., and Kisker, C. (2003) Crystal structure of *Mycobacterium tuberculosis* MenB, a key enzyme in vitamin K2 biosynthesis, *The Journal of biological chemistry* 278, 42352-42360.
  15. Leonard, P. M., and Grogan, G. (2004) Structure of 6-oxo camphor hydrolase H122A mutant bound to its natural product, (2S,4S)-alpha-campholinic acid: mutant structure suggests an atypical mode of transition state binding for a crotonase homolog, *The Journal of biological chemistry* 279, 31312-31317.
  16. Eberhard, E. D., and Gerlt, J. A. (2004) Evolution of function in the crotonase superfamily: the stereochemical course of the reaction catalyzed by 2-ketocyclohexanecarboxyl-CoA hydrolase, *J Am Chem Soc* 126, 7188-7189.
  17. Gasson, M. J., Kitamura, Y., McLauchlan, W. R., Narbad, A., Parr, A. J., Parsons, E. L., Payne, J., Rhodes, M. J., and Walton, N. J. (1998) Metabolism of ferulic acid to vanillin. A bacterial gene of the enoyl-SCoA hydratase/isomerase superfamily encodes an enzyme for the hydration and cleavage of a hydroxycinnamic acid SCoA thioester, *The Journal of biological chemistry* 273, 4163-4170.
  18. Engel, C. K., Mathieu, M., Zeelen, J. P., Hiltunen, J. K., and Wierenga, R. K. (1996) Crystal structure of enoyl-coenzyme A (CoA) hydratase at 2.5

- angstroms resolution: a spiral fold defines the CoA-binding pocket, *EMBO J* 15, 5135-5145.
19. Kurimoto, K., Fukai, S., Nureki, O., Muto, Y., and Yokoyama, S. (2001) Crystal structure of human AUH protein, a single-stranded RNA binding homolog of enoyl-CoA hydratase, *Structure* 9, 1253-1263.
  20. Modis, Y., Filppula, S. A., Novikov, D. K., Norledge, B., Hiltunen, J. K., and Wierenga, R. K. (1998) The crystal structure of dienoyl-CoA isomerase at 1.5 Å resolution reveals the importance of aspartate and glutamate sidechains for catalysis, *Structure* 6, 957-970.
  21. Whittingham, J. L., Turkenburg, J. P., Verma, C. S., Walsh, M. A., and Grogan, G. (2003) The 2-Å crystal structure of 6-oxo camphor hydrolase. New structural diversity in the crotonase superfamily, *The Journal of biological chemistry* 278, 1744-1750.
  22. Sleeman, M. C., Sorensen, J. L., Batchelar, E. T., McDonough, M. A., and Schofield, C. J. (2005) Structural and mechanistic studies on carboxymethylproline synthase (CarB), a unique member of the crotonase superfamily catalyzing the first step in carbapenem biosynthesis, *The Journal of biological chemistry* 280, 34956-34965.
  23. Ulaganathan, V., Agacan, M. F., Buetow, L., Tulloch, L. B., and Hunter, W. N. (2007) Structure of *Staphylococcus aureus* 1,4-dihydroxy-2-naphthoyl-CoA synthase (MenB) in complex with acetoacetyl-CoA, *Acta Crystallogr Sect F Struct Biol Cryst Commun* 63, 908-913.



24. Pilka ES, P. C., King ONF, Guo K, Von Delft F, Pike ACW, Arrowsmith CH, Weigelt J, Edwards AM, Oppermann U. (2007/12/19 ) Crystal Structure Of Human Beta-Hydroxyisobutyryl-Coa Hydrolase In Complex With Quercetin, *Structural Genomics Consortium (Sgc)*.
25. Lannergard, J., von Eiff, C., Sander, G., Cordes, T., Seggewiss, J., Peters, G., Proctor, R. A., Becker, K., and Hughes, D. (2008) Identification of the genetic basis for clinical menadione-auxotrophic small-colony variant isolates of *Staphylococcus aureus*, *Antimicrobial agents and chemotherapy* 52, 4017-4022.
26. Bryant, R. W., Jr., and Bentley, R. (1976) Menaquinone biosynthesis: conversion of o-succinylbenzoic acid to 1,4-dihydroxy-2-naphthoic acid and menaquinones by *Escherichia coli* extracts, *Biochemistry* 15, 4792-4796.
27. Heide, L., Arendt, S., and Leistner, E. (1982) Enzymatic synthesis, characterization, and metabolism of the coenzyme A ester of o-succinylbenzoic acid, an intermediate in menaquinone (vitamin K2) biosynthesis, *The Journal of biological chemistry* 257, 7396-7400.
28. Heath, R. J., and Rock, C. O. (2002) The Claisen condensation in biology, *Natural product reports* 19, 581-596.
29. Sedlak, J., and Lindsay, R. H. (1968) Estimation of total, protein-bound, and nonprotein sulfhydryl groups in tissue with Ellman's reagent, *Anal Biochem* 25, 192-205.

30. Grisostomi C., Kast P., Pulido R., Huynh J., and Hilvert, D. (1997) Efficient in vivo synthesis and rapid purification of chorismic acid using an engineered *Escherichia coli* Strain, *Bioorg Chem* 25, 297-305.
31. Kolkman R., and E., L. (1987) Synthesis, analysis and characterization of the coenzyme A esters of o-Succinylbenzoic acid, an intermediate in vitamin K2 (menaquinone) biosynthesis, *Z. Naturforsch.* 42c, 542-552.
32. Gallus, C., and Schink, B. (1994) Anaerobic degradation of pimelate by newly isolated denitrifying bacteria, *Microbiology (Reading, England)* 140 ( Pt 2), 409-416.
33. Kabsch, W., and Sander, C. (1983) Dictionary of protein secondary structure: pattern recognition of hydrogen-bonded and geometrical features, *Biopolymers* 22, 2577-2637.
34. Wen-Jin Wu, Y. F., Xiang He, Hilary A. Hofstein, Daniel P. Raleigh and Peter J. Tonge. (2000) Stereospecificity of the Reaction Catalyzed by Enoyl-CoA Hydratase, *J. Am. Chem. Soc.* 122, 3987.
35. Kurosawa, T., Sato, M., Nakano, H., Fujiwara, M., Murai, T., Yoshimura, T., and Hashimoto, T. (2001) Conjugation reactions catalyzed by bifunctional proteins related to beta-oxidation in bile acid biosynthesis, *Steroids* 66, 107-114.
36. Qin, Y. M., Haapalainen, A. M., Conry, D., Cuebas, D. A., Hiltunen, J. K., and Novikov, D. K. (1997) Recombinant 2-enoyl-CoA hydratase derived from rat peroxisomal multifunctional enzyme 2: role of the hydratase reaction in bile acid synthesis, *Biochem J* 328 ( Pt 2), 377-382.

37. Dieuaide-Noubhani, M., Asselberghs, S., Mannaerts, G. P., and Van Veldhoven, P. P. (1997) Evidence that multifunctional protein 2, and not multifunctional protein 1, is involved in the peroxisomal beta-oxidation of pristanic acid, *Biochem J* 325 ( Pt 2), 367-373.
38. Jiang, L. L., Kurosawa, T., Sato, M., Suzuki, Y., and Hashimoto, T. (1997) Physiological role of D-3-hydroxyacyl-CoA dehydratase/D-3-hydroxyacyl-CoA dehydrogenase bifunctional protein, *J Biochem* 121, 506-513.
39. Hiltunen, J. K., and Qin, Y. (2000) beta-oxidation - strategies for the metabolism of a wide variety of acyl-CoA esters, *Biochim Biophys Acta* 1484, 117-128.
40. Igbavboa, U., and Leistner, E. (1990) Sequence of proton abstraction and stereochemistry of the reaction catalyzed by naphthoate synthase, an enzyme involved in menaquinone (vitamin K2) biosynthesis, *Eur J Biochem* 192, 441-449.
41. Stern, J. R., Del Campillo, A., and Raw, I. (1956) Enzymes of fatty acid metabolism. I. General introduction; crystalline crotonase, *The Journal of biological chemistry* 218, 971-983.
42. Willadsen, P., and Eggerer, H. (1975) Substrate stereochemistry of the enoyl-CoA hydratase reaction, *Eur J Biochem* 54, 247-252.
43. Steinman, H. M., and Hill, R. L. (1975) Bovine liver crotonase (enoyl coenzyme A hydratase). EC 4.2.1.17 L-3-hydroxyacyl-CoA hydrolyase, *Methods Enzymol* 35, 136-151.

44. Bell, A. F., Feng, Y., Hofstein, H. A., Parikh, S., Wu, J., Rudolph, M. J., Kisker, C., Whitty, A., and Tonge, P. J. (2002) Stereoselectivity of enoyl-CoA hydratase results from preferential activation of one of two bound substrate conformers, *Chem Biol* 9, 1247-1255.
45. Meganathan, R. (2001) Biosynthesis of menaquinone (vitamin K2) and ubiquinone (coenzyme Q): a perspective on enzymatic mechanisms, *Vitamins and hormones* 61, 173-218.
46. Jiang, M., Chen, X., Guo, Z. F., Cao, Y., Chen, M., and Guo, Z. (2008) Identification and characterization of (1R,6R)-2-succinyl-6-hydroxy-2,4-cyclohexadiene-1-carboxylate synthase in the menaquinone biosynthesis of *Escherichia coli*, *Biochemistry* 47, 3426-3434.

## CHAPTER 3: MENB AND BADI CATALYZE DIECKMANN CONDENSATION AND REVERSE DIECKMANN CONDENSATION

### Background

In the crotonase superfamily, there are two enzymes which catalyze similar but totally reverse reactions. The carbon-carbon bond formation (Dieckmann condensation) catalyzed by MenB and carbon-carbon bond hydrolysis (reverse Dieckmann condensation) catalyzed by BadI (2-ketocyclohexanecarboxyl-CoA hydrolase) represent unique and rare reactions among enzymatic catalysts in general (**Figure 3.1**). mtMenB shares 35% sequence identity with orthologs of BadI. The proposed catalytic roles for the residues in the active site of MenB are possibly complementary to the roles proposed for the active-site residues of BadI.

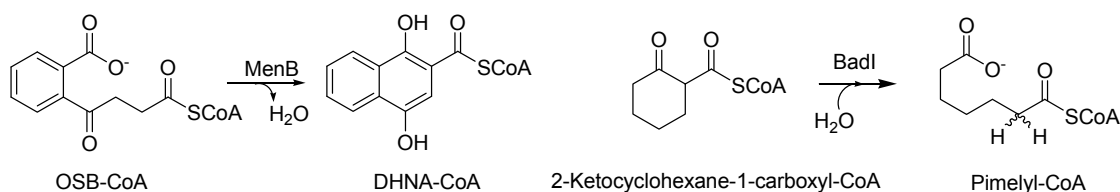


**Figure 3.1: Reactions catalyzed by MenB and BadI**

Both of the reactions are essentially irreversible. The MenB-catalyzed ring-forming reaction is rendered irreversible by the formation of an aromatic system. The BadI-catalyzed ring-cleaving reaction is not reversible because the product is ionized upon its release from the active site. Obviously, MenB and BadI share an intriguing evolutionary relationship. These two enzymes are likely to share similar active site configurations, and their active-site residues might serve

similar catalytic functions. Therefore it might be interesting to study BadI in order to further understand the mechanism of the MenB reaction.

BadI catalyzes the hydrolysis of 2-ketocyclohexanecarboxyl-CoA to pimelyl-CoA by a reverse Dieckmann condensation. This reaction is the last step in the anaerobic degradation pathway of benzoate in *Rhodospseudomonas palustris* which results in the cleavage of the six-membered ring (**Figure 3.2**) (1). The mechanism of this reaction is the reverse of the mechanism of the MenB-catalyzed reaction. The catalytic residues found in MenB are similarly conserved in BadI as Ser138, Asp140 and Tyr235 (**Figure 2.1**).

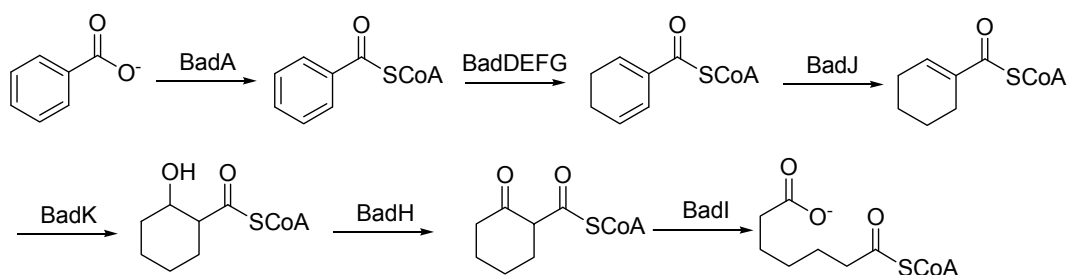


**Figure 3.2: Pathway for anaerobic benzoate degradation in *R. palustris***

The detailed mechanism of reaction catalyzed by mtMenB and ecMenB has been discussed in chapter 2. In this chapter, we will discuss the BadI reaction and then focus on comparing these two reverse reactions catalyzed by MenB and BadI.

## Materials and methods

### *Expression and purification of wild-type BadI from R. palustris*

The gene encoding BadI (*badI*) was cloned in pET17b vector and sequenced by Ellen D. Eberhard in the laboratory of Prof. John A. Gerlt at University of Illinois at Urbana-Champaign. The gene was cloned in frame with *NdeI* and *XhoI* restrictions sites and without a hexahistidine tag. Protein was optimally expressed from transformed *E. coli* BL21 (DE3) cells. BL21 cells (100  $\mu$ l) were transformed with 1  $\mu$ L of mini-prepped plasmid by heat shock. The transformants were resuspended in 700  $\mu$ L of LB, 200  $\mu$ L of which were plated on LB-Amp plate. The plate was incubated at 37 °C for overnight. A 15 mL starter culture (LB-Amp) was inoculated from a single colony and shaken at 37 °C for approximately 8 hours. 800 mL LB-Amp media was inoculated with 1 mL of starter culture, and shaken at 37 °C overnight.

The cells were collected by centrifugation at 5,000 rpm for 20 min at 4 °C, and resuspended in 30 mL of 20 mM Tris-HCl, pH 7.9. The cells were lysed by sonication (Sonicator 3000, Misonix) at level 5, alternating a 5 second pulse with a 10 second rest, for a total pulse time of 10 min. The cell debris was removed by centrifugation at 33,000 rpm for 90 min at 4 °C. The supernatant liquid was loaded onto a pre-equilibrated anion exchange column (DE52 resin, Whatman 2.6 cm  $\times$  70 cm). The column was washed with 300 mL of 20 mM Tris-HCl, pH 7.9. A linear gradient (800 mL, 0 to 0.5 M NaCl, 20 mM Tris-HCl, pH 7.9) was applied while collecting 8 mL fractions and monitoring the eluent at 280 nm. The column was then washed with 1 M NaCl and re-equilibrated in the starting buffer.

BadI was eluted in approximately fractions 27-40, appearing as the dominant band at 28 kDa as assessed by SDS-PAGE. The BadI-containing fractions were collected and concentrated to 20 mL in a Millipore stirred cell, using a 10,000 MWCO Millipore ultrafiltration membrane. The solution was then dialyzed at 4 °C against 20 mM Tris-HCl, pH 7.9, to remove salt.

The protein sample was further purified by strong anion exchange chromatography (Q sepharose, Pharmacia Biotech, 5 mm × 100 mm) at 4 °C. The protein was loaded in 20 mM Tris-HCl, pH 7.9. The column was washed with 15 mL of 20 mM Tris-HCl, pH 7.9. A linear gradient (400 mL, 0 to 0.35 M NaCl, 20 mM Tris-HCl, pH 7.9) was applied while 6 mL fractions were collected. BadI was eluted in fraction 40-70, appearing as the dominant band at 28 kDa as assessed by SDS-PAGE. The concentration of BadI was determined by measuring the absorption at 280 nm using an extinction coefficient of 32,790 M<sup>-1</sup>cm<sup>-1</sup> calculated from the primary sequence. The BadI containing fractions were collected, concentrated and stored at -80 °C. The non-His-tagged protein purified by this procedure was submitted for X-ray crystallography.

#### *Expression and purification of mutant BadI*

BadI mutants of S138A, D140N and Y235F were prepared by Ellen D. Eberhard in the laboratory of Prof. John A. Gerlt at University of Illinois at Urbana-Champaign. The procedure for the expression and purification of mutant BadI was used as described for wild-type BadI.



### *CD spectra of wild-type BadI and its Mutants*

The far-UV CD spectra of the wild-type BadI protein and its mutant variants were measured at a protein concentration of 20  $\mu\text{M}$  in 20 mM Tris-HCl, 150 mM NaCl, pH 7.9 buffer at 25  $^{\circ}\text{C}$  by using an AVIV 62 DS spectrometer equipped with a Peltier temperature control unit. CD spectra were obtained for all the mutant enzymes, and the resulting spectra were identical to that of the wild-type enzyme (**Figure 3.3**), suggesting that the mutagenesis did not alter the overall structure of the protein and the decrease of the activity is not due to the unfolding of the protein.

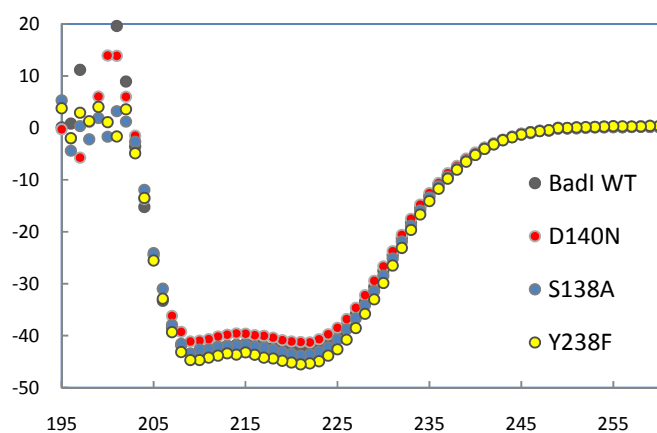


**Figure 3.3: CD spectra of wild-type and mutant BadI**

### *Assay of BadI reaction*

2-Ketohexanecarboxyl-CoA gives an absorbance peak at 314 nm when incubated in the presence of  $\text{Mg}^{2+}$  at pH 8 (**Figure 3.4**), which is due to the formation of an  $\text{Mg}^{2+}$ -enolate complex similar to that formed by acetoacetyl-CoA in the presence of  $\text{Mg}^{2+}$  ions at pH 8 (2, 3). BadI activity was assayed by monitoring the decrease of absorbance at 314 nm. The assay depends on the

loss of absorbance of an  $Mg^{2+}$ -enolate complex that occurs when the alicyclic ring of pimelyl-CoA is cleaved (**Figure 3.5**). BadI reaction performed in 20 mM Tris-HCl, 150 mM NaCl, and 100 mM  $MgCl_2$ , pH 8.0 buffer. Activity was calculated by using an extinction coefficient of  $1,210\ M^{-1}cm^{-1}$  for 2-ketohexanecarboxyl-CoA.

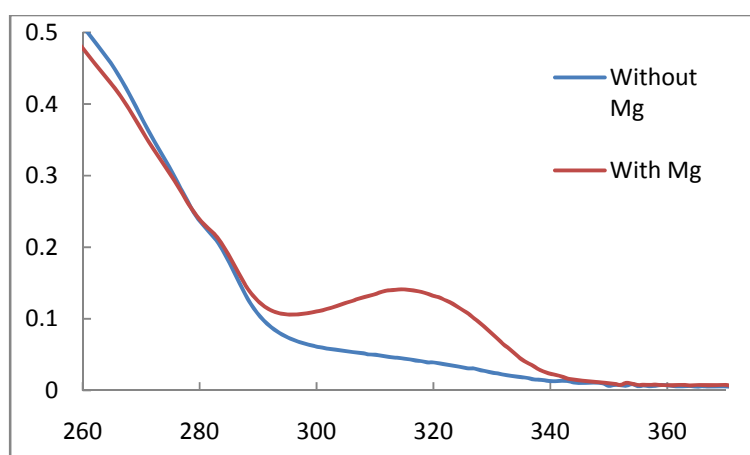


**Figure 3.4: Formation of an  $Mg^{2+}$ -enolate complex of 2-ketohexanecarboxyl-CoA**

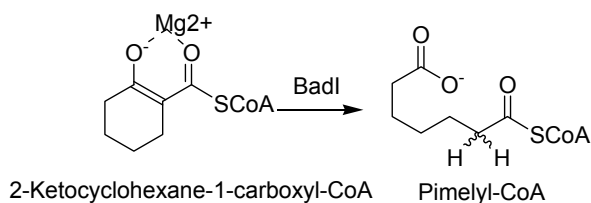


**Figure 3.5: Assay of BadI reaction based on the disappearance of  $Mg^{2+}$ -enolate complex**

#### *Magnesium dependence of BadI reaction*

In order to characterize the magnesium dependency for BadI reaction, the reaction catalyzed by BadI was incubated in 20 mM Tris-HCl, 150 mM NaCl, and 100 mM  $MgCl_2$ , pH 8.0 buffer and magnesium free buffer. Reaction mixtures

were characterized by HPLC (Phenomenex C18 analytical column, 5  $\mu\text{m}$  particle diameter, 4.6 mm i.d., 250 mm length). A linear gradient (0 to 40% acetonitrile, 40 min) was applied. Pimely-CoA was eluted at 11 min. When there was no magnesium in the reaction buffer, the same product was formed and eluted from HPLC at 11 min (**Figure 3.6**).

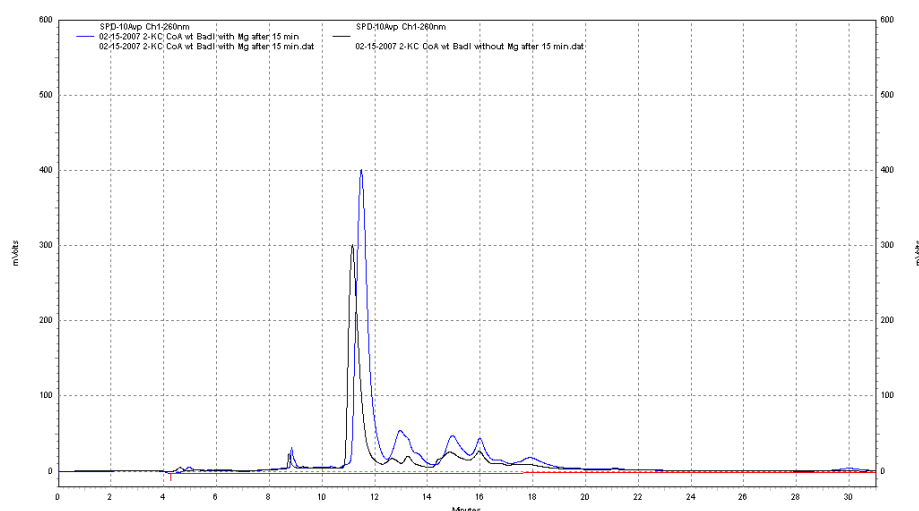


**Figure 3.6: BadI reaction is not magnesium dependent.** Without the incubation with magnesium, the same product was formed characterized by HPLC at 11 min.

#### *Synthesis of 2-ketohexanecarboxyl-CoA*

Ethyl 2-cyclohexanone-carboxylate (25 mmol) was hydrolyzed with 1 M NaOH in 50 mL of  $\text{H}_2\text{O}$  overnight at room temperature. After acidifying to pH 1-2 using 1 M HCl, 2-cyclohexanone-carboxylic acid (21 mmol) was precipitated from the cold water. The acid (1mmol) was dissolved in 20 mL of tetrahydrofuran, with stirring and external cooling by an ice bath. Dry triethylamine (2 mmol) was added, followed by dropwise addition of ethylchloroformate (2 mmol). After an additional hour of stirring in the ice bath, the precipitated triethyl ammonium

chloride was removed by gravity filtration. CoA (40  $\mu\text{mol}$ ) was dissolved in 10 mL of water, and the pH was adjusted to 7 with 0.1 M NaOH. The solution of activated acid was added dropwise over 30 min to the CoA solution, while maintaining pH at 7 by adding 0.1 M NaOH dropwise as necessary. After addition was complete, the reaction was allowed to stir another four hours. The reaction was acidified to pH 1-2 using 1 M HCl and extracted with ethyl acetate. The pH of the water layer was then raised to 10-11 with 5 M NaOH, kept at this pH for 1 h and then brought back to pH of 7 (**Figure 3.7**). The solution was frozen in liquid nitrogen and lyophilized. The product was purified from the lyophilized powder by semi-preparative HPLC (Vydac C18 column, 10  $\mu\text{m}$  particle diameter, 10 mm i.d., 250 mm length). A linear gradient (0 to 40% acetonitrile, 40 min) was applied. The absorbance of the eluent was monitored at 260 nm. The peak of interest was collected over several runs, frozen and lyophilized. ESI-MS  $[\text{M}-\text{H}]^-$ : calcd 890.17 ( $\text{C}_{28}\text{H}_{43}\text{N}_7\text{O}_{18}\text{P}_3\text{S}^-$ ); found 890.0.

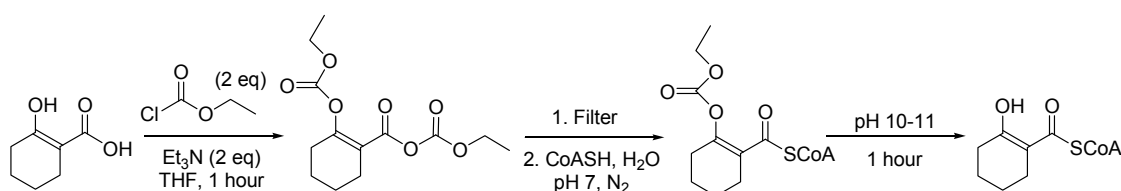


**Figure 3.7: Synthesis of 2-ketohexanecarboxyl-CoA**

#### *Synthesis of cyclohexenecarboxyl-CoA*

Starting with cyclohexenecarboxylic acid (Aldrich), the standard procedure on page 67 was used to synthesize cyclohexenecarboxyl-CoA. ESI-MS  $[\text{M}-\text{H}]^-$ : calcd 874.17 ( $\text{C}_{28}\text{H}_{43}\text{N}_7\text{O}_{17}\text{P}_3\text{S}^-$ ); found 874.0.

*X-Ray crystallography of BadI*

BadI along with cyclohexenecarboxy-CoA were submitted to Dr. Margaret Luk-Paszyc, Dr. Kolappan Subramaniapillai and Prof. Caroline Kisker at the Rudolf Virchow Center, DFG Research Center for Experimental Biomedicine (Germany). The structures were solved in *apo*- form and with cyclohexenecarboxyl-CoA bound in the active site.

## Results and discussion

### *Badl catalyzes reverse Dieckmann condensation*

Badl belongs to crotonase superfamily. It catalyzes the reverse Dieckmann Condensation which is reverse to the reaction catalyzed by MenB. The Badl from *R. palustris* was expressed without His-tag and purified by anion exchange chromatography as previously described in materials and methods section. The pure Badl protein was shown on SDS-PAGE as 28 kDa band (**Figure 3.8**).

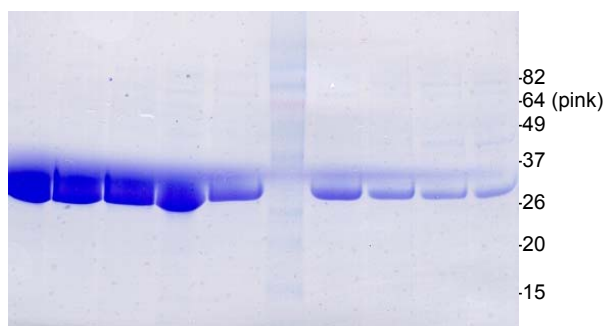


**Figure 3.8: SDS-PAGE gel of Badl after DE52 and Q sepharose columns**

The reaction catalyzed by Badl is not magnesium dependent as described in **Figure 3.6**. Two possible enantiomers of the substrate for Badl, *S*-2-ketohexanecarboxyl-CoA (*S*-KC-CoA) and *R*-2-ketohexanecarboxyl-CoA (*R*-KC-CoA) can interconvert *via* enolization (**Figure 3.9**). It has been reported that Badl can catalyze the hydrolysis of *S*-KC-CoA, but not *R*-KC-CoA (4). Badl can be assayed by monitoring the loss in absorbance due to the formation of a magnesium enolate with the substrate. However, complication in assaying the enzyme is that the substrate can exist as two enantiomers that are in equilibrium. Therefore an accurate measure of the concentration of the substrate is

impossible. The apparent the  $k_{cat}/K_m$  value of wild-type BadI is  $11.9 \pm 1.6 \text{ min}^{-1} \mu\text{M}^{-1}$  ( $k_{cat}$  and  $K_m$  values are  $3395.9 \pm 125.2 \text{ min}^{-1}$  and  $285.4 \pm 32.4 \mu\text{M}$ ).

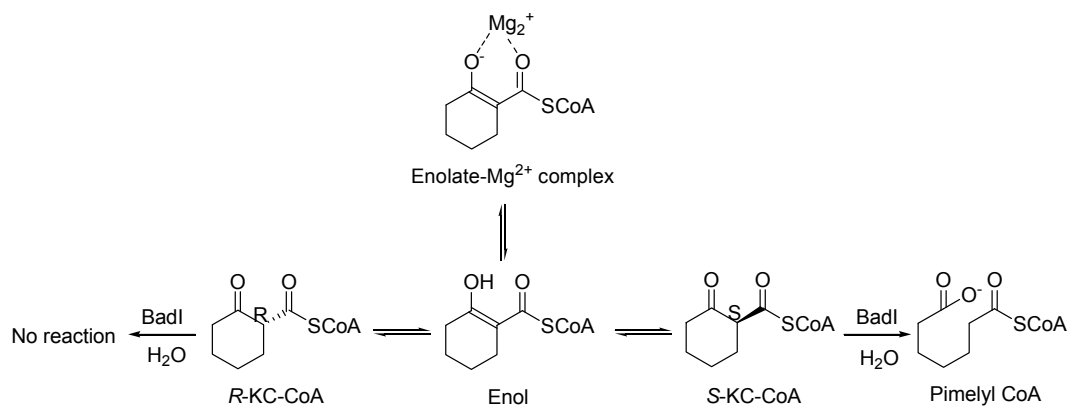


**Figure 3.9: Keto enol tautomerism of BadI substrates and interconversion of the S and R diastereomers**

S138, D140 and Y235 in BadI are conserved in MenB (**Figure 2.1**). The catalytic activities of BadI mutants of Y235 F, D140N and S138A were measured. Since the mutagenesis caused the  $K_m$  values of the mutants to increase to even bigger values, measurement of the apparent  $k_{cat}/K_m$  values of BadI mutants relied on the plot of the initial rate vs. substrate concentration when  $[S] \ll K_m$  ( $\frac{k_{cat}}{K_m} = \frac{V_i}{[S] \times [E]}$ ) (**Figure 3.10**). Y235 F, D140N and S138A catalyzed the reactions at rates which were 176, 313 and 4677 fold reduced, respectively, compared to wild-type BadI (**Table 3.1**). Therefore, the residues probably work together as a triad, with Ser 138 playing a central role.

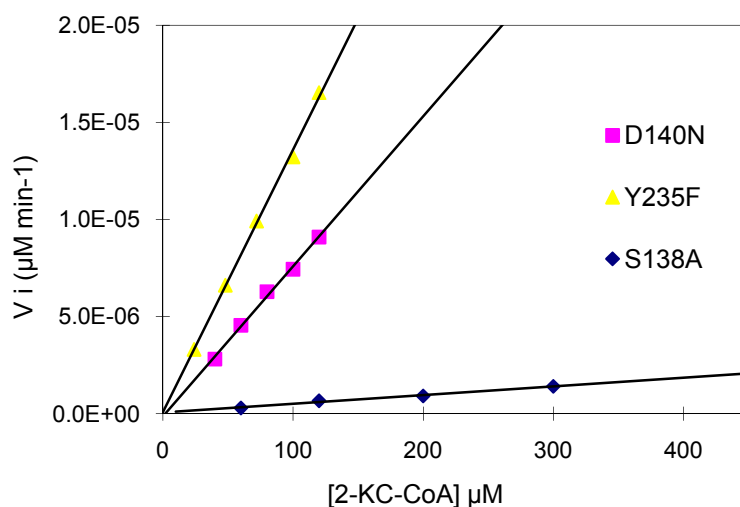


**Figure 3.10: Apparent  $k_{cat}/K_m$  values of BadI mutants.** Each mutant concentration was 2  $\mu\text{M}$ .

**Table 3.1: Apparent  $k_{cat}/K_m$  values of BadI and its mutants**

Enzyme	$k_{cat}/K_{m\ app}$ ( $\text{min}^{-1}\cdot\mu\text{M}^{-1}$ )	Ratio
Wild-type BadI	11.9	1
S138A	0.0025	1/4677
D140N	0.038	1/313
Y235F	0.067	1/176

The proposed mechanism of the reaction catalyzed by BadI is based on our mutagenic data and stereochemistry published in reference (4) (**Figure 3.11**). D140 may function as a base to activate the water molecular to attack the  $\beta$ -carbonyl of the substrate. The subsequent tetrahedral intermediate forms an enolate which is stabilized by oxyanion hole residues. S138 may direct the pro-2S proton to the enolate to yield the product.



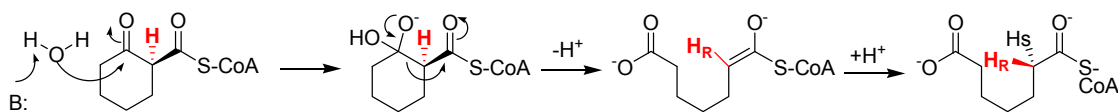


**Figure 3.11: Proposed mechanism of BadI reaction**

### *Comparison of crystal structures of mtMenB and BadI*

The *apo*- structure of BadI and the structure of BadI with cyclohexenecarboxyl-CoA (**Figure 3.12**) bound in the active site were solved by Dr. Margaret Luk-Paszyc, Dr. Kolappan Subramaniapillai and Prof. Caroline Kisker at the Rudolf Virchow Center, DFG Research Center for Experimental Biomedicine (Germany). Comparison of the active sites structure when the ligand is bound to that of the unliganded active site revealed minimal structural differences, indicating that the active site is rigid and that the binding of the substrate analogue would not be expected to induce any major structural perturbations in the protein.

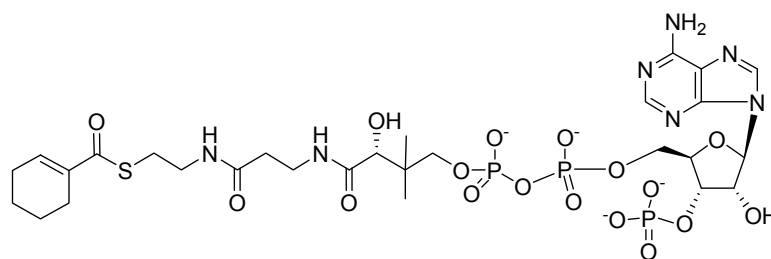


**Figure 3.12: Structure of cyclohexenecarboxyl-CoA**

Like many of the previously characterized members in the crotonase superfamily, BadI is hexamer (dimer of trimers). The overall fold displays a right hand spiral with a core composed of  $\beta$ -sheets surrounded by  $\alpha$ -helices. In

contrast to MenB, the C-terminus in each BadI monomer folds back to contribute residues to the active site in the same monomer. Consequently, the active site of each monomer contains residues only from that monomer (**Figure 3.13**).

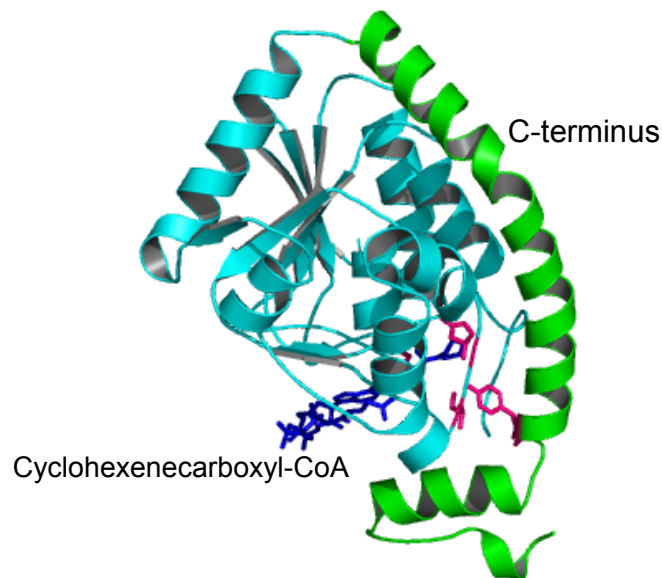


**Figure 3.13: Structure of BadI.** The C-terminal  $\alpha$ -helices involved in subunit interactions are colored in green. The side chains of the active site residues are displayed in pink. The substrate analogue, cyclohexenecarboxyl-CoA, is colored in blue.

The active site residues are located on the outer edge of the trimer, near the trimer-trimer interface. The cyclohexene portion of the substrate analogue is buried within a cleft in the enzyme, while the CoA portion threads out of the active site making enough contacts with water molecules on the surface. The thioester carbonyl forms hydrogen bonding interaction with the backbone amide protons of the residues of the oxyanion hole (Gly 66 and Gly 110). Catalytic residues S138, D140 and Y235 occur within 5 Å of the bound substrate analogue and are positioned on the same side of the molecule (**Figure 3.14**).

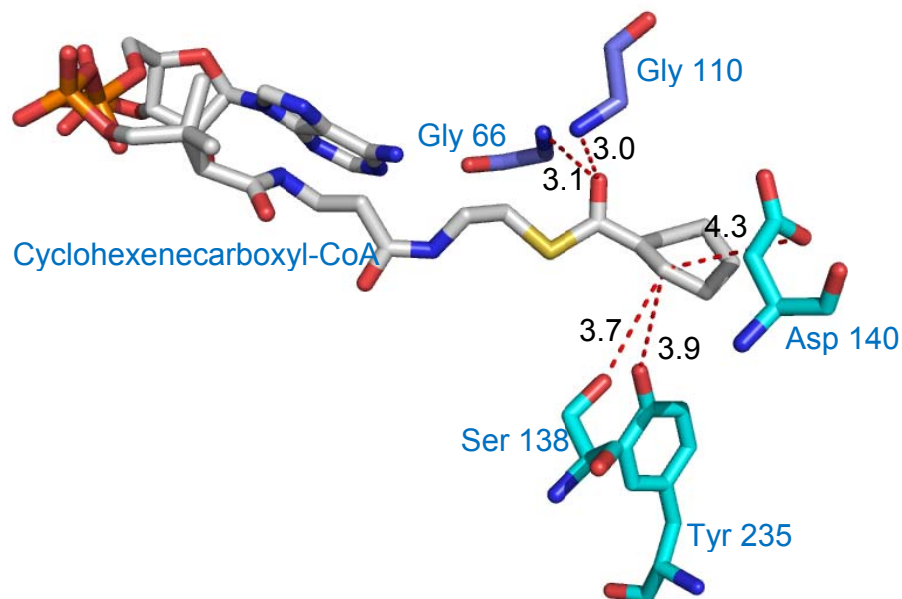


**Figure 3.14: Active site of BadI.** The distance between catalytic residues and oxyanion-hole residues to substrate analogue are in Angstroms.

Because the substrate analogue lacks an oxygen substituent on the  $\beta$ -carbon as occurs in the true substrate, it presumably lacks a major hydrogen-bonding contact. Therefore, the cyclohexene portion of the molecule may not be bound in a manner that represents the binding mode of the actual reaction.

mtMenB and BadI share 35% sequence identity. In both cases, the  $\alpha$ -helices of the C-terminus provide the major contacts between the subunits of the hexamer. In BadI, this region folds along the subunit and involves in the active site of the same subunit. In contrast, mtMenB's C-terminus folds back, crosses the trimer-trimer interface, and forms part of the active site of the opposing monomer. Remarkably, even with this structural difference, the active sites of mtMenB and BadI are superimposable (**Figure 3.15 A and B**). mtMenB S190 and

D192 are in the same position of BadI S138 and D140, while Tyr287 in mtMenB and Tyr235 points to the different direction. The position of BadI Y235 may represent the actual binding mode in the MenB active site since since cyclohexenecarboxy-CoA is a better mimic of the true BadI substrate than AcAc-CoA is of the MenB substrate. D185 mtMenB is not conserved in the BadI structure in which it is a glycine instead.

In both structures, the active site residues are all positioned on one side of the substrate analogues, which is similar to the active site of enoyl-CoA hydratase in that the catalytic residues all occur on the same side of the substrate with respect to the plane of the thioester (**Figure 3.15** C and D). The same architecture in the active site indicates that MenB, BadI and enoyl-CoA hydratase may share the comparable configuration of the reaction intermediates.

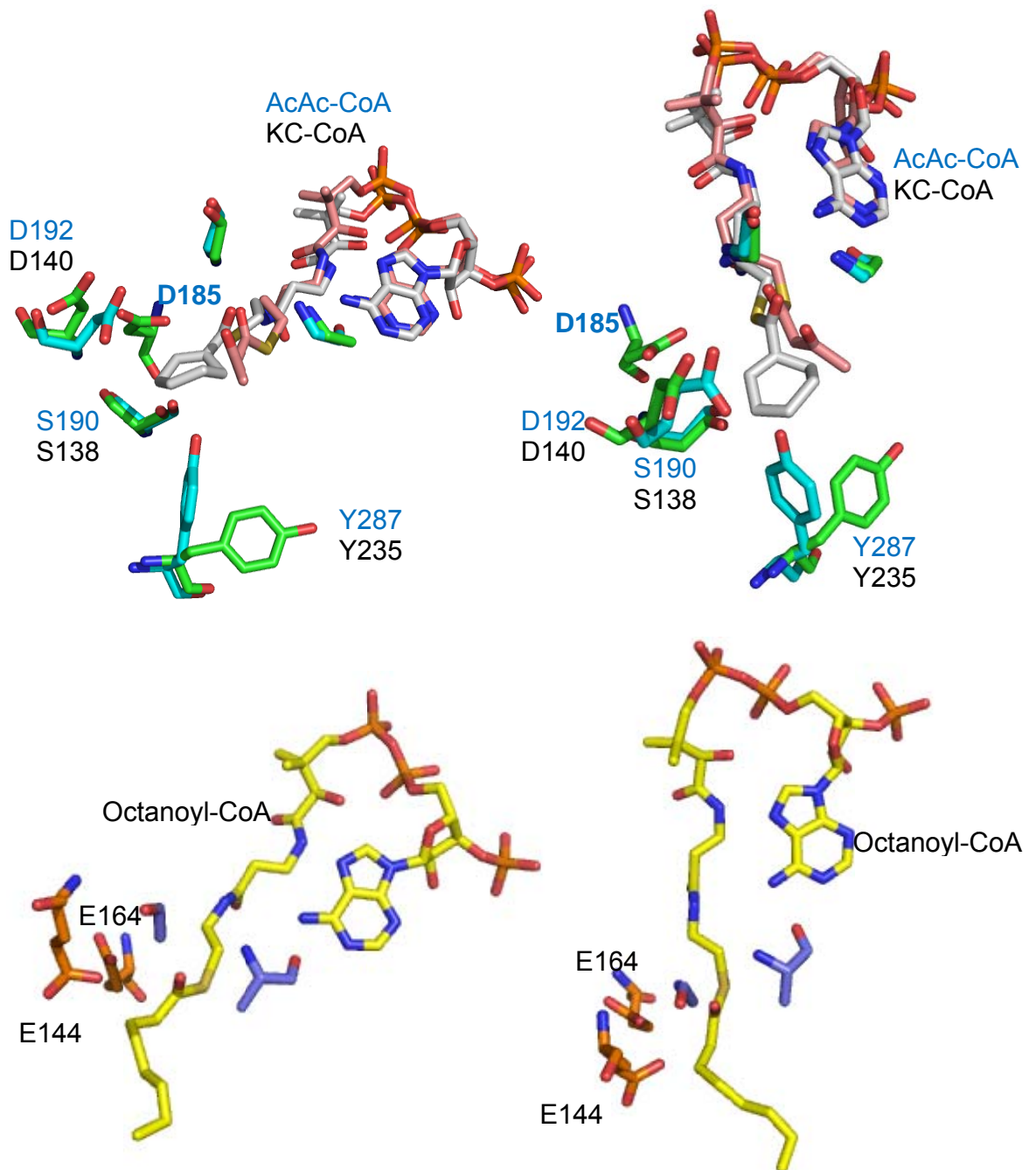


**Figure 3.15: Crystal structures of mtMenB, BadI and enoyl-CoA hydratase.** Figure A and B: superimposition of the active site of mtMenB and BadI (different view). MenB active-site residues are labeled in blue and BadI active-site residues are labeled in black. Figure C and D: The active site of enoyl-CoA hydratase (different view). All catalytic residues are positioned at the same side.

### *Stereochemistry of reactions catalyzed by MenB and BadI*

The reactions catalyzed by MenB and BadI are the mechanistic reverse of each other. The stereochemical courses of the reaction catalyzed by these two enzymes were elucidated. In contrast, the stereo-specificities of the analogous steps, enolate formation in the reaction catalyzed by MenB and enolate protonation in the reaction catalyzed by BadI, are divergent. MenB catalyzes the abstraction of the pro-2*R* proton in the initiation of the reaction (5), while BadI catalyzes the addition of the pro-2*S* proton in the termination step (4). The divergent stereo-specificities are likely due to the active-site architecture.

The pro-2*R* stereochemistry has also been found in the reaction catalyzed by enoyl-CoA hydratase. X-ray crystallography and site-directed mutagenesis of enoyl-CoA hydratase have demonstrated that the two glutamate residues, Glu-144 and Glu-164, form part of a catalytic diad and act in concert to facilitate the *syn* addition/elimination reaction (6-18) (**Figure 3.16**). E164 in enoyl-CoA hydratase, which is involved in the addition/abstraction of the pro-2*R* proton, is structurally homologous to D185 in mtMenB (**Figure 2.41**).

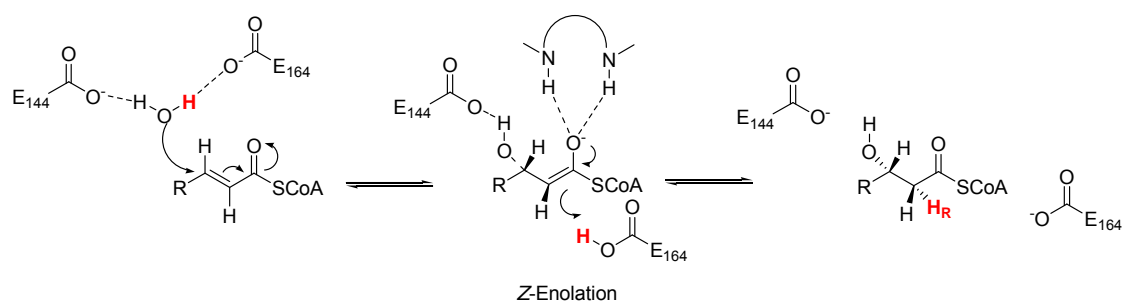


**Figure 3.16: Mechanism of the reaction catalyzed by rat mitochondrial enoyl-CoA hydratase**

The active sites of MenB, BadI and enoyl-CoA hydratase are similar in that the catalytic residues are arranged on the same side of the substrate, with respect to the plane of the thioester (**Figure 3.15**). The thioester moieties of the bound substrate analogues share similar positions in the active sites of all structurally characterized members in the crotonase superfamily. The oxygen atom of the thioester is bound in the conserved oxyanion hole, forming hydrogen bonds with two amide hydrogens of the peptide backbone. The sulfur atom of the thioester is fixed in its position by the coenzyme A portion of the molecule. Since the oxygen and the sulfur are anchored in the same positions, it can be assumed that the plane of the thioester does not rotate during catalysis within the active site. Therefore, the enolate, which is stabilized by the oxyanion hole, will also maintain the same plane.

However the stereochemistry of MenB, BadI and enoyl-CoA hydratase are different (**Figure 3.17**), thus substrate must orient differently with the active site residues. mtMenB and enoyl-CoA hydratase share the same pro-2*R* stereochemistry. Like enoyl-CoA hydratase, the substrate of mtMenB presents the pro-2*R* proton to D185, resulting in the Z-enolate configuration of the intermediate. However, in ecMenB which lacks D185, we propose that the substrate carboxyl abstracts the pro-2*R* proton, thus leading to an enolate intermediate with the *E* configuration. In the case of BadI, the substrate binds in a conformation similar to that required for the ecMenB. However in the case of BadI, enzyme group abstracts the pro-2*S* proton.

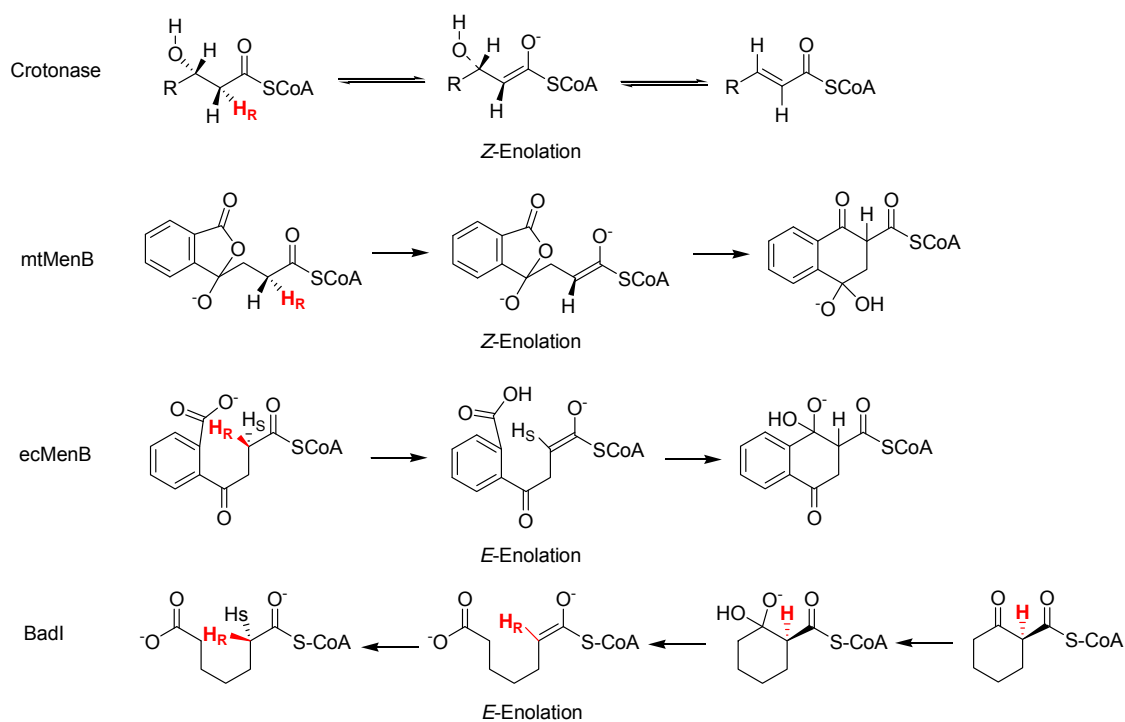


**Figure 3.17: The divergent stereo-specificities of the reactions catalyzed by enoyl-CoA hydratase, mtMenB, ecMenB, and BadI. Pro-2*R* proton is abstracted in enoyl-CoA hydratase and MenB reaction while it is retained in the  $\alpha$ -carbon in BadI reaction.**



## Conclusions

MenB and BadI belong to the crotonase superfamily and catalyze similar but totally reverse reactions. MenB catalyzes carbon-carbon bond formation (Dieckmann condensation) while BadI catalyzes the carbon-carbon bond hydrolysis (reverse Dieckmann condensation). Therefore it is interesting to compare the both enzymes.

The mutagenic data indicates that the conserved residues of S138, D140 and Y235 are important for the reaction, with Ser 138 playing a central role. The crystal structure of BadI in complex with cyclohexenecarboxyl-CoA also suggests that these three catalytic residues occur within 5 Å of the bound substrate analogue.

In crystal structures of MenB and BadI, the active site residues are all positioned on one side of the substrate analogues with respect to the plane of the thioester, which is similar to the active site of enoyl-CoA hydratase. However the stereochemistry of MenB, BadI and enoyl-CoA hydratase are different. mtMenB and enoyl-CoA hydratase share the pro-2*R* proton stereochemistry. In mtMenB, the substrate presents the pro-2*R* proton to D185, resulting in Z-enolate configuration of the intermediate. However, in ecMenB which lacks D185, we propose that the substrate carboxyl abstracts the pro-2*R* proton, thus leading to an enolate intermediate with the *E* configuration. In the case of BadI, the substrate binds in a conformation similar to that required for the ecMenB, but the pro-2*S* proton is added to the reaction.

## References

1. Eglund, P. G., Pelletier, D. A., Dispensa, M., Gibson, J., and Harwood, C. S. (1997) A cluster of bacterial genes for anaerobic benzene ring biodegradation, *Proceedings of the National Academy of Sciences of the United States of America* 94, 6484-6489.
2. Lynen, F., and Ochoa, S. (1953) Enzymes of fatty acid metabolism, *Biochim Biophys Acta* 12, 299-314.
3. Perrotta, J. A., and Harwood, C. S. (1994) Anaerobic Metabolism of Cyclohex-1-ene-1-Carboxylate, a Proposed Intermediate of Benzoate Degradation, by *Rhodopseudomonas palustris*, *Appl Environ Microbiol* 60, 1775-1782.
4. Eberhard, E. D., and Gerlt, J. A. (2004) Evolution of function in the crotonase superfamily: the stereochemical course of the reaction catalyzed by 2-ketocyclohexanecarboxyl-CoA hydrolase, *J Am Chem Soc* 126, 7188-7189.
5. Igbavboa, U., and Leistner, E. (1990) Sequence of proton abstraction and stereochemistry of the reaction catalyzed by naphthoate synthase, an enzyme involved in menaquinone (vitamin K<sub>2</sub>) biosynthesis, *Eur J Biochem* 192, 441-449.
6. Wen-Jin Wu, Y. F., Xiang He, Hilary A. Hofstein, Daniel P. Raleigh and Peter J. Tonge. (2000) Stereospecificity of the Reaction Catalyzed by Enoyl-CoA Hydratase, *J. Am. Chem. Soc.* 122, 3987.

7. Kurosawa, T., Sato, M., Nakano, H., Fujiwara, M., Murai, T., Yoshimura, T., and Hashimoto, T. (2001) Conjugation reactions catalyzed by bifunctional proteins related to beta-oxidation in bile acid biosynthesis, *Steroids* 66, 107-114.
8. Qin, Y. M., Haapalainen, A. M., Conry, D., Cuebas, D. A., Hiltunen, J. K., and Novikov, D. K. (1997) Recombinant 2-enoyl-CoA hydratase derived from rat peroxisomal multifunctional enzyme 2: role of the hydratase reaction in bile acid synthesis, *Biochem J* 328 ( Pt 2), 377-382.
9. Dieuaide-Noubhani, M., Asselberghs, S., Mannaerts, G. P., and Van Veldhoven, P. P. (1997) Evidence that multifunctional protein 2, and not multifunctional protein 1, is involved in the peroxisomal beta-oxidation of pristanic acid, *Biochem J* 325 ( Pt 2), 367-373.
10. Jiang, L. L., Kurosawa, T., Sato, M., Suzuki, Y., and Hashimoto, T. (1997) Physiological role of D-3-hydroxyacyl-CoA dehydratase/D-3-hydroxyacyl-CoA dehydrogenase bifunctional protein, *J Biochem* 121, 506-513.
11. Hiltunen, J. K., and Qin, Y. (2000) beta-oxidation - strategies for the metabolism of a wide variety of acyl-CoA esters, *Biochim Biophys Acta* 1484, 117-128.
12. Engel, C. K., Mathieu, M., Zeelen, J. P., Hiltunen, J. K., and Wierenga, R. K. (1996) Crystal structure of enoyl-coenzyme A (CoA) hydratase at 2.5 angstroms resolution: a spiral fold defines the CoA-binding pocket, *EMBO J* 15, 5135-5145.

13. Engel, C. K., Kiema, T. R., Hiltunen, J. K., and Wierenga, R. K. (1998) The crystal structure of enoyl-CoA hydratase complexed with octanoyl-CoA reveals the structural adaptations required for binding of a long chain fatty acid-CoA molecule, *J Mol Biol* 275, 847-859.
14. Bahnson, B. J., Anderson, V. E., and Petsko, G. A. (2002) Structural mechanism of enoyl-CoA hydratase: three atoms from a single water are added in either an E1cb stepwise or concerted fashion, *Biochemistry* 41, 2621-2629.
15. Muller-Newen, G., Janssen, U., and Stoffel, W. (1995) Enoyl-CoA hydratase and isomerase form a superfamily with a common active-site glutamate residue, *Eur J Biochem* 228, 68-73.
16. D'Ordine, R. L., Bahnson, B. J., Tonge, P. J., and Anderson, V. E. (1994) Enoyl-coenzyme A hydratase-catalyzed exchange of the alpha-protons of coenzyme A thiol esters: a model for an enolized intermediate in the enzyme-catalyzed elimination?, *Biochemistry* 33, 14733-14742.
17. Hanson, K. R. R., I. A. (1975) Interpretations of Enzyme Reaction Stereospecificity, *Acc. Chem. Res.* 8, 1.
18. Hofstein, H. A., Feng, Y., Anderson, V. E., and Tonge, P. J. (1999) Role of glutamate 144 and glutamate 164 in the catalytic mechanism of enoyl-CoA hydratase, *Biochemistry* 38, 9508-9516.

## CHAPTER 4: INHIBITION STUDIES OF MTMENB

### Introduction

The central goal of our project is based on the mechanistic understanding of bacterial menaquinone biosynthesis, to design and synthesize potent inhibitors against menaquinone biosynthetic enzymes and to validate menaquinone biosynthesis as a target for the development of novel anti-TB chemotherapeutics. In this chapter, we will discuss our inhibition studies of mtMenB which is in the early stage of the drug development process (**Figure 4.1**) including exploration and lead selection. Further steps will be continued in our group.

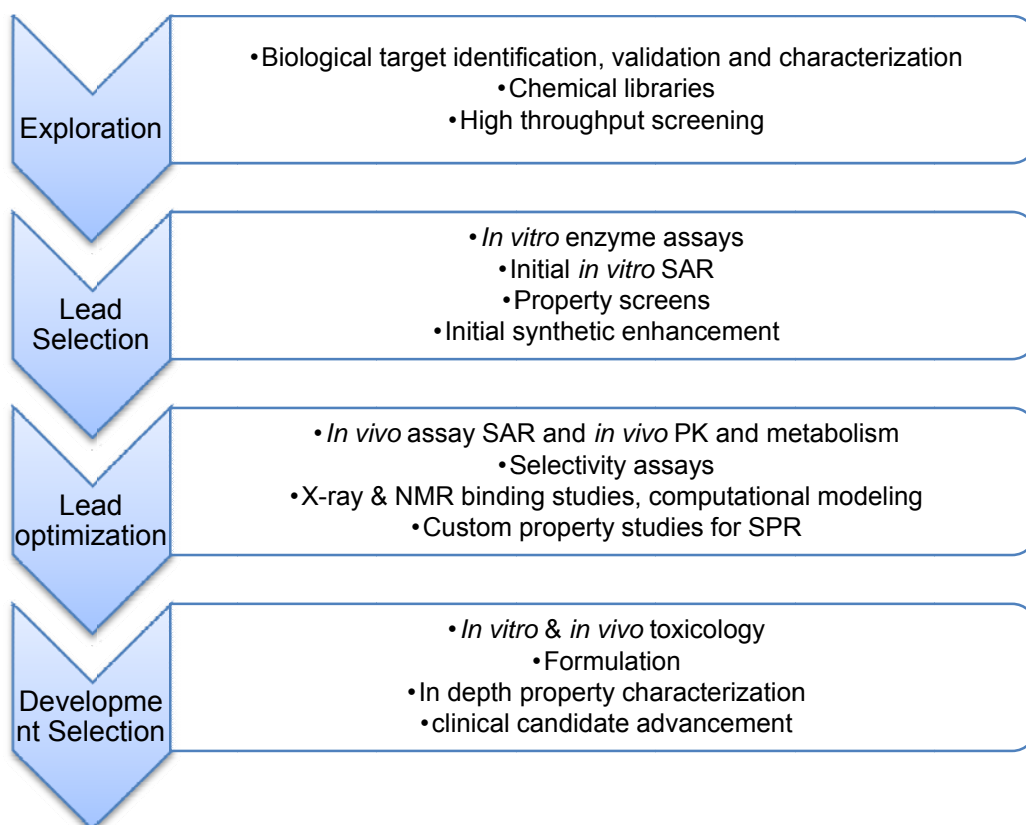


**Figure 4.1: Stages of drug discovery process**

## Materials and methods

### *Pilot screening to establish assay conditions for high throughput screening*

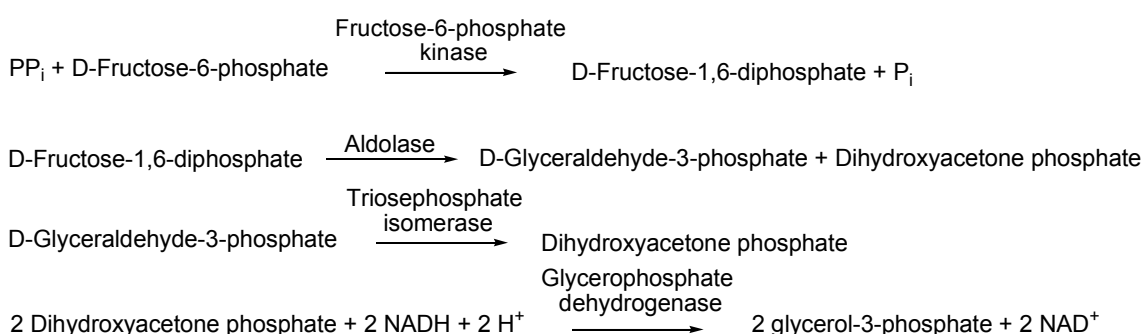
Pilot screens were performed to identify the most appropriate conditions for a high-throughput screen aimed at identifying lead MenB inhibitors. The MenE/MenB coupled assay was performed under the range of substrate concentration from 200  $\mu\text{M}$  to 300  $\mu\text{M}$ , and reaction time from 20 min to 60 min.

### *High throughput screening of potent inhibitors of mtMenB*

High throughput screening was carried out to select small molecules that inhibit mtMenB activity at the ICCB-Longwood Screening Facility at Harvard Medical School. Assays were carried out in 384-well plates at 25 °C. Each well contained of 40  $\mu\text{L}$  of mixture that included 250  $\mu\text{M}$  of OSB, ATP and CoA, 0.15  $\mu\text{M}$  of mtMenB, 3  $\mu\text{M}$  of *E. coli* MenE and ~ 23  $\mu\text{M}$  of screening compound in 20 mM  $\text{NaH}_2\text{PO}_4$ , 1 mM  $\text{MgCl}_2$ , 150 mM NaCl buffer (pH 7.0). OSB, ATP, CoA and mtMenB were mixed and then screening compounds were added by pin transfer. The reaction was initiated by adding *E. coli* MenE. After 60 min the extent of the reaction we assessed by measuring the absorbance of each reaction at 405 nm (since this the closest filter to 392 nm) using an *Envision* plate reader. The mtMenB mutant Y287F, which is inactive, was used as a positive control. The wells which were added with DMSO instead of screening compound were used as a negative control.

### Pyrophosphate release assay

Pyrophosphate (PPi) is released in the process of reaction catalyzed by MenE. PPi is determined in this procedure according to the following coupled reactions. Two moles of NADH are oxidized to NAD<sup>+</sup> per mole of pyrophosphate consumed. The reaction is monitored on a CARY-300 spectrophotometer at 25 °C at 340 nm using an extinction coefficient of 6, 220 M<sup>-1</sup>cm<sup>-1</sup>.



### Fluorescence titration of mtMenB with hexachlorophene

Equilibrium fluorescence titrations were performed at 25 °C in a Fluorolog-3-21 fluorimeter by making microliter additions of the ligand to a solution of mtMenB (5 μM). The excitation wavelength was 290 nm and the emission wavelength was 343 nm. A control experiment was performed following the same procedure but omitting enzyme from the cuvette. The data were fit to equation (1) to obtain K<sub>d</sub>.

$$\Delta F = \Delta F_{max} \left( \frac{K_d + [E] + [L] - \sqrt{K_d + [E] + [L]^2 - 4[L][E]}}{2[E]} \right) \quad (1)$$

### *Assay for inhibition of mtMenB*

Reactions were performed in 20 mM NaH<sub>2</sub>PO<sub>4</sub> pH 7.0, 150 mM NaCl, 1 mM MgCl<sub>2</sub> and were initiated by adding MenE (final concentration 4 μM) to a solution containing MenB (200 nM), ATP (120 μM), CoA (120 μM), OSB (30 μM) and inhibitor (0–200 μM). The formation of DHNA-CoA was monitored at 392 nm and initial velocities were determined using an extinction coefficient of 4,000 M<sup>-1</sup>cm<sup>-1</sup>. IC<sub>50</sub> values were calculated by fitting the initial velocity data ( $v_i$ ) obtained at different inhibitor concentrations ([I]) to equation (2) using Grafit 4.0.

$$v_i = \frac{100\%}{1 + [I]/IC_{50}} \quad (2)$$

The type of inhibition was determined by Lineweaver-Burk plot analysis. K<sub>i</sub> values for competitive inhibition were determined by fitting the data to equation (3) while equation (4) was used for non-competitive inhibition using Grafit 4.0.

$$v_i = \frac{V_{max} \times [S]}{K_m \left(1 + \frac{[I]}{K_i}\right) + [S]} \quad (3)$$

$$v_i = \frac{V_{max} \times [S]}{([S] + K_m) \left(1 + \frac{[I]}{K_i}\right)} \quad (4)$$

### *Determination of M. tuberculosis antimicrobial activity*

MIC<sub>90</sub> data for *M. tuberculosis* were acquired by Susan E. Knudson in the Department of Bioagricultural Sciences and Pest Management at Colorado State University.



#### *Determination of B. subtilis antimicrobial activity*

Whole-cell antimicrobial activity was determined by a broth microdilution procedure. Different inhibitors were dissolved in DMSO and serially diluted into VY medium (Veal-Yeast medium, ATCC medium) on a 96-well plate. The final test concentrations ranged from 300  $\mu\text{M}$  to 0.01  $\mu\text{M}$  of inhibitors. 10  $\mu\text{L}$  of overnight grown cells of *B. subtilis* were added into each well. Inoculated plates were incubated at 37 °C for 24 hours. The minimum inhibitory concentration (MIC) was determined as the lowest concentration of compound that inhibited visible growth as estimated by OD<sub>600</sub> reading using a 96-well plate reader.

#### *Supplement experiment with DHNA by agar overlay method*

Liquid growth experiments with DHNA in LB and VY media were unsuccessful. This is due to the instability of DHNA in aqueous aerated media which has been discussed in Chapter 2. Therefore, soft agar overlay procedures were used for supplement by DHNA (1). Approximately 5  $\mu\text{g}$  amounts of DHNA were spotted on blank paper disks placed on soft agar overlays with different concentration of inhibitors, and enhancement of growth around the disks was monitored after 24 hours of growth.

#### *Supplement experiment with menadione and menaquinone-7 (MK-7)*

Different concentration of menadione and menaquinone-7 (MK-7), from 10  $\mu\text{M}$  to 300  $\mu\text{M}$  was added to medium wells which contained different

concentration of inhibitors, ranging from 300  $\mu\text{M}$  to 0.01  $\mu\text{M}$ . The 96-well plates were incubated at 37 °C for 24 hours and read at  $\text{OD}_{600}$ .

## Results and discussion

### *Pilot screening of mtMenB and hexachlorophene*

Around 3,000 compounds were analyzed in a pilot screen to optimize the screening conditions.  $Z'$  factor is a simple statistical parameter for use in evaluation and validation of high throughput screening assays (2). The number of  $Z'$  factor was calculated based on the formula based on Equation (5). An optimal assay has a  $Z'$  score of greater than 0.7 and we generally achieved  $Z'$  scores in the range from 0.6 to 0.7 during the pilot as we increased the reaction time to 60 minutes (**Table 4.1**).

$$Z' = 1 - \frac{(3SD_+ + 3SD_-)}{|Ave_+ - Ave_-|} \quad (5)$$

SD<sub>+</sub> = positive control standard deviation

Ave<sub>+</sub> = positive control average

SD<sub>-</sub> = negative control standard deviation

Ave<sub>-</sub> = negative control average

**Table 4.1:  $Z'$  score of different reaction time**

Reaction time	SD <sub>+</sub>	SD <sub>-</sub>	Ave <sub>+</sub>	Ave <sub>-</sub>	$Z'$
20 min	0.0084	0.0086	0.052	0.143	0.44
30 min	0.0080	0.0083	0.052	0.157	0.54
40 min	0.0077	0.0081	0.052	0.166	0.60
60 min	0.0073	0.0079	0.052	0.173	0.63

The best positive result from the pilot screening was hexachlorophene (**Figure 4.2**), which is an antimicrobial compound, being most active against Gram-positive bacteria (3). Frederick has proposed that hexachlorophene appears to inhibit respiration by interfering with membrane-bound components of the electron transport chain (4). Since menaquinone is an essential component of

the electron transport chain, we propose that hexachlorophene could act by inhibiting MenB, thereby decreasing the amount of menaquinone in the membrane.

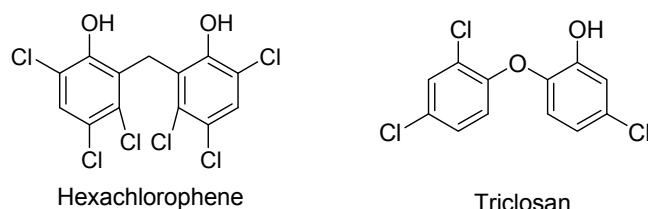


**Figure 4.2: The structures of hexachlorophene and triclosan**

In our *in vitro* enzymatic kinetic assay, hexachlorophene is a competitive inhibitor of mtMenB with an  $IC_{50}$  value of  $9.3 \pm 0.9 \mu\text{M}$ ,  $K_i$  value of  $7.4 \pm 0.8 \mu\text{M}$  and  $K_d$  value of  $17.2 \pm 0.5 \mu\text{M}$  (**Figure 4.3**). The  $MIC_{90}$  value of hexachlorophene against *M. tuberculosis* is  $< 0.78 \mu\text{g/mL}$ . Triclosan, an antibacterial chemical mainly targeting the FabI in bacteria fatty acid biosynthesis, has the similar structure of hexachlorophene. However, it showed very poor inhibition (more than  $200 \mu\text{M}$ ) against mtMenB.

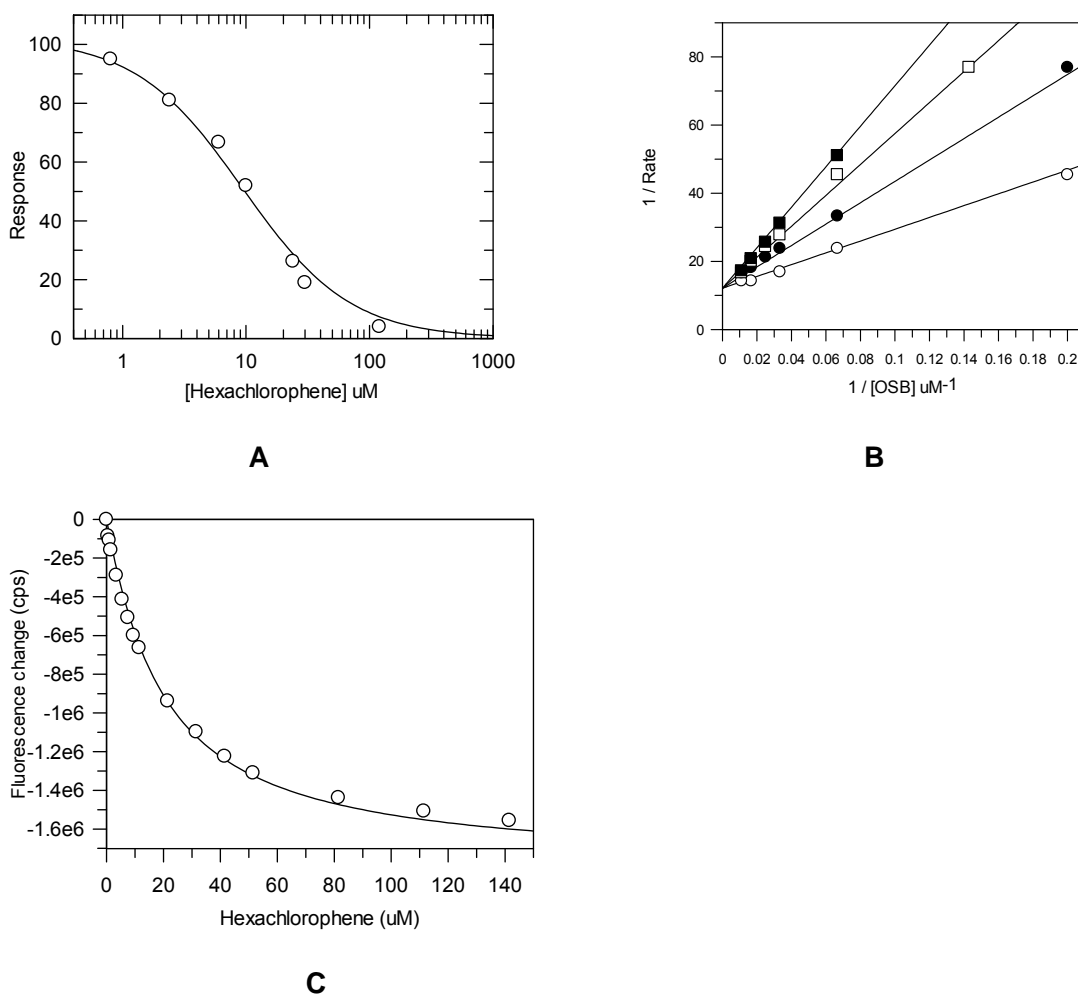


**Figure 4.3: Inhibition and binding data of hexachlorophene of mtMenB.** Figure A:  $IC_{50}$  of hexachlorophene versus mtMenB. B) Lineweaver-Burk plot. The inhibition hexachlorophene against mtMenB in the absence of inhibitor ( $\circ$ ), in the presence of 6  $\mu\text{M}$  of hexachlorophene ( $\bullet$ ), 12  $\mu\text{M}$  of hexachlorophene ( $\square$ ) or 18  $\mu\text{M}$  of hexachlorophene ( $\blacksquare$ ). C) Fluorescence titration of mtMenB with hexachlorophene. Excitation wavelength is 290 nm, and emission wavelength is 343 nm.

### *High throughput screening of mtMenB*

We screened around 100,000 small molecular compounds from the library of Known Bioactives (Pilot screening) and Commercial Compounds (**Table 4.2**) at the ICCB-Longwood Screening Facility at Harvard Medical School (June, September and October 2007).

**Table 4.2: Libraries of screened compounds**

	Library Name	Number of Compounds	Plate Numbers	Number of Plates
Known Bioactive	Biomol ICCB Known Bioactives2-High Conc.	480	1791-1792	2
	Biomol ICCB Known Bioactives1-Medium Conc.	480	1361-1362	2
	Ninds Custom Collection 2	1,040	1920-1923	4
	Prestwick 1 Collection	1,120	1568-1571	4
Commercial Compounds	Asinex 1	12,378	1671-1706	36
	ChemBridge 3	19,560	1577-1606	30
	ChemDiv 4	14,677	1607-1648	42
	Enamine 2	26,576	1715-1790	76
	Life Chemicals 1	3,893	1649-1660	12
	Maybridge 5	3,212	1661-1670	10
	ChemDiv3	16,544	1473-1519	47
	ChemDiv 5	1,249	1709-1712	4
	MixCommercial 5	268	1520	1
	Maybridge 4	4,576	1521-1533	13
Biomol-TimTec 1	8,518	1534-1558	25	

Microsoft Excel spreadsheet was used to organize and analyze screening data. Cut-offs for defining the potency of inhibitors were calculated as follows. We classified hits into three groups: strong hits are those compounds that inhibited the reaction greater than 70%, (**Figure 4.4**), medium hits are 50% < inhibition < 70% (**Figure 4.5**) and weak hits are 30% < inhibition < 50% (**Figure 4.6**).

$$30\% \text{ of inhibition: } N_{ave} - (N_{ave} - P_{ave}) \times 30\%$$

$$50\% \text{ of inhibition: } N_{ave} - (N_{ave} - P_{ave}) \times 50\%$$

$$70\% \text{ of inhibition: } N_{ave} - (N_{ave} - P_{ave}) \times 70\%$$

$N_{ave}$ : negative control average based on the absorbance of negative wells in each plate;

$P_{ave}$ : positive control average based on the absorbance of positive wells in each plate.

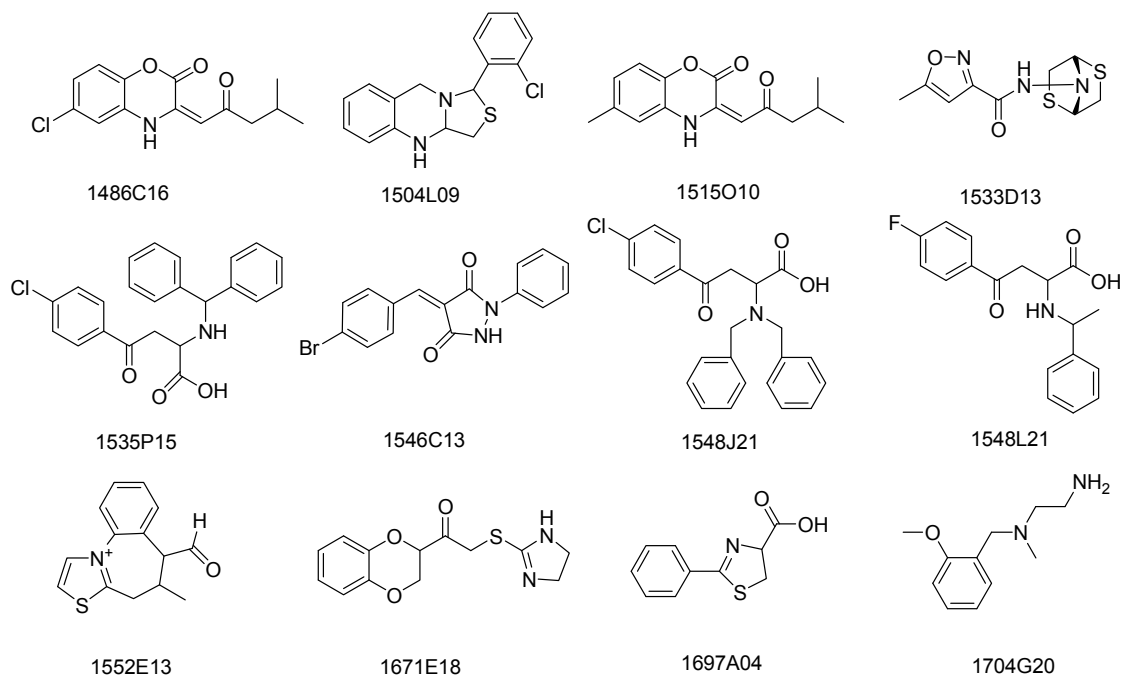


**Figure 4.4: High throughput screening hits with strong inhibition**

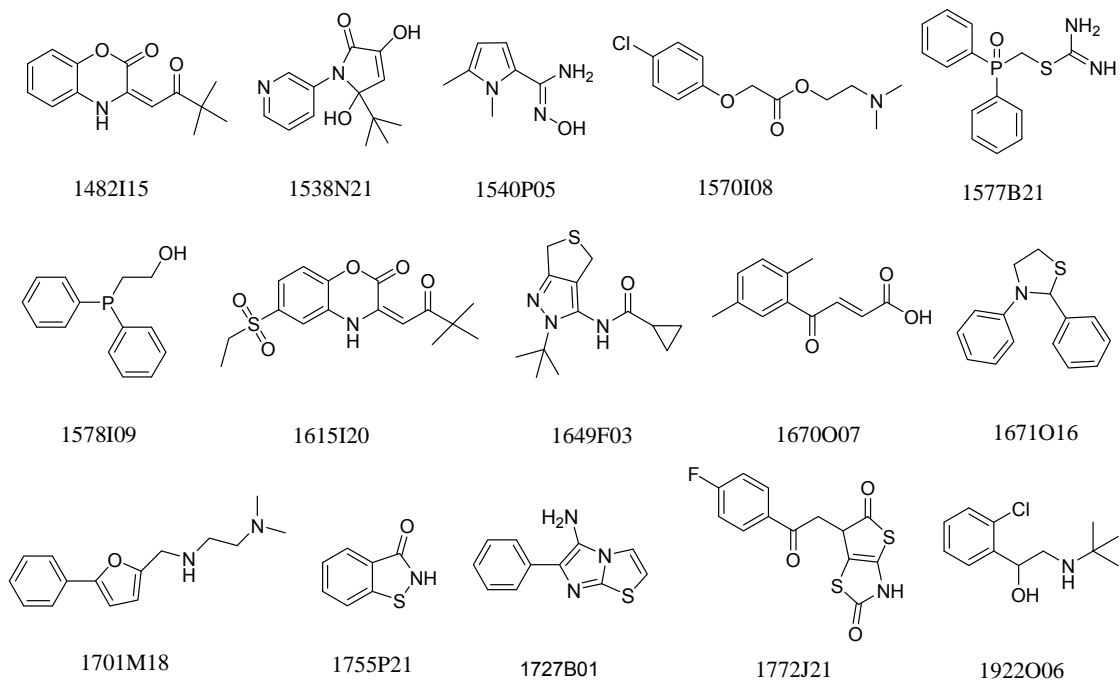


**Figure 4.5: High throughput screening hits with medium inhibition**



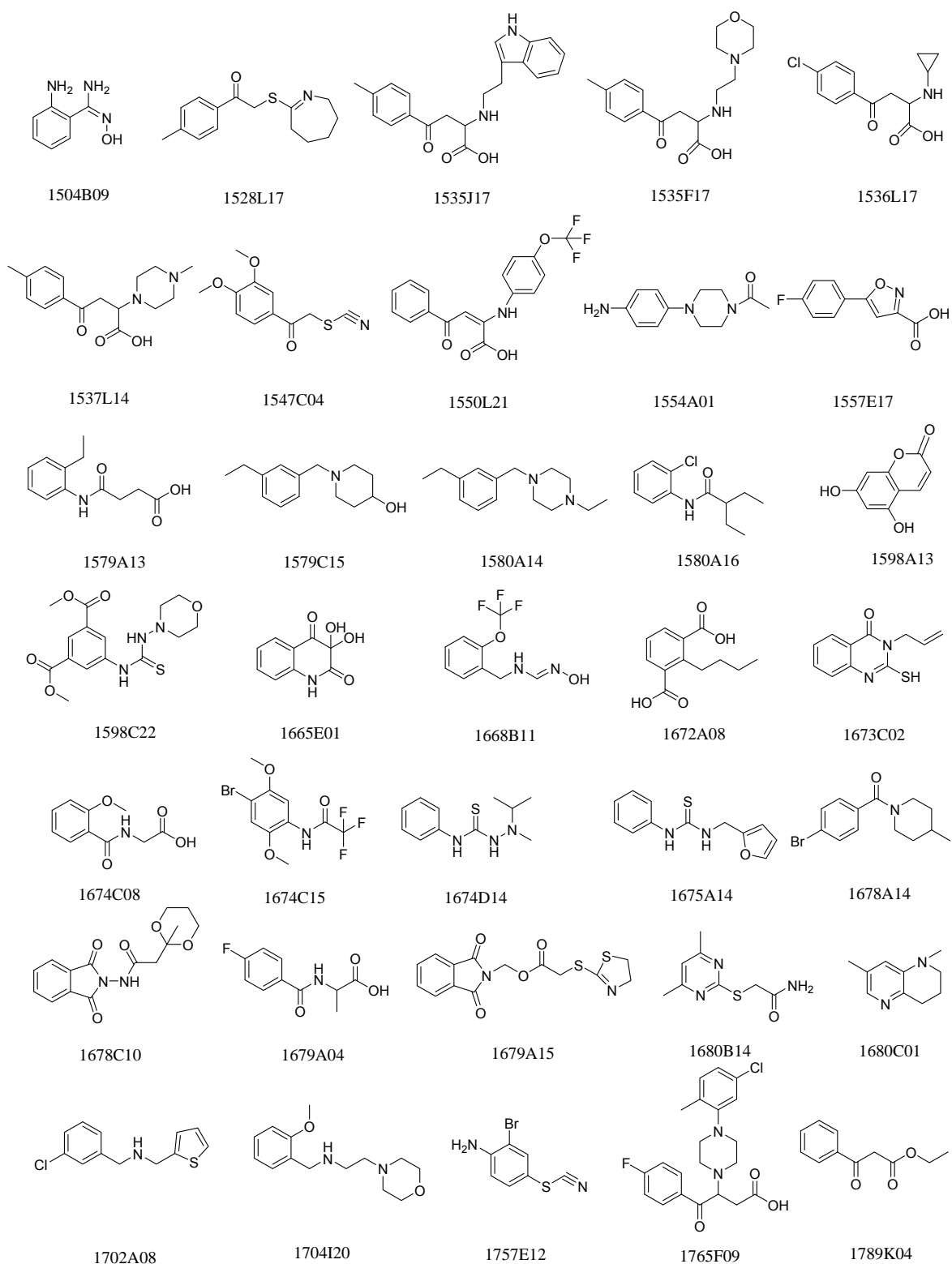


**Figure 4.6: The structures of high throughput screening hits with weak inhibition**

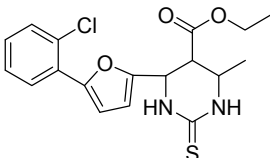
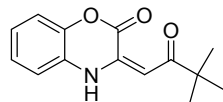
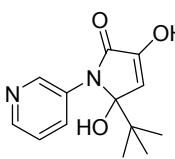
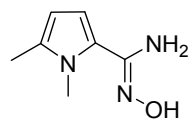
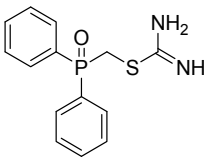
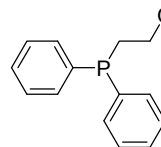
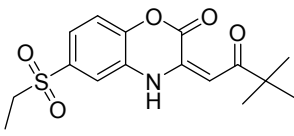
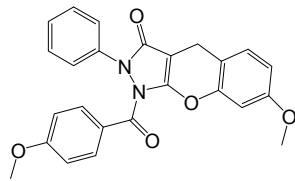
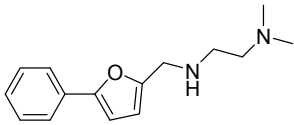
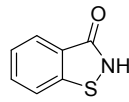
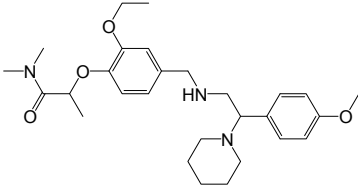
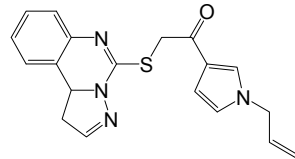
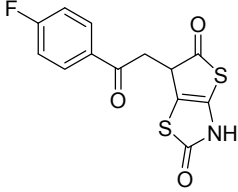
### *Second screens of “cherry picks”*

After completing the primary screen, we analyzed the structures of “positives” and selected some compounds for second screening called “cherry picks”. The requested compounds included all the “strong” hits, and the “medium” hits with reasonable structures. 1  $\mu$ l of each selected screening positive compound ( $\sim$ 5  $\mu$ g) was provided and the second screening was performed in our lab (**Table 4.3** and **Table 4.4**). For those compounds we are interested from the “cherry picks”, the inhibition was measured in the presence and absence of 0.1% Triton X-100 according to the Shoichet’s method (5); molecules that inhibit only in the absence of detergent are considered likely promiscuous aggregators.

**Table 4.3: Inhibition data of second screens for strong hits (inhibitor concentration is 12  $\mu$ M)**

ID No.	Structure	Activity (%)	ID No.	Structure	Activity (%)
1486 C16		79.4	1504 L09		74.1
1515 O10		64.7	1533 D13		78.2
1535 P15		23.5	1546 C13		67.6
1548 J21		5.0	1548 L21		64.7
1552 E13		82.3	1670 O07		52.9
1671 E18		64.7	1697 A04		82.3
1704 G20		94.1	1727 B01		100

**Table 4.4: Inhibition data of second screens for medium hits (inhibitor concentration is 37.5  $\mu$ M)**

ID No.	Structure	Activity (%)	ID No.	Structure	Activity (%)
1474 D06		18.9	1482 I15		61.1
1538 N21		66.7	1540 P05		66.7
1577 B21		66.7	1578 I09		75.0
1615 I20		16.7	1622 I10		66.7
1701 M18		66.7	1755 P21		72.2
1759 E18		61.1	1759 I10		55.6
1772 J21		44.4			

From the results of “cherry picks”, it can be noted that a series of positive compounds, such as 1548 L21, have the backbone of OSB moiety of MenB substrate. The inhibition activities of the “substrate-like” molecules were tested against ecMenE by using PPI release assay and MenE/MenB assay using limited concentration of mtMenB. However, there was no inhibition observed at the concentration of inhibitor of 200  $\mu$ M, suggesting that this compound class primarily targets MenB in the coupled assay. In contrast, compounds such as 1486 C16 are reminiscent of the DHNA MenB product. Therefore, our subsequent SAR studies have primarily focused on the structure of “substrate-like” 2-amino-4-oxo-phenylbutanoic acids and “product-like” benzoxazinones (Figure 4.7).

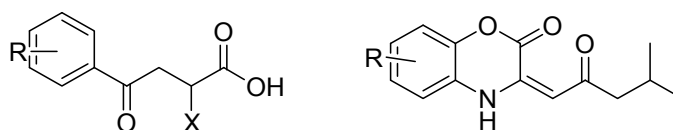
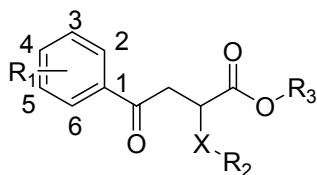


**Figure 4.7: Structure of 2-amino-4-oxo-phenylbutanoic acids and benzoxazinones**

#### *In vitro enzymatic inhibition assay of “substrate-like” inhibitors*

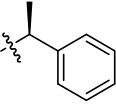
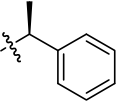
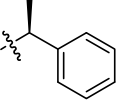
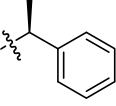
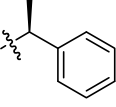
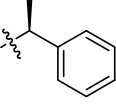
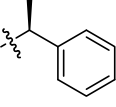
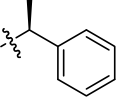
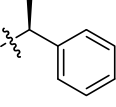
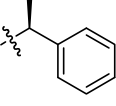
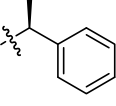
Our current SAR studies are primarily based on the structure of “substrate-like” 2-amino-4-oxo-phenylbutanoic acids. We have designed a series of molecules which contain the OSB moiety with the different substitutions in the aromatic ring and with different substitutions at the  $\alpha$ -carbon. These compounds were synthesized by Xiaokai Li in our group. The inhibition of different inhibitors was measured by ecMenE/mtMenB coupled assay which is described in the Materials and Methods section. The substrate and mtMenB were fixed as 30  $\mu$ M

and 200 nM, respectively. The enzyme inhibition data are summarized in **Table 4.5**.



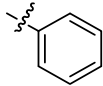
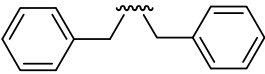
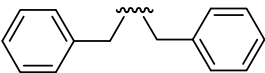
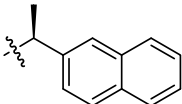
**Table 4.5: Inhibition of “substrate-like” inhibitors**

Compound	R <sub>1</sub>	X	R <sub>2</sub>	R <sub>3</sub>	IC <sub>50</sub> (μM)	MIC <sub>90</sub> <i>M. tb</i> (μg/mL)
1	H	NH		H	112.1 ± 10.7	7.81
2	4-F	NH		H	13.2 ± 0.75	8.46
3	4-Cl	NH		H	8.54 ± 0.80	7.52
4	4-Br	NH		H	105.4 ± 15.0	9.67
5	4-NO <sub>2</sub>	NH		H	>200	194.66
6	4-OMe	NH		H	>200	8.41
7	2-F	NH		H	8.70 ± 0.80	24.34
8	2-Cl	NH		H	8.50 ± 0.80	5.94

Compound	R <sub>1</sub>	X	R <sub>2</sub>	R <sub>3</sub>	IC <sub>50</sub> (μM)	MIC <sub>90</sub> <i>M. tb</i> (μg/mL)
9	2-Br	NH		H	0.600 ± 0.07	12.80
10	2-I	NH		H	0.630 ± 0.034	6.25
11	2-NO <sub>2</sub>	NH		H	2.1 ± 0.2	9.57
12	2-OMe	NH		H	>200	11.07
13	2-CF <sub>3</sub>	NH		H	2.10 ± 0.19	11.70
14	2-COOMe	NH		H	>200	>300
15	3-Cl	NH		H	>200	13.95
16	3-NO <sub>2</sub>	NH		H	>200	228.67
17	2,4-diF	NH		H	1.40 ± 0.18	7.11
18	2-Cl, 4-F	NH		H	1.10 ± 0.08	12.50
19	2-Br, 4-F	NH		H	0.430 ± 0.032	12.50

Compound	R <sub>1</sub>	X	R <sub>2</sub>	R <sub>3</sub>	IC <sub>50</sub> (μM)	MIC <sub>90</sub> <i>M. tb</i> (μg/mL)
20	2-CF <sub>3</sub> , 4-F	NH		H	0.823 ± 0.094	7.39
21	2,4-diCl	NH		H	0.262 ± 0.027	20.30
22	2,6-diCl	NH		H	7.11 ± 0.11	0.89
23	4-Cl	NH		H	41.9 ± 3.4	10.37
24	4-Cl	NH		H	17.2 ± 2.7	28.89
25	4-Cl	NH		H	>200	9.85
26	4-Cl	NH		H	18.1 ± 2.2	14.04
27	4-Cl	NH		H	3.25 ± 0.33	12.30
28	4-Cl	NH		H	10.0 ± 0.9	16.19
29	4-Cl	NH		H	7.25 ± 0.60	699.85
30	4-Cl	NH	n-octyl	H	15.1 ± 1.6	12.17
31(6)	4-Cl	S		H	>200	51.89

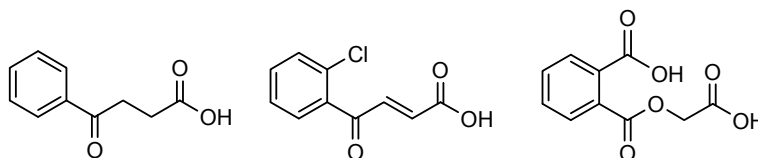


Compound	R <sub>1</sub>	X	R <sub>2</sub>	R <sub>3</sub>	IC <sub>50</sub> (μM)	MIC <sub>90</sub> <i>M. tb</i> (μg/mL)
32(7)	4-Cl	CH <sub>2</sub>		H	>200	45.41
33	4-Cl	N		H	2.2 ± 0.2	NA
34	4-Cl	N		CH <sub>3</sub>	NA	< 0.78
35	4-Cl	NH		H	25.1 ± 4.0	NA

One conclusion that can be drawn from the above data is that the addition of a bulky substituent (R<sub>1</sub>) at either the 2 or 4 position of the aromatic ring, or the addition of substitution at 3-position of the phenyl group resulted in significant reduction in enzymatic inhibition. In addition, while electron withdrawing groups increased the potency of inhibition, electron donating groups reduced the affinity of the compounds for MenB. The 2, 4-dichloro substituted compound **21** is the best inhibitor so far identified with an IC<sub>50</sub> value of 260 nM. Therefore, it can be concluded that two factors determine the inhibition activity for the aromatic substitutions: the size and electronic effect of the groups at the 2- and/or 4-position.

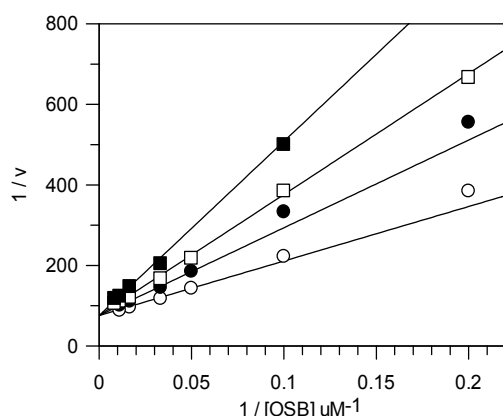
In addition to the importance of electron withdrawing substituents on the aromatic ring, the SAR data revealed two other important structural features for MenB inhibition: an amino group at position X and a hydrophobic R<sub>2</sub> group. Replacement of X with sulfur (compound **31**) or carbon (compound **32**) caused a significant reduction in inhibitory activity, while lower IC<sub>50</sub> values were observed

when R<sub>2</sub> was a (S)-1-phenylethyl (such as compound **21**), a (S)-1-cyclohexylethyl (compound **27**) or diphenylmethyl (compound **33**). In addition, a series of OSB analogues lack the corresponding R<sub>2</sub> substituents and don't show inhibition against mtMenB (**Figure 4.8**). Although structures of the inhibitors bound to MenB are not currently available, analysis of existing structural data suggests that the R<sub>2</sub> substituent may occupy the hydrophobic pocket revealed in the dimethoxy DHNA-CoA structure (**Figure 2.52**).



**Figure 4.8: Structures of compounds showed poor inhibition against mtMenB**

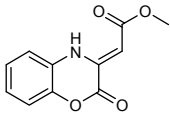
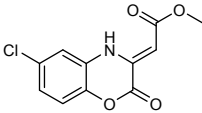
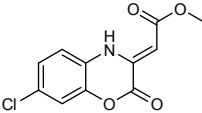
Compound **8** is a competitive inhibitor of mtMenB with a K<sub>i</sub> value of 8.1 ± 0.6 μM (**Figure 4.9**). It can be deduced that the “substrate-like” inhibitors occupy the active site and compete with substrate for the active site.



**Figure 4.9: Compound 8 is a competitive inhibitor.** The inhibition of compound **8** against mtMenB in the absence of inhibitor (○), in the presence of 5 μM of compound **8** (●), 10 μM of compound **8** (□) or 18 μM of compound **8** (■).

*In vitro* enzymatic inhibition assay of “product-like” inhibitors

The SAR studies on “product-like” benzoxazinone inhibitors are less well advanced. Compounds 35-37 were synthesized and their IC<sub>50</sub> values were measured (**Table 4.6**).

Compound	Structure	IC <sub>50</sub> (μM)	MIC <sub>90</sub> <i>M. tb</i> (μg/mL)
36		10.1 ± 0.9	<0.78
37		23.1 ± 1.0	NA
38		46.2 ± 2.9	NA

Unlike “substrate-like” inhibitors, compound **36** (“product-like”) is a non-competitive inhibitor with a K<sub>i</sub> value of 14.1 ± 0.6 μM (**Figure 4.10**). Non-competitive inhibition occurs when the inhibitor binds at a site away from the substrate binding site, causing a reduction in the catalytic rate. A non-competitive inhibitor could be a promiscuous inhibitor. However, the inhibition was not affected in the presence or absence of 0.1% Triton X-100, indicating that the inhibition of compound **36** is not due to the promiscuous aggregation. Further SAR studies as well as binding assays will be conducted.

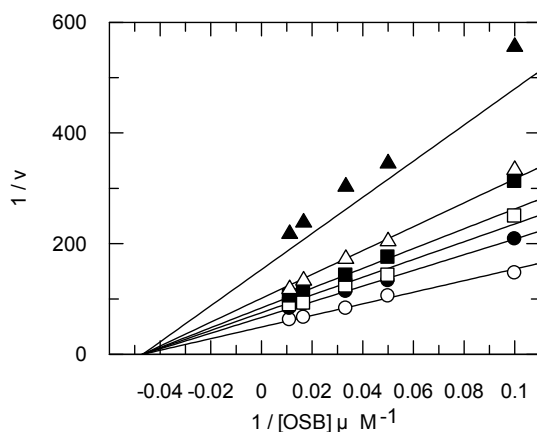


**Figure 4.10: Compound 36 is a non-competitive inhibitor.** The inhibition of compound 36 against mtMenB in the absence of inhibitor ( $\circ$ ), in the presence of 5  $\mu\text{M}$  of compound 36 ( $\bullet$ ), 7.5  $\mu\text{M}$  of compound 36 ( $\square$ ), 10  $\mu\text{M}$  of compound 36 ( $\blacksquare$ ), 15  $\mu\text{M}$  of compound 36 ( $\triangle$ ) or 30  $\mu\text{M}$  of compound 36 ( $\blacktriangle$ ).

#### *MK-7 can partially rescue the growth of B. subtilis*

In order to validate whether MenB and menaquinone biosynthesis are essential for bacterium growth, the supplement experiments with DHNA, menadione and MK-7 were performed. These experiments were performed with *B. subtilis* instead of *M. tuberculosis* since this organism can be grown in normal lab conditions (BSL-1) and MenB from *B. subtilis* and mtMenB share 50.6% identity over 265 residues overlap. *B. subtilis* is a fast growing Gram positive bacterium that also requires menaquinone for survival. The menaquinone biosynthetic pathway of *B. subtilis* is the same as in *M. tuberculosis* except that *M. tuberculosis* uses MK-9 while *B. subtilis* uses MK-7 for electron transportation.

The experiments using DHNA and menadione were unsuccessful since DHNA was unstable in solution and menadione indeed inhibited the growth of the

bacterium. However, supplement with MK-7 rescued the growth of *B. subtilis* (Figure 4.11). Figure 4.12 showed that compound 8 killed its growth at the concentration of <math><200 \mu\text{M}</math> (60  $\mu\text{g/mL}</math>). While the supplement of MK-7 partially overcome the inhibition, which indicates that menaquinone biosynthesis is required for bacterial survival.$

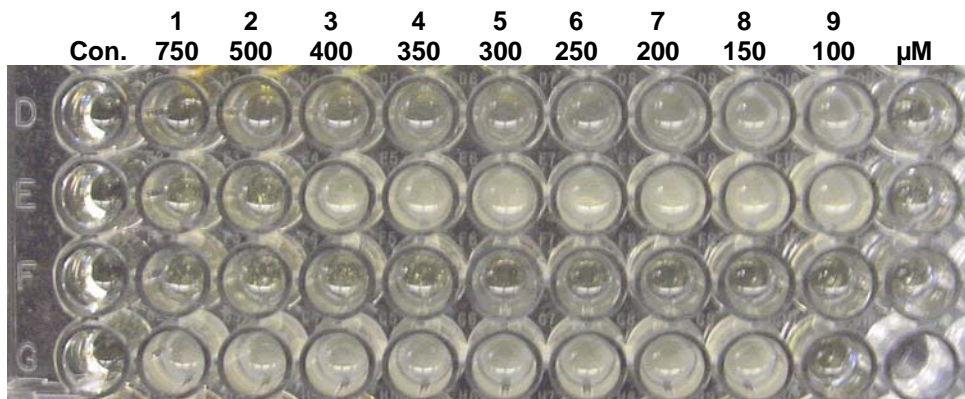


**Figure 4.11: Supplement experiment with MK-7.** Lane D1-D9 contained compound 8 (concentration from 750-100  $\mu\text{M}</math>). Lane E1-E9 contained same concentration of compound 8 and 200  $\mu\text{M}</math> of MK-7 each. Lane F1-F8 were negative control (no cells grew) and lance G1-G8 were positive controls (cells grew).$$

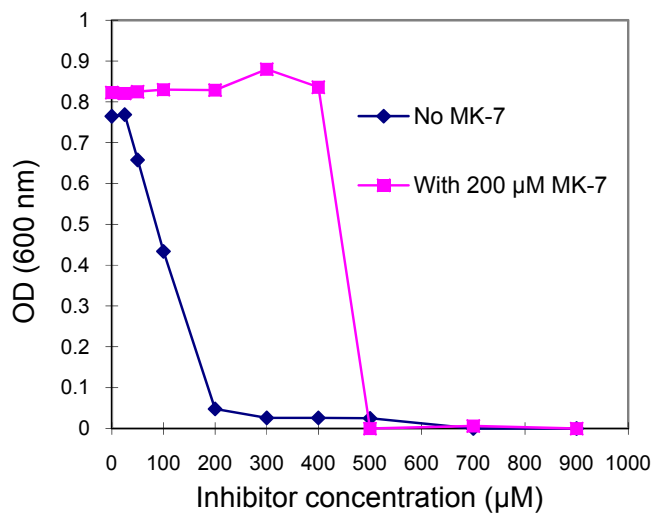


**Figure 4.12: MK-7 partially overcame the inhibition of compound 8**

*In vitro* antibacterial activity of inhibitors against *M. tuberculosis*

The MIC<sub>90</sub> values of different inhibitors against *M. tuberculosis* were measured by Susan E. Knudson in the Department of Microbiology, Immunology and Pathology, Colorado State University (**Table 4.5 and Table 4.6**). Basically, IC<sub>50</sub> and MIC<sub>90</sub> had a reasonable linear correlation with each other, which indicates these groups of compounds target mtMenB. However, it is important to note that several compounds have very good MIC<sub>90</sub> values but have poor IC<sub>50</sub> values, suggesting that mtMenB might not be the only target.

Interestingly, the methyl ester compound **34** has extremely good MIC<sub>90</sub> value of < 0.78 µg/mL. Although we don't have the MIC<sub>90</sub> value of its acid compound **33**, it can be deduced by comparing with other compounds that the methyl ester improves the antibacterial activity probably because it increases the molecule hydrophobicity and facilitates transport across the mycobacterial membrane.

## Conclusions

Two types of lead inhibitors of mtMenB including “substrate-like” 2-amino-4-oxo-phenylbutanoic acids and “product-like” benzoxazinones were identified from high throughput screening.

Our initial SAR studies on 2-amino-4-oxo-phenylbutanoic acids suggest that the introduction of electron withdrawing substituents on the aromatic ring ( $R_1$ ) is essential for inhibition. In addition, two other important structural features for MenB inhibition include an amino group at position X and a hydrophobic  $R_2$  group. The best inhibitor (compound **21**) indentified so far has an  $IC_{50}$  value of 260 nM. The “substrate-like” inhibitors are competitive inhibitors of mtMenB.

In contrast, the SAR studies on “product-like” inhibitors are less well advanced. Benzoxazinone compound **36** is a non-competitive inhibitor with an  $IC_{50}$  value of 10  $\mu$ M and a  $K_i$  value of 14  $\mu$ M.

Although we do not have structures of these inhibitors bound to mtMenB, the structure of the product analogue dimethoxy DHNA-CoA bound to mtMenB provides a clue concerning how the compounds may bind to the enzyme. The hydrophobic pocket might provide a potential location for the  $R_2$  group of 2-amino-4-oxo-phenylbutanoic acids and non-competitive inhibitors to bind.

The  $MIC_{90}$  values of different inhibitors against *M. tuberculosis* are basically correlated to their  $IC_{50}$  values, indicating MenB is the target for these two types of inhibitors. The inhibition can be partially overcome by the supplement with MK-7, which indicates that menaquinone biosynthesis is required for bacterial survival.

## References

1. Taber, H. W., Dellers, E. A., and Lombardo, L. R. (1981) Menaquinone biosynthesis in *Bacillus subtilis*: isolation of men mutants and evidence for clustering of men genes, *Journal of bacteriology* 145, 321-327.
2. Zhang, J. H., Chung, T. D., and Oldenburg, K. R. (1999) A Simple Statistical Parameter for Use in Evaluation and Validation of High Throughput Screening Assays, *J Biomol Screen* 4, 67-73.
3. Heath, R. J., Li, J., Roland, G. E., and Rock, C. O. (2000) Inhibition of the *Staphylococcus aureus* NADPH-dependent enoyl-acyl carrier protein reductase by triclosan and hexachlorophene, *The Journal of biological chemistry* 275, 4654-4659.
4. Frederick, J. J., Corner, T. R., and Gerhardt, P. (1974) Antimicrobial actions of hexachlorophene: inhibition of respiration in *Bacillus megaterium*, *Antimicrobial agents and chemotherapy* 6, 712-721.
5. Feng, B. Y., Shelat, A., Doman, T. N., Guy, R. K., and Shoichet, B. K. (2005) High-throughput assays for promiscuous inhibitors, *Nat Chem Biol* 1, 146-148.
6. Drakulic, B. J., Juranic, Z. D., Stanojkovic, T. P., and Juranic, I. O. (2005) 2-[(Carboxymethyl)sulfanyl]-4-oxo-4-arylbutanoic acids selectively suppressed proliferation of neoplastic human HeLa cells. A SAR/QSAR study, *Journal of Medicinal Chemistry* 48, 5600-5603.



7. Drake, N. L., and Tuemmler, W. B. (1955) PODOPHYLLOTOXIN AND PICROPODOPHYLLIN .2. THE SYNTHESIS OF AN OPEN-CHAIN ANALOG, *Journal of the American Chemical Society* 77, 1204-1209.

## CHAPTER 5: EXPRESSION AND INHIBITION STUDIES OF MENE

This chapter is based on part of work that has been published in: Mechanism-based inhibitors of MenE, an acyl-CoA synthetase involved in bacterial menaquinone biosynthesis. Lu X, Zhang H, Tonge PJ, Tan DS, Bioorg Med Chem Lett. 2008 Nov 15; 18(22):5963-6. Epub 2008 Aug 12.

### Background

OSB-CoA synthase (MenE), an acyl-CoA synthetase, catalyzes a magnesium-dependent multisubstrate reaction, resulting in the conversion of OSB to OSB-CoA *via* a two-step process involving the initial ATP-dependent adenylation of OSB to form a reactive OSB-AMP intermediate, followed by thioesterification with CoA to form OSB-CoA (**Figure 5.1**) (1, 2). The mutagenesis technology using transposon site hybridization (TraSH) identified *menE* gene is essential in *M. tuberculosis* (3).

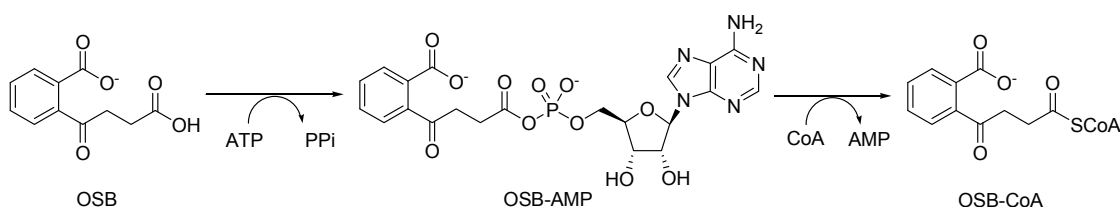


**Figure 5.1: MenE reaction**

The MenE reaction is analogous to that catalyzed by the long chain acyl-CoA synthetases (LC-FACS). Similarly, the synthesis of fatty acyl-CoA includes two discrete steps: 1) the formation of a fatty acyl-AMP molecule as a stable

intermediate and 2) the formation of a fatty acyl-CoA molecule as the final product (**Figure 5.2**) (4, 5).

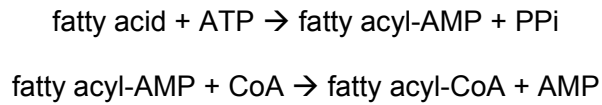


**Figure 5.2: Long chain fatty acyl-CoA synthetases reaction**

The molecular mechanism of LC-FACS is proposed to be compatible with the Bi Uni Uni Bi Ping-Pong based on the three high resolution structures of *Thermus thermophilus* HB8 LC-FACS (ttLC-FACS) (5) and extensive kinetic studies of the rat enzyme (6). The reaction scheme is summarized as follows (**Figure 5.3**). The binding of ATP triggers the closed conformation and opening of the W234 gate of the fatty acid-binding tunnel (**Figure 5.3 A and B**). After the fatty acid molecule binds and the fatty acyl-AMP intermediate is formed, the pyrophosphate molecule leaves (**Figure 5.3 C**). A CoA molecule then binds and the final product fatty acyl-CoA is formed (**Figure 5.3 C and D**). Finally, the fatty acyl-CoA followed by the AMP leave after opening of the C-terminal domain (**Figure 5.3 E**) (5, 7).

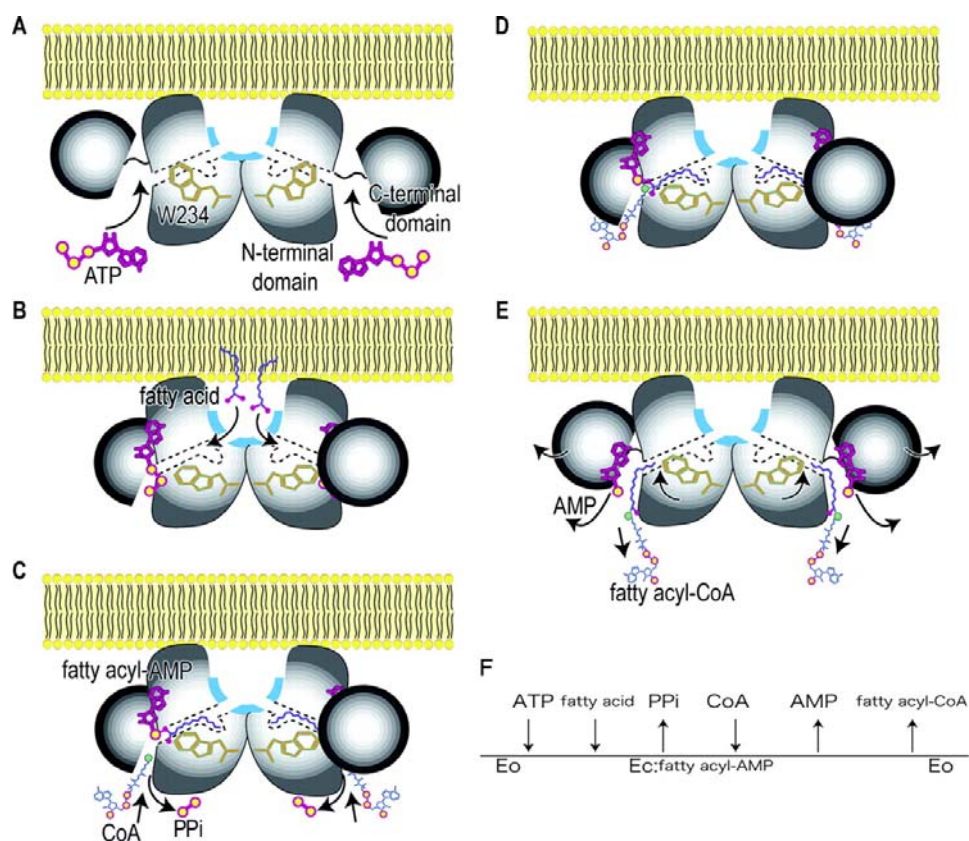


**Figure 5.3: The schematic mechanism for the catalysis by ttLC-FACS (taken from reference (5)).**

Acyl-CoA synthetases belong to a superfamily of structurally and mechanistically related adenylate-forming enzymes, and the crystal structures of several superfamily members have been solved (5, 8-10). Analogous adenylation reactions are also catalyzed by structurally unrelated aminoacyl-tRNA synthetases (11).

A series of 5'-O-(*N*-acylsulfamoyl) adenosines (acyl-AMS) and related compounds were reported to inhibit such adenylate-forming enzymes by mimicking the cognate, tightly bound acyl-AMP intermediates (12-22) (**Table 5.1**).

These molecules were inspired by a class of sulfamoyladenine natural products that includes nucleocidin and ascamycin (23, 24).

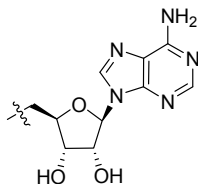


**Table 5.1: Representative inhibitors of aryl acid adenylation enzymes**

Inhibitor	Enzyme	$K_i^{\text{app}}/\text{nm}$	Organism
	YbtE	0.3–1.1	<i>Y. pestis</i>
	MbtA	5.1–6.6	<i>M. tuberculosis</i>
	MbtA	3.7–3.8	<i>M. tuberculosis</i>
	DhbE	85	<i>B. subtilis</i>
	EntE	9	<i>E. coli</i>
	AsbC	250 (IC <sub>50</sub> value)	<i>B. anthracis</i>

In this chapter, we will discuss our efforts to obtain the soluble mtMenE using the different expression hosts including *M. smegmatis* and *E. coli*. Although mtMenE has proven difficult to obtain, ecMenE expresses very well in *E. coli*. In addition, a series of mechanism-based inhibitors which mimic the tightly-bound

OSB-AMP intermediates were designed and their inhibition against MenE enzyme will be discussed.

## Materials and methods

### *Expression and purification of ecMenE*

The *menE* gene *b2260* (1356 bp), used for the overexpression and purification of ecMenE was previously isolated by PCR from genomic DNA, cloned into the pET-15b plasmid (Novagen) and placed in frame with an N-terminal His-tag sequence, by Yuguo Feng. Protein expression was performed using *E. coli* BL21 (DE3) cells. Transformed cells were grown in 800 mL of LB media containing 0.2 mg/mL ampicillin and induction was achieved using 1 mM IPTG overnight at 25 °C. Cells were harvested by centrifugation at 5,000 rpm for 20 min at 4 °C, resuspended in 30 mL of His-binding buffer (5 mM imidazole, 0.5 M NaCl, 20 mM Tris HCl, pH 7.9) and lysed by 3 passages through a French Press cell (1,000 psi). Cell debris was removed by centrifugation at 33,000 rpm for 90 min at 4 °C. MenB was purified using His affinity chromatography: the supernatant was loaded to a column containing 3 mL of His-bind resin (Novagen), charged with 9 mL of charge buffer (Ni<sup>2+</sup>). The column was washed with 20 mL of His-binding buffer and 20 mL of wash buffer (60 mM imidazole, 0.5 M NaCl, 20 mM Tris HCl, pH 7.9). ecMenB was eluted using a gradient of 20 mL elute buffer (0.5 M imidazole, 0.5 M NaCl, 20 mM Tris HCl, pH 7.9). Fractions containing ecMenE were collected and the imidazole removed by chromatography on G-25 resin using 20 mM NaH<sub>2</sub>PO<sub>4</sub>, 0.1 M NaCl at pH 7.0, as storing buffer. The concentration of ecMenE was determined by measuring the absorption at 280 nm using an extinction coefficient of 104,770 M<sup>-1</sup>cm<sup>-1</sup> calculated from the primary

sequence. The enzyme was concentrated by using Centricon-30 (Amicon) and stored at -80 °C.

#### *Cloning and expression of mtMenE in M. smegmatis cells*

The *mene* gene *Rv0542c* (1089 bp) was amplified from *M. tuberculosis* genomic DNA by PCR and cloned into the pVVAP, pVV16 and pJAM2 plasmid by using the following oligonucleotides (primers):

Vector	Primer sequence (from 5' to 3' sequence)	Restriction site
pVVAP and pVV16	F: GGAATTCCATATGGTGCTGGGTGGCAGCGACCC	NdeI
	R: CCCAAGCTTCTATTGATCGGCTTCACCGGCGAA	HindIII
pJAM2	F: CGGGATCCGTGCTGGGTGGCAGCGACCCGGAC	BamHI
	R: GCTCTAGACTATTGATCGGCTTCACCGGCGAA	XbaI

The above plasmids were transformed into *M. smegmatis* competent cell by electroporation (2.5 kV). The transformants were resuspended in 900 µL of 7H9 medium, 300 µL of which were plated on a 7H10-Kan plate. The plate was incubated at 35.5 °C for 3 to 4 days. A 15 mL rich culture (7H9 medium with 0.2% glycerol, 1.5 mL OADC and 5 µL Tween 80) with kanamycin (30 µg/mL) was inoculated from a single colony and shaken at 35.5 °C for approximately 36 hours. 800 mL 7H9 medium was inoculated with 1 mL of rich culture, and shaken at 35.5 °C for 24 hours or longer until the OD<sub>600</sub> value reached around 0.4. 0.4% acetamide was added to cells harboring the pVVAP and pJAM2, and the cells were incubated at 35.5 °C or 25 °C for an additional 24 hours (there is no



induction promoter in pVV16 vector). Cells were harvested by centrifugation at 5,000 rpm for 20 min at 4 °C.

*Cloning and expression of mtMenE in E. coli cells*

The *mene* gene *Rv0542c* (1089 bp) was amplified from *M. tuberculosis* genomic DNA by PCR and cloned into the pET23b and pET43b (N terminus and C terminus His-tag) plasmids by using the following oligonucleotides (primers). The gene was also cloned into pET15b plasmid by Hua Xu in our group.

Vector	Primer sequence (from 5' to 3' sequence)	Restriction site
pET23b	F: GGAATTCCATATGATGCTGGGTGGCAGCGACCC	NdeI
	R: CCGCTCGAGTTGATCGGCTTCACCGGCGAACCG	XhoI
pET43b N His-tag	F: TTCCCCCGGGATGCTGGGTGGCAGCGAC	SmaI
	R: CCGCTCGAGCTATTGATCGGCTTCACCGGCGAA	XhoI
pET43b C His-tag	F: GACTAGTATGCTGGGTGGCAGCGACCCGGCATT	BamHI
	R: CCGCTCGAGTTGATCGGCTTCACCGGCGAACCG	XhoI

Four plasmids were transformed into *E. coli* Rosette2 (DE3) (Novagen) competent cells by heat shock. Transformed cells were grown in 800 mL of LB medium containing 0.2 mg/mL ampicillin and induction was achieved using 0.5 mM IPTG overnight at 25 °C. Cells were harvested by centrifugation at 5,000 rpm for 20 min at 4 °C.

### *E. coli* rare codon mutagenesis

In order to improve the expression of heterologous *M. tuberculosis* MenE in *E. coli* cell, a series of mutagenesis were performed to mutant the rare *E. coli* codons to inherent codons. The primers are listed in **Table 5.2**.

**Table 5.2: Primer sequences for *E. coli* rare codon mutagenesis**

Primer (from 5' to 3' sequence)		
1	Forward	GCCGACGACCGTCTCGGTCAGCGTGTGGTC
	Reverse	GACCACACGCTGACCGAGACGGTCGTGGGC
2	Forward	ACCGCCGCGCCGCGTGAGCTGCATGTCGTG
	Reverse	CACGACATGCAGCTCACGCGGCGCGGCGGT
3	Forward	GTGAACGTGCTGCCGCGTCGCGGCATCGGC
	Reverse	GCCGATGCCGCGACGCGGCAGCACGTTAC
4	Forward	TTACCGAACGCGATCAAGCGTTTGGGTTCTGGC
	Reverse	GCCAGAACCCAAACGCTTGATCGCGTTCGGTAA
5	Forward	TTGGGTTCTGGCCGTCGTTACACGTCGCTG
	Reverse	CAGCGACGTGTAACGACGGCCAGAACCCAA
6	Forward	CTCGACGGGGTCCGTCTGCGTGTGCTGGCCGGC
	Reverse	GCCGGCCAGCACACGCAGACGGACCCCGTTCGAG
7	Forward	TTGCTGGGCGCTTTGCGTGTGGGCGAGCAGATT
	Reverse	AATCTGCTCGCCACACGCAAAGCGCCAGCAA
8	Forward	GGCGGGCCGGCCCCGCGTCCGATCCTGGACGCC
	Reverse	GGCGTCCAGGATCGGACGCGGGGCCGGCCCCGCC
9	Forward	GGTGGTTGCGACCTTCGCGACGCACGCGTACAG
	Reverse	GACATGCGCACGCAGCGCTTCCAGCGTTGGTGG

Primer (from 5' to 3' sequence)		
10	Forward	GAATTACCCAACGCGATCAAGAGATTGGGTTCTG
	Reverse	CAGAACCCAATCTCTTGATCGCGTTGGGTAATTC
11	Forward	AGAAGCGCTGCGTGCGCATGTCGCGCGCAC
	Reverse	GTGCGCGCGACATG CGCACG CAGCGCTTCT
12	Forward	ACCACCAACGCTGGAA GCG CTG CGT GCGCA
	Reverse	TGCGCACGCAGCGCTTC CAGCGTTGGTGGT
13	Forward	ACGCGATAAAGCGTTTGGGTTCTGGCCGGCGATAC
	Reverse	GTATCGCCGGCCAGAACCCAAACGCTTTATCGCGT

*Expression and purification of rare codon mutant of mtMenE in E. coli cells*

After 13 steps of rare codon mutagenesis, the plasmid was transformed into *E. coli* Rosette2 (DE3) (Novagen) competent cells by heat shock. Transformed cells were grown in 800 mL of LB medium containing 0.2 mg/mL ampicillin and 5% glycerol and induction was achieved using 0.5 mM IPTG overnight at 16 °C. Cells were harvested by centrifugation at 5,000 rpm for 20 min at 4 °C, resuspended in 30 mL of Ni-NTA Bind Buffer (10 mM imidazole, 300 mM NaCl, 50 mM sodium phosphate buffer, pH 8.0) and lysed by 3 passages through a French Press cell (1,000 psi). Cell debris was removed by centrifugation at 33,000 rpm for 90 min at 4 °C. MenB was purified using His affinity chromatography: the supernatant was loaded to a column containing 3 mL of Ni-NTA His-Bind resins (Novagen). The column was washed with 20 mL of Ni-NTA Bind Buffer and 20 mL of wash buffer (20 mM imidazole, 300 mM NaCl, 20 mM sodium phosphate buffer, pH 8.0). mtMenE was eluted using a gradient of 20 mL elute buffer (250 mM

imidazole, 300 mM NaCl, 20 mM sodium phosphate buffer, pH 8.0). The concentration of MenB was determined by measuring the absorption at 280 nm using an extinction coefficient of  $17,900 \text{ M}^{-1}\text{cm}^{-1}$  calculated from the primary sequence. SDS-PAGE gel showed not a pure band as 37 kDa.

#### *Coupled assay of MenE reaction*

The coupled reactions were performed in 20 mM  $\text{NaH}_2\text{PO}_4$  pH 7.0, 150 mM NaCl, 1 mM  $\text{MgCl}_2$  buffer. 20 nM of ecMenE was incubated with ATP (120  $\mu\text{M}$ ), CoA (120  $\mu\text{M}$ ), OSB (0-120  $\mu\text{M}$ ) and excess MenB (4  $\mu\text{M}$ ). The formation of DHNA-CoA was monitored at 392 nm and initial velocities were determined using an extinction coefficient of  $4,000 \text{ M}^{-1}\text{cm}^{-1}$ .  $V_{\max}$  and  $K_m$  values were obtained by fitting all the data to the Michaelis-Menten equation (1) using GraFit 4.0.  $k_{\text{cat}}$  values were obtained using the equation (2) .

$$v = \frac{V_{\max}[S]}{K_m + [S]} \quad (1)$$

$$V_{\max} = k_{\text{cat}} \times [E] \quad (2)$$

#### *Assay for inhibition of ecMenE*

Reactions were performed in 20 mM  $\text{NaH}_2\text{PO}_4$  pH 7.0, 150 mM NaCl, 1 mM  $\text{MgCl}_2$  buffer. 20 nM of ecMenE was incubated with inhibitor (0–200  $\mu\text{M}$ ), ATP (120  $\mu\text{M}$ ) and CoA (120  $\mu\text{M}$ ) for 10 minutes prior to the addition of MenB (4  $\mu\text{M}$ ) and OSB (30  $\mu\text{M}$ ). The formation of DHNA-CoA was monitored at 392 nm and initial velocities were determined using an extinction coefficient of  $4,000 \text{ M}^{-1}\text{cm}^{-1}$ .

IC<sub>50</sub> values were calculated by fitting the initial velocity data ( $v_i$ ) obtained at different inhibitor concentrations ([I]) to equation (3) using Grafit 4.0.

$$v_i = \frac{100\%}{1 + [I]/IC_{50}} \quad (3)$$

## Results and discussion

### *Expression of ecMenE and enzymatic activity*

ecMenB was expressed and purified as pure protein band as 52 kDa (**Figure 5.4**). Compared to mtMenE whose molecular weight is 37 kDa, ecMenE is much larger. They share 29.8% identity in 275 residues overlap. Instead of using PPI release assay which only represents the first step of MenE reaction, ecMenE/mtMenB coupled assay was employed to determine the enzymatic activity. The  $k_{cat}$  and  $K_m$  value are  $140.0 \pm 2.5$  and  $4.9 \pm 0.3$ , respectively, for ecMenE when the concentration of ATP and CoA were fixed.

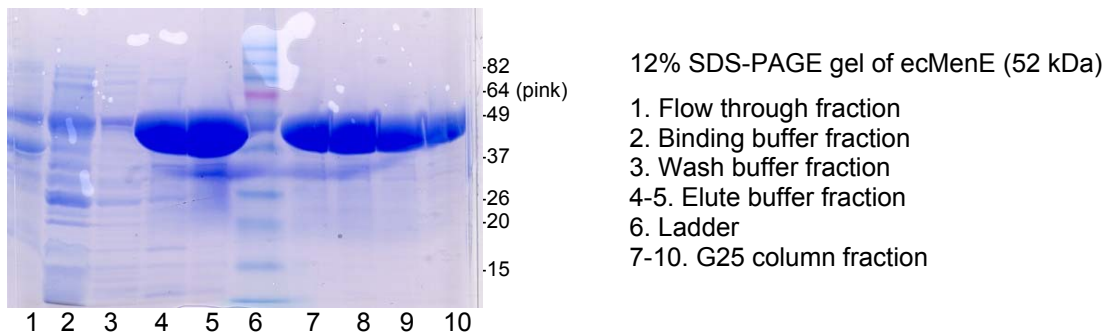


**Figure 5.4: SDS-PAGE gel of ecMenE**

### *Expression of mtMenE*

We have encountered an enormous difficulty during the process of expressing mtMenE in heterologous systems. In *M. smegmatis* cells, there was no expression of the protein by using pVVAP, pVV16 and pJAM2 expression vectors. Similarly, the expression in *E. coli* pET15b, pET23b and pET43b (designed N- and C-terminus His-tag) all failed. We speculated that the lack of success at expressing mtMenE in *E. coli* might be due to the presence of a large number of rare codons (35 rare codons among 362 residues) (**Figure 5.5**).

GTG CTG GGT GGC AGC GAC CCG GCA TTG GTC GCG GTG CCC ACC CAG CAT  
 GAG TCC TTG CTG GGC GCT TTG CGA GTG GGC GAG CAG ATT GAC GAC GAC  
 GTC GCC CTG GTA GTG ACG ACG TCA GGA ACC ACG GGA CCG CCC AAG GGC  
 GCC ATG TTG ACC GCG GCG GCC TTG ACC GCC AGC GCC TCG GCC GCC CAC  
 GAC CGG CTC GGC GGA CCG GGC AGC TGG CTG TTG GCT GTG CCG CCG TAT  
 CAC ATC GCC GGG CTG GCG GTG CTG GTG CGC AGC GTG ATC GCC GGA TCA  
 GTT CCT GTC GAA CTG AAC GTC TCC GCG GGA TTC GAT GTC ACC GAA TTA  
 CCC AAC GCG ATA AAG AGA TTG GGT TCT GGC CGG CGA TAC ACG TCG CTG  
 GTC GCC GCA CAG TTG GCC AAG GCA CTT ACC GAC CCG GCG GCC ACG GCC  
 GCG CTG GCC GAA TTG GAC GCG GTG CTG ATC GGC GGC GGG CCG GCC CCC  
 CGG CCC ATC CTG GAC GCC GCG GCC GCC GCC GGC ATC ACG GTG GTG CGC  
 ACC TAC GGC ATG AGC GAG ACC TCG GGC GGC TGT GTC TAC GAC GGC GTT  
 CCG CTC GAC GGG GTC CGG CTG AGG GTG CTG GCC GGC GGC CGC ATA GCT  
 ATC GGC GGT GCG ACC CTG GCC AAG GGC TAT CGC AAC CCG GTC TCG CCC  
 GAT CCG TTC GCC GAG CCA GGC TGG TTT CAC ACC GAC GAC CTT GGC GCC  
 CTT GAA TCG GGT GAT TCG GGT GTG CTG ACC GTG CTG GGC CGA GCC GAC  
 GAA GCG ATC AGC ACG GGC GGA TTC ACC GTG CTG CCG CAG CCA GTG GAG  
 GCC GCA CTG GGC ACC CAC CCT GCG GTG CGT GAC TGC GCG GTT TTT GGA  
 CTT GCC GAC GAC CGA CTC GGT CAG CGA GTG GTC GCC GCG ATT GTG GTC  
 GGC GAC GGA TGC CCA CCA CCA ACG CTA GAA GCG CTG CGG GCG CAT GTC  
 GCG CGC ACC CTG GAC GTC ACC GCC GCG CCC CGA GAG CTA CAT GTC GTG  
 AAC GTG CTA CCG CGA CGC GGC ATC GGC AAG GTG GAC CGG GCA GCG TTG  
 GTG CGC CGG TTC GCC GGT GAA GCC GAT CAA TAG

**Figure 5.5: Rare *E. coli* codons in *M. tuberculosis mene* DNA sequence.** Red = rare Arg codons; green = rare Leu codon; blue = rare Ile codon; orange = rare Pro codon; and pink = rare Gly codon. Residues with yellow background are mutation sites.

Most amino acids are encoded by more than one codon, and *E. coli*, and indeed all cells, uses a specific subset of the 61 available amino acid codons for the production of most mRNA molecules (25, 26). So-called major codons are those that occur in highly expressed genes, whereas the minor or rare codons tend to be in genes expressed at a low level. When the mRNA of heterologous target genes is overexpressed in *E. coli*, differences in codon usage can disturb translation due to the demand for one or more tRNAs that may be rare or lacking in the population (27-29). Approaches normally used to overcome this problem include targeted mutagenesis to remove rare codons or the addition of rare codon tRNAs in specific cell lines. The commercial available Rosetta2 (DE3) host strain (Novagen) which is compatible with pET vectors, is designed to enhance the production of rare codon tRNAs. However, the expression by using Rosetta2 competent cells was unsuccessful again.

Therefore, 14 rare *E. coli* codon sites among 35 rare codon sites were mutated into major codon (**Figure 5.5**). The mutation plasmid was expressed in Rosetta2 (DE3) cells. Although the expression level has been greatly improved, most of the expressed mtMenE protein was found in the pellet (**Figure 5.6** lane 1-3). Two methods including lowering the induction temperature and adding glycerol were employed to improve the solubility of mtMenE protein. It can be noted that a small portion of the protein was soluble when 4% of glycerol was added and 16 °C was used for induction (**Figure 5.6** lane 4-11). However, SDS-PAGE gel showed that mtMenE was not pure with a distinct lower band around 20 kDa after purification (**Figure 5.7**). The lower band could be the truncated



mtMenE. The purified fraction showed the MenE activity. The detailed kinetic analysis was not conducted due to the impurity. Therefore, the solubility problem should be addressed in the future.

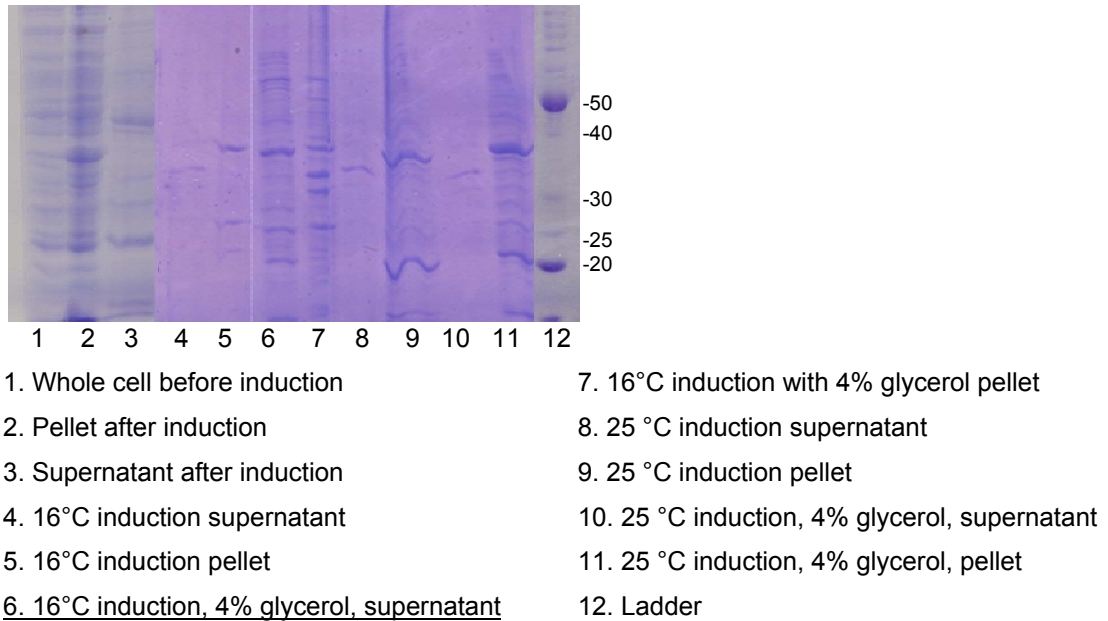


**Figure 5.6: Expression of mtMenE after rare codon mutations.** Sample in lane 4-11 were pre-treated with 5  $\mu$ L of His-Bind resin and loaded with the resin, so they basically represented proteins with His-tag.

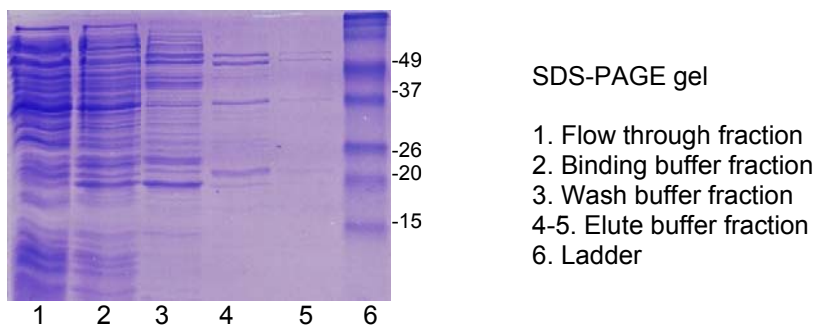


**Figure 5.7: The SDS-PAGE gel showed mtMenE was not pure after purification.**

Recently, our collaborator, Professor Kisker's lab, completed the total synthesis of *menE* DNA without *E. coli* codon bias and they successfully obtained the good expression and soluble protein, indicating the expression problem in *E. coli* is due the high frequency of rare codons in the mtMenE gene.

#### *Design of mechanism-based inhibitors of MenE*

MenE converts OSB to OSB-CoA *via* a two-step process involving initial ATP-dependent adenylation of OSB to form a reactive OSB-AMP intermediate, followed by thioesterification with CoA to form OSB-CoA (**Figure 5.1**). Based on the structure of intermediate, 5'-O-(*N*-acylsulfamoyl) adenosines (acyl-AMS) and related compounds were designed to inhibit MenE by mimicking tightly-bound OSB-AMP intermediates. To avoid potential pharmacological liabilities, we replaced aromatic carboxylate of OSB with a neutral methyl ester, since this carboxylate is not directly involved in the reaction mechanism (30, 31) and we have found that the aromatic methyl ester OSB-CoA (MeOSB-CoA) is more stable than OSB-CoA which has been discussed in chapter 2. Thus, we envisioned that MeOSB-AMS (**1**) or its sulfamide analog MeOSB-AMSN (**2**) might be effective inhibitors of MenE and menaquinone biosynthesis (**Figure 5.8**).

We also considered that the corresponding vinyl sulfonamide MeOSB-AVSN (**3**) might inhibit MenE through covalent binding to the incoming CoA thiol nucleophile during the second half-reaction (**Figure 5.9**), forming a mimic of the tetrahedral intermediate. Michael acceptors have been used extensively to inhibit cysteine proteases (32), and also to target protein thiol nucleophiles in

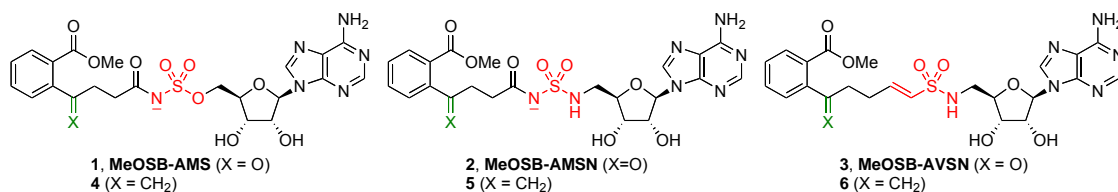


**Figure 5.8: Structures of designed inhibitors of MenE.** The sulfamate (1, 4) and sulfamide (2, 5) functionalities (red) are designed to mimic the phosphate group in the cognate OSB-AMP reaction intermediate. The vinyl sulfonamide moiety (3, 6) is designed to trap the incoming CoA nucleophile covalently. The corresponding *exo*-methylene analogs (4–6) are designed to probe the importance of the aromatic ketone functionality (green) for binding.

polyketide and non-ribosomal peptide synthetases (33, 34). Based on studies of Roush and coworkers on the inherent reactivity of various sulfonyl-based Michael acceptors (35), we selected the vinyl sulfonamide moiety to provide the requisite balance of reactivity and selectivity to bind CoA in the MenE active site without reacting promiscuously with other nucleophiles.

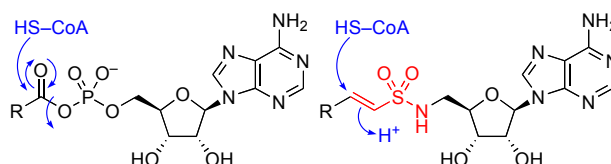


**Figure 5.9: Mechanism of covalent inhibition.** (*left*) The CoA thiol nucleophile attacks the carbonyl group in the acyl-AMP intermediate during the second half-reaction catalyzed by acyl-CoA synthetases. (*right*) A vinyl sulfonamide Michael acceptor is appropriately positioned to trap the incoming nucleophile and form a covalent adduct.

### *Inhibition of ecMenE*

Since we were unable to reliably express mtMenE, IC<sub>50</sub> values were determined against ecMenE (**Table 5.3**). We were gratified to find that both the sulfamate MeOSB-AMS (**1**) and sulfamide MeOSB-AMSN (**2**) were effective inhibitors of MenE (**Table 5.3**). Moreover, the vinyl sulfonamide analog MeOSB-AVSN (**3**) was proved to be the most potent inhibitor, with an IC<sub>50</sub> value of 5.7 ± 0.7 μM; kinetic analysis indicated that this compound is a slow-binding inhibitor, suggesting a conformational change during binding. In contrast, none of the corresponding *exo*-methylene analogs (**4–6**) inhibited the enzyme at up to 200 μM concentration. No inhibition was observed when assays were performed using a limiting concentration of MenB (200 nM) in the presence of excess MenE (5 μM), indicating that the compounds do not inhibit MenB.

**Table 5.3: Inhibition of ecMenE by designed inhibitors 1–6**

Compound	IC <sub>50</sub> (μM)	Compound	IC <sub>50</sub> (μM)
<b>1</b>	38.0 ± 3.0	<b>4</b>	>200
<b>2</b>	34.1 ± 2.8	<b>5</b>	>200
<b>3</b>	5.7 ± 0.7	<b>6</b>	>200

It is interesting to note that the vinyl sulfonamide analog MeOSB-AVSN (**3**) is the most potent inhibitor of MenE. In contrast to the sulfamate and sulfamide analogs **1** and **2**, this compound lacks the carbonyl and adjacent heteroatom of the acyl phosphate group in OSB-AMP, which may be involved in hydrogen bonding interactions, based on the cocrystal structure of a related fatty acyl-CoA synthetase with myristoyl-AMP. These results also contrast with the relative

potencies of related inhibitors which are nM inhibitors of the NRPS salicylate adenylation enzyme MbtA (**Table 5.1**). This may be due to the structure differences between the methyl ester OSB-AMP intermediate analogues and OSB-AMP. Although the aromatic carboxyl group in OSB is not directly involved in the formation of OSB-CoA, we note that the OSB methyl ester (**Figure 5.10**) is not a substrate for MenE. Thus removal of the methyl ester functionality in compounds **1-3** may significantly improve their affinity for MenE. Our results also suggest that the OSB ketone group is required for inhibition, as shown by the complete lack of activity in *exo*-methylene analogs **4-6**. Therefore, modified compound **1-3** could show better inhibition potency if the methyl group is removed.

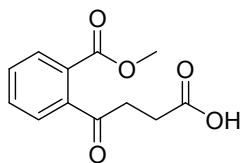


**Figure 5.10: The structure of OSB methyl ester**

## Conclusions

OSB-CoA synthase (MenE), an acyl-CoA synthetase, catalyzes a magnesium-dependent multisubstrate reaction, resulting in the conversion of OSB to OSB-CoA *via* a two-step process involving the initial ATP-dependent adenylation of OSB to form a reactive OSB-AMP intermediate, followed by thioesterification with CoA to form OSB-CoA. Based on the structure of intermediate, 5'-O-(*N*-acylsulfamoyl) adenosines (acyl-AMS) and related compounds were designed to inhibit MenE by mimicking tightly-bound OSB-AMP intermediates.

The mtMenE enzyme has proven difficult to be expressed heterologously even using *M. smegmatis* as an expression host. We started to obtain small amounts of active enzyme having optimized the first 14 codons in the gene for expression in *E. coli*. The rare codon mutagenesis improved the expression level of mtMenE in the *E. coli* host; however, the protein was not very soluble. In contrast, ecMenE expresses very well in *E. coli*.

Since we were unable to reliably express mtMenE, IC<sub>50</sub> values were determined against ecMenE. Both the sulfamate MeOSB-AMS (**1**) and sulfamide MeOSB-AMSN (**2**) were effective inhibitors of MenE. Moreover, the vinyl sulfonamide analog MeOSB-AVSN (**3**) was proved to be the most potent inhibitor, with an IC<sub>50</sub> value of 5 μM. Although the aromatic carboxyl group in OSB is not directly involved in the formation of OSB-CoA, we note that the OSB methyl ester is not a substrate for MenE. Therefore we propose that removal of the methyl ester functionality in compounds **1-3** could show better inhibition potency.

## References

1. Driscoll, J. R., and Taber, H. W. (1992) Sequence organization and regulation of the *Bacillus subtilis* menBE operon, *Journal of bacteriology* 174, 5063-5071.
2. Sharma, V., Hudspeth, M. E., and Meganathan, R. (1996) Menaquinone (vitamin K2) biosynthesis: localization and characterization of the menE gene from *Escherichia coli*, *Gene* 168, 43-48.
3. Sasseti, C. M., Boyd, D. H., and Rubin, E. J. (2003) Genes required for mycobacterial growth defined by high density mutagenesis, *Mol Microbiol* 48, 77-84.
4. Bar-Tana, J., Rose, G., and Shapiro, B. (1971) The purification and properties of microsomal palmitoyl-coenzyme A synthetase, *Biochem J* 122, 353-362.
5. Hisanaga, Y., Ago, H., Nakagawa, N., Hamada, K., Ida, K., Yamamoto, M., Hori, T., Arai, Y., Sugahara, M., Kuramitsu, S., Yokoyama, S., and Miyano, M. (2004) Structural basis of the substrate-specific two-step catalysis of long chain fatty acyl-CoA synthetase dimer, *The Journal of biological chemistry* 279, 31717-31726.
6. Bar-Tana, J., Rose, G., Brandes, R., and Shapiro, B. (1973) Palmitoyl-coenzyme A synthetase. Mechanism of reaction, *Biochem J* 131, 199-209.
7. Cleland, W. W. (1963) The kinetics of enzyme-catalyzed reactions with two or more substrates or products. I. Nomenclature and rate equations, *Biochim Biophys Acta* 67, 104-137.

8. Gulick, A. M., Starai, V. J., Horswill, A. R., Homick, K. M., and Escalante-Semerena, J. C. (2003) The 1.75 Å crystal structure of acetyl-CoA synthetase bound to adenosine-5'-propylphosphate and coenzyme A, *Biochemistry* 42, 2866-2873.
9. Gulick, A. M., Lu, X., and Dunaway-Mariano, D. (2004) Crystal structure of 4-chlorobenzoate:CoA ligase/synthetase in the unliganded and aryl substrate-bound states, *Biochemistry* 43, 8670-8679.
10. Jogl, G., and Tong, L. (2004) Crystal structure of yeast acetyl-coenzyme A synthetase in complex with AMP, *Biochemistry* 43, 1425-1431.
11. Ibba, M., and Soll, D. (2000) Aminoacyl-tRNA synthesis, *Annual review of biochemistry* 69, 617-650.
12. Nakatsu, T., Ichiyama, S., Hiratake, J., Saldanha, A., Kobashi, N., Sakata, K., and Kato, H. (2006) Structural basis for the spectral difference in luciferase bioluminescence, *Nature* 440, 372-376.
13. Cisar, J. S., and Tan, D. S. (2008) Small molecule inhibition of microbial natural product biosynthesis-an emerging antibiotic strategy, *Chem Soc Rev* 37, 1320-1329.
14. Ueda, H., Shoku, Y., Hayashi, N., Mitsunaga, J., In, Y., Doi, M., Inoue, M., and Ishida, T. (1991) X-ray crystallographic conformational study of 5'-O-[N-(L-alanyl)-sulfamoyl]adenosine, a substrate analogue for alanyl-tRNA synthetase, *Biochim Biophys Acta* 1080, 126-134.
15. Finking, R., Neumuller, A., Solsbacher, J., Konz, D., Kretschmar, G., Schweitzer, M., Krumm, T., and Marahiel, M. A. (2003) Aminoacyl



- adenylate substrate analogues for the inhibition of adenylation domains of nonribosomal peptide synthetases, *Chembiochem* 4, 903-906.
16. May, J. J., Finking, R., Wiegeshoff, F., Weber, T. T., Bandur, N., Koert, U., and Marahiel, M. A. (2005) Inhibition of the D-alanine:D-alanyl carrier protein ligase from *Bacillus subtilis* increases the bacterium's susceptibility to antibiotics that target the cell wall, *FEBS J* 272, 2993-3003.
  17. Ferreras, J. A., Ryu, J. S., Di Lello, F., Tan, D. S., and Quadri, L. E. (2005) Small-molecule inhibition of siderophore biosynthesis in *Mycobacterium tuberculosis* and *Yersinia pestis*, *Nat Chem Biol* 1, 29-32.
  18. Somu, R. V., Boshoff, H., Qiao, C., Bennett, E. M., Barry, C. E., 3rd, and Aldrich, C. C. (2006) Rationally designed nucleoside antibiotics that inhibit siderophore biosynthesis of *Mycobacterium tuberculosis*, *J Med Chem* 49, 31-34.
  19. Miethke, M., Bisseret, P., Beckering, C. L., Vignard, D., Eustache, J., and Marahiel, M. A. (2006) Inhibition of aryl acid adenylation domains involved in bacterial siderophore synthesis, *FEBS J* 273, 409-419.
  20. Pfleger, B. F., Lee, J. Y., Somu, R. V., Aldrich, C. C., Hanna, P. C., and Sherman, D. H. (2007) Characterization and analysis of early enzymes for petrobactin biosynthesis in *Bacillus anthracis*, *Biochemistry* 46, 4147-4157.
  21. Cisar, J. S., Ferreras, J. A., Soni, R. K., Quadri, L. E., and Tan, D. S. (2007) Exploiting ligand conformation in selective inhibition of non-ribosomal peptide synthetase amino acid adenylation with designed macrocyclic small molecules, *J Am Chem Soc* 129, 7752-7753.

22. Ferreras, J. A., Stirrett, K. L., Lu, X., Ryu, J. S., Soll, C. E., Tan, D. S., and Quadri, L. E. (2008) Mycobacterial phenolic glycolipid virulence factor biosynthesis: mechanism and small-molecule inhibition of polyketide chain initiation, *Chem Biol* 15, 51-61.
23. Waller, C. W., Patrick, J. B., Fulmor, W., and Meyer, W. E. (1957) The structure of nucleocidin. I, *J. Am. Chem. Soc.* 79 79, 1011.
24. Isono, K., Uramoto, M., Kusakabe, H., Miyata, N., Koyama, T., Ubukata, M., Sethi, S. K., and McCloskey, J. A. (1984) Ascamycin and dealanylascamycin, nucleoside antibiotics from *Streptomyces* sp, *J Antibiot (Tokyo)* 37, 670-672.
25. Zhang, S. P., Zubay, G., and Goldman, E. (1991) Low-usage codons in *Escherichia coli*, yeast, fruit fly and primates, *Gene* 105, 61-72.
26. Wada, K., Wada, Y., Ishibashi, F., Gojobori, T., and Ikemura, T. (1992) Codon usage tabulated from the GenBank genetic sequence data, *Nucleic Acids Res* 20 Suppl, 2111-2118.
27. Kane, J. F. (1995) Effects of rare codon clusters on high-level expression of heterologous proteins in *Escherichia coli*, *Curr Opin Biotechnol* 6, 494-500.
28. Kurland, C., and Gallant, J. (1996) Errors of heterologous protein expression, *Curr Opin Biotechnol* 7, 489-493.
29. Goldman, E., Rosenberg, A. H., Zubay, G., and Studier, F. W. (1995) Consecutive low-usage leucine codons block translation only when near the 5' end of a message in *Escherichia coli*, *J Mol Biol* 245, 467-473.

30. Kolkman, R., and Leistner, E. (1985) Synthesis and revised structure of the o-succinylbenzoic acid coenzyme A ester, an intermediate in menaquinone biosynthesis, *Tetrahedron Lett.* 26, 1703-1704.
31. Kolkman, R., and Leistner, E. (1987) Synthesis, analysis and characterization of the coenzyme A esters of o-Succinylbenzoic acid, an intermediate in vitamin K2 (menaquinone) biosynthesis, *Zeitschrift fur Naturforschung* 42, 542-552.
32. Santos, M. M., and Moreira, R. (2007) Michael acceptors as cysteine protease inhibitors, *Mini Rev Med Chem* 7, 1040-1050.
33. Worthington, A. S., Rivera, H., Torpey, J. W., Alexander, M. D., and Burkart, M. D. (2006) Mechanism-based protein cross-linking probes to investigate carrier protein-mediated biosynthesis, *ACS Chem Biol* 1, 687-691.
34. Qiao, C., Wilson, D. J., Bennett, E. M., and Aldrich, C. C. (2007) A mechanism-based aryl carrier protein/thiolation domain affinity probe, *J Am Chem Soc* 129, 6350-6351.
35. Reddick, J. J., Cheng, J., and Roush, W. R. (2003) Relative rates of Michael reactions of 2'-(phenethyl)thiol with vinyl sulfones, vinyl sulfonate esters, and vinyl sulfonamides relevant to vinyl sulfonyl cysteine protease inhibitors, *Org Lett* 5, 1967-1970.

## REFERENCES

### Chapter 1 References

1. World Health Organization (WHO) REPORT 2008: Global Tuberculosis Control.
2. Bloom, B. R., and Murray, C. J. (1992) Tuberculosis: commentary on a reemergent killer, *Science*. 257, 1055-1064.
3. Kochi, A. (1991) The global tuberculosis situation and the new control strategy of the World Health Organization, *Tubercle* 72, 1-6.
4. Kumar, V., Abbas, A. K., Fausto, N., and Mitchell, R. N., (Eds.) (2007) *Robbins Basic Pathology (8th ed.)*, Saunders Elsevier.
5. Rothschild, B. M., Martin, L. D., Lev, G., Bercovier, H., Bar-Gal, G. K., Greenblatt, C., Donoghue, H., Spigelman, M., and Brittain, D. (2001) Mycobacterium tuberculosis complex DNA from an extinct bison dated 17,000 years before the present, *Clin Infect Dis* 33, 305-311.
6. Zink, A. R., Sola, C., Reischl, U., Grabner, W., Rastogi, N., Wolf, H., and Nerlich, A. G. (2003) Characterization of Mycobacterium tuberculosis complex DNAs from Egyptian mummies by spoligotyping, *J Clin Microbiol* 41, 359-367.
7. Pearce-Duvel, J. M. (2006) The origin of human pathogens: evaluating the role of agriculture and domestic animals in the evolution of human disease, *Biol Rev Camb Philos Soc* 81, 369-382.
8. Cox, R. A. (2004) Quantitative relationships for specific growth rates and macromolecular compositions of Mycobacterium tuberculosis,

- Streptomyces coelicolor A3(2) and Escherichia coli B/r: an integrative theoretical approach, *Microbiology (Reading, England)* 150, 1413-1426.
9. Madison, B. M. (2001) Application of stains in clinical microbiology, *Biotech Histochem* 76, 119-125.
  10. Ryan, K. J., and Ray, C. G., (Eds.) (2004) *Sherris Medical Microbiology (4th ed.)*, McGraw Hill.
  11. Finlay, B. B., and Falkow, S. (1997) Common themes in microbial pathogenicity revisited, *Microbiol Mol Biol Rev* 61, 136-169.
  12. Cole, E. C., and Cook, C. E. (1998) Characterization of infectious aerosols in health care facilities: an aid to effective engineering controls and preventive strategies, *Am J Infect Control* 26, 453-464.
  13. Nicas, M., Nazaroff, W. W., and Hubbard, A. (2005) Toward understanding the risk of secondary airborne infection: emission of respirable pathogens, *J Occup Environ Hyg* 2, 143-154.
  14. (December 2004) World Health Organization Disease Watch: Focus: Tuberculosis.
  15. (March 2006) Tuberculosis Fact sheet N°104 - Global and regional incidence, World Health Organization (WHO).
  16. (2000) *Core Curriculum on Tuberculosis: What the Clinician Should Know (4th edition)*, Centers for Disease Control and Prevention (CDC), Division of Tuberculosis Elimination.

17. Bonah, C. (2005) The 'experimental stable' of the BCG vaccine: safety, efficacy, proof, and standards, 1921-1933, *Stud Hist Philos Biol Biomed Sci* 36, 696-721.
18. Comstock, G. W. (1994) The International Tuberculosis Campaign: a pioneering venture in mass vaccination and research, *Clin Infect Dis* 19, 528-540.
19. Pfuetze, K. H., Pyle, M. M., Hinshaw, H. C., and Feldman, W. H. (1955) The first clinical trial of streptomycin in human tuberculosis, *Am Rev Tuberc* 71, 752-754.
20. Medical\_Research\_Council. (1948) Streptomycin treatment of pulmonary tuberculosis, *BMJ* 2, 769-782.
21. Medical\_Research\_Council. (1952) The prevention of streptomycin resistance by combined chemotherapy, *BMJ*, 1157-1162.
22. (1952) ISONIAZID in pulmonary tuberculosis, *Lancet* 2, 19-21.
23. (1953) Second report to the Medical Research Council by their Tuberculosis Chemotherapy Trials Committee. Isoniazid in the treatment of pulmonary tuberculosis, *BMJ* 71 (4809), 521-536.
24. (1955) Seventh report to the Medical Research Council by their Tuberculosis Chemotherapy Trials Committee. Various combinations of isoniazid with streptomycin or with PAS in the treatment of pulmonary tuberculosis, *BMJ* 4911, 435-445.
25. Covacev, L., and Monzali, G. (1966) [Rifamycin SV in the therapy of tuberculosis], *Clin Ter* 39, 547-566.

26. Lucchesi, M., Pallotta, G., Rossi, P., and Sbampato, M. (1967) [The therapeutic action of Rifampicin, a derivative of 3-(4-methyl-1-piperazinyl-iminomethyl)-rifamycin SV, in pulmonary tuberculosis], *Ann Ist Carlo Forlanini* 27, 199-227.
27. Nitti, V., Catena, E., Bariffi, F., and Delli Veneri, F. (1967) [Therapeutic activity of the Rifampicin in pulmonary tuberculosis], *Arch Tisiol Mal Appar Respir* 22, 417-462.
28. Onyebujoh, P., Zumla, A., Ribeiro, I., Rustomjee, R., Mwaba, P., Gomes, M., and Grange, J. M. (2005) Treatment of tuberculosis: present status and future prospects, *Bull World Health Organ* 83, 857-865.
29. Mitchison, D. A. (2005) Shortening the treatment of tuberculosis, *Nat Biotechnol* 23, 187-188.
30. Zhang, Y., and Amzel, L. M. (2002) Tuberculosis drug targets, *Curr Drug Targets* 3, 131-154.
31. Zhang, Y. (2005) The magic bullets and tuberculosis drug targets, *Annu Rev Pharmacol Toxicol* 45, 529-564.
32. Schroeder, E. K., de Souza, N., Santos, D. S., Blanchard, J. S., and Basso, L. A. (2002) Drugs that inhibit mycolic acid biosynthesis in *Mycobacterium tuberculosis*, *Curr Pharm Biotechnol* 3, 197-225.
33. Janin, Y. L. (2007) Antituberculosis drugs: ten years of research, *Bioorg Med Chem* 15, 2479-2513.
34. (1998) Prevention and treatment of tuberculosis among patients infected with human immunodeficiency virus: principles of therapy and revised

recommendations, in *MMWR Recomm Rep.*, pp 1-58, Centres for Disease Control and Prevention.

35. Geneva\_World\_Health\_Organization. (2006) Guidelines for the programmatic management of drug-resistant tuberculosis., *HTM/TB*, 361.
36. Sander, P., De Rossi, E., Boddinhaus, B., Cantoni, R., Branzoni, M., Bottger, E. C., Takiff, H., Rodriguez, R., Lopez, G., and Riccardi, G. (2000) Contribution of the multidrug efflux pump LfrA to innate mycobacterial drug resistance, *FEMS microbiology letters* 193, 19-23.
37. De Rossi, E., Branzoni, M., Cantoni, R., Milano, A., Riccardi, G., and Ciferri, O. (1998) mmr, a Mycobacterium tuberculosis gene conferring resistance to small cationic dyes and inhibitors, *Journal of bacteriology* 180, 6068-6071.
38. Ainsa, J. A., Blokpoel, M. C., Otal, I., Young, D. B., De Smet, K. A., and Martin, C. (1998) Molecular cloning and characterization of Tap, a putative multidrug efflux pump present in Mycobacterium fortuitum and Mycobacterium tuberculosis, *Journal of bacteriology* 180, 5836-5843.
39. Saltini, C. (2006) Chemotherapy and diagnosis of tuberculosis, *Respir Med* 100, 2085-2097.
40. Mitchison, D. A., and Nunn, A. J. (1986) Influence of initial drug resistance on the response to short-course chemotherapy of pulmonary tuberculosis, *Am Rev Respir Dis* 133, 423-430.
41. Shah, N. S., Wright, A., Bai, G. H., Barrera, L., Boulahbal, F., Martin-Casabona, N., Drobniowski, F., Gilpin, C., Havelkova, M., Lepe, R., Lumb,



- R., Metchock, B., Portaels, F., Rodrigues, M. F., Rusch-Gerdes, S., Van Deun, A., Vincent, V., Laserson, K., Wells, C., and Cegielski, J. P. (2007) Worldwide emergence of extensively drug-resistant tuberculosis, *Emerg Infect Dis* 13, 380-387.
42. Parrish, N. M., Dick, J. D., and Bishai, W. R. (1998) Mechanisms of latency in Mycobacterium tuberculosis, *Trends Microbiol* 6, 107-112.
43. Houben, E. N., Nguyen, L., and Pieters, J. (2006) Interaction of pathogenic mycobacteria with the host immune system, *Curr Opin Microbiol* 9, 76-85.
44. Herrmann, J. L., and Lagrange, P. H. (2005) Dendritic cells and Mycobacterium tuberculosis: which is the Trojan horse?, *Pathol Biol (Paris)* 53, 35-40.
45. Agarwal, R., Malhotra, P., Awasthi, A., Kakkar, N., and Gupta, D. (2005) Tuberculous dilated cardiomyopathy: an under-recognized entity?, *BMC Infect Dis* 5, 29.
46. Kaufmann, S. H. (2002) Protection against tuberculosis: cytokines, T cells, and macrophages, *Ann Rheum Dis* 61 Suppl 2, ii54-58.
47. Jozefowski, S., Sobota, A., and Kwiatkowska, K. (2008) How Mycobacterium tuberculosis subverts host immune responses, *Bioessays* 30, 943-954.
48. Wayne, L. G., and Hayes, L. G. (1996) An in vitro model for sequential study of shutdown of Mycobacterium tuberculosis through two stages of nonreplicating persistence, *Infection and immunity* 64, 2062-2069.

49. Lim, A., Eleuterio, M., Hutter, B., Murugasu-Oei, B., and Dick, T. (1999) Oxygen depletion-induced dormancy in *Mycobacterium bovis* BCG, *Journal of bacteriology* 181, 2252-2256.
50. Wayne, L. G., and Sohaskey, C. D. (2001) Nonreplicating persistence of *Mycobacterium tuberculosis*, *Annu Rev Microbiol* 55, 139-163.
51. Boshoff, H. I., and Barry, C. E., 3rd. (2005) Tuberculosis - metabolism and respiration in the absence of growth, *Nat Rev Microbiol* 3, 70-80.
52. Dick, T. (2001) Dormant tubercle bacilli: the key to more effective TB chemotherapy?, *J Antimicrob Chemother* 47, 117-118.
53. Wayne, L. G., and Sramek, H. A. (1994) Metronidazole is bactericidal to dormant cells of *Mycobacterium tuberculosis*, *Antimicrobial agents and chemotherapy* 38, 2054-2058.
54. Wayne, L. G. (1994) Dormancy of *Mycobacterium tuberculosis* and latency of disease, *Eur J Clin Microbiol Infect Dis* 13, 908-914.
55. Stover, C. K., Warrener, P., VanDevanter, D. R., Sherman, D. R., Arain, T. M., Langhorne, M. H., Anderson, S. W., Towell, J. A., Yuan, Y., McMurray, D. N., Kreiswirth, B. N., Barry, C. E., and Baker, W. R. (2000) A small-molecule nitroimidazopyran drug candidate for the treatment of tuberculosis, *Nature* 405, 962-966.
56. Barry, C. E., 3rd, Lee, R. E., Mdluli, K., Sampson, A. E., Schroeder, B. G., Slayden, R. A., and Yuan, Y. (1998) Mycolic acids: structure, biosynthesis and physiological functions, *Prog Lipid Res* 37, 143-179.

57. Boshoff, H. I., Myers, T. G., Copp, B. R., McNeil, M. R., Wilson, M. A., and Barry, C. E., 3rd. (2004) The transcriptional responses of *Mycobacterium tuberculosis* to inhibitors of metabolism: novel insights into drug mechanisms of action, *The Journal of biological chemistry* 279, 40174-40184.
58. Weinstein, E. A., Yano, T., Li, L. S., Avarbock, D., Avarbock, A., Helm, D., McColm, A. A., Duncan, K., Lonsdale, J. T., and Rubin, H. (2005) Inhibitors of type II NADH:menaquinone oxidoreductase represent a class of antitubercular drugs, *Proceedings of the National Academy of Sciences of the United States of America* 102, 4548-4553.
59. Lester, R. L., and Crane, F. L. (1959) The natural occurrence of coenzyme Q and related compounds, *The Journal of biological chemistry* 234, 2169-2175.
60. Bishop, D. H., Pandya, K. P., and King, H. K. (1962) Ubiquinone and vitamin K in bacteria, *Biochem J* 83, 606-614.
61. Rao, S. P. S., Alonso, S., Rand, L., Dick, T., and Pethe, K. (2008) The protonmotive force is required for maintaining ATP homeostasis and viability of hypoxic, nonreplicating *Mycobacterium tuberculosis*, *Proceedings of the National Academy of Sciences of the United States of America* 105, 11945-11950.
62. Dowd, P., Ham, S. W., Naganathan, S., and Hershline, R. (1995) The mechanism of action of vitamin K, *Annu Rev Nutr* 15, 419-440.

63. Meganathan, R. (2001) Biosynthesis of menaquinone (vitamin K<sub>2</sub>) and ubiquinone (coenzyme Q): a perspective on enzymatic mechanisms, *Vitamins and hormones* 61, 173-218.
64. Rowland, B., Hill, K., Miller, P., Driscoll, J., and Taber, H. (1995) Structural organization of a *Bacillus subtilis* operon encoding menaquinone biosynthetic enzymes, *Gene* 167, 105-109.
65. Rowland, B. M., Grossman, T. H., Osburne, M. S., and Taber, H. W. (1996) Sequence and genetic organization of a *Bacillus subtilis* operon encoding 2,3-dihydroxybenzoate biosynthetic enzymes, *Gene* 178, 119-123.
66. Rowland, B. M., and Taber, H. W. (1996) Duplicate isochorismate synthase genes of *Bacillus subtilis*: regulation and involvement in the biosyntheses of menaquinone and 2,3-dihydroxybenzoate, *Journal of bacteriology* 178, 854-861.
67. Azerad, R., Bleiler-Hill, R., Catala, F., Samuel, O., and Lederer, E. (1967) Biosynthesis of dihydromenaquinone-9 by *Mycobacterium phlei*, *Biochem Biophys Res Commun* 27, 253-257.
68. Catala, F., Azerad, R., and Lederer, E. (1970) [Properties of demethylmenaquinone C-methylase from *Mycobacterium phlei*], *Int Z Vitaminforsch* 40, 363-373.
69. Dansette, P., and Azerad, R. (1970) A new intermediate in naphthoquinone and menaquinone biosynthesis, *Biochem Biophys Res Commun* 40, 1090-1095.

70. Leduc, M. M., Dansette, P. M., and Azerad, R. G. (1970) [Incorporation of shikimic acid into the ring of bacterial and plant naphthoquinones], *Eur J Biochem* 15, 428-435.
71. McGovern, E. P., and Bentley, R. (1978) Isolation and properties of naphthoate synthetase from *Mycobacterium phlei*, *Arch Biochem Biophys* 188, 56-63.
72. Meganathan, R., and Bentley, R. (1979) Menaquinone (vitamin K2) biosynthesis: conversion of o-succinylbenzoic acid to 1,4-dihydroxy-2-naphthoic acid by *Mycobacterium phlei* enzymes, *Journal of bacteriology* 140, 92-98.
73. Meganathan, R., Folger, T., and Bentley, R. (1980) Conversion of o-succinylbenzoate to dihydroxynaphthoate by extracts of *Micrococcus luteus*, *Biochemistry* 19, 785-789.
74. Meganathan, R., Bentley, R., and Taber, H. (1981) Identification of *Bacillus subtilis* men mutants which lack O-succinylbenzoyl-coenzyme A synthetase and dihydroxynaphthoate synthase, *Journal of bacteriology* 145, 328-332.
75. Heide, L., Arendt, S., and Leistner, E. (1982) Enzymatic synthesis, characterization, and metabolism of the coenzyme A ester of o-succinylbenzoic acid, an intermediate in menaquinone (vitamin K2) biosynthesis, *The Journal of biological chemistry* 257, 7396-7400.
76. Igbavboa, U., and Leistner, E. (1990) Sequence of proton abstraction and stereochemistry of the reaction catalyzed by naphthoate synthase, an

- enzyme involved in menaquinone (vitamin K<sub>2</sub>) biosynthesis, *Eur J Biochem* 192, 441-449.
77. Daruwala, R., Kwon, O., Meganathan, R., and Hudspeth, M. E. (1996) A new isochorismate synthase specifically involved in menaquinone (vitamin K<sub>2</sub>) biosynthesis encoded by the menF gene, *FEMS microbiology letters* 140, 159-163.
78. Meganathan, R., and Bentley, R. (1983) Thiamine pyrophosphate requirement for o-succinylbenzoic acid synthesis in *Escherichia coli* and evidence for an intermediate, *Journal of bacteriology* 153, 739-746.
79. Palaniappan, C., Sharma, V., Hudspeth, M. E., and Meganathan, R. (1992) Menaquinone (vitamin K<sub>2</sub>) biosynthesis: evidence that the *Escherichia coli* menD gene encodes both 2-succinyl-6-hydroxy-2,4-cyclohexadiene-1-carboxylic acid synthase and alpha-ketoglutarate decarboxylase activities, *Journal of bacteriology* 174, 8111-8118.
80. Jiang, M., Cao, Y., Guo, Z. F., Chen, M., Chen, X., and Guo, Z. (2007) Menaquinone biosynthesis in *Escherichia coli*: identification of 2-succinyl-5-enolpyruvyl-6-hydroxy-3-cyclohexene-1-carboxylate as a novel intermediate and re-evaluation of MenD activity, *Biochemistry* 46, 10979-10989.
81. Jiang, M., Chen, X., Guo, Z. F., Cao, Y., Chen, M., and Guo, Z. (2008) Identification and characterization of (1R,6R)-2-succinyl-6-hydroxy-2,4-cyclohexadiene-1-carboxylate synthase in the menaquinone biosynthesis of *Escherichia coli*, *Biochemistry* 47, 3426-3434.

82. Sharma, V., Meganathan, R., and Hudspeth, M. E. (1993) Menaquinone (vitamin K2) biosynthesis: cloning, nucleotide sequence, and expression of the menC gene from *Escherichia coli*, *Journal of bacteriology* 175, 4917-4921.
83. Sharma, V., Hudspeth, M. E., and Meganathan, R. (1996) Menaquinone (vitamin K2) biosynthesis: localization and characterization of the menE gene from *Escherichia coli*, *Gene* 168, 43-48.
84. Truglio, J. J., Theis, K., Feng, Y., Gajda, R., Machutta, C., Tonge, P. J., and Kisker, C. (2003) Crystal structure of *Mycobacterium tuberculosis* MenB, a key enzyme in vitamin K2 biosynthesis, *The Journal of biological chemistry* 278, 42352-42360.
85. Suvarna, K., Stevenson, D., Meganathan, R., and Hudspeth, M. E. (1998) Menaquinone (vitamin K2) biosynthesis: localization and characterization of the menA gene from *Escherichia coli*, *Journal of bacteriology* 180, 2782-2787.
86. Lee, P. T., Hsu, A. Y., Ha, H. T., and Clarke, C. F. (1997) A C-methyltransferase involved in both ubiquinone and menaquinone biosynthesis: isolation and identification of the *Escherichia coli* ubiE gene, *Journal of bacteriology* 179, 1748-1754.
87. Bentley, S. D., Chater, K. F., Cerdeno-Tarraga, A. M., Challis, G. L., Thomson, N. R., James, K. D., Harris, D. E., Quail, M. A., Kieser, H., Harper, D., Bateman, A., Brown, S., Chandra, G., Chen, C. W., Collins, M., Cronin, A., Fraser, A., Goble, A., Hidalgo, J., Hornsby, T., Howarth, S.,

- Huang, C. H., Kieser, T., Larke, L., Murphy, L., Oliver, K., O'Neil, S., Rabbinowitsch, E., Rajandream, M. A., Rutherford, K., Rutter, S., Seeger, K., Saunders, D., Sharp, S., Squares, R., Squares, S., Taylor, K., Warren, T., Wietzorrek, A., Woodward, J., Barrell, B. G., Parkhill, J., and Hopwood, D. A. (2002) Complete genome sequence of the model actinomycete *Streptomyces coelicolor* A3(2), *Nature* 417, 141-147.
88. Borodina, I., Krabben, P., and Nielsen, J. (2005) Genome-scale analysis of *Streptomyces coelicolor* A3(2) metabolism, *Genome Res* 15, 820-829.
89. Collins, M. D., Pirouz, T., Goodfellow, M., and Minnikin, D. E. (1977) Distribution of menaquinones in actinomycetes and corynebacteria, *J Gen Microbiol* 100, 221-230.
90. Tomb, J. F., White, O., Kerlavage, A. R., Clayton, R. A., Sutton, G. G., Fleischmann, R. D., Ketchum, K. A., Klenk, H. P., Gill, S., Dougherty, B. A., Nelson, K., Quackenbush, J., Zhou, L., Kirkness, E. F., Peterson, S., Loftus, B., Richardson, D., Dodson, R., Khalak, H. G., Glodek, A., McKenney, K., Fitzegerald, L. M., Lee, N., Adams, M. D., Hickey, E. K., Berg, D. E., Gocayne, J. D., Utterback, T. R., Peterson, J. D., Kelley, J. M., Cotton, M. D., Weidman, J. M., Fujii, C., Bowman, C., Watthey, L., Wallin, E., Hayes, W. S., Borodovsky, M., Karp, P. D., Smith, H. O., Fraser, C. M., and Venter, J. C. (1997) The complete genome sequence of the gastric pathogen *Helicobacter pylori*, *Nature* 388, 539-547.
91. Parkhill, J., Wren, B. W., Mungall, K., Ketley, J. M., Churcher, C., Basham, D., Chillingworth, T., Davies, R. M., Feltwell, T., Holroyd, S., Jagels, K.,



- Karlyshev, A. V., Moule, S., Pallen, M. J., Penn, C. W., Quail, M. A., Rajandream, M. A., Rutherford, K. M., van Vliet, A. H., Whitehead, S., and Barrell, B. G. (2000) The genome sequence of the food-borne pathogen *Campylobacter jejuni* reveals hypervariable sequences, *Nature* 403, 665-668.
92. Marcelli, S. W., Chang, H. T., Chapman, T., Chalk, P. A., Miles, R. J., and Poole, R. K. (1996) The respiratory chain of *Helicobacter pylori*: identification of cytochromes and the effects of oxygen on cytochrome and menaquinone levels, *FEMS microbiology letters* 138, 59-64.
93. Moss, C. W., Lambert-Fair, M. A., Nicholson, M. A., and Guerrant, G. O. (1990) Isoprenoid quinones of *Campylobacter cryaerophila*, *C. cinaedi*, *C. fennelliae*, *C. hyointestinalis*, *C. pylori*, and "*C. upsaliensis*", *J Clin Microbiol* 28, 395-397.
94. Hiratsuka, T., Furihata, K., Ishikawa, J., Yamashita, H., Itoh, N., Seto, H., and Dairi, T. (2008) An alternative menaquinone biosynthetic pathway operating in microorganisms, *Science (New York, N.Y)* 321, 1670-1673.
95. Seto, H., Jinnai, Y., Hiratsuka, T., Fukawa, M., Furihata, K., Itoh, N., and Dairi, T. (2008) Studies on a new biosynthetic pathway for menaquinone, *J Am Chem Soc* 130, 5614-5615.

## Chapter 2 References

1. Gerlt, J. A., and Babbitt, P. C. (2001) Divergent evolution of enzymatic function: mechanistically diverse superfamilies and functionally distinct suprafamilies, *Annual review of biochemistry* 70, 209-246.
2. Glasner, M. E., Gerlt, J. A., and Babbitt, P. C. (2006) Evolution of enzyme superfamilies, *Curr Opin Chem Biol* 10, 492-497.
3. Gerlt, J. A., and Babbitt, P. C. (1998) Mechanistically diverse enzyme superfamilies: the importance of chemistry in the evolution of catalysis, *Curr Opin Chem Biol* 2, 607-612.
4. Babbitt, P. C., and Gerlt, J. A. (1997) Understanding enzyme superfamilies. Chemistry As the fundamental determinant in the evolution of new catalytic activities, *The Journal of biological chemistry* 272, 30591-30594.
5. Bahnson, B. J., Anderson, V. E., and Petsko, G. A. (2002) Structural mechanism of enoyl-CoA hydratase: three atoms from a single water are added in either an E1cb stepwise or concerted fashion, *Biochemistry* 41, 2621-2629.
6. Mohrig, J. R., Moerke, K. A., Cloutier, D. L., Lane, B. D., Person, E. C., and Onasch, T. B. (1995) Importance of historical contingency in the stereochemistry of hydratase-dehydratase enzymes, *Science (New York, N.Y)* 269, 527-529.

7. Bell, A. F., Wu, J., Feng, Y., and Tonge, P. J. (2001) Involvement of glycine 141 in substrate activation by enoyl-CoA hydratase, *Biochemistry* 40, 1725-1733.
8. Wong, B. J., and Gerlt, J. A. (2004) Evolution of function in the crotonase superfamily: (3S)-methylglutaconyl-CoA hydratase from *Pseudomonas putida*, *Biochemistry* 43, 4646-4654.
9. Mursula, A. M., van Aalten, D. M., Hiltunen, J. K., and Wierenga, R. K. (2001) The crystal structure of delta(3)-delta(2)-enoyl-CoA isomerase, *J Mol Biol* 309, 845-853.
10. Zhang, D., Liang, X., He, X. Y., Alipui, O. D., Yang, S. Y., and Schulz, H. (2001) Delta 3,5,delta 2,4-dienoyl-CoA isomerase is a multifunctional isomerase. A structural and mechanistic study, *The Journal of biological chemistry* 276, 13622-13627.
11. Benning, M. M., Haller, T., Gerlt, J. A., and Holden, H. M. (2000) New reactions in the crotonase superfamily: structure of methylmalonyl CoA decarboxylase from *Escherichia coli*, *Biochemistry* 39, 4630-4639.
12. Wong, B. J., and Gerlt, J. A. (2003) Divergent function in the crotonase superfamily: an anhydride intermediate in the reaction catalyzed by 3-hydroxyisobutyryl-CoA hydrolase, *J Am Chem Soc* 125, 12076-12077.
13. Benning, M. M., Taylor, K. L., Liu, R. Q., Yang, G., Xiang, H., Wesenberg, G., Dunaway-Mariano, D., and Holden, H. M. (1996) Structure of 4-chlorobenzoyl coenzyme A dehalogenase determined to 1.8 Å resolution:

- an enzyme catalyst generated via adaptive mutation, *Biochemistry* 35, 8103-8109.
14. Truglio, J. J., Theis, K., Feng, Y., Gajda, R., Machutta, C., Tonge, P. J., and Kisker, C. (2003) Crystal structure of *Mycobacterium tuberculosis* MenB, a key enzyme in vitamin K2 biosynthesis, *The Journal of biological chemistry* 278, 42352-42360.
  15. Leonard, P. M., and Grogan, G. (2004) Structure of 6-oxo camphor hydrolase H122A mutant bound to its natural product, (2S,4S)-alpha-campholinic acid: mutant structure suggests an atypical mode of transition state binding for a crotonase homolog, *The Journal of biological chemistry* 279, 31312-31317.
  16. Eberhard, E. D., and Gerlt, J. A. (2004) Evolution of function in the crotonase superfamily: the stereochemical course of the reaction catalyzed by 2-ketocyclohexanecarboxyl-CoA hydrolase, *J Am Chem Soc* 126, 7188-7189.
  17. Gasson, M. J., Kitamura, Y., McLauchlan, W. R., Narbad, A., Parr, A. J., Parsons, E. L., Payne, J., Rhodes, M. J., and Walton, N. J. (1998) Metabolism of ferulic acid to vanillin. A bacterial gene of the enoyl-SCoA hydratase/isomerase superfamily encodes an enzyme for the hydration and cleavage of a hydroxycinnamic acid SCoA thioester, *The Journal of biological chemistry* 273, 4163-4170.
  18. Engel, C. K., Mathieu, M., Zeelen, J. P., Hiltunen, J. K., and Wierenga, R. K. (1996) Crystal structure of enoyl-coenzyme A (CoA) hydratase at 2.5

angstroms resolution: a spiral fold defines the CoA-binding pocket, *EMBO J* 15, 5135-5145.

19. Kurimoto, K., Fukai, S., Nureki, O., Muto, Y., and Yokoyama, S. (2001) Crystal structure of human AUH protein, a single-stranded RNA binding homolog of enoyl-CoA hydratase, *Structure* 9, 1253-1263.
20. Modis, Y., Filppula, S. A., Novikov, D. K., Norledge, B., Hiltunen, J. K., and Wierenga, R. K. (1998) The crystal structure of dienoyl-CoA isomerase at 1.5 Å resolution reveals the importance of aspartate and glutamate sidechains for catalysis, *Structure* 6, 957-970.
21. Whittingham, J. L., Turkenburg, J. P., Verma, C. S., Walsh, M. A., and Grogan, G. (2003) The 2-Å crystal structure of 6-oxo camphor hydrolase. New structural diversity in the crotonase superfamily, *The Journal of biological chemistry* 278, 1744-1750.
22. Sleeman, M. C., Sorensen, J. L., Batchelar, E. T., McDonough, M. A., and Schofield, C. J. (2005) Structural and mechanistic studies on carboxymethylproline synthase (CarB), a unique member of the crotonase superfamily catalyzing the first step in carbapenem biosynthesis, *The Journal of biological chemistry* 280, 34956-34965.
23. Ulaganathan, V., Agacan, M. F., Buetow, L., Tulloch, L. B., and Hunter, W. N. (2007) Structure of *Staphylococcus aureus* 1,4-dihydroxy-2-naphthoyl-CoA synthase (MenB) in complex with acetoacetyl-CoA, *Acta Crystallogr Sect F Struct Biol Cryst Commun* 63, 908-913.

24. Pilka ES, P. C., King ONF, Guo K, Von Delft F, Pike ACW, Arrowsmith CH, Weigelt J, Edwards AM, Oppermann U. (2007/12/19 ) Crystal Structure Of Human Beta-Hydroxyisobutyryl-Coa Hydrolase In Complex With Quercetin, *Structural Genomics Consortium (Sgc)*.
25. Lannergard, J., von Eiff, C., Sander, G., Cordes, T., Seggewiss, J., Peters, G., Proctor, R. A., Becker, K., and Hughes, D. (2008) Identification of the genetic basis for clinical menadione-auxotrophic small-colony variant isolates of *Staphylococcus aureus*, *Antimicrobial agents and chemotherapy* 52, 4017-4022.
26. Bryant, R. W., Jr., and Bentley, R. (1976) Menaquinone biosynthesis: conversion of o-succinylbenzoic acid to 1,4-dihydroxy-2-naphthoic acid and menaquinones by *Escherichia coli* extracts, *Biochemistry* 15, 4792-4796.
27. Heide, L., Arendt, S., and Leistner, E. (1982) Enzymatic synthesis, characterization, and metabolism of the coenzyme A ester of o-succinylbenzoic acid, an intermediate in menaquinone (vitamin K2) biosynthesis, *The Journal of biological chemistry* 257, 7396-7400.
28. Heath, R. J., and Rock, C. O. (2002) The Claisen condensation in biology, *Natural product reports* 19, 581-596.
29. Sedlak, J., and Lindsay, R. H. (1968) Estimation of total, protein-bound, and nonprotein sulfhydryl groups in tissue with Ellman's reagent, *Anal Biochem* 25, 192-205.

30. Grisostomi C., Kast P., Pulido R., Huynh J., and Hilvert, D. (1997) Efficient in vivo synthesis and rapid purification of chorismic acid using an engineered *Escherichia coli* Strain, *Bioorg Chem* 25, 297-305.
31. Kolkman R., and E., L. (1987) Synthesis, analysis and characterization of the coenzyme A esters of o-Succinylbenzoic acid, an intermediate in vitamin K2 (menaquinone) biosynthesis, *Z. Naturforsch.* 42c, 542-552.
32. Gallus, C., and Schink, B. (1994) Anaerobic degradation of pimelate by newly isolated denitrifying bacteria, *Microbiology (Reading, England)* 140 ( Pt 2), 409-416.
33. Kabsch, W., and Sander, C. (1983) Dictionary of protein secondary structure: pattern recognition of hydrogen-bonded and geometrical features, *Biopolymers* 22, 2577-2637.
34. Wen-Jin Wu, Y. F., Xiang He, Hilary A. Hofstein, Daniel P. Raleigh and Peter J. Tonge. (2000) Stereospecificity of the Reaction Catalyzed by Enoyl-CoA Hydratase, *J. Am. Chem. Soc.* 122, 3987.
35. Kurosawa, T., Sato, M., Nakano, H., Fujiwara, M., Murai, T., Yoshimura, T., and Hashimoto, T. (2001) Conjugation reactions catalyzed by bifunctional proteins related to beta-oxidation in bile acid biosynthesis, *Steroids* 66, 107-114.
36. Qin, Y. M., Haapalainen, A. M., Conry, D., Cuebas, D. A., Hiltunen, J. K., and Novikov, D. K. (1997) Recombinant 2-enoyl-CoA hydratase derived from rat peroxisomal multifunctional enzyme 2: role of the hydratase reaction in bile acid synthesis, *Biochem J* 328 ( Pt 2), 377-382.

37. Dieuaide-Noubhani, M., Asselberghs, S., Mannaerts, G. P., and Van Veldhoven, P. P. (1997) Evidence that multifunctional protein 2, and not multifunctional protein 1, is involved in the peroxisomal beta-oxidation of pristanic acid, *Biochem J* 325 ( Pt 2), 367-373.
38. Jiang, L. L., Kurosawa, T., Sato, M., Suzuki, Y., and Hashimoto, T. (1997) Physiological role of D-3-hydroxyacyl-CoA dehydratase/D-3-hydroxyacyl-CoA dehydrogenase bifunctional protein, *J Biochem* 121, 506-513.
39. Hiltunen, J. K., and Qin, Y. (2000) beta-oxidation - strategies for the metabolism of a wide variety of acyl-CoA esters, *Biochim Biophys Acta* 1484, 117-128.
40. Igbavboa, U., and Leistner, E. (1990) Sequence of proton abstraction and stereochemistry of the reaction catalyzed by naphthoate synthase, an enzyme involved in menaquinone (vitamin K2) biosynthesis, *Eur J Biochem* 192, 441-449.
41. Stern, J. R., Del Campillo, A., and Raw, I. (1956) Enzymes of fatty acid metabolism. I. General introduction; crystalline crotonase, *The Journal of biological chemistry* 218, 971-983.
42. Willadsen, P., and Eggerer, H. (1975) Substrate stereochemistry of the enoyl-CoA hydratase reaction, *Eur J Biochem* 54, 247-252.
43. Steinman, H. M., and Hill, R. L. (1975) Bovine liver crotonase (enoyl coenzyme A hydratase). EC 4.2.1.17 L-3-hydroxyacyl-CoA hydrolyase, *Methods Enzymol* 35, 136-151.



44. Bell, A. F., Feng, Y., Hofstein, H. A., Parikh, S., Wu, J., Rudolph, M. J., Kisker, C., Whitty, A., and Tonge, P. J. (2002) Stereoselectivity of enoyl-CoA hydratase results from preferential activation of one of two bound substrate conformers, *Chem Biol* 9, 1247-1255.
45. Meganathan, R. (2001) Biosynthesis of menaquinone (vitamin K2) and ubiquinone (coenzyme Q): a perspective on enzymatic mechanisms, *Vitamins and hormones* 61, 173-218.
46. Jiang, M., Chen, X., Guo, Z. F., Cao, Y., Chen, M., and Guo, Z. (2008) Identification and characterization of (1R,6R)-2-succinyl-6-hydroxy-2,4-cyclohexadiene-1-carboxylate synthase in the menaquinone biosynthesis of *Escherichia coli*, *Biochemistry* 47, 3426-3434.

### Chapter 3 References

1. Eglund, P. G., Pelletier, D. A., Dispensa, M., Gibson, J., and Harwood, C. S. (1997) A cluster of bacterial genes for anaerobic benzene ring biodegradation, *Proceedings of the National Academy of Sciences of the United States of America* 94, 6484-6489.
2. Lynen, F., and Ochoa, S. (1953) Enzymes of fatty acid metabolism, *Biochim Biophys Acta* 12, 299-314.
3. Perrotta, J. A., and Harwood, C. S. (1994) Anaerobic Metabolism of Cyclohex-1-ene-1-Carboxylate, a Proposed Intermediate of Benzoate Degradation, by *Rhodopseudomonas palustris*, *Appl Environ Microbiol* 60, 1775-1782.
4. Eberhard, E. D., and Gerlt, J. A. (2004) Evolution of function in the crotonase superfamily: the stereochemical course of the reaction catalyzed by 2-ketocyclohexanecarboxyl-CoA hydrolase, *J Am Chem Soc* 126, 7188-7189.
5. Igbavboa, U., and Leistner, E. (1990) Sequence of proton abstraction and stereochemistry of the reaction catalyzed by naphthoate synthase, an enzyme involved in menaquinone (vitamin K<sub>2</sub>) biosynthesis, *Eur J Biochem* 192, 441-449.
6. Wen-Jin Wu, Y. F., Xiang He, Hilary A. Hofstein, Daniel P. Raleigh and Peter J. Tonge. (2000) Stereospecificity of the Reaction Catalyzed by Enoyl-CoA Hydratase, *J. Am. Chem. Soc.* 122, 3987.

7. Kurosawa, T., Sato, M., Nakano, H., Fujiwara, M., Murai, T., Yoshimura, T., and Hashimoto, T. (2001) Conjugation reactions catalyzed by bifunctional proteins related to beta-oxidation in bile acid biosynthesis, *Steroids* 66, 107-114.
8. Qin, Y. M., Haapalainen, A. M., Conry, D., Cuebas, D. A., Hiltunen, J. K., and Novikov, D. K. (1997) Recombinant 2-enoyl-CoA hydratase derived from rat peroxisomal multifunctional enzyme 2: role of the hydratase reaction in bile acid synthesis, *Biochem J* 328 ( Pt 2), 377-382.
9. Dieuaide-Noubhani, M., Asselberghs, S., Mannaerts, G. P., and Van Veldhoven, P. P. (1997) Evidence that multifunctional protein 2, and not multifunctional protein 1, is involved in the peroxisomal beta-oxidation of pristanic acid, *Biochem J* 325 ( Pt 2), 367-373.
10. Jiang, L. L., Kurosawa, T., Sato, M., Suzuki, Y., and Hashimoto, T. (1997) Physiological role of D-3-hydroxyacyl-CoA dehydratase/D-3-hydroxyacyl-CoA dehydrogenase bifunctional protein, *J Biochem* 121, 506-513.
11. Hiltunen, J. K., and Qin, Y. (2000) beta-oxidation - strategies for the metabolism of a wide variety of acyl-CoA esters, *Biochim Biophys Acta* 1484, 117-128.
12. Engel, C. K., Mathieu, M., Zeelen, J. P., Hiltunen, J. K., and Wierenga, R. K. (1996) Crystal structure of enoyl-coenzyme A (CoA) hydratase at 2.5 angstroms resolution: a spiral fold defines the CoA-binding pocket, *EMBO J* 15, 5135-5145.

13. Engel, C. K., Kiema, T. R., Hiltunen, J. K., and Wierenga, R. K. (1998) The crystal structure of enoyl-CoA hydratase complexed with octanoyl-CoA reveals the structural adaptations required for binding of a long chain fatty acid-CoA molecule, *J Mol Biol* 275, 847-859.
14. Bahnson, B. J., Anderson, V. E., and Petsko, G. A. (2002) Structural mechanism of enoyl-CoA hydratase: three atoms from a single water are added in either an E1cb stepwise or concerted fashion, *Biochemistry* 41, 2621-2629.
15. Muller-Newen, G., Janssen, U., and Stoffel, W. (1995) Enoyl-CoA hydratase and isomerase form a superfamily with a common active-site glutamate residue, *Eur J Biochem* 228, 68-73.
16. D'Ordine, R. L., Bahnson, B. J., Tonge, P. J., and Anderson, V. E. (1994) Enoyl-coenzyme A hydratase-catalyzed exchange of the alpha-protons of coenzyme A thiol esters: a model for an enolized intermediate in the enzyme-catalyzed elimination?, *Biochemistry* 33, 14733-14742.
17. Hanson, K. R. R., I. A. (1975) Interpretations of Enzyme Reaction Stereospecificity, *Acc. Chem. Res.* 8, 1.
18. Hofstein, H. A., Feng, Y., Anderson, V. E., and Tonge, P. J. (1999) Role of glutamate 144 and glutamate 164 in the catalytic mechanism of enoyl-CoA hydratase, *Biochemistry* 38, 9508-9516.

## Chapter 4 References

1. Taber, H. W., Dellers, E. A., and Lombardo, L. R. (1981) Menaquinone biosynthesis in *Bacillus subtilis*: isolation of men mutants and evidence for clustering of men genes, *Journal of bacteriology* 145, 321-327.
2. Zhang, J. H., Chung, T. D., and Oldenburg, K. R. (1999) A Simple Statistical Parameter for Use in Evaluation and Validation of High Throughput Screening Assays, *J Biomol Screen* 4, 67-73.
3. Heath, R. J., Li, J., Roland, G. E., and Rock, C. O. (2000) Inhibition of the *Staphylococcus aureus* NADPH-dependent enoyl-acyl carrier protein reductase by triclosan and hexachlorophene, *The Journal of biological chemistry* 275, 4654-4659.
4. Frederick, J. J., Corner, T. R., and Gerhardt, P. (1974) Antimicrobial actions of hexachlorophene: inhibition of respiration in *Bacillus megaterium*, *Antimicrobial agents and chemotherapy* 6, 712-721.
5. Feng, B. Y., Shelat, A., Doman, T. N., Guy, R. K., and Shoichet, B. K. (2005) High-throughput assays for promiscuous inhibitors, *Nat Chem Biol* 1, 146-148.
6. Drakulic, B. J., Juranic, Z. D., Stanojkovic, T. P., and Juranic, I. O. (2005) 2-[(Carboxymethyl)sulfanyl]-4-oxo-4-arylbutanoic acids selectively suppressed proliferation of neoplastic human HeLa cells. A SAR/QSAR study, *Journal of Medicinal Chemistry* 48, 5600-5603.

7. Drake, N. L., and Tuemmler, W. B. (1955) PODOPHYLLOTOXIN AND PICROPODOPHYLLIN .2. THE SYNTHESIS OF AN OPEN-CHAIN ANALOG, *Journal of the American Chemical Society* 77, 1204-1209.

## Chapter 5 References

1. Driscoll, J. R., and Taber, H. W. (1992) Sequence organization and regulation of the *Bacillus subtilis* menBE operon, *Journal of bacteriology* 174, 5063-5071.
2. Sharma, V., Hudspeth, M. E., and Meganathan, R. (1996) Menaquinone (vitamin K<sub>2</sub>) biosynthesis: localization and characterization of the menE gene from *Escherichia coli*, *Gene* 168, 43-48.
3. Sassetti, C. M., Boyd, D. H., and Rubin, E. J. (2003) Genes required for mycobacterial growth defined by high density mutagenesis, *Mol Microbiol* 48, 77-84.
4. Bar-Tana, J., Rose, G., and Shapiro, B. (1971) The purification and properties of microsomal palmitoyl-coenzyme A synthetase, *Biochem J* 122, 353-362.
5. Hisanaga, Y., Ago, H., Nakagawa, N., Hamada, K., Ida, K., Yamamoto, M., Hori, T., Arai, Y., Sugahara, M., Kuramitsu, S., Yokoyama, S., and Miyano, M. (2004) Structural basis of the substrate-specific two-step catalysis of long chain fatty acyl-CoA synthetase dimer, *The Journal of biological chemistry* 279, 31717-31726.
6. Bar-Tana, J., Rose, G., Brandes, R., and Shapiro, B. (1973) Palmitoyl-coenzyme A synthetase. Mechanism of reaction, *Biochem J* 131, 199-209.
7. Cleland, W. W. (1963) The kinetics of enzyme-catalyzed reactions with two or more substrates or products. I. Nomenclature and rate equations, *Biochim Biophys Acta* 67, 104-137.

8. Gulick, A. M., Starai, V. J., Horswill, A. R., Homick, K. M., and Escalante-Semerena, J. C. (2003) The 1.75 Å crystal structure of acetyl-CoA synthetase bound to adenosine-5'-propylphosphate and coenzyme A, *Biochemistry* 42, 2866-2873.
9. Gulick, A. M., Lu, X., and Dunaway-Mariano, D. (2004) Crystal structure of 4-chlorobenzoate:CoA ligase/synthetase in the unliganded and aryl substrate-bound states, *Biochemistry* 43, 8670-8679.
10. Jogl, G., and Tong, L. (2004) Crystal structure of yeast acetyl-coenzyme A synthetase in complex with AMP, *Biochemistry* 43, 1425-1431.
11. Ibba, M., and Soll, D. (2000) Aminoacyl-tRNA synthesis, *Annual review of biochemistry* 69, 617-650.
12. Nakatsu, T., Ichiyama, S., Hiratake, J., Saldanha, A., Kobashi, N., Sakata, K., and Kato, H. (2006) Structural basis for the spectral difference in luciferase bioluminescence, *Nature* 440, 372-376.
13. Cisar, J. S., and Tan, D. S. (2008) Small molecule inhibition of microbial natural product biosynthesis-an emerging antibiotic strategy, *Chem Soc Rev* 37, 1320-1329.
14. Ueda, H., Shoku, Y., Hayashi, N., Mitsunaga, J., In, Y., Doi, M., Inoue, M., and Ishida, T. (1991) X-ray crystallographic conformational study of 5'-O-[N-(L-alanyl)-sulfamoyl]adenosine, a substrate analogue for alanyl-tRNA synthetase, *Biochim Biophys Acta* 1080, 126-134.
15. Finking, R., Neumuller, A., Solsbacher, J., Konz, D., Kretschmar, G., Schweitzer, M., Krumm, T., and Marahiel, M. A. (2003) Aminoacyl



- adenylate substrate analogues for the inhibition of adenylation domains of nonribosomal peptide synthetases, *Chembiochem* 4, 903-906.
16. May, J. J., Finking, R., Wiegeshoff, F., Weber, T. T., Bandur, N., Koert, U., and Marahiel, M. A. (2005) Inhibition of the D-alanine:D-alanyl carrier protein ligase from *Bacillus subtilis* increases the bacterium's susceptibility to antibiotics that target the cell wall, *FEBS J* 272, 2993-3003.
  17. Ferreras, J. A., Ryu, J. S., Di Lello, F., Tan, D. S., and Quadri, L. E. (2005) Small-molecule inhibition of siderophore biosynthesis in *Mycobacterium tuberculosis* and *Yersinia pestis*, *Nat Chem Biol* 1, 29-32.
  18. Somu, R. V., Boshoff, H., Qiao, C., Bennett, E. M., Barry, C. E., 3rd, and Aldrich, C. C. (2006) Rationally designed nucleoside antibiotics that inhibit siderophore biosynthesis of *Mycobacterium tuberculosis*, *J Med Chem* 49, 31-34.
  19. Miethke, M., Bisseret, P., Beckering, C. L., Vignard, D., Eustache, J., and Marahiel, M. A. (2006) Inhibition of aryl acid adenylation domains involved in bacterial siderophore synthesis, *FEBS J* 273, 409-419.
  20. Pfleger, B. F., Lee, J. Y., Somu, R. V., Aldrich, C. C., Hanna, P. C., and Sherman, D. H. (2007) Characterization and analysis of early enzymes for petrobactin biosynthesis in *Bacillus anthracis*, *Biochemistry* 46, 4147-4157.
  21. Cisar, J. S., Ferreras, J. A., Soni, R. K., Quadri, L. E., and Tan, D. S. (2007) Exploiting ligand conformation in selective inhibition of non-ribosomal peptide synthetase amino acid adenylation with designed macrocyclic small molecules, *J Am Chem Soc* 129, 7752-7753.

22. Ferreras, J. A., Stirrett, K. L., Lu, X., Ryu, J. S., Soll, C. E., Tan, D. S., and Quadri, L. E. (2008) Mycobacterial phenolic glycolipid virulence factor biosynthesis: mechanism and small-molecule inhibition of polyketide chain initiation, *Chem Biol* 15, 51-61.
23. Waller, C. W., Patrick, J. B., Fulmor, W., and Meyer, W. E. (1957) The structure of nucleocidin. I, *J. Am. Chem. Soc.* 79 79, 1011.
24. Isono, K., Uramoto, M., Kusakabe, H., Miyata, N., Koyama, T., Ubukata, M., Sethi, S. K., and McCloskey, J. A. (1984) Ascamycin and dealanylascamycin, nucleoside antibiotics from *Streptomyces* sp, *J Antibiot (Tokyo)* 37, 670-672.
25. Zhang, S. P., Zubay, G., and Goldman, E. (1991) Low-usage codons in *Escherichia coli*, yeast, fruit fly and primates, *Gene* 105, 61-72.
26. Wada, K., Wada, Y., Ishibashi, F., Gojobori, T., and Ikemura, T. (1992) Codon usage tabulated from the GenBank genetic sequence data, *Nucleic Acids Res* 20 Suppl, 2111-2118.
27. Kane, J. F. (1995) Effects of rare codon clusters on high-level expression of heterologous proteins in *Escherichia coli*, *Curr Opin Biotechnol* 6, 494-500.
28. Kurland, C., and Gallant, J. (1996) Errors of heterologous protein expression, *Curr Opin Biotechnol* 7, 489-493.
29. Goldman, E., Rosenberg, A. H., Zubay, G., and Studier, F. W. (1995) Consecutive low-usage leucine codons block translation only when near the 5' end of a message in *Escherichia coli*, *J Mol Biol* 245, 467-473.

30. Kolkmann, R., and Leistner, E. (1985) Synthesis and revised structure of the o-succinylbenzoic acid coenzyme A ester, an intermediate in menaquinone biosynthesis, *Tetrahedron Lett.* 26, 1703-1704.
31. Kolkmann, R., and Leistner, E. (1987) Synthesis, analysis and characterization of the coenzyme A esters of o-Succinylbenzoic acid, an intermediate in vitamin K2 (menaquinone) biosynthesis, *Zeitschrift fur Naturforschung* 42, 542-552.
32. Santos, M. M., and Moreira, R. (2007) Michael acceptors as cysteine protease inhibitors, *Mini Rev Med Chem* 7, 1040-1050.
33. Worthington, A. S., Rivera, H., Torpey, J. W., Alexander, M. D., and Burkart, M. D. (2006) Mechanism-based protein cross-linking probes to investigate carrier protein-mediated biosynthesis, *ACS Chem Biol* 1, 687-691.
34. Qiao, C., Wilson, D. J., Bennett, E. M., and Aldrich, C. C. (2007) A mechanism-based aryl carrier protein/thiolation domain affinity probe, *J Am Chem Soc* 129, 6350-6351.
35. Reddick, J. J., Cheng, J., and Roush, W. R. (2003) Relative rates of Michael reactions of 2'-(phenethyl)thiol with vinyl sulfones, vinyl sulfonate esters, and vinyl sulfonamides relevant to vinyl sulfonyl cysteine protease inhibitors, *Org Lett* 5, 1967-1970.